Genetic approaches to the therapy of hepatocellular carcinoma

Thesis

UNRESTRICTED

GENETIC APPROACHES TO THE THERAPY OF HEPATOCELLULAR CARCINOMA

BORIS ROMAN ALEXANDER BLECHACZ

M.D., Dr. med.

A dissertation submitted in partial fulfillment of the requirements of the
Open University for the degree of
Doctor of Philosophy

January 2009

Dept. of Molecular Medicine
Mayo Clinic College of Medicine
Rochester, Minnesota
USA

Submission date: 15 January 2009
Date of award: 30 September 2009

Abstract

Hepatocellular carcinoma (HCC) is a devastating malignancy originating from hepatocytes. There is an urgent need for novel therapeutic approaches. Currently explored gene therapy systems have not yet achieved significant survival benefits. The aim of this thesis was the development and evaluation of novel genetic approaches to this malignancy.

The results of this thesis show that the only non-conjugated gene delivery system achieving significant intratumoral transgene expression is direct injection. Systemic gene delivery systems based upon Tf-shielded, polyethylenimine (PEI) based polyplexes and stabilized plasmid lipid particles (SPLP) do achieve efficient intratumoral transgene expression levels comparable to direct intratumoral injection, but their use is limited by their low intratumoral biodistribution. Further, this study shows that the use of non-viral replicon vectors based on the autonomously replicating parvoviruses minute virus of mice (pMVM) is feasible. In contrast to its viral equivalent, it allows expansion of its genome size to >106% and avoids immunogenicity. It maintains its tumorselectivity, but loses its cytotoxicity. The results of this thesis show that the Edmonston strain of measles virus (MV-Edm) efficiently infects human HCC cell lines resulting in syncytia formation followed by apoptotic cell death. The use of recombinant MV-Edm expressing marker genes allows non-invasive tracking of MV-Edm infection and kinetics. Treatment of mice bearing subcutaneous human HCC xenografts with recombinant MV-Edm resulted in significant survival benefits and tumor regression in up to one third of animals.

Acknowledgement

I would like to express my deep and sincere gratitude to Dr. Stephen J. Russell, the outstanding mentor who guided me through this project, continuously giving me support and encouragement. Working with him was an extraordinary experience, shaping my scientific development for this project and my academic future. His approach to science, his great wealth of knowledge and logic will always serve me as a role model.

My deep gratitude goes to Dr. Richard G. Vile for giving me the opportunity to pursue the Ph.D., his advice, continuous support and enthusiasm.

My sincere thanks also go to the examiners Drs. Farzin Farzaneh and Yasuhiro Ikeda for their time and effort, and for creating a friendly, collegial and educational atmosphere during the viva voce.

I also would like to thank my colleagues Drs. David Dingli, Louay K. Hallak, Takafumi Nakamura, Ianko D. Iankov, Apollina Goel, Jie Zhang and Jaime R. Merchan, for creating an enjoyable atmosphere and providing productive scientific discussions. I am highly grateful to Dr. Jean Rommelaere for his advice and support leading to my research pursuit in the United States. Thanks go to Drs. Kah-Whye Peng, Annick Brandenburger, Jan J. Cornelis, Christiane Dinsart and Ernst Wagner who helped with various aspects of this project.

Finally, I would like to thank my family: my parents for awakening and supporting my interest in science, their encouragement throughout my academic development and their continuous motivation throughout this project, and my wife for sustaining me throughout my journey and her words of encouragement.

Table of contents

TITLE PAGE I

ABSTRACT II

ACKNOWLEDGEMENT III

TABLE OF CONTENTS IV

LIST OF FIGURES VII

LIST OF TABLES X

I. INTRODUCTION 1

1. Hepatocellular Carcinoma 1
1.1. Introduction 1
1.2. Epidemiology 2
1.3. Etiology 3
1.4. Prognosis and staging 5
1.5. Therapy 9

2. Genetic approaches to the therapy of cancer 17
2.1. Introduction 17
2.2. Immunogene therapy 18
2.3. Anti-angiogenic cancer gene therapy 19
2.4. Cytoreductive cancer gene therapy 20
2.5. HSC transduction with drug-resistance genes 20

3. Parvoviridae 22
3.1. Introduction 22
3.2. Parvoviridae biology 22
3.3. Infectivity, pathogenicity and oncosuppression 26
3.4. Tissue targeting with parvovirinae vectors 27
3.5. Parvovirinae in cancer gene therapy 28
3.6. Summary 33

4. Measles virus 34
4.1. Introduction 34
4.2. Measles Virus biology 35
4.3. Tumor selectivity 37
4.4. Measles virus and the immune system 39
4.5. MV-Edm as a viral vector for cancer gene therapy 42
4.6. Trackable MV-Edm for pharmacodynamic and pharmacokinetic analysis 46
4.7. Summary 48

5. Non-viral gene deliver systems **50**
5.1. Introduction 50
5.2. Biologic barriers 50
5.3. Uncomplexed DNA gene delivery 52
5.4. Synthetic gene delivery systems 56

6. Specific aims of the thesis **63**
6.1. Background 63
6.2. Specific aim 1 63
6.3. Specific aim 2 64
6.4. Specific aim 3 65

II. MATERIAL & METHODS 66

1. Cell biological methods **66**
1.1. Cell lines 66
1.2. Long-term storage of cells 66
1.3. Passaging of established cell lines 67
1.4. Assessment of cell numbers 68
1.5. Cell staining 68
1.6. Cytotoxicity assays 70
1.7. Flow cytometry 72
1.8. In vitro ^{123}I uptake studies 72

2. Molecular biological methods **73**
2.1. Nucleic acid transduction 73
2.2. Isolation and purification of nucleic acids 74
2.3. Nucleic acid analysis 76
2.4. Nucleic acids cloning 79

3. Virologic methods **85**
3.1. Amplification of recombinant measles virus 85
3.2. Infection of eukaryotic cells 85

4. Biochemical methods **86**
4.1. Stabilized plasmid lipid particles 86
4.2. PEI-Polyplexes 87
4.3. LipT complexes 89
4.4. Protein concentration analysis 89
4.5. Luciferase assay 90
4.6. β-Galactosidase assay 90

5. Animal experimental methods **91**
5.1. Subcutaneous tumor xenograft implantation 91
5.2. Tumor marker analysis 91
5.3. *In vivo* iodine uptake studies 92
5.4. *In vivo* gene expression analysis 92
5.5. Statistical Methods 92

III. RESULTS 93

1. Nonviral gene delivery systems **93**
1.1. Introduction 93
1.2. Un-conjugated plasmid DNA transfer 93
1.3. Conjugated DNA transfer systems 100

2. Expanded parvoviral replicons as novel nonviral gene therapy vectors **109**
2.1. Introduction 109
2.2. Generation of recombinant MVM-replicons 110
2.3. Functionality of recombinant parvoviral replicon vectors 117
2.4. Effect of palindrome restoration on MVM-replicon efficacy 124
2.5. Expanded parvoviral replicons 128
2.6. Parvoviral replicons in comparison to other expression systems 133
2.7. Tumor selectivity of parvoviral replicon vectors 136
2.8. MVM-replicon cytotoxicity 140

3. Viral gene therapy using recombinant measles virus **142**
3.1. Introduction 142
3.2. Human HCC express high levels of CD46 143
3.3. Infectivity, syncytia formation and cytotoxicity of MV-Edm in HCC 145
3.4. Measles virus induces apoptosis in HCC 147
3.5. Transgene expression in MV-Edm infected human HCC cell lines 150
3.6. Intratumoral MV-Edm therapy in human HCC-xenografts 153
3.7. Non-invasive *in vivo* monitoring after MV-CEA therapy of HCC 155
3.8. Non-invasive *in vivo* imaging after MV-NIS therapy of HCC 156
3.9. Intravenous MV-Edm therapy of human HCC-xenografts 158

IV. DISCUSSION 160

1. Nonviral gene delivery systems **160**

2. Parvoviral replicon vectors **169**

3. Viral gene therapy using recombinant measles virus **175**

V. LITERATURE 182

VI. ABBREVIATIONS 214

List of figures

Figure	Title	Page
Figure 1:	HCC incidence	2
Figure 2:	Staging and treatment assignment for HCC patients according to the BCLC system	8
Figure 3:	Genome organisation of autonomously replicating parvovirus	24
Figure 4:	Measles virus genome	36
Figure 5:	Measles virus structure	37
Figure 6:	Liposome preparation	58
Figure 7:	SPLP-purification	87
Figure 8:	SPLP size analysis	88
Figure 9:	Gene expression after intravenous injection of naked plasmid DNA	94
Figure 10:	Gene expression after intra-arterial injection of naked plasmid DNA	96
Figure 11:	Gene expression after hydrodynamic injection of naked plasmid DNA	98
Figure 12:	Gene expression after direct intratumoral injection of naked plasmid DNA	100
Figure 13:	*In vivo* gene expression after systemic therapy with DNA/Tf-PEI25/PEI22-polyplexes	102
Figure 14:	SPLP biodistribution	105
Figure 15:	*In vivo* gene expression after systemic therapy with SPLP	107

Figure 16:	Intratumoral distribution of transduced cells after SPLP treatment.	108
Figure 17:	Parvovirus MVM left palindrome	110
Figure 18:	Cloning strategy for insertion of stuffer DNA	112
Figure 19:	Cloning strategy of recombinant parvoviral replicons vectors	115-116
Figure 20:	Parvoviral replicons vectors	118
Figure 21:	Excision and amplification of recombinant parvoviral replicons	119
Figure 22:	^{125}I-uptake after pUC-MVMp+-NIS transfection	121
Figure 23:	CEA expression after pUC-MVMp+-CEA transfection	122
Figure 24:	Transgene expression after transfection with recombinant parvoviral replicons	123
Figure 25:	Comparison of parvoviral DNA-replication with incomplete and restored left palindrome	125
Figure 26:	Effect of left palindrome restoration on transgene expression	127
Figure 27:	Transcriptional efficiency of expanded parvoviral replicon vectors	129
Figure 28:	Replication of expanded parvoviral replicon vectors	131
Figure 29:	Transgene expression after transfection with expanded parvoviral replicon vectors	132
Figure 30:	Comparison of parvoviral replicon vectors with replicating and non-replicating high-level expression vectors	135
Figure 31:	Tumorselectivity of parvoviral replicon vectors	138
Figure 32:	Tumorselectivity of parvoviral replicon vectors	139
Figure 33:	MVM replicon cytotoxicity	141
Figure 34:	Schematic representation of recombinant MV-Edm	143

Figure 35:	CD46-overexpression in HCC in comparison to normal hepatic tissue	144
Figure 36:	Infectivity, syncytia-induction and CPE of MV-Edm in HCC	146
Figure 37:	MV-Edm induced apoptosis	148
Figure 38:	Caspase 3/7 activity after MV-Edm infection	149
Figure 39:	Transgene expression in human HCC cell lines after infection with MV-CEA and MV-NIS	152
Figure 40:	Tumor-suppression and survival after intratumoral MV-CEA therapy of HCC-xenografts	154
Figure 41:	Syncytia formation after intratumoral MV-Edm therapy	155
Figure 42:	Serum CEA concentrations after intratumoral MV-CEA therapy of HCC-xenografts	156
Figure 43:	Increased ^{123}I-uptake in HCC-tumors after intravenous MV-NIS therapy	157
Figure 44:	Tumor-suppression in HCC-tumors after intravenous MV-NIS therapy	159

List of tables

Table	Title	Page
Table 1:	Risk factors for HCC	4
Table 2:	AASLD HCC screening recommendations	5
Table 3:	TNM staging classification for HCC	6
Table 4:	The Barcelona Clinic Liver Cancer (BCLC) staging Classification	8
Table 5:	Requirements of a gene delivery system with respect to different target cells	18
Table 6:	The parvovirinae subfamily	22
Table 7:	Preclinical studies evaluating MV-Edm as a cancer therapy agent	45
Table 8:	Cell lines used in for experiments	67

I. Introduction

1. Hepatocellular Carcinoma

1.1. Introduction

Hepatocellular carcinoma (HCC) is a malignancy originating from hepatocytes. It is the most common primary hepatic malignancy constituting 84% of primary liver cancers. Globally, it is one of the leading causes of cancer mortality and its incidence is increasing, especially in Western countries. Its prognosis is fatal with a median survival of less than one year after onset of symptoms. There are a variety of different therapeutic approaches including surgical, local ablative and systemic treatments. Unfortunately, the majority of patients present with advanced stage disease, at which curative therapies are not feasible. Hence, surveillance of patients at risk is essential [1]. New therapeutic approaches are being explored and novel targeted therapies have been developed. Most recently, the kinase inhibitor Sorafenib has been shown to achieve significant prolongation of survival in intermediate stage HCC patients and is now commonly used in this patient subgroup. However, surgery continues to remain the only potentially curative treatment. Therefore, there is an urgent need for new curative approaches for HCC. The aim of this study was the development and evaluation of novel genetic therapies for HCC.

1.2. Epidemiology

HCC is the fifth most common cancer in the world and the third most common cause of cancer mortality worldwide [2]. The annual incidence for HCC has been estimated as high as 564,000 cases worldwide and its mortality as 548,554 cases in 2000. The distribution of HCC is heterogenous (Fig. 1) [3].

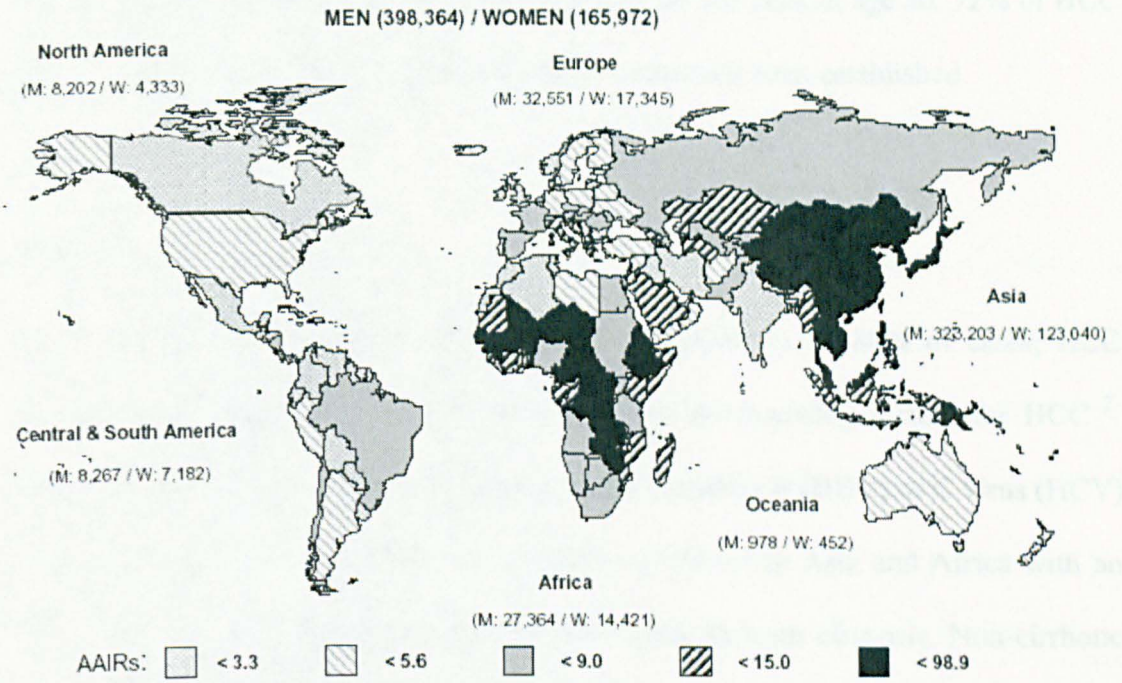

Figure 1 HCC incidence. World map depicting estimated age-adjusted incidence rates of HCC cases among men in 2000. The corresponding age-adjusted incidence rates for women follows a similar pattern [4].

The highest incidence rates are being reported in Eastern Asia and Middle Africa with age-adjusted incidence rates (AAIR) of up to 98.9/100,000. In Australia, New Zealand, Europe and the American continents, the incidence of HCC is consistently below 10/100,000 [4]. However, incidence rates of HCC in USA and Europe have increased more than two-fold in the last three decades from 1.3/100,000 in 1976-1980 to 3.0/100,000 in 1991-1998 [5, 6]. Age-adjusted mortality rates (AAMR) of HCC follow a

geographic pattern consistent with the incidence rates. Mortality rates of HCC in the USA have also increased significantly in the last three decades and were estimated to be 3.7/100,000 in 2001 [5, 6]. The average age at diagnosis in Western countries is 65; HCC in patients younger than 40 years of age is rare. Starting at age 40 the risk increases progressively and peaks at age 70-75. In high-risk areas such as South East Asia and the West Coast of Africa, HCC is frequently diagnosed between age 20 and 35. HCC incidence rates in these countries increase from age 20 and peak at age 50. 72% of HCC patients are male. Causes of the gender difference have not been established.

1.3. Etiology

Several risk factors for HCC have been identified (Tab. 1). In 80% of cases, HCC develops in cirrhosis which is considered the most predisposing factors for HCC [7]. Frequently, HCC is the long-term result of chronic Hepatitis B (HBV) or C virus (HCV) infection. Hepatitis B virus (HBV) is the main risk factor in Asia and Africa with an annual incidence rate of 2-6% in chronic HBV patients with cirrhosis. Non-cirrhotic chronic hepatitis B patients have an annual HCC incidence rate of 0.4%. In developed countries, HCC predominantly develops in the setting of cirrhosis secondary to chronic alcohol abuse or chronic HCV infection. Up to one third of cirrhotic, chronic HCV infected patients develop HCC; the annual incidence rate of HCC in this setting is 3-5%. The carcinogen aflatoxin B1 increases the neoplastic risk three-fold and has been linked to mutations in the tumor suppressor gene p53. Other risk factors include α-1-antitrypsin deficiency, hemochromatosis and non-alcoholic fatty liver disease.

- Cirrhosis
- Chronic hepatitis B, C, D
- Toxins (e.g. alcohol, aflatoxins)
- Hemochromatosis
- a-1-antitrypsin deficiency
- Non-alcoholic fatty liver disease
- Autoimmune hepatitis

Table 1 Risk factors for HCC. Shown are conditions considered to be significant risk factors for the development of HCC [8].

Current surveillance and prevention recommendations are based upon the above-described etiologic factors. Nationwide vaccination of infants for HBV in Taiwan between 1984-1986 decreased the prevalence of HBV carriers in childhood from 15% to 1%, and simultaneously decreased HCC in vaccinated children by 60% compared to non-vaccinated children [9, 10]. Current screening recommendations by the American Association of the Study of Liver Disease (AASLD) are summarized in Table 2. Goal of regular screening of patients at risk is the early detection of HCC at a stage where the cancer is amenable to curative therapy. The recommended screening intervals are 6-12 months based upon tumor doubling times [11]. Most centers use a 6-months interval, although survival has not shown to be improved through 6- versus 12-months intervals [12]. The most commonly used screening tests are serum alphafetoprotein (AFP) and ultrasound of the liver. However, both tests have limitations as screening tests. AFP has a sensitivity of only 60% at a cut-off level of 20 ng/ml and a positive predictive value of 41.5% in a population with a prevalence of 5% as usually seen in specialized centers. Ultrasound of the liver has a sensitivity of 65-80% and a specificity of >90% as a screening test for HCC. False-positive rates increase with combined use of these tests to 7.5% and costs to $3,000 per detected tumor [11].

- Hepatitis B carriers:
- Asian males ≥40 years
- Asian females ≥50 years
- All cirrhotic hepatitis B carriers
- Family history of HCC
- Africans >20 years
- Non-hepatitis B cirrhosis:
- Hepatitis C
- Alcoholic cirrhosis
- Genetic hemochromatosis
- Primary biliary cirrhosis

Table 2 AASLD HCC screening recommendations. These are level III recommendations issued by the AASLD in 2005. Conditions such as α-1-antitrypsin deficiency, non-alcoholic steatohepatitis and autoimmune hepatitis are not included in these recommendations due to the lack of data regarding the benefit of surveillance.

1.4. Prognosis and staging

The majority of HCC patients are diagnosed at an advanced stage due to the clinically silent character of this tumor. Tumor growth rates display a great variety with a median doubling time of 117 days. Its subclinical development lasts a median time period of 3.2 years [13, 14]. There are only few reports on the natural course and prognosis of HCC in patients receiving only symptomatic treatment. Earlier studies reported 1.6 to 4 months survival from onset of symptoms in symptomatically treated HCC patients [15, 16]. More recent studies described median survival of 17 month with an overall probability of survival at 1, 2 and 3 years of up to 54%, 40% and up to 28% in cirrhotic patients with HCC receiving only symptomatic treatment [17, 18]. However, the increase in median survival over time has been attributed to lead-time bias as patients at risk are more aggressively screened, and diagnostic techniques are more advanced [19]. As for most

cancers, prognosis of HCC is related to its tumor stage [20]. Very early stage HCC has 5-year survival rates between 71-89% after therapy and 3-year recurrence rate of 8%. 5-year survival rates in early HCC range between 50-70% with treatment [21]. 1-, 2- and 3 year survival of intermediate stage HCC is 80%, 65% and 50%, and 29%, 16% and 8% for advanced stage HCC. Different staging systems have been implemented in order to

TNM	Variable
T1	Solitary tumor w/o vascular invasion
T2	Solitary tumor with vascular invasion OR multiple tumors, none >5 cm
T3	Multiple tumors >5 cm OR tumor involving major branch of portal or hepatic veins
T4	Tumor(s) w. direct invasion of adjacent organs other than gallbladder OR w. perforation of visceral peritoneum
N0	No regional lymph node metastases
N1	Regional lymph node metastases
M0	No distant metastases
M1	Distant metastases
Stage	
I	T1 N0 M0
II	T2 N0 M0
IIIA	T3 N0 M0
IIIB	T4 N0 M0
IIIC	Any T N1 M0
IV	Any T Any N M1

Table 3 TNM staging classification for HCC. HCC staging classification according to International Union Against Cancer (UICC) and the American Joint Committee on Cancer (AJCC). The system is based on tumor extent (T), extent of lymph node involvement (N) and presence of metastases.

establish an optimal predictor of prognosis; these include the Okuda staging system, the CLIP-score, the TNM-staging system and the BCLC staging system. In contrast to most other tumor-types, prognosis of HCC is highly complex and depends on different factors, including tumor stage, liver function, patient's general condition and treatment

efficacy [19]. At present, there is no consensus on one gold standard staging system for HCC [11, 22]. Classical cancer staging systems, such as the TNM- classification (Table 3), have been shown to be inaccurate in predicting survival or guiding management. In order to combine the two variables of liver function and tumor extent, the Okuda system was developed [16]. This system grouped patients in three groups defined by tumor volume, ascites, jaundice and serum albumin concentration. The Okuda system was commonly used for two decades. In the 1990's, improvement in imaging technology allowed identification of hepatic lesions at earlier stages. With these techniques, the Okuda system was not sufficient anymore as it missed early and intermediate stage HCC. As a consequence a great variety of different scoring system was developed such as a modified TNM systems, the Cancer of the Liver Italian Program (CLIP) score and the Barcelona Clinic Liver Cancer (BCLC) staging system (Table 6) [23-25]. Comparison of the Okuda and CLIP systems with the TNM system showed that neither one was superior to the TNM system in regard to their prognostic value in patients undergoing surgical resection [26]. The BCLC staging system is based upon results of several independent studies and includes variables such as tumor stage, hepatic functional status, physical status and cancer related symptoms. It links staging with treatment modalities, and thereby provides survival estimates based upon published data on response rates to different treatments (Figure 2). Currently, there is no global consent on a preferred staging system for HCC. However, the BCLC system is the only staging system that includes information on the impact of treatment on life expectancy, and is therefore recommended by the AASLD practice guidelines [11].

Stage	PST	Tumor	Hepatic status
Stage A (early HCC)			
A1	0	Single tumor	No portal hypertension, Normal bilirubin
A2	0	Single tumor	Portal hypertension, Normal bilirubin
A3	0	Single tumor	Portal hypertension, Abnormal bilirubin
A4	0	3 tumors, all <3 cm	Child-Pugh A-B
Stage B (intermediate HCC)			
B	0	Large multinodular	Child-Pugh A-B
Stage C (advanced stage)			
C	1-2	Vascular invasion OR Extrahepatic spread	Child-Pugh A-B
Stage D (end-stage HCC)			
D	3-4	Any	Child-Pugh C

Table 4 The Barcelona Clinic Liver Cancer (BCLC) staging classification.

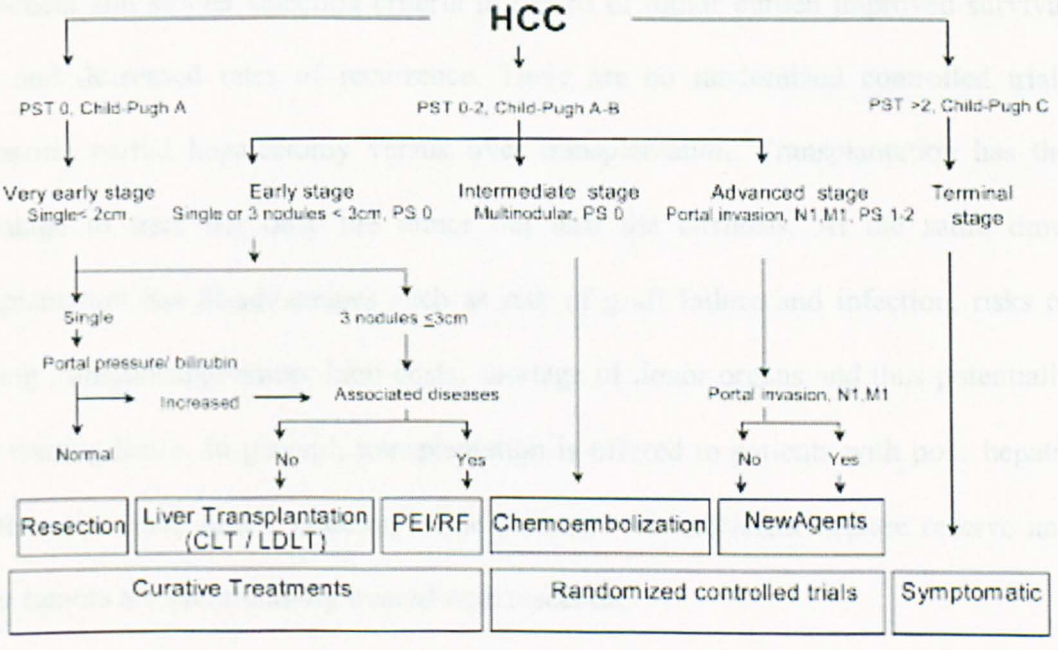

Figure 2 Staging and treatment assignment for HCC patients according to the BCLC system [11].

1.5. Therapy

A variety of therapeutic options are available for HCC including surgery, chemotherapy, local ablative therapies and hormone therapy. Surgery is considered to be the only potentially curative treatment. Most of the other treatment modalities are palliative or used as adjuvant or neoadjuvant treatment. More than 80% of HCC patients are diagnosed at an advanced stage at which they are not eligible for potentially curative treatments such as transplantation, surgical resection or liver-directed therapies [3].

1.5.1. Surgery

Partial hepatic resection and transplantation are the only potentially curative treatments. Unfortunately, only a minority of patients is eligible for these procedures. Initially, outcomes were poor in terms of recurrence and survival. Advances in pre-operative assessment and stricter selection criteria in regard of tumor burden improved survival rates and decreased rates of recurrence. There are no randomized controlled trials comparing partial hepatectomy versus liver transplantation. Transplantation has the advantage to treat not only the tumor but also the cirrhosis. At the same time, transplantation has disadvantages such as risk of graft failure and infection, risks of lifelong immunosuppression, high costs, shortage of donor organs and thus potentially long waiting times. In general, transplantation is offered to patients with poor hepatic function and small tumor nodules, while patients with sufficient hepatic reserve and larger tumors are preferentially treated with resection.

1.5.1.1. Resection

Resection is the initial treatment of choice. Especially patients with a small, unifocal tumor qualify for this treatment. Liver reserve and regenerative capacity are major

determinants of post-operative liver failure. As a majority of HCC patients have compromised hepatic function, the choice of candidates is restricted. The operative risk is especially in the setting of cirrhosis increased due to complications such as hemorrhage, infections, wound-related complications and respiratory compromise. It has been shown that cirrhosis is a factor associated with poor outcome [27]. The ideal candidate is considered one with Child-Pugh class A cirrhosis, age <65 years, a single tumor nodule with a diameter of <5cm and no portal vein invasion. Contraindications for resection are advanced cirrhosis, multilocular HCC and extrahepatic metastases. Resectability of the tumor is dependent on its anatomic location and the absence of major vascular invasion. Non-cirrhotic patients recover well from partial hepatectomy preserving at least two segments of functional liver tissue. In well-compensated cirrhosis, resection of up to two functional segments is well tolerated. The operative mortality is reported to be up to 10% and 5-year survival ranges between 20-60%. Recurrence is the main reason for late post-operative mortality. 5-year recurrence rates are reported to be 50-100%; in the majority of the cases tumor recurrence is diagnosed within the first 3 years following resection. Early recurrence (12 months to 3 years) is thought to represent residual tumor spread, and is considered to be a poor prognostic factor. Late recurrence is thought to result from new tumor formation within the cirrhotic liver. In general, the following parameters are thought to correlate with surgical failure: vascular invasion, presence of satellite nodules, large tumor size, advanced pTNM stage, hepatitis activity in the non-cancerous hepatic tissue and perioperative transfusion.

1.5.1.2. Transplantation

Initially, outcome of liver transplantation for HCC were poor, recurrence rates high and 5-year survival only 18-40% [28, 29]. Limitation of candidates based upon established selection criteria has resulted in improved results. Most liver transplantation centers as well as the United Network for Organ Sharing (UNOS) apply the Milan selection criteria [30]. According to these criteria, patients are eligible for liver transplantation, if they have a solitary tumor nodule with a diameter $\leq$ 5 cm or fewer than 3 tumor nodules, no more than 3 cm each; vascular invasion and extrahepatic manifestations are considered contraindications. Restriction of patients fulfilling these criteria resulted in 5-year survival rates of 70%. Attempts to expand Milan criteria resulted in worse outcomes with 5-year survival of 44% [31]. A study comparing the Milan criteria with the expanded UCSF-criteria - defined as single tumor nodule $\leq$ 6.5 cm or up to 3 lesions with the largest not exceeding 4.5 cm and the sum of tumor diameters not exceeding 8 cm -showed no significant difference in survival, but significantly higher recurrence rates in the UCSF-criteria group [29, 32]. However, donor organ shortage results in long waiting times and as a consequence drop out rates are high with up to 25% drop out rate at 12 months [33]. Living donor liver transplantation is an alternative approach achieving similar 5-year survival outcomes as deceased donor transplantation [28]. However, it is also correlated with morbidity and mortality rates of 14-21% and 0.25-1% [28].

1.5.1.3. Neoadjuvant and adjuvant therapy

The aim of neoadjuvant therapy is to downstage tumors in order to facilitate resection or transplantation, or to prevent tumor progression prior to liver transplantation. However, systemic therapies for neoadjuvant treatment do not provide survival benefits in HCC [20]. Local ablative methods are frequently used as a neoadjuvant treatment for bridging

time to liver transplantation [34]. However, also these approaches have not been proven to provide significant survival benefits [35]. Adjuvant chemotherapy has been evaluated in a variety of trials due to the high recurrence rate of HCC. However, adjuvant treatments do not improve overall survival or disease-free survival [36, 37].

1.5.2. Local ablative methods

Local ablative treatments are beneficial in patients who do not qualify for resection or transplantation. There are a variety of different techniques used for this approach including percutaneous ethanol injection (PEI), radiofrequency ablation and transarterial chemoembolization (TACE).

1.5.2.1. Percutaneous ethanol injection

PEI is a widely accepted and commonly used therapeutic method for small, localized HCC. 95% ethanol is intratumorally injected under ultrasound guidance. As a general rule, the total number of injections in order to ablate the tumor equals twice the tumor-diameter measured in centimeters [38]. This technique is indicated for HCC-patients with a tumor-nodule of $\leq$2 cm in diameter who are not being suitable candidates for liver-transplantation or hepatic resection [39, 40]. Treatment of tumors larger in size resulted in incomplete ablation, high rates of relapse and decreased survival; therefore, they are not considered suitable for PEI-therapy. Also, superficially located tumor-nodules are not suitable due to increased extravasation of ethanol and suboptimal treatment of tumor margins [39]. Complication rate of PEI-treatment is 1.7% and mortality 0.1% [39]. Overall 1- and 3-year survival rates in patients with HCC-nodules $\leq$ 3 cm treated with PEI is 90% and 63% but recurrence rates are high with up to 66% per year [41-43].

1.5.2.2. Radiofrequency ablation

Thermal ablation is based on the principle of irreversible tissue damage caused by exposure to high temperatures. Temperatures between 60^0 C and 100^0 C cause cellular protein coagulation with irreversible damage to cellular enzymes and nucleic acid-histone complexes. Several techniques have been used for induction of thermal injury such as radiofrequency ablation, microwave, laser and high-intensity focused ultrasound [44]. Radiofrequency ablation is the most established of these methods [45]. A grounding pad is placed on the patients back and a partially insulated electrode is placed within the tumor tissue. High-frequency alternating current is applied to tumor tissue resulting in heat energy of $>60^0$ C in the area of the electode [46]. This technique achieves similar response rates as PEI in tumors <2 cm but better outcomes in larger tumors. However, a significant long-term survival benefit has not been shown [8, 20].

1.5.2.3. Chemoembolization

HCC is a highly vascularized tumor deriving its main blood supply through the hepatic artery. In contrast, hepatic parenchyma derives its main blood supply from the portal vein. Selective intra-arterial embolization of the tumor-supplying artery (TAE) was shown to have therapeutic efficacy [47, 48]. However, it does not have any beneficial effects on overall survival and is therefore not recommended as routine treatment for HCC [49-52].

Transcatheter arterial chemoembolization (TACE) is defined as local delivery of chemotherapeutic agents conjugated to an embolic agent to the tumor. Embolization results in prolonged exposure of tumor tissue to the chemoterapeutic agent and reduced systemic side effects in comparison to systemic chemotherapy. Chemotherapeutic agents used for TACE include doxorubicin, farmorubicin, adriamycin, eporubicin and

cisplatin [53-57]. Embolizing agents include lipiodol, gelatin sponge particles, starch, collagen or blood clots [53]. TACE can be repeated after 6 to 12 weeks [38]. Response rates to TACE are are reported as 33-55% [51, 53]. Initial analyses showed mixed results in regard of its effect on survival [48, 49, 51, 58-60]. Modification of protocols and analysis of patient characteristics showed that therapeutic benefit of TACE depends on hepatic function and tumor stage [61-63]. Restriction of patient selection to Child-Pugh class A and Okuda stage I and II resulted in 1-, 2- and 3-year survival rates of 57%, 31% and 26% after TACE compared to 32%, 11% and 3% with symptomatic treatment only [50, 52]. In patients with Child C cirrhosis, the rate of complication is significantly higher with mortality rates up to 30% [64]. Therefore, cirrhosis Child-Pugh class C cirrhosis as well as portal vein thrombosis and presence of a portosystemic shunt are considered contraindications for TACE reducing the number of eligible candidates to 12% [50, 53, 65].

1.5.3. Systemic therapies

Systemic therapies for HCC are considered non-curative. The spectrum of this therapeutic mode includes chemotherapy, hormonal therapy and biologic therapies. A great variety of clinical trials have been conducted in patients with unresectable HCC. Chemotherapeutics were used either as single agents or as combination chemotherapy. The most common chemotherapeutic agents used were doxorubicin and its less hepatotoxic derivative epirubicin, 5-FU, cisplatin and gemcitabine [66].

However, systemic chemotherapy for HCC shows only low response rates between 0-30%, no survival benefit, and is correlated with significant adverse effects and complications [3, 20, 67-81]. Factors such as high albumin, low total bilirubin levels, low transaminase levels, absence of ascites, non-elevated serum-AFP, absence of vascular

involvement and small tumor size have been associated with better response to chemotherapy [82-84]. These factors reflect liver function and it has been hypothesized that better hepatic function allows better cytotoxic delivery [84]. At the present time, there are no chemotherapeutic drug regimens considered standard of care for HCC [85].

Based upon demonstration of over-expression of hormonal receptors – e.g. estrogen- and androgen receptors - in HCC, it was hypothesized that inhibition of these receptors might elicit therapeutic effects [86]. Initial results in small, uncontrolled trials using the estrogen receptor inhibitor tamoxifen for HCC were promising, reporting significant survival benefits [49, 87-90]. However, re-evaluation of tamoxifen in large, randomized trials failed to show a significant therapeutic effect [91-97]. Also, studies with the somatostatin analogue octreotide, initially reported to be beneficial in HCC, showed no therapeutic efficacy in more recent, large randomized controlled clinical trials. In conclusion, hormonal therapy is not considered to be of significant benefit in HCC [85, 96].

Results from trials evaluating biologic and biochemical agents such as interferon and thalidomide are inconclusive and can therefore not be recommended for HCC [85].

1.5.4. Radiation therapy

External beam radiation is not feasible for HCC as at least 50 Gy are required for tumor ablation but radiation hepatitis is induced by doses >30 Gy [98]. Conformational radiotherapy did not show significant survival benefits despite tumor response. Newer techniques involve micropsheres such as Yttrium-90 TheraSpheres, which are currently under evaluation.

1.5.5. Novel therapies

The growing understanding of the molecular pathogenesis of HCC has identified new therapeutic targets. A great variety of new agents have been developed and are being evaluated for their potential as novel treatment options. These include small-molecule inhibitors, monoclonal antibodies and others [99]. The majority of these agents target tyrosine kinases such as epidermal growth factor receptor (EGFR), vascular endothelial growth factor receptor (VEGFR), MAPK kinases or Raf kinase. Other targets include mTOR or members of the Bcl-2 family. Recent evaluation of the multikinase inhibitor Sorafenib in the clinical SHARP (Sorafenib HCC Assessment Randomized Protocol) demonstrated significant prolongation of survival by 3 months and longer time to progression in patients with advanced HCC resulting in its approval for HCC by the FDA [100].

1.5.5. Summary

In summary, despite intense research efforts, surgery continues to be the only curative therapeutic option for HCC. However, only a minority of patients qualifies for an invasive approach and the dropout rates for patients awaiting transplantation are relatively high. Novel therapies have resulted only in modest prolongation of survival. Therefore, there is an urgent need for new therapeutic approaches. Genetic approaches to the therapy of HCC might be a potent tool in its treatment.

2. Genetic approaches to the therapy of cancer

2.1. Introduction

Gene therapy is one of the most promising approaches to treat cancer as it has the potential to provide tumour cell selectivity and/or protection of untransformed cells of the body. There are four main strategies in cancer gene therapy: (1) immunogene therapy to produce an antitumour vaccine effect or to enhance T-cell antitumour capability; (2) anti-angiogenic gene therapy; (3) cytoreductive gene therapy; and (4) transduction of haematopoetic stem cells (HSCs) with drug-resistance genes to enhance their resistance to cytotoxic drugs. In order to transduce the gene of interest, either nonviral vectors or viral vectors are used. Nonviral vector strategies include naked plasmid DNA, liposome–DNA complexes, peptide-bound DNA and electroporation [101-103, 104]. The most widely used viral vectors are retroviruses, adenoviruses, adeno-associated viruses (AAVs; members of the parvoviridae family and discussed further below) and herpesviruses, and there is a great diversity of new vector systems being developed [105, 106, 107, 108].

Depending on the desired gene therapy approach, there are different requirements the vector must fulfill, including safety and efficiency of the vector, specific targeting of gene transduction, expression level of the transduced gene and ease of manufacture [109]. The specific requirements for vectors in the various gene therapy strategies are discussed in the following sections and are summarised in Table 5.

Two viral vector systems fulfilling the majority of these requirements are autonomously replicating parvoviruses and measles virus. In the following sections, cancer gene therapy strategies will be discussed, followed by overviews over both viral systems and their use in cancer gene therapy.

	Tumour cells ex vivo	Tumour cells in vivo	VECs	T cells or HSCs ex vivo	T cells or HSCs in vivo
Transfer to progeny	–	–	–	+	+
Expression in nondividing cells	+	+	+	–	+
In vivo stability	–	+	+	–	+
Transcriptional targeting	–	+	+	–	+
Targeted attachment	–	+	+	–	+

Table 5 Requirements of a gene delivery system with respect to different target cells. The table shows the requirements vector systems have to fulfil in the different cancer gene therapy strategies. Further details and explanations are described in the text of the corresponding sections. (Abbreviations: + = required, - = not required; VEC = vascular endothelial cell; HSC = haemopoietic stem cell)

2.2. Immunogene therapy

In oncologic diseases, neoplastic cells have escaped the immune surveillance that normally prevents tumour formation. Mechanisms by which tumors escape an immune response include development of tolerance towards tumour-associated antigens (TAAs), development in an immunoprivileged site, and suppression of cytotoxic T lymphocytes (CTLs) by immunosuppressive factors expressed on the tumour cell surface (e.g. apoptotic ligands) or secreted by the tumour cells (e.g. interleukin 10 (IL-10), transforming growth factor β (TGF-β)) [110]. The rationale underlying immunogene therapy is to enhance either tumour immunogenicity or the antitumour effector capability of T cells to overcome the tolerance of the immune system.

The first approach can be achieved by transduction of tumour cells or antigen-presenting cells (APCs) such as dendritic cells with cytokine genes, costimulatory molecules, strong immunogenic tumor rejection antigens or foreign MHC molecules. This can be accomplished either by *ex vivo* transduction of explanted tumor cells for use

as cell-based cancer vaccines, or by *in vivo* transduction of tumour cells or APCs to achieve a vaccine effect. In the second approach, immune effector cells can be retargeted by transduction of T cells with chimaeric antigen receptors (CARs) or human leukocyte antigen (HLA)-restricted αβ heterodimeric T-cell receptors (TCRs). Both strategies aim at immune-mediated destruction of the tumour [110, 111, 112, 113, 114].

2.3. Anti-angiogenic cancer gene therapy

Tumor growth is dependent on angiogenesis as it supplies the tumor tissue with oxygen and other factors required for its survival and growth. The degree of vascularisation of a tumor has been associated with its aggressiveness [115, 116, 117]. Tumour angiogenesis is driven by the proliferation and migration of vascular endothelial cells (VECs), which are therefore important targets in cancer therapy. VECs are stimulated by pro-angiogenic proteins such as vascular endothelial growth factor (VEGF), basic fibroblast growth factor (bFGF) and platelet-derived endothelial growth factor-β (PDGF-β). These proteins are synthesised by tumor cells, endothelial cells or both. VEGF in particular is highly expressed in many different tumor cells and has been correlated with tumor growth, invasion and metastasis [118, 119].

In cancer therapy, there are three different strategies to disrupt tumour vessel growth. In the first, direct, strategy, endothelial cells are directly targeted to block proliferation or migration or to induce apoptosis. The second strategy is to attack tumor-associated endothelial cells indirectly by blocking the expression or activity of tumor proteins that stimulate angiogenesis. This can be achieved by neutralising pro-angiogenic proteins in the microcirculation, by preventing their binding to their cognate receptors or by blocking signal transduction by targeting the intracellular domains of receptor tyrosine

kinases. For example, the inhibition of epidermal growth factor receptor (EGFR) blocks the synthesis of VEGF, bFGF and TGF-α. A third strategy is the inhibition of multiple signal transduction pathways on both the tumor-associated endothelial cells and the tumor cells. These various anti-angiogenic approaches can be used in combination [120]. The requirements vectors must fulfill for anti-angiogenic gene therapy approaches are demanding. Since the route of administration has to be systemic, vectors have to be stable *in vivo*. Also, they have to provide stable transgene expression since tumors can reoccur as soon as inhibition of tumor angiogenesis is stopped. Although no toxic side effects have been observed up to now, there are still concerns about the effect of angiogenesis inhibition on physiologic angiogenesis.

2.4. Cytoreductive cancer gene therapy

Cytoreductive cancer gene therapy is used to reduce the number of tumor cells by transducing them with a therapeutic gene encoding a cytotoxic protein or a prodrug-sensitizing protein [109]. In order to succeed with this approach, vectors require *in vivo* stability, high transduction efficiency and their trangene expression needs to be targeted in order to protect non-malignant tissue, either through transcriptional control using a tumour-specific promoter or transductional targeting [121, 122].

2.5. HSC transduction with drug-resistance genes

One of the limiting factors in chemotherapy of malignancy is myelosuppression [123]. Autologous stem cell transplantation is therefore a widely used method to facilitate high-dose chemotherapies. However, as the transplant is harvested before the therapy, the possibility of contamination of the transplant with tumor cells remains. As an alternative to this procedure, transduction of HSCs with a drug-resistance gene makes

these stem cells, as well as their offspring, more resistant to the cytotoxic effect of the chemotherapeutic agent, allowing the administration of higher doses of chemotherapy, which in turn increases the likelihood of a curative therapy of the malignancy [109]. The most widely used multidrug-resistance gene is the gene encoding MDR1. Other examples of genes having a protective potential against chemotherapeutic drugs are those encoding dihydrofolate reductase (DHFR), O^6-methylguanine-DNA methyltransferase (MGMT), aldehyde dehydrogenase (ALDH), glutathione-S-transferase (GST), cytidine deaminase (CDD) and dihydropyrimidine dehydrogenase (DPD) [124]. The major requirement for the transduction of drug-resistance genes is the restriction of their expression to HSCs, because transduction of even a small number of tumor cells with drug-resistance genes would render them resistant to chemotherapy. HSCs can be collected from bone marrow, peripheral blood or umbilical cord blood, and selective transduction can be achieved *ex vivo* by transduction of the HSCs after CD34 selection and stimulation with growth factors [109, 125, 126]. For direct *in vivo* gene transfer, the vectors would have to be targeted against proteins such as CD34 and c-kit, both of which are human haematopoetic progenitor cell-surface markers [127, 128, 128].

3. Parvoviridae

3.1. Introduction

The family parvoviridae is subdivided into the subfamily parvovirinae (which use vertebrate hosts) and the subfamily densovirinae (using arthropod hosts). The subfamily parvovirinae includes three genera: parvovirus, erythrovirus and dependovirus (Table 6). Members of the genus parvovirus are characterised by their oncotropism and oncosuppression, and their ability to mediate long-term gene expression. Together with their human apathogenicity, these characteristics make parvoviruses highly interesting vector systems for cancer gene therapy. The following section will focus on the autonomously replicating parvoviruses (ARP).

Genus	Virus[b]
Parvovirus (PV)	**H1** **LuIII** **MVM** (minute virus of mice) CPV (canine parvovirus) FPV (feline parvovirus)
Erythrovirus	**B19**
Dependovirus	**AAV** (Adeno-associated virus) serotypes 1–8

Table 6. The parvovirinae subfamily. Viruses of the parvovirinae subfamily that are commonly used for gene therapy are shown in bold.

3.2. Parvoviridae biology

3.2.1. Structure

Parvoviridae are are among the smallest known viruses. They are icosahedral, nonenveloped viruses with a diameter of 18–26 nm and a molecular mass of 5.5–6.2 x 10^6 Da [129]. Virions consist to 50% of protein and 50% DNA [130]. The capsid is formed

by three capsid proteins VP1, VP2 and VP3 – 90% of the capsid is formed by VP3, 5% by VP1 and 5% by VP2 – and encapsidates a single-stranded DNA molecule.

3.2.2. Genome

The ARP genome has a size of approximately 5.1 kb. It consists of single-stranded, linear DNA of negative polarity. At both termini, it has palindromic sequences that serve as self-priming origins of replication (Fig. 3) [131, 132]. For the genus parvovirus, these inverted repeats at the left and right end are unique and form Y-shaped and T-shaped hairpin loops, respectively. In the MVM genome, the 3'-palindrome is approximately 115 nucleotides and the 5'-palindrome 207 nucleotides in length. These termini contain the *cis*-acting elements required for replication [133]. Additional sequences essential for efficient MVM replication include two regions inboard of the right palindrome called element A and B. Within the genome there are two overlapping open reading frames (ORFs) coding for the nonstructural and structural viral proteins. Expression of these proteins is regulated by two parvoviral promoters: the P4 promoter and the P38 promoter. [134, 135, 136, 137, 138]. Expression of the nonstructural proteins (NS1 and 2) is under the control of the P4 promoter. This promoter is induced at the G1–S-phase transition and stimulated by oncoproteins [139]. The P38 promoter is trans-activated by the NS1 protein and regulates transcription of the capsid-coding genes (VP1 and VP2) [140, 141, 142, 143]. VP1 and VP2 are derived from alternatively spliced mRNA transcripts. VP3 is synthesized by proteolytic cleavage of approximately 25 N-terminal amino acids of VP2, a process only observed in DNA-containing virions [144]. Unique regions in VP1 contain phospholipase A activity and nuclear localization signals [130]. NS1 is an 83 kDa phosphoprotein that has helicase, ATPase, DNA-nicking and sequence-specific DNA-binding activities. It is therefore a multifunctional protein

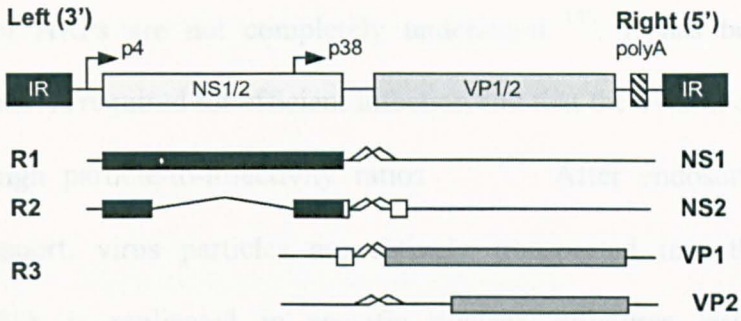

Figure 3 Genome organisation of autonomously replicating parvovirus (ARP). The 5.1 kb single-stranded linear DNA genome has inverted repeat (IR) sequences at the termini that serve as self-priming origins of replication. There are two open-reading frames, coding for the structural (VP1 and VP2) and nonstructural (NS1 and NS2) proteins. Transcription is regulated by the promoters P4 and P38. The transcripts R1–3 and their corresponding parvoviral proteins are indicated below the schematic figure of the genome.

essential for viral replication and promoter transactivation [145, 146, 147, 148, 149, 150, 151, 152, 153]. It is also considered the major mediator of cytotoxicity [154]. NS2 is a 22 kDa protein that is essential for replication, virus production, nuclear egress of progeny virions and host-specific infection [155-160]. In addition, NS2 enhances NS1-mediated cytotoxicity [161, 162].

3.2.3. Life cycle

The life cycle of the parvoviridae starts with receptor-mediated binding of the virus to the cell surface. Although not yet completely characterised, the receptor for binding of MVM (minute virus of mice) and H1 is known to contain *N*-acetylneuraminic acid (sialyl)-containing glycoproteins [132]. For the erythrovirus B19, erythrocyte P antigen has been identified as a binding receptor and $\alpha5\beta1$ integrin as a cellular coreceptor [163-165]. Recently, the differential use of the transferrin receptor (TfR) as a binding receptor for canine parvovirus (CPV) and feline parvovirus (FPV) has been shown [166-169]. Following cellular receptor binding, viral particles are internalized via receptor–mediated

endocytosis. Endosomal trafficking and escape, uncoating and nuclear entry mechanisms of ARPs are not completely understood [170]. It has been shown that endosomal transit is required for efficient infection and that the overall efficiency is low resulting in high particle-to-infectivity ratios [171, 172]. After endosomal release and cytosolic transport, virus particles are actively transported into the nucleus [130]. Parvoviral DNA is replicated in specific nuclear structures termed autonomos parvovirus-associated replication bodies [173, 174]. ARP are not integrated into the host genome [175]. Parvoviral replication follows the "rolling hairpin model" and strictly depends on S-phase specific cellular factors [174, 176]. Parvoviral DNA replication starts with synthesis of a complementary strand converting its single-stranded genome into a double-stranded monomer replicative form (mRF) [132]. This initial conversion is independent from viral proteins, but requires cellular cyclin A that is induced at the G1/S-transition. Cyclin A induction results in polymerase-δ mediated complementary DNA synthesis starting from the self-primed, palindromic parvoviral 3'-terminus [173, 174]. The right hand hairpin is nicked by NS1 at a nicking site 18 bp downstream of the original 5'terminus followed by new formation of two hairpins. The newly formed 3'-terminus serves as primer for repair DNA synthesis extending through both strands of the mRF resulting in formation of di- and multimeric, double-stranded replicative forms (dRF). Both termini of this replication intermediate consist of the original 5'-terminus while the original left terminus is located in the middle forming the so called dimer bridge. The dimer bridge is asymmetrically resolved through single-strand nicking reactions followed by displacement syntheses and religations resulting in the formation of new replication intermediates which serve as templates for further replication, gene expression and single-strand DNA [129, 130, 132]. Cytosolic synthesized capsid proteins are transported into the nucleus where they undergo assembly followed by NS1-dependent

incorporation of single-stranded parvoviral DNA. Using VP2 as a nuclear export signal, virions are transported from the nucleus into the cytosol followed by cellular release, a process frequently leading to cell death [130].

3.3. Infectivity, pathogenicity and oncosuppression

Viruses of the parvovirinae subfamily have the ability to infect a variety of different vertebrates. Although the natural hosts of parvovirus H1, MVM and LuIII are rodents, they also have the ability to infect human cells [129]. However, ARPs are not pathogenic in humans. Although viraemia after human exposure to H1 has been described, B19 (of the erythrovirus genus) is the only virus of the parvovirinae subfamily known to cause human diseases, which include erythema infectiosum, hydrops fetalis, transient aplastic anaemia, myocarditis, hepatitis, arthritis, vasculitis and neurological disorders [177].

In the context of cancer, ARPs have special characteristics. They were first isolated from human tumour tissue and for that reason were believed to be oncogenic [178]. It was then observed that ARPs possess an oncosuppressive potential, inhibiting the formation of spontaneous and chemically or virally induced tumours *in vivo* and *in vitro* [179, 180, 178, 181, 182, 183, 184, 185, 186, 185, 187]. Oncogenic transformation of several human and rodent cells resulted in an enhanced capacity for parvoviral DNA amplification and gene expression, and correlated with significantly increased susceptibility towards the parvoviral cytotoxicity [188, 189, 190]. It has been shown that oncogenic transformation of cells resulted in P4 promoter activation [139, 191, 192]. A precondition for parvoviral cytotoxicity is cell proliferation. Parvovirus P4 promoter activation and replication is S-phase dependent [174, 193, 176]. Several oncoproteins have been shown to contribute to the activation of the P4 promoter during its stimulation at the G1/S-phase transition

resulting in NS1-production high enough to initiate viral replication [139, 174, 176, 191-193]. The exact mechanism of parvoviral tumour suppression is not completely understood but is thought to involve several factors, with the NS1 protein as the major mediator of parvoviral cytotoxicity [194, 195, 196, 197]. Depending on the cell line, the mechanism of parvovirus-mediated cytotoxicity is either apoptosis or necrosis [198, 199, 200].

3.4. Tissue targeting with parvovirinae vectors

In order to prevent damage to non-malignant tissue, the specificity of a therapeutic agent for tumor cells is of high importance, particularly when the vector is to be used systemically. Unfortunately, the therapeutic index of most existing vectors is low [201], and the undesired transduction of non-malignant tissue can result in damage and cell death. Specificity of a gene therapy vector can be achieved by transductional or transcriptional targeting [201, 202]. Transductional targeting describes the selective uptake of the vector into the cells of interest, where the transgene is transcribed. Depending on the gene therapy strategy, this can be tumor cells, endothelial cells of tumor vasculature or other target cells. Selective uptake can be achieved by various strategies, such as modification of the viral capsid or pseudotyping of viruses. In transcriptional targeting, the vector might be taken up by many different cell types but is only transcribed in the target cells. In this approach, selective expression of the transgene is achieved by replacement of the natural promoter or by modification of the transcription factor binding sites within a promoter. There are promoters based on aberrant tumour biology (e.g. promoter induction by telomerase), tissue-specific expression (e.g. promoter induction by tyrosinase for cell type-specific expression in melanomas) and externally inducible promoters (e.g. heat shock protein 70). Transductional re-targeting of ARPs

has been reported for feline parvovirus (FPV), a parvovirus that normally infects feline cells, with the aim of modifying it to target human tumor cells for cancer gene therapy. Although modification of the FPV capsid to bind αv integrins enabled transduction of a human rhabdomyosarcoma cell line, other human tumor cell lines expressing αv integrins were not transduced [203]. Thus, other factors are likely to be required.

Transcriptional targeting of ARPs has the advantage that the vectors are already oncoselective, as explained above. Transcriptional targeting of ARPs has been used to achieve cell-type specific transgene expression of the parvovirus LuIII: recombinant LuIII vectors expressing the luciferase marker gene under the control of a chimaeric promoter containing a liver-specific enhancer directed the preferential expression of the luciferase marker in transduced human hepatoma cells [121, 204]. In another approach, targeted hybrid H-1/MVM parvovirus vectors were used. Transcription factor binding sites for the heterodimeric β-catenin/Tcf transcription factor were inserted in the P4 promoter. Activation of the wnt signaling pathway results in activation of promoters containing Tcf binding sites. The wnt signaling pathway is constitutively activated in colon carcinoma so that this system was used to target specifically colon carcinoma. The authors observed NS1 expression and viral burst size similar to wild-type levels in colon carcinoma cell lines but a 1000-fold reduction of viral burst size in wnt-inactive cell lines [205].

3.5. Parvovirinae in cancer gene therapy

The aim of cancer gene therapy is the transduction of a specific cell population with a specific gene in order to destroy the tumor, or to protect noncancerous cells and thereby enable high-dose chemotherapy. Due to their oncoselectivity and human apathogenicity,

ARPs are highly suitable vectors for selective infection of tumor cells and have been used especially for immuno- and cytoreductive gene therapy.

3.5.1. Immunogene therapy

Unmodified parvoviridae (MVM, H-1) are not able to induce significant cytokine production [interferon (IFN), tumour necrosis factor α (TNF-α), IL-6] either in rodent or human cells [206]. However, induction of heat shock protein release after H1 infection has been reported [207]. Heat shock proteins are intracellular molecules that are released in necrotic but not apoptotic cell death; their antigenic peptides are chaperoned into APCs and induce an immune response after presentation to CTLs [208]. Enhancement of the immune-mediated parvoviral antitumor effect can be achieved by transduction of tumour cells or APCs with specific transgenes. Both *ex vivo* and *in vivo* transduction approaches have been used.

3.5.1.1. Ex vivo transduction

In *ex vivo* transduction, tumor cells are explanted, transduced with the therapeutic gene and readministered to provoke a host immune response. The vector must be capable of mediating relatively short-term gene expression in the explanted tumor cell, a requirement fulfilled by ARPs.

Cytokines such as IL-2, IL-12 and granulocyte–macrophage–colony-stimulating factor (GM-CSF) have shown their antitumor potential in different models [209, 210, 211, 212, 213, 214, 215, 216, 217]. IL-2 and IL-12 mediate their antineoplastic potential mainly by activation and expansion of tumor-specific T cells and the activation of the cytotoxic activity of natural killer (NK) cells. In addition, they are able to stimulate IFN-γ production, induce the differentiation of T helper type 1 (Th1) cells and activate lymphokine-activated

killer cells (LAKs) [212, 217]. GM-CSF stimulates $CD11c^+$ dendritic cells type 1 (DC1), resulting in an enhancement of antigen processing and presentation [110]. The use of ARP vectors (MVM, H-1) resulted in high, although not stable, IL-2 levels after transduction of transformed cells [218, 219], and *in vivo* experiments showed up to 90% tumor reduction of human cervical carcinoma (HeLa) xenografts [219]. In a subcutaneous melanoma xenografts model, tumor growth was inhibited by infection with an IL-2 expressing MVM vector prior to implantation; animals were also partially protected against re-challenge with uninfected tumor cells [220].

Another widely used family of proteins for cancer gene therapy are the monocyte chemotactic proteins (MCP), which belong to the chemokine family. MCP-1 mostly recruits monocyte/macrophages; MCP-3 exerts its effect on a broader variety of cells including monocytes, T cells, basophils, eosinophils, neutrophils, granulocytes, NK cells and DCs [221, 222, 223, 224, 225, 226, 227, 228]. Transduction of tumor cells with MCPs has been shown to have a tumor-suppressive effect. The observation that endogenous MCP-1 is absent in human cervical carcinoma cell lines made it a therapeutic transgene of interest for cancer gene therapy [229, 230]. Recombinant parvoviruses H1 and MVM carrying a transgene encoding for MCP-3, were able to delay tumor growth in subcutaneous cervical cancer and melanoma xenograft mouse models; however, a complete tumor suppression could not be achieved [231, 232].

Another popular approach to enhance tumor immunogenicity is transduction with costimulatory molecules, resulting in an induction of an antitumour CTL response. CD80 (B7.1) and CD86 (B7.2) stimulate CD28, which is expressed on the T-cell surface; the costimulation of CD28 and the TCR leads to expansion of $CD8^+$ CTLs. Expression of B7 proteins in tumors has been shown to increase antitumor immune responses, resulting in rejection, and even protection against tumors not expressing B7

proteins [233, 234, 235, 236, 237]. MVM has been used *in vitro* for this approach. Recombinant MVM coding for CD80 or CD86 resulted in tumor cell-specific expression of these proteins. However, their tumorsuppressive potential was not evaluated [238].

3.5.1.2. In vivo transduction

The requirements a vector must fulfil for *in vivo* transduction are more demanding compared with the *ex vivo* approach. The vector should be transductionally or transcriptionally targeted to the tumor. In addition, it has to be sufficiently stable *in vivo* to tolerate systemic administration, although direct intratumoral delivery is also possible. MVMp has been used for *in vivo* transduction of metastatic haemangiosarcoma with interferon-inducible protein 10 (IP-10) with very promising results; a significant slowing of recurring haemangiosarcoma growth and metastasis suppression was observed in immunocompetent mice, as well as survival up to 6 months in a third of the animals [239]. IP-10 is a chemokine with previously demonstrated antitumor potential, which is thought to be mediated by antiangiogenic factors as well as immune stimulation [240, 241].

3.5.3. Cytoreductive cancer gene therapy

Cytoreductive cancer gene therapy is used to reduce the number of tumor cells by transducing them with a therapeutic gene encoding a cytotoxic protein or a prodrug-sensitizing protein [109]. To achieve this, a vector requires *in vivo* stability, high transduction efficiency and the ability to target, either by transcriptional control using a tumor-specific promoter or transductional targeting, to avoid damage to normal tissue [121, 122].

ARPs are characterised by their oncotropism and oncosuppressive potential and provide high-level transgene expression. These characteristics make them promising vectors for cytoreductive cancer gene therapy. In general, the parvoviral cytotoxicity is not sufficiently potent to achieve 100% tumor regression. The resistance of some tumor cells to parvoviral cytotoxicity is thought to be in part correlated to the p53 status of the cell, as wild-type p53 cells are less susceptible to parvoviral cytotoxicity [200, 242]. One approach to overcome this problem of tumor cell resistance towards parvoviral cytotoxicity is through the use of cytotoxic transgenes. This can be achieved by either replacing the capsid-coding region with a therapeutic transgene or by replacing the complete parvoviral coding region with a different expression cassette flanked by parvoviral palindromic sequences. Great efforts have been made to modulate the parvoviral genome to enhance its cytotoxicity and two transgenes that have been used are apoptin and HSV-TK.

Apoptin is a 13.8 kDa protein encoded by the chicken anaemia virus [243]. It induces apoptosis in tumor cells in a p53-independent manner. Apoptin-induced apoptosis is mediated by the caspase-signalling pathway. Interestingly, apoptin does not harm untransformed cells most probably owing to a cytosolic localisation in contrast to its nuclear localisation in transformed cells. Its antitumoral potential has been shown in different tumor models [244, 245, 246, 247, 248]. The susceptibility of H1-resistant tumor cell lines was increased by infection with the recombinant hH1–apoptin resulting in up to three-fold higher cytotoxicity than with parvovirus hH1–GFP infection. It remains to be determined if this effect can also be achieved *in vivo* [249].

In *in vitro* tumor models of melanoma, breast cancer and glioma, HSV-TK was tested as a therapeutic transgene cloned in MVMp [250]. Infection of these tumor cell lines with the recombinant MVMp–HSV-TK followed by the addition of ganciclovir resulted in up to

95% cell killing dependent on the tumor type. Ganciclovir-independent MVM-mediated cytotoxicity was 30–65%.

3.6. Summary

Parvoviridae are highly promising vectors for gene therapy of cancer. ARPs are appealing vectors for cytoreductive gene therapy as well as immunogene therapy approaches to target tumor cells. They have the advantage of being oncotropic, oncosuppressive, human apathogenic and providing high-level transgene expression.

A disadvantage of ARPs is the limitation of transgene size owing to inefficient encapsidation beyond a size limit of 106% of the wild-type genome size [133, 251].

In summary, parvoviridae have highly advantageous characeristics as cancer gene therapy vectors. However, their efficacy is limited by their genomic size restriction and immunogenicity.

4. Measles virus

4.1. Introduction

In the 1970's, several cases of temporary tumor regression were observed in hematologic malignancies during wild type measles virus infection [252-254]. However, a systemic approach of using measles virus for cancer virotherapy was not pursued until 2001 [107, 255]. Measles virus was first isolated by Enders and Peebles in 1954 from a throat swap of David Edmonston, an 11 year old child suffering from measles. Adaptation of the isolated Edmonston strain of measles virus to chick embryos with subsequent serial passaging in chick embryo fibroblasts resulted in the Edmonston B strain of measles virus [256, 257]. Further passaging of the Edmonston or the Edmonston B strain of measles virus in different cell culture systems generated a variety of other attenuated measles virus vaccine strains (e.g. Schwarz strain, Moraten strain, Edmonston-Zagreb strain) [258-261]. Adverse effects of measles vaccine are rare and include expected effects such as fever (5%), rash (1.6%) and conjunctivitis (2.1%), as well as rare unexpected events as anaphylaxis, thought to be secondary to gelatin [262]. One of the premises for the generation of engineered measles viruses was the first successful rescue of measles virus from an infectious molecular clone of the attenuated Edmonston B strain [263]. The resulting infectious virus was named Edmonston tag strain and will be referred to as MV-Edm [263]. Based upon this viral strain, a variety of recombinant measles viruses have been generated with additional functions including enhanced cytotoxicity, the potential for noninvasive monitoring and retargeted viruses. The advances and applications of recombinant measles virus vectors will be discussed in the following sections.

4.2. Measles Virus biology

4.2.1. Genome and structure

Measles virus (MV) is an enveloped, negative strand RNA-virus belonging to the family *Paramyxoviridae*, genus *Morbillivirus* and order *Mononegavirales*. Its virions are characterized by their pleomorphic structure with a diameter of 120 to >300 nm and their capacity for polyploidy [264]. The envelope carrries protrusions formed by the fusion glycoprotein and the viral transmembrane hemagglutinine. Measles virus has a nonsegmented RNA genome of negative polarity, which is 15,894 nucleotides in size (Fig. 4). The genome is encapsidated by a helical array of nucleocapsid proteins and encodes six structural and two non-structural proteins: nucleocapsid protein (N), viral RNA-polymerase (L), phosphoprotein (P), matrix protein (M), haemagglutinin protein (H) and fusion protein (F). Two non-structural proteins, C and V, are encoded by the P-cistron [265, 266]. The relative position of genes in relation to the 3'-end is negatively correlated with their level of protein transcription [267]. The viral genome is encapsidated by nucleocapsid and associated with polymerase and its cofactor phosphoprotein forming the ribonucleoprotein complex. The ribonucleoprotein complex is surrounded by matrix proteins, located beneath the viral envelope, and interacts with the cytoplasmic domains of haemagglutinin and fusion proteins [268] (Fig. 5). Measles virus infection begins with its binding to its cellular receptors CD46 and SLAM, which are discussed in more detail below. H-protein is a type II transmembrane glycoprotein responsible for the interaction of measles virus with its cellular target receptors. The type I glycoprotein F mediates membrane fusion [269, 270]. Both glycoproteins are required for effective fusion [271]. Receptor binding of the H-protein induces conformational changes in the F-protein resulting in insertion of hydrophobic fusion domains into the

target cell membrane and approximation of the two membranes facilitating membrane fusion [272, 273]. Subsequently, the ribonuclein complex is released into the cytoplasm where transcription of viral mRNA is initiated. Rescue of recombinant measles virus vectors is facilitated by the reverse genetics system and has first been described for measles virus

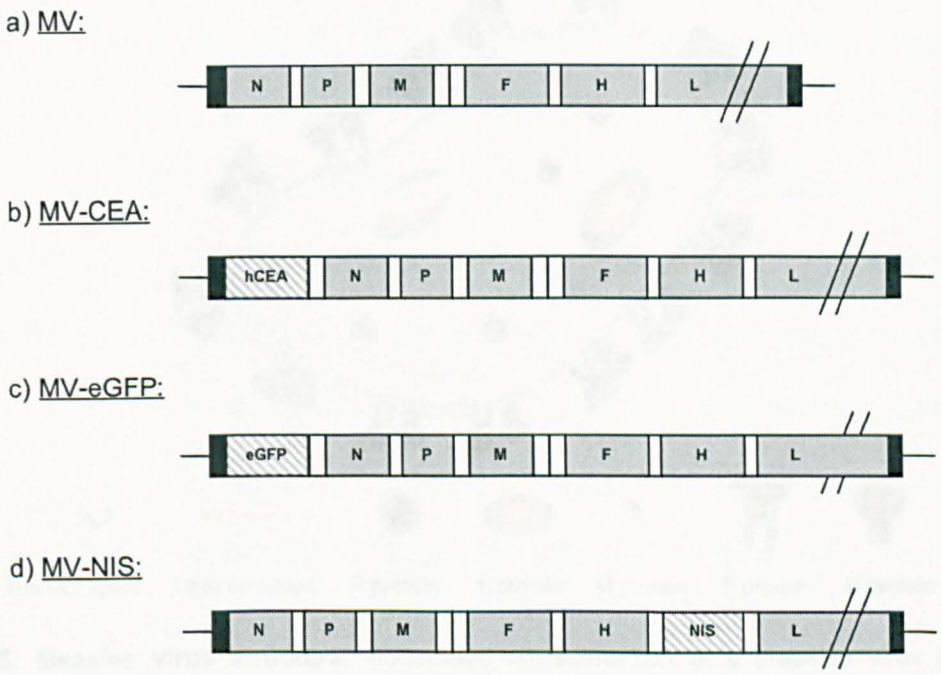

Figure 4 Measles virus genome. Schematic representation of the genome of unmodified and recombinant MV-Edm constructs. Viral proteins and their relative positions within the genome are indicated by gray boxes, intergenic regions by white boxes and transgenes by shaded boxes. Viral proteins include nucleoprotein (N), phosphoprotein (P), matrix protein (M), fusion protein (F), hemagglutinin protein (H), polymerase (L). Two additional proteins C and V protein are encoded on the P cistron. a) wildtype MV-Edm, b) recombinant MV-Edm coding for carcinoembryonic antigen (hCEA), c) recombinant MV-Edm encoding enhanced green fluorescent protein (eGFP), d) recombinant MV-Edm encoding the human sodium iodide symporter (hNIS).

by Radecke et al. [263]. This rescue system uses a stably transfected cell line expressing measles virus N- and P-protein, as well as the T7-polymerase. These helper cells are co-transfected with plasmids encoding measles virus polymerase (L-protein) and the full-

length measles virus antigenome regulated by a T7-promoter. Successful rescue of infectious measles virus was shown. The successful establishment of this system allowed genetic modification of measles virus.

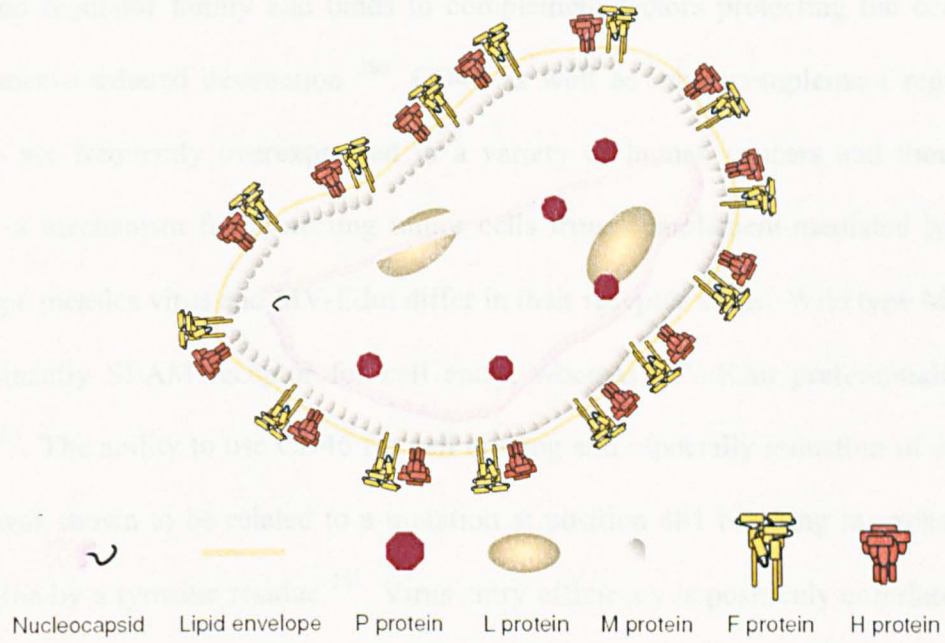

Figure 5: Measles virus structure. Schematic representation of a measles virus particle. Within the particle is the genome, which is encapsidated by the nucleoprotein and associated with the viral polymerase complex consisting of the polymerase (L) and its cofactor phosphoprotein (P). The resulting complex forms the ribonucleoprotein complex which is linked to the envelope by the matrix protein. The two viral glycoproteins hemagglutinin protein (H) and fusion (F) project from the envelope are essential for viral attachment and fusion as described in the text.

4.3. Tumor selectivity

Measles virus tropism is substantially determined by its receptor usage. Two receptors have been identified for measles viruses binding: CD46 and SLAM [274-276]. However, infection in the absence of these receptors has been observed, indicating the possibility of a third receptor [277-279]. Signaling lymphocyte activation molecule (SLAM, CD150) is

a 70 kDa transmembrane glycoprotein expressed on activated T- and B-cells, memory lymphocytes, dendritic cells and immature thymocytes [280]. It is involved in T-cell activation, induction of T-cell proliferation and Th1 cytokine-production [281]. CD46 (MCP, membrane cofactor protein) is a 57-67 kDa transmembrane glycoprotein ubiquitously expressed on all nucleated human cells. It belongs to the complement activation regulator family and binds to complement factors protecting the cell from complement-mediated destruction [280]. CD46 as well as other complement regulatory proteins are frequently overexpressed in a variety of human cancers and thought to provide a mechanism for protecting tumor cells from complement-mediated lysis [282]. Wild type measles virus and MV-Edm differ in their receptor usage. Wild type MV uses predominantly SLAM receptor for cell entry, whereas MV-Edm preferentially uses CD46 [283]. The ability to use CD46 for cell binding and especially induction of cell-cell fusion was shown to be related to a mutation at position 481 resulting in exchange of asparagine by a tyrosine residue [283]. Virus entry efficiency is positively correlated with increasing CD46 density. In the absence of syncytia formation, viral gene expression after MV-Edm infection was comparable in normal cells and their transformed counterparts despite differences in CD46 density. However, for efficient induction of syncytia formation and cytotoxicity, a "threshold" receptor density was required [284, 285]. In addition, syncytia formation resulted in an at least 5-fold amplification of viral gene expression [284]. The positive correlation between extent of cytopathic effect and CD46 receptor density was confirmed in primary human multiple myeloma cells [286].

Additional factors contributing to MV-Edm tumor selectivity are likely. Defects of intracellular innate immune response pathways in tumor cells allow efficient propagation of RNA viruses in these cells but not in untransformed cells. Wild type measles virus has the ability to inactivate these pathways in normal cells. In contrast,

MV-Edm has lost this ability due to mutations in the V protein. This might help to explain why MV-Edm propagates efficiently in transformed but not in untransformed cells. These pathways will be discussed in more detail in the following section.

4.4. Measles virus and the immune system

The interactions between measles virus and the immune system have two major aspects: the effect of measles virus on the host and the host's immune response against the virus. Wild type measles virus infection is associated with immunosuppression to non-MV antigens. Characteristic findings include suppression of delayed-type hypersensitivity reactions and marked lymphopenia affecting mainly the T-cell population. Cellular and humoral responses to new antigens are impaired. These changes can last from several weeks to months and increase significantly the host's susceptibility to secondary infections. The mechanisms of measles induced immunosuppression include functional abnormalities of immune cells as well as suppression of cytokine synthesis [287, 288].

The other aspect is the antiviral immune defense. During the prodromal phase of the disease, the early innate immune response is induced followed by the adaptive immune response with MV-specific humoral as well as cellular responses [287]. Due to widespread measles vaccination, average titers of measles antibodies in healthy humans are 100 $\pm$ 59.2 EU/ml and serum titers of >20 EU/ml are considered measles immune [289]. In addition, intracellular antiviral response mechanisms are induced inhibiting viral replication and protein synthesis as discussed below. The sum of these antiviral mechanisms is highly efficient in virus elimination and thereby a major barrier to successful measles virotherapy.

4.4.1. Circumventing antiviral antibodies

In order to circumvent these barriers and enhance transduction efficiencies of MV-Edm therapy, different delivery strategies have been evaluated. One of the first strategies was the use of MV-Edm infected cells as delivery system [290, 291]. There is a strong rationale for this approach since measles virus naturally disseminates via the bloodstream inside infected monocytes or T cells, not as cell free virus. Also, passive serotherapy with measles hyperimmune serum is ineffective when given more than one week after initial exposure to the virus (i.e. before the virus disseminates via the bloodstream) proving that antibodies cannot prevent the cell-associated virus from trafficking to distant sites. The feasibility of this approach was shown *in vitro* using different cells as transport cells including the monocytic cell-line U-937, the endothelial cell line OEC, PBMCs and human T-cells [290, 291]. Even in the presence of highly neutralizing anti-measles human serum, these infected carrier cells were able to fuse with cancer cells – a process referred to as heterofusion - and transfer successfully measles infectivity to lymphoma, multiple myeloma or ovarian cancer cells. *In vivo*, the feasibility of this approach was shown in different tumor models. In intraperitoneal xenograft models of multiple myeloma, ovarian and hepatocellular carcinoma, as well as in a disseminated lymphoma model, successful heterofusion and infection was shown after intraperitoneal treatment with MV-preinfected OEC or U-937 cells. The therapeutic efficacy was shown in an intraperitoneal ovarian cancer xenograft model in mice, in which tumor regression was achieved in more than half of the animals after treatment with only a single intraperitoneal dose of 1 x 10^6 MV-GFP-preinfected U-937 cells. Successful tumor infection was also achieved in mice passively immunized with human anti measles virus antibodies [291]. Data from these studies show the general feasibility of cell delivery systems for measles virus treatment in the presence of an immune response.

4.4.2. Combating innate immunity

The intracellular innate immune response system has also been targeted in order to enhance MV efficacy [285]. Virus infection results in activation of transcription factors that regulate immediate early genes including type I interferons (IFN-α/β) and other antiviral cytokines. IFN-α/β activate interferon regulated transcription factors through JAK/STAT-signaling pathways resulting in expression of antiviral proteins which inhibit viral replication and expression [292, 293]. Wild type measles virus as well as several other viruses have developed mechanisms inhibiting the type I interferon response pathways [292]. Paramyxovirus-induced IFN-response inhibition is mediated by P, V and C proteins [294]. Measles virus P, V and C proteins have been shown to inhibit IFN-induced STAT activation and nuclear translocation [295-298]. In contrast to wild type measles virus, MV-Edm was shown to be impaired in its ability to block the IFN-response due to P/V protein Y110H and V protein C272R mutations [298, 299].

In tumor cells, it has been reported that these intracellular antiviral response pathways are defective [300]. However, it was shown *in vitro* that primary ovarian cancer as well as myeloma cells produce significant amounts of IFN-α and IFN-β following MV-Edm infection [285]. Pretreatment of these cells with IFN-α or IFN-β followed by infection with a CEA-expressing recombinant MV-Edm resulted in up to 50-fold reduction of transgene protein expression and an up to two logs lower virus progeny production. In order to enhance MV-Edm efficacy, recombinant MV-Edm were generated expressing the unmutated wild type P-protein (MV-GFP-Pwt). Maximum titers and cytotoxicity of MV-GFP-Pwt were similar to MV-GFP. However, IFN-α/β induction was significantly lower and virus growth kinetics of the chimeric measles virus faster than MV-GFP. *In*

vivo comparison of MV-GFP with MV-GFP-Pwt in a human myeloma xenograft model in mice showed increased potency and accelerated tumor suppression with wildtype P-expressing measles virus.

4.4.3. Boosting antitumor immunity

The immune system may also have a supportive role in measles virus mediated oncolysis. Polymorphonuclear neutrophils have been described to mediate tumor destruction by direct tumor cell destruction as well as cytokine and chemokine mediated activation of reactive cells and inhibition of angiogenesis [301]. Intratumoral treatment with UV-inactivated MV, an active MV or a recombinant MV expressing murine granulocyte macrophage colony-stimulating factor (mGM-CSF) were compared in human CD46 transgenic, IFN-α/β receptor knockout mice (Ifnar^{tm}-CD46Ge) bearing subcutaneous lymphoma xenografts [302]. Intratumoral accumulation of neutrophils was observed in mice treated with the active viruses but not in inactivated virus-treated ones. In parallel, the rate of tumor regression was positively correlated with the percentage of intratumoral neutrophil infiltration. The data of this study indicate that measles virus replication stimulates intratumoral infiltration with neutrophils causing an enhancement of MV-mediated oncolysis.

4.5. MV-Edm as a viral vector for cancer gene therapy

In 1971, a case of transient tumor regression in a patient with Burkitt lymphoma was reported; an observation potentially explained by the ability of wild type measles virus to propagate in EBV transformed cells [252]. However, wild type measles virus fails to propagate in other (SLAM-negative) transformed cell lines, e.g. human sarcomas or

epithelial malignancies [300]. In contrast, MV-Edm has been shown to be oncolytic in a variety of different human tumor models *in vitro* as well as *in vivo* [107, 255, 303, 304]. The basis for the wide oncolytic potential of MV-Edm is thought to be its preferential use of CD46 and the overexpression of this receptor on transformed cells compared to their non-transformed counterparts as discussed above [284]. Infection of transformed cells by MV-Edm results in syncytia formation. The recruitment of surrounding cells into syncytia causes an enhancement of the cytotoxic effect through a bystander effect. Syncytia formation is followed by cell death through apoptosis or a bioenergetic form of cell death with necrosis [303, 305, 306].

The following section will give an overview of different human malignancies in which the oncolytic potential of MV-Edm was evaluated. A summary of preclinical studies evaluating the therapeutic potential of MV-Edm is provided in table 7.

4.5.1. MV-Edm for hematologic malignancies

B-cell Non-Hodkin lymphoma. MV-Edm was evaluated for its therapeutic potential for B-cell Non-Hodgkin lymphoma (NHL) [255]. Infection with MV-Edm or a β-galactosidase expressing recombinant MV-Edm (MV-lacZ) at a MOI as low as 0.001 resulted in efficient MV-Edm amplification, multinucleated giant cell formation of the suspension cells and cytotoxicity. The tumor suppressive effect was confirmed in mice bearing established tumors. Intratumoral treatment resulted in complete tumor regression in up to 25% of treated animals and systemic treatment was also able to slow tumor-progression.

Multiple Myeloma. The therapeutic potential of MV-Edm has also been shown for multiple myeloma (MM) [107]. Replication, syncytia formation and cytotoxicity were

shown *in vitro* in a variety of established and primary human multiple myeloma cell lines after infection with a GFP-expressing recombinant MV-Edm (MV-GFP). *In vivo* tumor formation could be inhibited by preinfection of the human MM cell lines. Intratumoral as well as intravenous treatment of established subcutaneous MM xenografts resulted in complete tumor regression in up to 100% of animals. In a murine MM xenograft model resistant to MV-Edm as well as radioiodine monotherapy, combined radiovirotherapy using human sodium iodide symporter gene (NIS) expressing MV-Edm in combination with ^{131}I achieved complete tumor regression in 40% of treated animals [304]. NIS is a membrane ion channel transporter mainly expressed in the follicular cells of the thyroid where it facilitates iodine uptake in the thyrocytes [307]. The promising results of these studies resulted in an FDA-approved protocol for clinical phase I testing of MV-NIS as systemic therapy in MM-patients.

Cutaneous T-cell lymphoma. Measles virus Edmonston-Zagreb strain (MV-EZ) – a vaccine strain derived from the Edmonston-Enders strain - was evaluated for its virotherapeutic potential in a non-randomized phase I dose-escalation study in five patients with cutaneous T-cell lymphoma (CTCL) [308]. Treatment was well tolerated. Evaluation of overall response showed partial response in one, stable disease in 2 and progressive disease in 2 patients. Preclinical data showing therapeutic efficacy of measles in a CTCL xenograft model was reported in a later manuscript [309].

4.5.2. MV-Edm for gynecologic malignancies

Ovarian cancer. Using a trackable measles virus expressing the extracellular domain of carcinoembryonic antigen (MV-CEA), recombinant measles virus was evaluated for its

potential as a viral therapeutic for ovarian cancer [107]. Intratumoral treatment of established subcutaneous ovarian cancer xenografts in mice resulted in complete tumor regression in 80% of treated mice and enhancement of median survival by 105% compared to the negative controls. Enhancement of survival by more than 250% was shown in an orthotopic model of ovarian cancer. Currently, MV-CEA is being evaluated in a clinical phase I study in patients with ovarian cancer.

Tumor type	Virus	Transgene	Retargeted
B-cell NHL	MV-Edm MV-lacZ MVHαCD20 MV2 MV-PNP Hblind^{anti}CD20	– B-gal – – PNP	– – CD20 CD38 CD20
Fibrosarcoma	MV-Edm MVHαCD20 MV^{green}-MMP-A1 MV^{green}	– – GFP GFP	– CD20 MMP-2 –
Multiple Myeloma	MV-Edm MV-GFP MV-NIS MV-ERV MV-αCD38	– GFP NIS – –	– – – Echistatin CD38
Cutaneous T-cell lymphoma	MV-GFP	GFP	–
Ovarian cancer	MV-CEA MV-GFP MV-FRα MV-αHER	CEA GFP – GFP	– – Folate receptor HER2
Breast cancer	MV-CEA	CEA	
Glioblastoma multiforme	MV-CEA MV-GFP MV-GFP-H_{AA}-scEGFR MV-GFP-H_{SNS}-scEGFRvIII	CEA GFP GFP GFP	– – EGFR EGFRvIII
Colon carcinoma	MV-PNP-antiCEA	PNP	CEA
MHC-peptide complex	MV-m33 (scTCR)	GFP	MHC-peptide complex

Table 7 Preclinical studies evaluating MV-Edm as a cancer therapy agent (for further details, see section 4.5.)

Breast cancer. MV-CEA was also evaluated for its potential as a therapeutic agent for breast cancer [310]. *In vitro* infection of several established human breast cancer cell lines resulted in infection, virus replication and transgene expression as well as cytotoxicity. Significant therapeutic potential was also confirmed *in vivo*.

4.5.3. MV-Edm for neurologic malignancies

Glioblastoma multiforme: *In vitro* as well as *in vivo* evaluation of MV-CEA in human glioblastoma multiforme (GBM) cell lines has shown strong cytopathic effects [303]. Intravenous treatment of mice bearing subcutaneous GBM xenografts resulted in complete tumor regression in all of the treated animals and significant prolongation of median survival. Similarly, evaluation in an orthotopic model with stereotactic intratumoral injection showed also complete tumor regression and prolongation of survival in the majority of treated animals. The oncolytic effect of MV-CEA was synergistically enhanced by combination with radiation treatment *in vitro* and *in vivo* [311]. The synergistic effect was shown to be due to increased MV-CEA propagation in tumor cells and enhanced apoptosis. Measles virus is currently being evaluated in a clinical phase 1 study of intratumoral inoculation in patients with glioma.

4.6. Trackable MV-Edm for pharmacodynamic and pharmacokinetic analysis

In order to gain understanding of the mechanisms responsible for different tumor response rates as well as for optimization of dosing and administration schedules in virotherapy, it is important to monitor viral replication and gene expression. Marker genes expressed in tumor cells after successful infection enable noninvasive monitoring.

Recombinant measles viruses were generated expressing marker genes including the soluble extracellular domain of carcinoembryonic antigen (CEA), the β-chain of human chorionic gonadotropin (βhCG) and the human sodium iodide symporter (NIS) [106, 304, 312]. Serum markers CEA and βhCG are non-immunogenic, have no relevant biological function and have relatively short half-life. Intraperitoneal administration of MV-CEA or MV-βhCG in CD46 transgenic mice followed by serum analysis showed that serum concentrations of these proteins correlate with viral gene expression and reflect total number of viable cells expressing the viral genome [106]. Peak serum concentrations of marker proteins were virus-dose dependent. Treatment of mice bearing measles-susceptible myeloma or measles-resistant human fibrosarcoma xenografts showed correlation of serum marker concentrations with tumor response rates after infection with trackable measles virus. In animals with resistant tumors, no marker proteins were detected in serum. In mice bearing susceptible tumors, serum levels of marker proteins were elevated and their expression pattern correlated with the tumor response. Rapid tumor response was associated with a brisk rise and fall of marker protein levels, slow responding tumors showed prolonged expression with lower peak levels [313]. In an orthotopic ovarian cancer mouse model, a significant correlation between intraperitoneal tumor burden and serum marker protein concentration was shown [312]. MV-CEA gave valuable insight in viral kinetics at different treatment doses, showing that high viral doses achieved more efficient initial cell killing in an intraperitoneal SKOV3ip.1 ovarian cancer xenograft model. However, the final outcome of therapy over a wide range of different virus doses was shown to be an equilibrium between the virus and the tumor confirming experimentally previously formulated mathematical models of oncolytic virotherapy [312, 314].

The human sodium iodide symporter (NIS) is another marker gene used for non-invasively tracking measles virus *in vivo* [304]. As described above, it is a membrane transporter facilitating intracellular iodine uptake. For in vivo monitoring, treatment with MV-NIS is followed by the application of ^{123}I and gamma-camera imaging. This approach enables monitoring of viral gene expression, replication and virus spread. In summary, the generation of trackable measles virus allows non-invasive monitoring of virus spread and will provide valuable pharmacodynamic information. These data will be helpful in adjusting viral doses, treatment schedules and to monitor tumor as well as viral biostribution.

4.7. Summary

The Edmonston strain of measles virus is a highly promising viral vector system for gene therapy of cancer. It has shown significant oncolytic potential in a variety of different models of human malignancies. The possibility of genetic engineering MV-Edm and the stability of recombinant MV-Edm allow the generation of viral vectors with enhanced oncolytic potential. In addition, genetic engineering of MV-Edm has allowed the generation of trackable measles viruses allowing non-invasive monitoring of virus replication and spread. These viruses will provide valuable pharmacokinetic information for the optimization of virotherapy. MV-Edm has an excellent safety record. Based upon the experience of the last four decades during which MV vaccine strains were safely administered to millions of patients as well as current experimental data evaluating measles virus as an oncolytic virotherapy platform in CD46 transgenic mice, virus-mediated adverse effects in humans are not expected. Valuable information is expected from ongoing clinical phase I trials. In addition, recent advances in targeting strategies for MV-Edm allow complete retargeting of MV-Edm. The immune system is

a significant barrier for viral gene therapy systems. It still needs to be determined if the immune system will negate the therapeutic effect of MV-Edm by virus neutralization or enhance the therapeutic effect by elimination of virus infected tumor cells. Several strategies for immune evasion have been developed and evaluated for measles virus showing promising results. Concomitant immunosuppression is another strategy currently being evaluated in a clinical phase I study in multiple myeloma patients.

In conclusion, MV-Edm is an ideal oncolytic virotherapy platform for cancer therapy characterized by its oncolysis, tumorselectivity and non-pathogenicity. Currently, it is being evaluated in several clinical phase I trials with additional clinical studies in the planning stages.

5. Non-viral gene deliver systems

5.1. Introduction

Non-viral gene delivery vector systems are an attractive alternative to viral vectors. In contrast to viruses, they are characterized by low toxicity and immunogenicity, lack of pathogenicity, and ease of production [315]. However, multiple biologic barriers impair the efficiency of systemic gene transfer systems. In order to overcome these barriers, an immense variety of different transfer strategies were developed. Non-viral gene delivery systems are classified into two distinct groups: 1. physical transfer of uncomplexed DNA and 2. carrier-molecule mediated DNA transfer. Both systems have been shown to possess *in vivo* gene transduction potential but differ in biodistribution and transduction efficiencies. In the following section, biologic barriers and different non-viral gene delivery systems will be reviewed.

5.2. Biologic barriers

Gene delivery systems are exposed to biologic barriers on multiple levels starting from the moment of vector administration to nuclear transport [316-318]. The first barriers are found in the intravascular and intercellular compartments. Serum nucleases rapidly degrade DNA after intravenous administration [319]. Large amounts of intravenously administered DNA are taken up and degraded by non-parenchymal hepatic cells, especially Kupffer cells, resulting in further decrease of input DNA [319]. Interaction of positively charged non-viral delivery systems with negatively charged blood components such as albumin results in charge neutralization and particle size increase. This can result in dissociation of carrier molecule and DNA, or particle aggregation

with other blood components and secondary size increase; size increases to >5 μm can result in capillary filtration [320, 321]. Administered DNA is further reduced through unspecific cell interactions and filtration in first pass organs such as lungs and spleen. Extravasation is the next barrier and its efficacy depends on the endothelial type; discontinuous and fenestrated endothelium allow passage of small DNA complexes, while continuous endothelium does not [104]. Interstitial transport is another limiting factor. Once the vector reaches the target-cell, it needs to bind and be taken up by the cell. Dependent on the type of non-viral vector system, cellular binding can be receptor mediated, non-receptor mediated through electrophilic interactions, or both. The main mechanisms of cell entry of non-viral vectors are clathrin and caveolae-mediated endocytosis, and macropinocytosis [322]. Following endocytosis, endosomal release is vital for the vector as lysosomal enzymes can inactivate and degrade DNA. Endosomal release is followed by cytosolic trafficking to the nucleus. This constitutes another barrier. The cytoskeleton inhibits diffusion of extended plasmid DNA molecules though the cytosol and cytosolic nucleases degrade DNA at a fast rate [323-325]. The last major barrier in gene delivery is nuclear transport. In dividing cells the nuclear membrane breaks down during mitosis allowing nuclear import of DNA. In non-dividing cells, nuclear DNA import has been shown to occur through nuclear pore complexes in an energy and time-dependent manner [326, 327]. However, in mitotic as well as non-mitotic cells nuclear import is an inefficient system with cell line-dependent nuclear import of 1-60% of input DNA [328, 329].

The sum of these barriers results in a significant inefficiency of non-viral gene delivery systems. Different non-viral vector systems were developed targeting different components of this barrier cascade in order to increase transduction efficiency. The

most relevant *in vivo* non-viral gene delivery systems will be discussed in the following sections.

5.3. Uncomplexed DNA gene delivery

The most direct way of DNA administration is injection of uncomplexed DNA. This system has been used with some success in tissues such as skeletal muscle, liver and skin although overall expression levels are suboptimal. Intravenous administration of uncomplexed DNA for systemic gene delivery is highly inefficient. Various physical methods have been developed in order to improve gene transfer efficiencies.

5.3.1. Sonoporation

Sonoporation describes the enhancement of gene transfer by ultrasound. This method has been used for gene therapy since the mid 1990's. Biophysically, ultrasound creates cavitation - defined as growth, oscillation and/or collapse of microbubbles - radiation pressure and acoustic microstreaming causing shear forces. Cavitation resulting in microbubble collapse is thought to be one of the main mechanisms of sonoporation. Energy released during microbubble collapse permeabilizes adjacent cells and results in transient pore formation in the cell membrane [330-332]. DNA uptake is enhanced by the use of contrast agents containing stabilized microbubbles [333, 334]. Transfection efficiency depends on transducer frequency, acoustic pressure, pulse duration and exposure duration. Different tissue types have successfully been transfected *in vivo* including skin, skeletal muscle, kidneys, liver and subcutaneous tumor xenografts [335-340]. The advantages of sonoporation include bypassing of endosomal cell entry and thereby evasion of lysosomal degradation. However, it does not protect against cytosolic

nuclease degradation and also the influence of sonoporation on nuclear entry is not well understood. For cancer gene therapy its use is limited as it is a localized, non-systemic approach.

5.3.2. Electroporation

Electroporation as a method for gene transfer was first described *in vitro* 25 years ago [341]. Since the 1990's, it is also used as a tool for *in vivo* DNA transfer [342]. The principle of electroporation is a transient and localized destabilization of the cell membrane through generation of a high-intensity electrical field. During destabilization, the cell membrane becomes permeable for exogenous molecules such as DNA [343]. Exact mechanisms of electric field-induced membrane pore generation as well as DNA uptake are not completely understood [344]. Also, intracellular DNA trafficking and nuclear uptake during and following electroporation is relatively unknown [345]. *In vivo*, this approach has been used for a variety of different internal and external tissues. The most commonly targeted tissues are tumors and muscle. Efficient *in vivo* gene transfer has been described in a variety of different tissue types including cardiac and skeletal muscle, lungs and subcutaneous tumor xenografts [346-349]. Intratumoral biodistribution patterns in tumor xenografts using this method were heterogenous [348]. Similar to sonoportion, electroporation bypasses endosomal uptake and lysosomal degradation but does not protect from cytosolic degradation. Also, it does not provide systemic gene transfer.

5.3.3. Hydrodynamic gene transfer

Hydrodynamic gene transfer was first described in 1998 by Butker et al. and is based on the use of hydrodynamic pressure for enhancement of endothelial and cell permeability

[350]. Butker and his group used a combination-approach of blood vessel occlusion and high-volume rapid DNA injection, and achieved transfection of all limb muscles with transfection efficiencies of up to 50%. The same group had also shown that portal vein injection of plasmid DNA with increased osmotic and hydrostatic pressure causing widening of sinusoidal fenestrae results in enhanced DNA extravasation [351]. Based on these observations, Liu et al. and Zhang et al. established the hydrodynamic gene delivery method [352, 353]. This method involves tail vein injection of DNA dissolved in a volume equivalent to 8-10% of the animals bodyweight over an injection time of 5-7 seconds [352, 353]. The result of this rapid volume overload is a transient cardiac congestion leading to a reverse flow in the inferior vena cava and the hepatic veins. This leads to disruption of hepatic sinusoids allowing DNA extravasation [354, 355]. Pericentrally located hepatocytes are preferentially transfected during hydrodynamic gene delivery, likely due to the close proximity of sinusoidal capillaries and peri-central hepatic parenchymal cells [356]. On a cellular level, hydrodynamic injection results in transient membrane permeabilization with pore formation facilitating cellular DNA entry [355, 357]. More recently, intracellular vesicle formation has been observed and endosomal uptake mechanisms following hydrodynamic gene transfer have been proposed [354, 358]. Hydrodynamic gene delivery is mainly being used for gene delivery to the liver but it has also been used successfully in other tissue such as kidney, myocardium and skeletal muscle [359-361]. Advantages of this technique include the enhancement of extravasation and, dependent on the uptake mechanism, the bypassing of lysosomal degradation. It does not protect against cytosolic degradation and does not enhance nuclear import. Hydrodyamic gene delivery has been used in larger animals such as pigs and even monkeys. In these studies, target organs were selectively catheterized and efferent vessels blocked before gene transfer [361-363].

5.3.4. Particle bombardment

Particle bombardment – also known as gene gun – was first described in 1987 in plant cells and was used in eukaryotic cells since the 1990's [364-366]. Its principle is the transport of DNA on an accelerated carrier molecule, usually gold particles. These DNA-coated particles are deployed by a "gene gun" into the target tissue [343]. They penetrate the cell membrane and deliver the DNA directly into the cytosol and eventually into the nucleus bypassing the endosome/lysosome and thereby avoiding lysosomal degradation. Efficiency of this approach depends on particle size, total number of DNA-coated particles, degree of particle coating and timing of delivery [367, 368]. Further, transfection efficiency is tissue dependent; e.g. epidermal cell and muscle transduction efficiencies have been reported to be 10-20% and 1-5%, respectively [365, 366, 369]. *In vivo*, it is mainly used for gene transfer to skin and liver tissue due to the shallow penetration depth of this method [369-371]. It has mostly been applied in cytokine expression and vaccination therapies [371, 372]. However, *in vivo* it achieves only short-term and low-level gene expression. The shallow penetration depth and its localized, non-systemic approach are additional limiting factors in its use for cancer gene therapy.

5.3.5. Other physical methods

Other physical gene transfer methods include laser irraditiation mediated gene transfer and magnetofection. In comparison to other gene delivery methods, these methods are not widely used. The use of laser irradiation for gene transfer dates back to the 1980's [373, 374]. Its principle is based on the thermal force of a laser beam causing penetration of the cell membrane. Membrane pores can be up to 2 μm in diameter and are only transient [373, 375]. More recently, use of this technique has also been described *in vivo* in

accessible tissues such as skin and muscle [376, 377]. Magnetofection uses a magnetic field for transfer of DNA complexed to iron oxide particles. This method has successfully been applied *in vitro* and *in vivo*. Gene delivery using magnetofection was shown in a variety of different tissues such as endothelium, gastrointestinal and respiratory tissue [378-380]. However, similar to the other physical gene transfer methods, these methods achieve gene transfer only in a localized field. They do not provide systemic treatment and are therefore of only limited use in cancer gene therapy.

5.4. Synthetic gene delivery systems

Another alternative approach for non-viral gene transfer is the use of synthetic gene delivery systems. These systems use chemical carriers for nucleic acid transfer. Carrier molecules fulfill several functions including protection of DNA from serum nucleases and other blood components, enhancement of cell binding, cell type-specific targeting, enhancement of endosomal escape and thereby protection from lysosomal degradation. Cationic lipids and polymer-based systems are the most commonly used chemical carriers for that purpose. In the following sections principles of these delivery systems will be discussed.

5.4.1. Lipoplex

Lipoplex DNA transfer systems are based on liposomes, which are defined as vesicular, colloidal particles composed of self-assembled amphiphilic molecules. Currently, the majority of liposomal systems use cationic lipids. Cationic lipids are amphiphilic molecules consisting of a positively charged polar headgroup linked to a hydrophobic domain of alkyl chains. They associate with negatively charged DNA via electrostatic

interaction resulting in positively charged lipoplexes. The charge of the cationic lipid depends on its amine groups. The ratio of lipid amine groups to DNA phosphate groups – known as the N/P-ratio - defines the lipoplex net charge and thereby its physicochemical and transfection properties. The use of cationic lipids for gene transfer was first described *in vitro* by Felgner et al. two decades ago [381]. Since then, a great variety of different liposomal formulations have been described mostly differing in the type of cationic lipid; these different types are similar in regard to their hydrophobic region but vary in regard to polar linker and cationic head groups [317]. For liposome synthesis, lipid solutions are being hydrated in aqueous solution. Neutral helper lipids such as dioleoyl-L-α-phosphatidylethanolamine (DOPE) or cholesterol are added to these formulations for endosomal escape as discussed below [382]. While single-chain amphiphilic molecules form micelles in aqueous solution, double-chain amphiphiles form lipid bilayers. Hydration concomitant with agitation results in formation of large multilamellar vesicle (LMV). During lipoplex formation, lipid restructuring occurs. Smaller vesicles are preferred due to their higher amenability to transformation. Size reduction of LMVs can be achieved through different methods, e.g. sonication, extrusion or homogenization. Resulting particles are small unilamellar vesicles (SUV) or large unilamellar vesicles (LUV) (Fig. 6). Combination of liposomes with DNA results in generation of lipoplexes [317]. Characteristics of the resulting lipoplex are influenced by thermodynamic and kinetic factors, charge ratios, lipid concentration, ionic strength, pH and temperature. Cationic lipid-to-DNA charge ratio determines lipoplex size as well as the ability of the lipoplex complex to protect DNA from nuclease degradation.

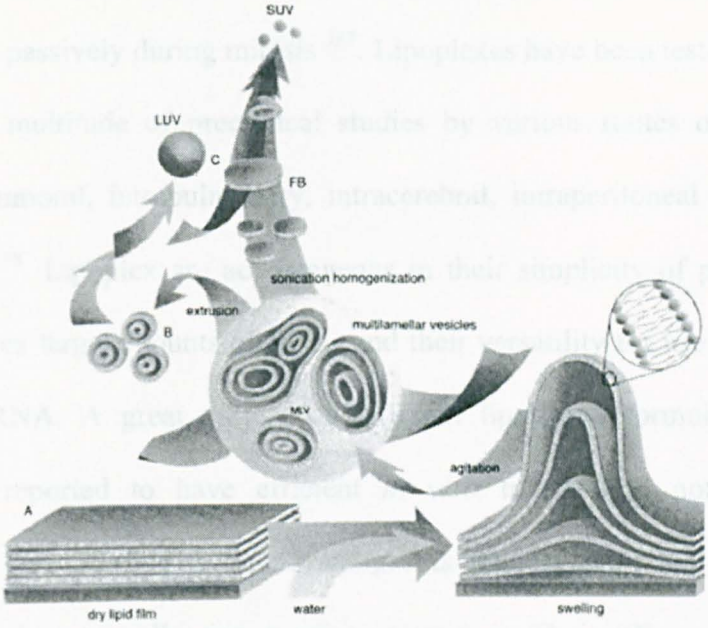

Figure 6 Liposome preparation. Shown is the generation of liposomes. Lipids are mixed in an organic solvent, dried and hydrated. Hydration and agitation results in formation of large, multilamellar vesicles (LMV). Through different methods such as sonication, extrusion or homogenization, small unilamellar vesiles can be generated for lipoplex synthesis (image obtained from http://www.avantilipids.com).

Cell membrane binding of lipoplex vectors is mediated through unspecific ionic interactions between the positively charged complex and negatively charged proteoglycans of the cell membrane [328, 383, 384]. Hence, overall net charge influences the transfection efficiency. Following cell binding, lipoplexes enter the cell via endocytosis [328, 385]. Endosomal escape is a key step in gene transfer as failure of this step results in lysosomal degradation. Fusogenic helper lipids, such as DOPE or cholesterol, are thought to facilitate this escape. DOPE forms stable lipid layers at pH of ~7 but transitions to an inverted hexagonal form at pH 5 to 6. This transition results in fusion and destabilization of the endosomal membrane resulting in release of the lipoplex [382]. The mechanism of DNA-dissociation from the liposome is not well understood but thought to occur either during or after endosomal escape [386, 387]. Nuclear entry is not

well understood in lipoplex gene transfer but thought to follow DNA release over nuclear pores or passively during mitosis [387]. Lipoplexes have been tested for safety and efficiency in a multitude of preclinical studies by various routes of administration including intratumoral, intrapulmonary, intracerebral, intraperitoneal and intravenous administration [388]. Lipoplex are advantageous in their simplicity of preparation, their ability to complex large amounts of DNA, and their versatility for use with any size or type of DNA/RNA. A great variety of different liposomal formulations has been described and reported to have efficient *in vivo* transfection potential in tumor xenografts [389]. One of their main advantages is their relative non-immunogenicity compared to viral vectors allowing repetitive treatment. Their efficiency is limited due to relatively low transgene expression levels after systemic application.

5.4.2. Polyplex

Polyplexes describe complexes of polymers and DNA. They are similar to lipoplexes as their assembly is based on the association of negatively charged DNA to positively charged polymers through electrostatic interactions. In contrast to cationic liposomes, cationic polymers condense DNA more efficiently, and as they do not contain hydrophobic moieties, they are water-soluble. Polymers can be modified in regard of their length and their geometry, e.g. linear or branched. Linear polymers differ from branched polymers in DNA compaction, nuclear uptake, transfection efficiency and toxicity. The positive charge of cationic polymers facilitates binding to extracellular proteoglycans, e.g. heparin/heparan sulfate proteoglycans [390]. As for liposomes, the N/P-ratio is critical for transfection efficiency. At high N/P ratios, the positive net charge of polyplexes increases resulting in improved cell interaction as well as

enhanced cellular and nuclear uptake, and retention [391]. An N/P ratio of >1 results in optimal efficiency, while a ratio of <1 yields only low level efficiency [384].

Examples of frequently used polymers include include poly(L-lysine) and poly(ethylenimine). Poly(L-lysine) (PLL)-based polyplexes were shown to bind to DNA and protect it from nuclease digestion [392]. However, their use was limited due to complex aggregation and precipitation, rapid systemic clearance due to non-specific interaction with serum proteins, their high cytotoxicity and low transfection efficiency. Modifications such as the use of high molecular weight PLL, conjugation with polyethylene glycol (PEG), synthesis of PLL-based polyion complex micelles (PIC) and conjugation of targeting molecules resulted in improvement of transfection efficiencies; however, other polycations such as poly(ethylenimine) (PEI) were found to achieve higher transfection rates [393]. PEI is a polyamine molecule synthesized from ethylenemine (aziridine) or oxazoline monomers. Polymerization of these monomers results in the formation of a branched or linear backbone of repeating 43 Da CH2-CH2-NH ethyleneimine motifs. Particle size depends on molecular weight of the branched PEI derivative, method of particle formation, and N/P ratio. The polyplex size decreases with increasing molecular weight, excess of polyamine and low ionic strength media. Polymer size is correlated with transfection efficiency. PEI of molecular weight between 10 and 22 kDa achieve the highest transfection efficiencies; below 10 kDa transfection efficiency decreases and above 22 kDa toxicity increases [394, 395]. Cell binding of PEI/DNA complexes is facilitated through the polyanionic heparan sulfate moieties of syndecans, ubiquitous transmembrane adhesion molecules. Cell uptake of PEI/DNA complexes is mediated by phagocytosis, followed by endosomal trafficking [396]. Endosomal escape of PEI-based polyplexes is facilitated by their buffering capacity within the normal pH range, a process known as the "proton sponge" hypothesis [383].

Protonation of ionizable amine groups causes intraendosomal chloride ion accumulation resulting in osmotic swelling and endosome rupture allowing endosomal escape of the PEI/DNA complex into the cytosol. Within the cytosol, complexion of DNA to PEI allows the cytosolic transport and protects DNA from degradation [396]. DNA dissociates from the polyplex-complex spontaneously. Kinetics and location are thought to be polymer dependent and have been observed cytosolic as well as intranuclear [397].

Polyplex gene delivery systems are commonly used for *in vitro* gene transfer and have also been evaluated *in vivo* as gene delivery vector systems [398-404]. Their high DNA-compaction ability, their intrinsic endosomolytic activity and their ability for efficient *in vivo* gene transfer, make them a highly promising non-viral gene delivery system.

5.4.3. Other synthetic gene delivery systems

The field of synthetic non-viral gene delivery systems is rapidly evolving. In order to enhance transfection efficiencies, different cationic or anionic lipids are being explored, changes in liposomal or polycationic formulations are evaluated for their effect on physicochemical properties, and existing liposomes and polyplexes are being modified. In general, the purpose of these modifications is to overcome the above-discussed biologic barriers. Poly(ethylene glycol) and targeting ligands are conjugated to non-viral vectors in order to prolong circulation times and decrease unspecific binding [405, 406]. Incorporation of nuclear localization signals aims at enhancement of nuclear transport efficiencies [407, 408]. The use of different fusogenic lipids and polycations aims at improvement of endosomal release. A variety of new molecules have been established as synthetic gene transfer systems such as protamine, chitosan and dendrimers [409, 410]. Recently, biodegradable polymers, virosomes and lipopolyplexes

have been added to the armory of non-viral gene transfer systems [411-413]. These new innovative approaches have resulting in improved transfection efficiencies. However, the remaining biologic barriers continue to impair the feasibility of these approaches for efficient clinical tools in oncology.

6. Specific aims of the thesis

6.1. Background

Hepatocellular carcinoma is a devastating malignancy. Its high global prevalence and its increasing incidence in Western countries make this neoplasm a highly significant disease. Its devastating prognosis and the lack of effective non-surgical treatments warrant the development of new therapeutic approaches to this malignancy.

In contrast to other oncologic approaches such as chemo- and radiation therapy, genetic approaches are a highly specific. A variety of different viral and non-viral gene delivery systems have been developed and tested in HCC. The majority of these studies used viral vector systems such as adenovirus, herpes simplex virus type 1 (HSV-1) and vesicular stomatitis virus (VSV) [414-416]. Different cancer gene therapy strategies have been studied in HCC including tumor-suppressor gene p53 transfer, suicide gene transduction, antiangiogenic strategies, immunogene therapy as well as oncolytic viral therapy [417-422]. Very few of these vectors were tested clinically, and although biologic responses were observed, their overall efficacy was low [423-426]. Failure of efficacy was attributed to insufficient tumor transduction and antibody formation efficiently neutralizing vectors during repeated dosing [423, 427, 428]. Alternative gene transfer systems are urgently needed. The overall goal of this thesis is the development and evaluation of alternative viral and non-viral gene delivery systems for this devastating disease.

6.2. Specific aim 1

Specific aim 1 of this thesis is the establishment, evaluation and comparison of different non-viral gene delivery systems *in vivo*. The rationale of non-viral gene delivery is the

low immunogenicity and toxicity of these vectors allowing repetitive dosing regimens. A variety of non-viral gene delivery systems are described in the current literature. However, the majority of these non-viral gene delivery systems suffer from their low transduction efficiency. Identification of the most promising non-viral gene delivery system is the overall goal of the first part of this thesis. Feasibility and transduction efficencies will be used as criteria for identification of the most promising approaches. These systems will be established according to published methodologies and evaluated *in vivo* using subcutaneous murine tumor xenograft models.

6.3. Specific aim 2

Specific aim 2 of this thesis is the development and evaluation of non-viral, expanded parvoviral genome-based replicon vectors. Parvovirus MVM is human apathogenic, tumor selective, oncolytic and provides high-level transgene expression. Their efficacy is limited by their immunogenicity and genomic size restrictions. Genomic size limitation to 106% of the wild type size are due to significant decrease in virion packaging efficiency. The rationale of the second aim of this thesis is the avoidance of parvoviral limitations through their use as replicating plamid expression vectors while oncotherapeutically advantageous charateristics will be maintained. Tolerance to genomic expansion would allow enhancement of parvoviral cytotoxcity through the use of therapeutic transgenes. Efficient replication and high-level transgene expression could potentially compensate for low transduction efficiencies of non-viral gene delivery systems. Expanded MVM-based replicon vectors will be generated and evaluated for their replication and transgene expression. Maintenance of tumor

selectivity and cytotoxicity will be analyzed and comparison to other expression systems performed.

6.4. Specific aim 3

Specific aim 3 of this thesis is the evaluation of recombinant MV-Edm as an oncolytic viral vector for HCC. The rational for the choice of this viral agent is its previously shown therapeutic potential in different models of human malignancies (Table 7). These preclinical studies have resulted in clinical phase I studies for ovarian cancer, multiple myeloma, and glioblastoma multiforme. Its potential as a virotherapeutic agent for HCC has never been evaluated. Infectivity and cytotoxicity of recombinant MV-Edm will be evaluated *in vitro* using human HCC cell lines. Mechanisms of cell death and expression of transgenes will be evaluated. *In vivo* oncolytic effects and tumor suppression will be analyzed.

II. Material & Methods

1. Cell biological methods

1.1. Cell lines

HUH-7 and Hep-3B cells were a kind gift of Dr. G. J. Gores. Transformed cell lines Wi38V13 and Mcl-5V1 were a kind gift of Prof. Rommelaere (DKFZ, Heidelberg). All other cell lines were obtained through the American Type Culture Collection (ATCC, Manassas, VA) and CellzDirect (Durham, NC). Growth media, serum and supplements were purchased from Gibco BRL (Grand Island, NY). All cells used in this study were cultured at a humidified atmosphere of 5% CO_2 and 37^0 C. Cell culture medium was supplemented with 10% heat-inactivated FBS, and 1% Sodium-Pyruvat. All media used in this study contained 100 U/ml penicillin-streptomycin.

1.2. Long-term storage of cells

Cells can be frozen and stored in liquid nitrogen for several months without impairment of their viability. Cells can either be stored directly in the liquid phase of nitrogen at -196^0 C or above within the gas phase between -150^0 C and -160^0 C. The following points are important for optimal results: prolonged freezing process, fast thawing, a high protein concentration and addition of 5-10% DMSO to the freezing medium. These measurements will increase membrane permeability, prevent partial dehydration of cyoplasma and prevent intra- as well as extracellular crystal formation.

Cell line	Type	Culture medium	Origin
Hep-3B	Human HCC	MEM	Dr. G.J. Gores
HUH-7	Human HCC	DMEM	Dr. G.J. Gores
Hepatocytes	Primary human hepatocytes	Williams medium E	CellzDirect
293-T	SV40-transformed human kidney cells	DMEM	ATCC
A9	Mouse fibroblast	DMEM	ATCC
Mcl-5	Human lung fibroblast	MEM	ATCC
Mcl-5/V1	SV40 transformed Mcl-5	MEM	Dr. Rommelaere
NIH-3T3	Rat fibroblast	DMEM	ATCC
V12-3T3	SV40 transformed NIH-3T3	DMEM	ATCC
Wi38	Human lung fibroblast	DMEM	ATCC
Wi38/V13	SV40 -transformed human lug fibroblast	DMEM	Dr. Rommelaere
N2A	Mouse neuroblastoma	DMEM	ATCC
Vero	African green monkey kidney	DMEM	ATCC

Table 8: Cell lines used in for experiments.

For recovery of frozen cells, cryo-tubes containing aliquots of the cell suspension were thawed in a 37^0 C water bath. For prevention of an osmotic shock, prewarmed medium was added to the cell suspension. Cell culture medium was exchanged 24h after cell adhesion.

1.3. Passaging of established cell lines

After removal of medium, cells were washed with 1x PBS, 2 ml of 2% Trypsin/EDTA added and cells incubated for 2 min at 37^0 C. Trypsin/EDTA was removed and the cells dissolved in 10 ml of the corresponding medium for inactivation of remaining trypsin. Cell clumps were dissociated through several cycles of pipetting. Cells were diluted to the density required for the corresponding experiment.

1.4. Assessment of cell numbers

After detachment of adherent cells with trypsin, 20 µl of the cellsuspension were mixed with 0.4% Trypan-blue solution (w/v) at a ratio of 1:1. Trypan-blue is an acidic dye, which binds easily to proteins due to its anionic characteristics. The dye is only taken up by non-viable cells, thereby facilitating the distinction between viable and non-viable cells. Counting of the cell number was performed using a Neubauer chamber. Number of viable cells in 1 ml of the cell suspension, equals the product of stastical mean value of the 4 main quadrants, the chamber factor (10^4 cells/ ml) and the dilution. Total number of cells is being calculated as the product of cell concentation (cells per ml) and the total volume of the cell suspension.

1.5. Cell staining

1.5.1. Fixation of cells

Before staining, cells required fixation. Medium was removed, cells washed once with 1x PBS. Acetic-ethanol mixture, pre-chilled to 4^0 C, was added to the cells and cells incubated at 4^0 C for 20 min. Cells were washed carefully with 1x PBS and once with H_2O, followed by removal of excess fluid and staining.

1.5.2. Crystal violet stain

Crystal violet is a methyl aniline dye with a high degree of blue. It has the ability to bind DNA and can be used for cell viability assays. After fixation, cells were incubated with 0.13% crystal violet solubilized in ethanol-formaldehyde (2:1). The stained

product was subsequently washed twice with H_2O and air-dried. Cell viability was evaluated optically and documented by digital photography

1.5.3. DAPI-stain

4,6-Diamidino-2-phenylidone (DAPI)-stain is used for nuclear staining of chromatin allowing morphologic analysis of chromosomal changes. This method can be used for identification of cells underoing apoptosis. After fixation of cells, cells were incubated with DAPI-dye for 5 min at RT under the exclusion of light. DAPI-dye was removed, cells washed twice with 1x PBS and excess fluid removed. Analysis was performed using fluorescence-microscopy.

1.5.4. Tunel-stain

Apoptotic data were confirmed by a TdT-mediated dUTP nick-end labeling (TUNEL) assay using TUNEL Label Mix (Roche Diagnostics). The assay is based upon nuclear DNA cleavage into oligonucleosome-sized fragments during apoptosis. In the TUNEL-assay, DNA-strand breaks are being labeled with fluorescein-dUTP and analyzed by fluorescence microscopy. TUNEL-assay was performed according to manufacturers recommendations. After fixation, cells were permeabilized in freshly prepared 0.1% sodium citrate containing 0.1% X-100 Triton for 2 min at 4^0 C. Cells were washed twice followed by addition of 50 µl TUNEL-reaction mixture containing the TUNEL-enzyme and labeling solution. Cells were incubated for 60 min at 37^0 C. After washing the cells for three times in PBS, they were analyzed using fluorescence microscopy at an excitation wavelength of 450-500 nm and detection range of 515-565 nm.

1.5.5. Immunohistochemistry

Paraffin-embedded liver sections of HCC- and healthy patients were incubated with mouse anti-human CD46 primary antibody (BD Biosciences, Pharmingen) for 30 min at 37 °C, then incubated with fluorescein isothiocyanate-conjugated anti-mouse IgG secondary antibody (1:300 dilution) (Santa Cruz Biotechnology, Santa Cruz, CA) for 30 min at room temperature. Cells were washed in phosphate-buffered saline three times each for 3 min. Immunofluorescence microscopic analysis was performed with a Zeiss LSM 510 using a 100x Pan-Apochromat 1.4-nm oil objective (Carl Zeiss Inc., Thornwood, NY).

1.6. Cytotoxicity assays

Cytotoxicity was evaluated quantitatively as well as morphologically using different modes of detection. Viability of cells was evaluated using crystal violet staining. For quantitative confirmation, viability of cells was analyzed using the CellTiter 96 AQueous nonradioactive cell proliferation assay kit (Promega Corp., Madison, Wis.). For mechanistic cell death analysis –apoptosis versus necrosis- cells were analyzed morphologically using fluorescence microscopy after DAPI- (1.5.3.) or TUNEL-staining. Apoptosis was confirmed by quantitation of caspase 3/7 activities using the Apo-ONE® Homogenous Caspase-3/7 Assay (Promega Corp., Madison, Wis.).

1.6.1. CellTiter 96® AQ_{ueous} Non-Radioactive Cell Proliferation Assay

The CellTiter 96® AQ_{ueous} Non-Radioactive Cell Proliferation Assay is a colorimetric method for determining the number of viable cells in proliferation or chemosensitivity assays. The assay is composed of tetrazolium compound 3-(4,5-dimethylthiazol-2-yl)-5-

(3-carboxymethoxyphenyl)-2-(4-sulfophenyl)-2H-tetrazolium (MTS) and an electron coupling reagent (PMS). MTS is reduced to aqueous, soluble formazan by cellular dehydrogenase in metabolically active, viable cells. The amount of formazan product can be quantitated by fluorometric analysis with the absorbance at 490nm being directly proportional to the number of viable cells. The CellTiter 96 AQueous nonradioactive cell proliferation assay kit was performed according to manufacturers recommendations. Briefly, cells were cultured and treated in 96-well tissue culture plates. At the designated time points, cells were incubated with 20 μL of MTS reagent solution for 2 h at 37^0 C. Absorbance at 490 nm was recorded using an ELISA plate reader.

1.6.2. Caspase 3/7 assay

Apo-ONE® Homogenous Caspase-3/7 Assay (Promega Corp., Madison, Wis.) contains profluorescent, rhodamine 110-labeled caspase-3/7 substrate bis-(N-CBZ-L-aspartyl-L-glutamyl-L-valyl-L-aspartic acid amide) (Z-DEVD-R110). Activated caspase-3/7 cleaves non-fluoroescent Z-DEVD-R110 resulting in release of fluorescent rhodamine-110. Fluorescence is positively correlated to caspase-3/7 activity and can be quantitated by spectrofluorometric analysis at an excitation wavelength of 499 nm with an emission maximum at 521 nm. The assay was performed according to manufacturers recommendations. Briefly, cells were cultured and treated in black 96-multiwell cell culture plates. At the experimental time points, the Apo-ONE reaction buffer was added to the sample at a 1:1 ratio, followed by incubation for 1-18h at RT. Caspase-3/7 activity in the sample was quantitated by spectrofluorometry and statistically analyzed.

1.7. Flow cytometry

Cells were harvested, washed twice in cold 2% BSA-PBS, and incubated with a FITC-labeled monoclonal mouse anti-human CD46 antibody (PharMingen, San Diego, USA) for 1h on ice. Following, the cells were washed twice and run on a Becton-Dickinson FACScan Plus cytometer and analyzed using the CellQuest software (Becton-Dickinson, San Jose, USA).

1.8. In vitro ^{123}I uptake studies

Cells were infected with MV-NIS at MOI 0.01, 0.1 and 1.0 for 2 h in Opti-MEM. Virus-suspension was removed and growth medium added to the cells. *In vitro* iodine uptake studies were performed 24h, 48h and 72h after infection as previously described [429]. Briefly, cells were washed twice in Hanks balanced salt solution (HBSS) and resuspended in HBSS with 10 mM HEPES (*N*-2-hydroxyethylpiperazine-*N'*-ethanesulfonic acid, pH 7.3). Potassium perchlorate was added to half of the samples to a final concentration of 1 μM. 1 x 10^5 cpm ^{125}I were added to each sample. After 50 min incubation at 37^0 C, cells were washed twice with cold HBSS and lysed by addition of 1M NaOH. Activity in the cell lysates was determined using a gamma counter.

2. Molecular biological methods

2.1. Nucleic acid transduction

2.1.1. Bacterial cells

For amplification of plasmid DNA, the chemically competent, recombinase deficient (*rec A*) E. coli strain SURE® 2 supercompetent cells (Stratagene, CA) were used. For transformation of DNA into the bacterial cells, competent bacteria were rapidly thawed at RT and 10-100 ng plasmid DNA or 1-5 µl of ligation mix added. Sample was gently mixed and incubated on ice for 30 min, followed by 30 sec incubation at 42^0 C. 250 µl prewarmed S.O.C. medium were added to transformed bacteria and the suspension incubated at 37^0 C on a shaker at 225 rpm for 1h. 100 µl of the bacterial suspension was transferred to a prewarmed antibiotic containing LB-agar plates (antibiotic corresponding to resistance gene encoded by transformed plasmid). Plates were incubated overnight at 37^0 C, resulting bacterial clones were collected (1-10/plate) and further amplified by overnight incubation at 37^0 C on a rotary shaker in 3 ml antibiotic-containing LB-medium. Following incubation, DNA was isolated and analyzed as described below.

2.1.2. Eukaryotic cells

For transfection of plasmid DNA in eukaryotic cell lines, Lipofectamine™2000 (Invitrogen, CA) was used according to the manufacturers recommendations. Lipofectamine™2000 is a cationic lipid formulation. Briefly, cells were plated the day prior to transfection so that cell density at day of transfection was 60-75%. Plasmid DNA as well as Lipofectamine™2000 reagent were diluted in Opti-MEM (Invitrogen,

CA), incubated for 5 min at RT and then combined and mixed; optimal DNA: Lipofectamine™2000 ratio was predetermined by preliminary experiments for optimization of transfection efficiency. For cotransfection experiments with two plasmids, equal copy numbers of each plasmid were used; however, total amount of DNA was sustained in order to preserve the DNA-to-lipid ratio. The DNA-lipid suspension was added to medium and cells were incubated for 4h at 37^0 C in a CO_2 incubator. After 4h of incubation, transfection medium was exchanged with regular cell culture medium.

2.2. Isolation and purification of nucleic acids

2.2.1. Bacterial cells

For isolation and purification of nucleic acids "Plasmid Mini Prep", "Endofree Plasmid Maxi Prep" and "Endofree Plasmid Giga Prep"-Kits (QIAGEN, CA) were used according to manufacturers recommendations. Briefly, after transformation, transduced bacteria were amplified in antibiotic containing LB-medium (volume: 3 ml for mini-culture, 500 ml for Maxi-prep, 5 L for Giga-prep); antibiotic was chosen according to antibiotic resistance gene encoded on the plasmid DNA. The bacterial culture was incubated at 37^0 C on a rotational shaker until reaching the log-phase, mostly 14-18 h. 850 µl of the bacterial culture were removed and mixed with 150 µl of autoclaved glycerol. Sample was stored at – 80^0 C for long-term storage. The rest of the bacterial culture was centrifuged using a Sorvall GSA-rotor with 5000 RPM for 10 min at 4^0 C. Supernatant was discarded and the bacterial sediment was resuspended in buffer P1. Lysis-buffer P2 was added and the culture incubated for 5 min at RT. Neutralization buffer P3 was added, the culture mixed by invertion and incubated for 20 min on ice.

The lysed bacterial culture was centrifuged at 16,500 RPM at 4^0 C, followed by filtration of the clear supernatant using a QBT-equilibrated anion exchange column. The columns were washed twice with QC-buffer, followed by elution of the plasmid DNA with QF-buffer. Plasmid DNA was precipitated using 0.7 volume parts isopropanolol followed by centrifugation with 10,000 RPM for 10 min at 4^0 C. DNA was washed with 70% ethanol and dried at room air. DNA was resuspended in an appropriate volume of TE-buffer and DNA concentration determined by photometric analysis.

2.2.2. Eukaryotic cells

Isolation of low molecular weight DNA from eukaryotic cells was performed as described by Hirt [430]. Cells were washed with 1x PBS, lysed in Hirt-lysis buffer (10 mM Tris/HCl pH 7.4, 10 mM EDTA pH 8.0, 0.6% SDS) and transferred to a 1.8 ml Eppendorf tube. 250 µg/ml Proteinase K was added to the lysed cells and samples incubated for 1h at 37^0 C. NaCl concentration was adjusted to 1.25 M, samples incubated for 12h at 4^0 C followed by centrifugation for 30 min at 12,000 RPM at 4^0 C. Supernatant was transferred to a new tube and low molecular weight DNA extracted by phenol/choroform extraction followed by isopropanol precipitation. DNA was washed with 70% ethanol and resuspended in TE-buffer. DNA concentration was determined by photometric analysis.

2.3. Nucleic acid analysis

2.3.1. Concentration and purity of nucleic acids

Absorption. The DNA concentration in solutions was measured using UV-spectrophotometry. Nucleic acids have an absorption maximum for UV-light at a wavelength of 260 nm. The absorption maximum of proteins is at a wavelength of 280 nm. The concentration of a nucleic acids can be estimated by measuring the absorbance at 260nm (A_{260}), adjusting the A_{260} measurement for turbidity (measured by absorbance at 320nm), multiplying by the dilution factor, and using the relationship that an A_{260} of 1.0 = 50µg/ml pure DNA (Concentration (µg/ml) = (A_{260} reading – A_{320} reading) × dilution factor × 50µg/ml). DNA purity can be estimated from the A_{260}/A_{280} ratio after correction for turbidity (DNA Purity (A_{260}/A_{280}) = (A_{260} reading – A_{320} reading) ÷ (A_{280} reading – A_{320} reading)). An A_{260}/A_{280} ratio between 1.7 and 2.0 generally represents a high-quality DNA sample. Lower ratios indicate the presence of proteins in the solution, higher ratios the presence of RNA.

PicoGreen assay. For measurement of DNA concentrations between 25 and 1000 pg/ml fluorescent PicoGreen® reagent (Molecular Probes, OR) was used. PicoGreen® reagent is not specific for dsDNA, but it shows a >1000-fold fluorescence enhancement upon binding to dsDNA, and much less fluorescence enhancement upon binding to single-stranded DNA (ssDNA) or RNA, making it possible to quantitate dsDNA in the presence of equimolar amounts of ssDNA, RNA or proteins. The assay was performed according to the manufacturers recommendations. Briefly, PicoGreen® reagent was added to samples and DNA standard curve dilutions, mixed and incubated for 5 min at RT. Fluorescence was measured using a spectrofluorometer at an excitation wavelength

of 480 nm and an emission wavelength of 520 nm. Based upon measured fluorescence of the standard curve DNA, concentration of DNA in the samples was calculated.

2.3.2. Nucleic acid sequence analysis

Nucleic acid sequencing analysis was required for confirmation of complete parvoviral DNA sequence –especially in the palindromic 5'- and 3'- termini. Parvoviral clones were sequenced by the Molecular Core Facility at Mayo on an ABI 377 sequencer and analyzed for sequence alterations.

2.3.3. Agarose gel electrophoresis

For analysis of DNA or isolation of DNA fragments for further cloning, DNA was separated using agarose gel electrophoresis. Agarose was dissolved in TAE or TBS buffer by boiling the solution in a microwave oven. Agarose concentration was chosen in dependence of DNA fragment size (100-500 bp: 2% agarose, 500-10,000 bp: 1% agarose). After agarose was completely dissolved, ethidiumbromide was added to a final concentration of 1 µg/ml and solution transferred to a gel electrophoresis apparatus. DNA was separated at an electrical current of 8 V/cm. DNA fragments migrate through the agarose gel negatively proportional to their size and were visualized after intercalation with ethidium bromide under UV-light (wavelength 312 nm).

2.3.4. Southern blot

Southern blot technique was used for transfer of DNA to nylon membranes. Briefly, after separation of DNA by agarose gel electrophoresis, DNA was denatured by

incubation of the gel in denaturation solution (1.5 M NaCl/0.5 M NaOH) for 30 min followed by 30 min incubation in neutralization solution (1.5 M NaCl/0.5 M Tris·Cl, pH 7.0). If DNA fragments were >15 kb, gel was prior to denaturation, depurinated by 30 min incubation in 0.25 M HCl. For capillary transfer of DNA, gel was transferred to a Southern blot apparatus and placed on a bridge consisting of Whatman 3MM filter paper sheets continuously in contact with 20x SSC buffer (3 M NaCl, 0.3 M tri-sodium citrate). A nylon membrane (Hybond-N+, Amersham) was placed on the gel, followed by three layers of Whatman 3 mm blotting paper and a stack of paper towels allowing buffer transfer by capillary action from a region of high water potential to a region of low water potential. The blot was performed overnight, followed by permanent fixation of DNA to the nylon membrane through UV-crosslinking (UV transilluminator, 254-nm wavelength).

2.3.5. Hybridisation

For DNA-DNA hybridization, the non-radioactive DIG labeling and detection method was used according to the manufacturers recommendations. Briefly, using the PCR DIG Probe Synthesis kit (Roche Applied Science, IN) a Digoxigenin (DIG)-labeled hybridization probe was synthesized by PCR; the probe was designed to bind to a 390 bp area in the parvoviral NS1-coding region. Labeling efficiency was analyzed by agarose-gel electrophoresis. The Southern blot nylon membrane was incubated for 30 min in prewarmed prehybridisation buffer (DIG Easy Hyb, Roche Applied Science, IN). Optimal hybridisation temperature was calculated according to the formula $T_{Hyb} = T_m$-(20^0C to 25^0 C) with Tm = 49.82+0.41 (% G+C)-600/length of hybrid in bp. Meanwhile, 2 µl of the PCR DIG-labeled DNA hybridization probe was diluted in 50 µl

H_2O, boiled for 5 min at 95^0 C for denaturation and chilled on ice. The hybridization probe was diluted in prewarmed hybridization buffer (DIG Easy Hyb, Roche Applied Science, IN) and the solution was added to the membrane after discarding the prehybridization buffer. Hybridisation was performed overnight at the appropriate hybridization temperature in a designated rotating hybridization oven. Following the hybridization, the membrane was washed twice for 5 min each in low stringency buffer (2x SSC, 0.1% SDS) at RT, followed by washing of the membrane twice for 15 min each in high stringency buffer (0.5% SSC, 0.1% SDS) at 65^0 C. For chemoluminescent detection of the probe bound to the membrane, ready-to-use CSPD assay (Roche Applied Science, IN) was used according to the manufacturers recommendations. Membrane was washed for 2 min at RT in detection washing buffer (0.1 M Maleic acid, 0.15 M NaCl pH 7.5, 0.3% Tween 20), followed by incubation for 0.5 to 3h in blocking buffer. The washing buffer was replaced with antibody solution containing anti-Digoxigenin antibody at a 1:10,000 dilution and incubated for 30 min at RT. Then, the membrane was washed twice for 15 min each with washing buffer and incubated for 3 min in detection buffer (0.1 M Tris-HCl, 0.1 M NaCl pH 9.5). After removal of the detection buffer, 1 ml/100 cm^2 ready-to-use CSPD was added onto the membrane, the membrane incubated at 37^0 C for 10 min followed visualization by exposure to a X-ray film.

2.4. Nucleic acids cloning

Plasmid DNA can be modified through cloning strategies aiming at introduction or deletion of nucleic acid sequences. The following techniques were used for cloning strategies in the studies described in this thesis.

2.4.1. Restriction hydrolysis

Restriction endonucleases are bacterial enzymes that cut double-stranded DNA molecules at specific recognition sites. There are three types of restriction endonucleases; Type II cuts at the recognition site and is therefore the most important for molecular biologic techniques. All enzymes were obtained from New England Biolabs (NEB, MA) and used according to the manufacturers recommendations. For analytical restriction hydrolysis of plasmid DNA, 0.5 to 2 µg were used, for preparative restriction hydrolysis an amount was chosen which would result in approximately 1 µg of the desired product. Reaction volume was for most reactions 20 µl and the reaction time at least 1 h. Restriction enzymes were given at a concentration of at least 2 Units/µg DNA but did not exceed 10% (v/v) of the reaction volume.

2.4.2. Polymerase chain reaction

For generation of modified nucleic acid sequences, polymerase chain reaction (PCR) was used. Briefly, primers were designed according to desired application (e.g. ligation, DNA sequencing) and template DNA. Primers were synthesized by the Mayo Clinic DNA synthesis core facility. 10-100 ng template DNA was combined with primers, dNTP, 5x reaction buffer and *Pfu* polymerase or Platinum®*Pfx* polymerase. The reaction mix was filled up to 20 microliter with H_2O. For DNA amplification, primer-annealing temperature was calculated based upon primer G/C and A/T content, duration of primer extension based upon length of PCR-product (1 min/kb) and cycle number dependent PCR efficiency and application between 25 and 30 cycles.

2.4.3. Reverse-transcriptase polymerase chain reaction

Reverse-transcriptase polymerase chain reaction (RT-PCR) is a two-step process during which RNA is reverse-transcribed to cDNA, followed by PCR amplification, thereby allowing quantification of transcription. For RT-PCR, Omniscript transverse transcription (QIAGEN, CA) was used according to manufacturers recommendations. Briefly, RNA was isolated using RNeasy kit (QIAGEN, CA) followed by analysis of RNA concentration. 50 µg RNA was combined with 10x reaction buffer, 5 mM of each dNTP, 10 Units RNase inhibitor, 1 µM oligo dT-primer, 4 Units of Omniscript reverse transcriptase and RNase-free water to a final volume of 20 µl. The sample was incubated at 37^0 C for 60 min. The resulting cDNA product was subsequently used in a PCR reaction using NS1-specific primers (nucleotide sequences: forward primer: TCACTG CCTGACACAAGAACC; reverse primer: TTGTGGTCATGATGACTGGTGTTG).

2.4.4. Mutagenesis

Mutagensis was used for generation or deletion of restriction sites within nucleotide sequences. For mutagenesis, QuickChange® XL Site-directed Mutagenesis Kit (Stratagene, CA) was used according to the manufacturers recommendations. Briefly, mutagenic primers were designed to contain the mutated sequence in the middle and 10-15 nt in 5'- and 3'-prime direction to a total primer length of 25-40 nt. Final reaction sample volume was 50 µl containing 10x reaction buffer, 10 ng of DNA template, 125 ng of forward and reverse mutagenic primer, 1 µl dNTP mix, 3 µl QuickSolution and H_2O ad 50 µl, and 5 Units *Pfu turbo* DNA polymerase. Mutated DNA sequences were amplified in a thermal block over 18 cycles, followed by DpnI restriction hydrolsis for

removal of unmutated, parental methylated DNA, and transformed in XL10-Gold ultracompetent bacteria for amplification.

2.4.5. Blunt-ending of restriction sites

The generation of blunt-ended double-stranded DNA was required for ligation of sticky-end restriction hydrolysed, non-cohesive DNA fragments. Two strategies were used: 1. fill-in of 5'-overhang DNA fragments or 2. removal of 3'-overhangs.

2.4.5.1. Fill-in of 5'-overhang DNA fragments

For fill-in of a 5'-overhang DNA fragments, Klenow-fragment of *E. coli* –DNA-polymerase I was used. This enzyme has DNA-polymerase activity, and no 5'-3'-exonuclease activity. Its 3'-5'-exonuclease activity is 200x-times less than T4 polymerase. DNA was diluted in Klenow reaction buffer to a final concentration of 50 ng/µl, 33 µM of each dNTP as well as 1 Unit/µg DNA added and the reaction incubated at 25^0 C for 15 min. DNA was then isolated by agarose gel-electrophoresis followed by gel-extraction.

2.4.5.2. Removal of 3'-overhangs

T4 DNA-polymerase has 200x more 3'-5'-exonuclease activity than Kenow DNA-polymerase; in addition it has 5'-3'-polymerase activity and no 5'-3'-exonuclease activity. For removal of 3'-overhangs, DNA was diluted in T4 DNA-polymerase reaction buffer reaction buffer to a final concentration of 50 ng/µl, 33 µM of each dNTP as well as 1 Unit/µg DNA of T4 DNA-polymerase was added and the reaction

incubated at 37^0 C for 30 min. DNA was then isolated gel-extraction following agarose gel-electrophoresis.

2.4.6. Ligation of DNA fragments

Ligation was used for linking double-stranded DNA-fragments - with either cohesive overhanging or blunt ends - after restriction hydrolysis or for linking PCR-fragments to restriction hydrolyzed DNA-molecules. T4-DNA-ligase was used for catalyzing covalent phosphodiester bonds between 5'-phosphate and 3'-hydroxyl groups of nucleotides. Ligations were performed overnight at 14^0 C in a reaction volume of 20 µl containing 1 Unit T4 DNA ligase (Invitrogen, CA), 14 µl 5x ligase buffer (250 mM Tris-HCl pH 7.8, 50 mM $MgCl_2$, 5 mM ATP, 5 mM DDT, 25% w/v PEG-8000), 50-200 ng DNA at a vector to insert ratio of 1:3.

2.4.6. Removal of 5' terminal phosphate groups

In order to avoid undesired re-ligation of vector DNA with cohesive ends, 5' terminal phosphate groups were removed by treatment with calf intestinal phosphatase (CIAP). Briefly, following restriction hydrolsis of vector DNA, 1 Unit of CIAP (Promega, WI) and 10x reaction buffer (50 mM Tris-HCl pH 9.3, 1 mM $MgCl_2$, 0.1 mM $ZnCl_2$, 1 mM spemidine) were added to reaction sample. H_20 was added to a total volume of 50 µl. Sample was incubated at 37^0 C for 60 min, followed by agarose gel-electrophoresis and isolation by gel extraction.

2.4.7. Gel extraction

For isolation of DNA fragments, agarose gel-electrophoresis was performed followed by gel-extraction. For gel extraction, QIAEX II-gel extraction kit (QIAGEN, CA) was used according to manufacturers recommendation. The method is based on binding of DNA to silica under high salt conditions. Briefly, DNA was separated by agarose gel electrophoresis, visualized by UV transillumination and bands of interest excised using a scalpel blade. Band was weighed and dissolved in 3 volumes buffer QX1 followed by incubation at 50^0 C for 10 min. The sample was centrifuged for 30 sec at 12,000 RPM, followed by removal of supernatant The pellet was washed once with 500 µl wash buffer QX1 followed by two wash steps using 500 µl buffer PE. The resulting pellet was air-dried and resuspended in 20 µl H_2O by incubation for 5 min at RT or 50^0 C in dependence of DNA size.

2.4.8. Nucleotide annealing

For annealing of oligo nucleotides, DNA was first 5'-phosphorylated using T4 polynuleotide kinase (T4 PNK) followed by step-down PCR. Briefly, 0.25 µg of each DNA strand was combined with T4 PNK kinase, 10x T4-ligase reaction buffer and H_2O to a final volume of 50 µl. The sample was incubated at 37^0 C for 30 min. In a thermo cycler, sample was denatured for 10 min at 94^0 C followed by decrease of temperature at a rate of 0.01^0 C/sec until Tm where it was held for 5 min followed by decrease to 24^0 C at a rate of 0.01^0 C/sec. Annealed DNA was gel-purified after agarose gel-electrophoresis.

3. Virologic methods

Virologic methods described in this section were used for experiments using recombinant measles virus.

3.1. Amplification of recombinant measles virus

Recombinant measles viruses including MV-Edm encoding the soluble extracellular domain of human CEA (MV-CEA), MV-Edm encoding the green fluorescent marker protein GFP (MV-GFP) and MV-Edm encoding the human NIS protein (MV-NIS) were generated and propagated on Vero cells as described previously [431]. Briefly, Vero cells were infected with virus stocks (generous gift by Dr. K.-W. Peng) at a MOI of 0.02 to 0.05 and incubated for 2h at 37^0 C. Subsequently, 5% FCS containing DMEM medium was added and cells incubated under normal culture conditions until 80-90% syncytia formation was observed. Cell-syncytia were harvested in Opti-MEM using a cell scraper and lysed by two freeze-thaw cycles followed by centrifugation with 1500 RPM for 2.5 min. Supernatant was transferred to a new reaction tube and stored at -80 ^{0} Celsius. Titers of viral stocks were determined by 50% end point dilution assays ($TCID_{50}$) on Vero cells.

Virus stocks were only thawed once in order to avoid alterations of virus concentration.

3.2. Infection of eukaryotic cells

For virus infection assays, $2x10^5$ cells were incubated with recombinant MV-Edm diluted in 1.0 ml of Opti-MEM (Life Technologies, Inc.) at a predetermined MOI for 2 h at 37^0 C. At the end of the incubation period, the virus was removed, and the cells maintained in standard medium until further analysis.

4. Biochemical methods

4.1. Stabilized plasmid lipid particles

Stabilized plasmid lipid particles (SPLP) were synthesized by the detergent dialysis method as described previously [432]. DOPE, DODAC and PEGC20 were mixed at a ratio of 82.5:7.5:10 and dissolved to a final lipid concentration of 10 mg/ml in sterile-filtered 1x HBS-buffer (10 mM HEPES, 150 mM NaCl, pH 7.4) containing 200 mM OGD detergent. DNA was added to a final concentration of 400 μg DNA/10 mg lipid. In order to determine the required ionic conditions for maximum packaging efficiency, aliquots of the sample were dialyzed overnight at RT against HBS-buffer containing NaCl at concentrations between 100 and 150 nM. Percentage of entrapped DNA was analyzed by PicoGreen Assay performed prior to and after Triton mediated lysis of particles; percentage of DNA entrapment was calculated according to the following formula: % encapsulation = ([+Triton]-[-Triton])*100)/[+Triton]. Particle size was analyzed by QELS (= Quasi-Elastic Light Scattering) analysis. Once the optimal buffer conditions were determined, Lipid/DNA sample was dialyzed against the corresponding HBS-buffer for 48h at RT; buffer was exchanged every 12h. Untrapped DNA was removed by DEAE-sepharose CL-6B chromatography, followed by purification of plasmid DNA containing SPLP by sucrose gradient centrifugation (1%, 2.5%, and 10.0% w/v sucrose in 1 x HBS) at 28,000 rpm for 18 h at 20^0 C. DNA-containing SPLP particles accumulate at the 2.5% and 10% interface and empty liposomal particles and unbound lipids in the 1.0% and 2.5% cellulose layers (Fig. 7). DNA entrapping-SPLP were collected, pooled and dialyzed against 1x HBS overnight at RT for removal of sucrose. DNA content and entrapment were analyzed by PicoGreen analysis as described above. SPLP particle size was confirmed by QELS analysis (Fig. 8).

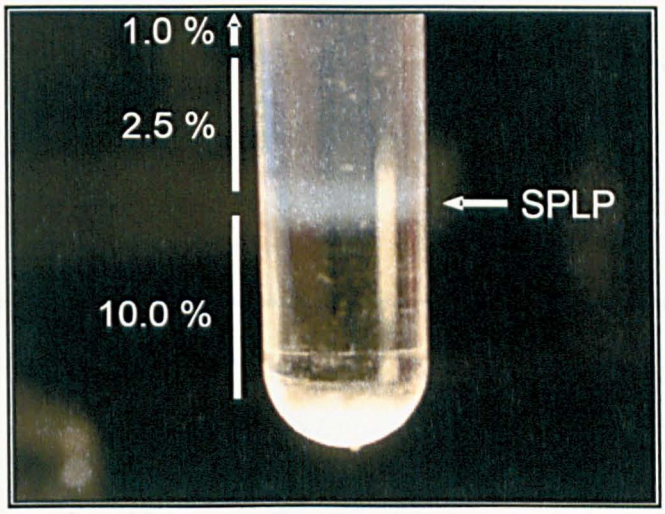

Figure 7: SPLP-purification. SPLP were synthesized by the detergent dialysis method. Following encapsulation of DNA in SPLP, free DNA was removed by DEAE-sepharose CL-6B chromatography. SPLP containing DNA were isolated from empty SPLP and free lipids by sucrose gradient centrifugation. DNA entrapping SPLP were located at the 2.5% and 10% interface as indicated in figure 7. The 2.5% and 1% layers contained empty SPLP and lipids. The DNA encapsidating SPLP were recovered by perforation of the centrifuge tube at the bottom of the band and collection in reaction tubes.

Sample was concentrated using an Amicon®Ultra-15 centifugal column (Millipore, Billerica, MA) and adjusted to a final concentration of 0.5 mg DNA/ml. After preparation was complete, SPLP were reanalyzed for particle size by QELS-analysis. As shown in Fig. 8, SPLP particles population had a mean diameter of 64.5 nm.

4.2. PEI-Polyplexes

PEI-based polyplexes were synthesized as previously described [393]. Linear polyethylenimine with molecular weight of 22 kDa (PEI22) as well as branched, 25 kDa PEI conjugated to transferrin ligand (Tf-PEI25) were a generous gift from Dr. E. Wagner. Briefly, DNA was dissolved in 0.5 HBS buffer (75 mM NaCl, 20 mM Hepes pH 7.4) to a final concentration of 0.4 µg/µl. Tf-PEI25 and PEI22 were combined at a

ratio of 1:3 and dissolved in 0.5 HBS buffer. PEI-solution and DNA-solution were combined by flash-mixing; resulting N/P-ratio was 4.8. The solution was incubated for 20 min at RT. For *in vivo* application, complexes were dissolved in 0.5 HBS containing 2.5% glucose.

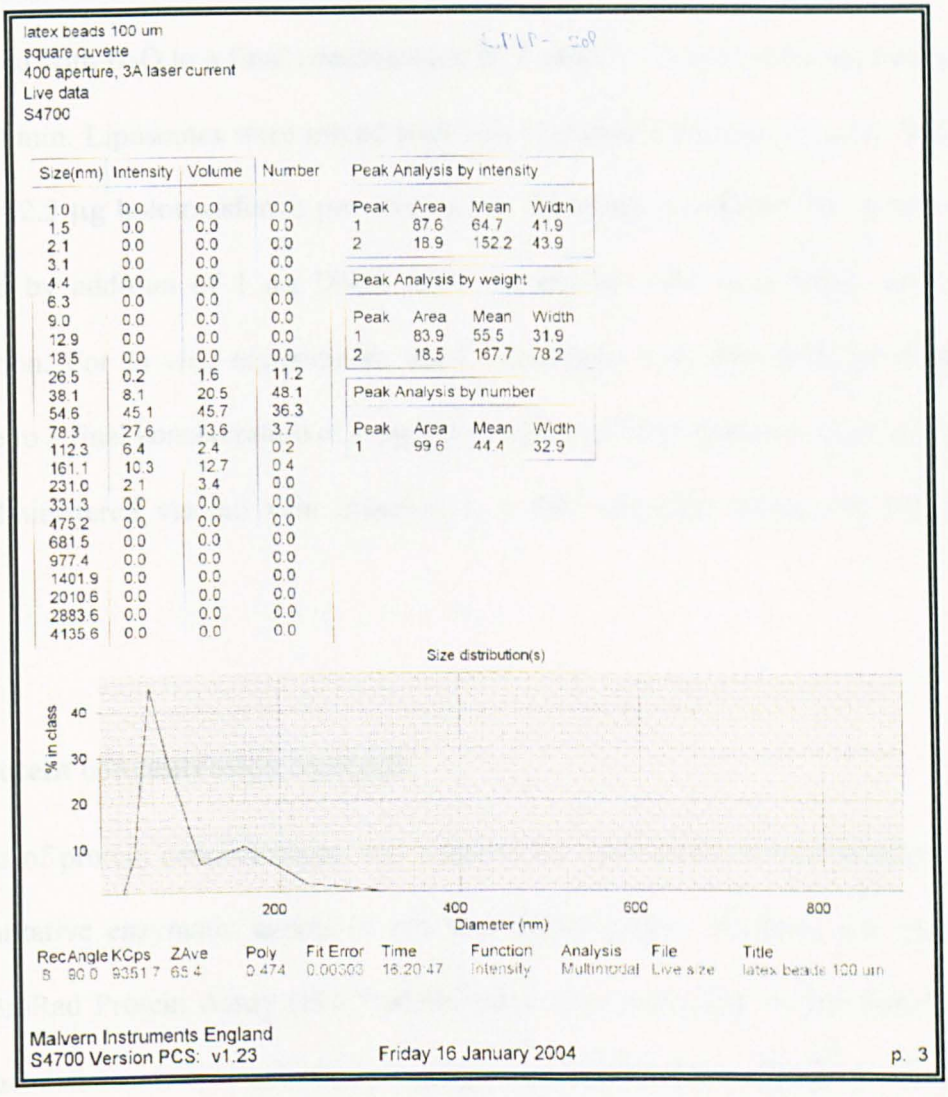

Figure 8: SPLP size analysis. SPLP size was measured by quasi-elastic light scattering (QELS) analysis. This technique is used to determine the size distribution profile of small particles in solution. It is based on the principle of diffuse light scattering by small particles and uses a laser light source for analysis. The scattered light undergoes either constructive or destructive interference by the surrounding particles, and within this intensity fluctuation information is contained allowing calculation of size and size distribution of the particles contained in a solution. As figure 8 indicated, 87.6% of SPLP in the solution have a mean SPLP-size of 64.7 nm.

4.3. LipT complexes

Transferrin-liposome-DNA (LipTcomplex) were synthesized as previously described [389]. Briefly, 1,2-dioleoyl-3-trimethylammoniumpropane (DOTAP) and dioleoylphosphatidyl-ethanolamine (DOPE) (Avanti Polar Lipids, Alabaster, AL) were dissolved in chloroform and mixed at a 1:1 ratio. Chloroform was evaporated and lipids rehydrated with H_2O to a final concentration of 2 μmol/ml followed by sonication at 4^0 C for 10 min. Liposomes were mixed with holo-transferrin (Sigma, St. Lois, MO) at a ratio of 12.5 μg holotransferrin per 10 nmol of liposome, incubated for 10 min at RT followed by addition of 1 μg DNA. LipT complexes were used wthin an hour of preparation. For *in vivo* experiments, LipT complexes were dissolved in sterile 5% dextrose to a final concentration of 1 μg DNA-LipT per 10 μl dextrose. LipT complexes were administered via tail vein injection in a total injcetion volume of 300 μl per animal.

4.4. Protein concentration analysis

Analysis of protein concentrations was required for corrections of total protein content in quantitative enzymatic assays of cell and tissue lysates. Analysis was performed using BioRad Protein Assay (Bio Rad,Hercules, CA) according to the manufacturers recommendations. It is a colorimetric assay based upon color change of Coomassie Brilliant Blue G-250 dye in response to various concentrations of proteins due to a shift of its absorption maximum from 465 nm to 595 nm. As the reaction is not linear over a range of different protein concentrations, measured absorption has to be correlated to a protein standard. Briefly, different dilutions were made of the protein solution of interest and a bovine serum albumin solution. 200 μl dye reagent was added to 800 μl of

protein solution and absorption measured at a wavelength of 595 nm. Protein concentration was read on the standard curve obtained from bovine serum albumin absorption values.

4.5. Luciferase assay

For analysis of luciferase activity Steady-Glo® Luciferase Assay System (Promega, Madison, WI) was used according to the manufacturers recommendation. This assay allows high throughput analysis in multiple samples, such as ain 96-well plates. Briefly, Steady-Glo® substrate was directly added to cell culture medium at a 1:1 ratio, followed by incubation for 5 min at RT and luciferase activity measurement in a luminometer. In experiments in which cells were co-transfected with a control vector for correction of transfection efficiency, medium was removed, cells washed once and lysed in Glo-Lysis buffer (Promega, Madison, WI) by incubation for 5 min at RT. The cell lysate was transferred to a luminometer tube and Steady-Glo® substrate added at a 1:1 ratio. After an additional incubation period of 5 min at RT, luciferase activity was analyzed using a luminometer.

4.6. β-Galactosidase assay

In studies in which correction for differences in transfection efficiencies was required, co-transfection with β-galactosidase expressionvector pSV-β-gal was performed. β-galactosidase was analyzed using β-Galactosidase Enzyme Assay System (Promega, Madison, WI) according to the manufacturers recommendations. Briefly, cells were lysed in Glo-Lysis buffer (Promega, Madison, WI) by incubation for 5 min at RT.

Assay reaction buffer containing substrate ONPG (o-nitrophenyl-beta-D-galactopyranoside) was added to cell lysate at a 1:1 ratio.

5. Animal experimental methods

5.1. Subcutaneous tumor xenograft implantation

All procedures involving animals were approved by and performed according to guidelines of the Institutional Animal Care and Use Committee of the Mayo Clinic. Animals were kept under pathogen-free conditions, fed standard food, and given free access to sterilized water. Female SCID and nude mice (4-6 weeks of age; Harlan Laboratories, Indianapolis, IN) were injected with 5 x 10^5 HUH-7 cells/100 µl PBS and 5 x 10^5 Hep-3B cells/100 µl PBS subcutaneously in the right flank with a 27-gauge needle. Mice were examined daily for tumor growth. Length, width and height of tumors were measured with calipers. Tumor volume was calculated according to the formula $\pi/6$ x width x length x height [433]. When tumors reached a maximum diameter of 0.5 cm, treatments were initiated. Animals were euthanized when tumor diameter reached 1 cm or mice lost 10% of body weight.

5.2. Tumor marker analysis

For in vivo experiments, blood samples were collected from mice by retro-orbital bleeding and serum analyzed for CEA concentration. For *in vitro* experiments, supernatant from MV-CEA infected and uninfected HCC cells was collected and

analyzed for CEA concentration. CEA levels were measured using the Bayer Centaur Immunoassay System.

5.3. *In vivo* iodine uptake studies

Subcutaneous HCC-xenografts were implanted as described above. Once the tumors reached a maximum diameter of 0.5 cm, animals were treated with a single-shot dose of 2×10^6 $TCID_{50}$ of MV-NIS by intravenous tail vein injection. 3, 7, 10 and 14 days after MV-NIS treatment, mice were injected intraperitoneally with 500 µCi ^{123}I. 1 h after injection of the isotope, whole-body imaging for ^{123}I activity was performed using a gamma camera (Helix System; Elscint, Haifa, Israel).

5.4. *In vivo* gene expression analysis

5.5. Statistical Methods

The statistical analysis for significance of differences in survival of mice treated with recombinant MV-Edm and UV-inactivated MV-Edm was performed using the log-rank test in the JMP-program. $P \leq 0.05$ indicates significant difference.

III. Results

1. Nonviral gene delivery systems

1.1. Introduction

Nonviral gene delivery systems possess lower immunogenicity and toxicity than viral vectors, thereby allowing use of higher doses and repetitive treatments. There are a great variety of different non-viral gene delivery systems. However, the majority of these systems are suboptimal due to their low transduction efficiency caused by multiple *in vivo* barriers. It was the initial goal of this thesis to identify the most promising of these delivery systems based upon their reported *in vivo* transduction efficiency, establish these systems independently in the laboratory, and compare them *in vivo* for identification of the most efficient one. Selection of the most promising appearing systems was based on thorough review of the current literature. These systems included conjugated and physical, non-conjugated gene delivery systems. All systems were evaluated *in vivo* in mice bearing subcutaneous tumor xenografts as specified in the following sections.

1.2. Un-conjugated plasmid DNA transfer

1.2.1. Intravenous injection of naked plasmid DNA

Intravenous injection of naked plasmid DNA was evaluated in the subcutaneous N2A neuroblastoma xenograft mouse model. Luciferase expressing plasmid pCi-luc was used as an expression vector. Plasmid DNA was prepared using endotoxin-free Maxi Prep Kits (QIAGEN, CA) for avoidance of endotoxin mediated complications.

Once tumors had a maximum diameter of 0.5 cm, animals were treated with 50 µg of plasmid DNA dissolved in a total volume of 100 µl sterile PBS per animal by intravenous tail vein injection. Luciferase activity in tumor, liver, spleen, lung, kidneys, muscle, heart and brain tissue was analyzed 8, 24, and 48h after injection. In order to correct for unspecific background luciferase activity, luciferase activity in organs of untreated mice was subtracted from luciferase activity of lysates from the corresponding organs of treated animals.

After intravenous injection of naked plasmid DNA, very low levels of luciferase activity were observed in all organ systems including the tumor (Fig. 9). Intratumoral luciferase activity was 197.8 ± 73.9 RLU/g tissue 8h after treatment, increased to 333.1 ± 182.0 RLU/g tissue 24h after treatment and decreased to undetectable levels 48h after treatment. Comparable or higher luciferase activity was detected in lungs and spleen.

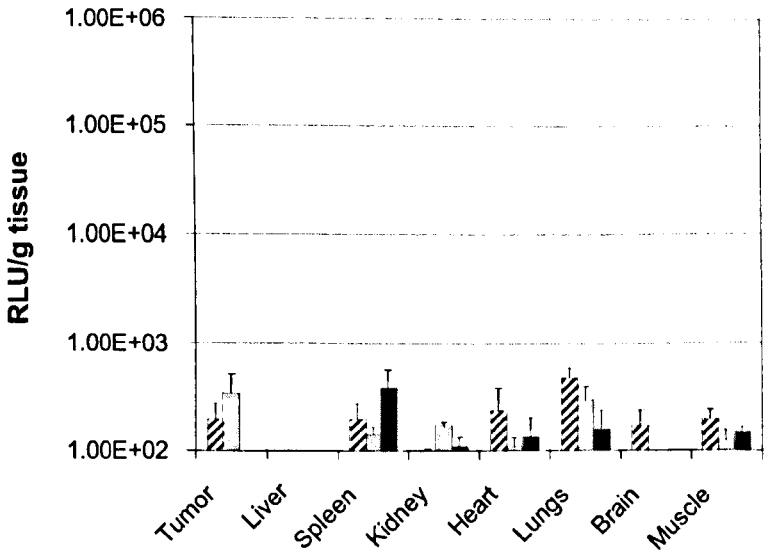

Figure 9: Gene expression after intravenous injection of naked plasmid DNA. Animals bearing subcutaneous N2A-xenografts were treated with 50 µg of pCi-luc plasmid DNA by direct intravenous tail vein injection. 8, 24 and 48h after injection, organs were harvested and analyzed for luciferase expression. Shown are means with standard error (n = 3).

(▨ = 8h p.i., □ = 24h p.i., ■ = 48h p.i.)

Luciferase activity in lung lysates was 475.0 ± 115.5 RLU/g tissue 8h after injection, and decreased to 292.0 ± 101.3 RLU/g tissue and 157.9 ± 82.1 RLU/g tissue 24h and 48h after injection. Luciferase activity in splenic lysate was 198.9 ± 73.1 RLU/g tissue, 140.6 ± 25.0 RLU/g tissue and 383.3 ± 184.9 RLU/g tissue at 8, 24 and 48h after intravenous DNA injection. Lower luciferase activities were observed in kidney, heart, brain and muscle tissue between with luciferase activity varying between 71 and 193 RLU/g tissue. The lowest luciferase activity was observed in liver tissue lysates with activities between 10.7 and 21.3 RLU/g tissue.

1.2.2. Intra-arterial injection of naked plasmid DNA

As shown above, intravenous DNA transfer achieved only very low-levels of transgene expression. Entrapment of systemically administered vectors in first pass organs contributes to vector reduction in the circulation. The results of intravenous DNA treatment showed the highest transgene expression in the lungs indicating entrapment of a significant amount of administered plasmid DNA in this organ. It was hypothesized in this thesis that bypassing the lungs would result in an increased amount of plasmid DNA in the arterial system resulting in increased vector delivery to tumor tissue. In order to achieve arterial delivery, naked plasmid DNA was transthoracically injected in the left cardiac ventricle. 50 µg of pCi-luc dissolved in 100 µl sterile PBS was used per animal. Luciferase activity was analyzed 8, 24 and 48h after injection in tumor, liver, spleen, kidneys, heart, lungs, brain and muscle tissue.

In comparison to the intravenous route, intra-arterial injection of plasmid DNA resulted in higher luciferase activity in all organs. The distribution pattern of luciferase expression differed between the two routes of administration (Fig. 10). With the

exception of muscle tissue, the highest transgene expression was observed 48h after injection. Intratumoral luciferase activity was 301.2 ± 169.1 RLU/g tissue 8h after treatment, increased to 977.8 ± 578.1 RLU/g tissue in the following 16h and decreased to 187.3 ± 43.7 RLU/g tissue 48h after injection. The highest luciferase activity was observed in cardiac lysates with 1151.2 ± 128.4 RLU/g tissue 8h after treatment, followed by an increase to 23265.1 ± 23027.8 RLU/g tissue 24h after treatment. 48h after injection, luciferase activity had decreased to 131.7 ± 38.7 RLU/g tissue. High luciferase activity was also observed in the spleen with 111.0 ± 28.1 RLU/g tissue, 3609.6 ± 3364.8 RLU/g tissue, 154.5 ± 13.0 RLU/g tissue 8, 24 and 48h after injection.

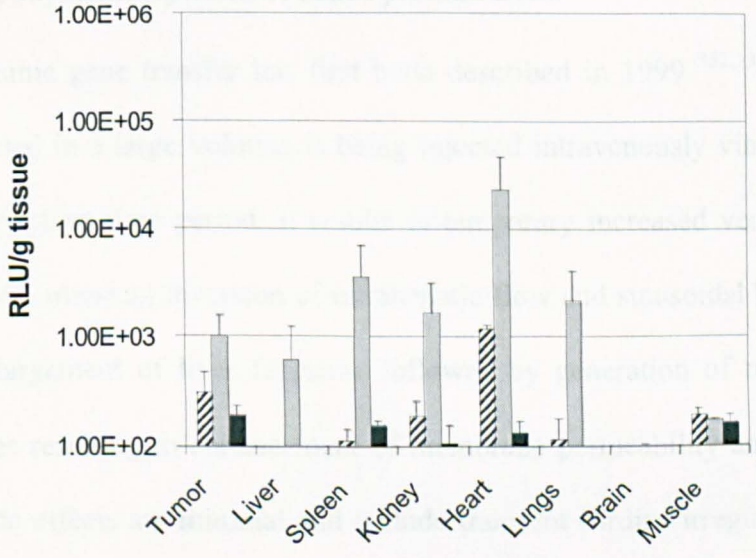

Figure 10: Gene expression after intraarterial injection of naked plasmid DNA. Animals bearing subcutaneous N2A-xenografts were treated with 50 µg of pCi-luc plasmid DNA by direct intraarterial injection in the left cardiac ventricle. 8, 24 and 48 h after injection, organs were harvested and analyzed for luciferase expression. Shown are means with standard error (n = 3). (▨ = 8 h p.i., □ = 24 h p.i., ■ = 48 h p.i.)

Intra-arterial treatment resulted in higher hepatic luciferase expression than intravenous injection. Luciferase activity was 25.6 ± 13.2 RLU/g tissue, 614.1 ± 605.7 RLU/g tissue

and 6.0 ± 2.0 RLU/g tissue at 8, 24 and 48h after vector administration. Luciferase expression was also observed in lung lysates with 113.9 ± 62.5 RLU/g tissue at 8h, 2129.7 ± 2031.3 RLU/g tissue at 24h and 61.7 ± 11.8 RLU/g tissue at 48h after intra-arterial injection. Luciferase expression in kidneys was 185.6 ± 65.7 RLU/g tissue, 1627.3 ± 1530.5 RLU/g tissue, 106.4 ± 47.8 RLU/g tissue 8, 24 and 48h after treatment. Low but persistent transgene expression was observed in muscle lysates with maximum luciferase activity of 192.5 ± 28.6 RLU/g tissue. Brain was the only organ in which lower transgene expression was observed than after intravenous treatment with a maximum of 83.4 ± 18.0 RLU/g tissue 24h after treatment.

1.2.3. Hydrodynamic injection of naked plasmid DNA

Hydrodynamic gene transfer has first been described in 1999 [352, 353]. Naked plasmid DNA, diluted in a large volume, is being injected intravenously via tail vein injection over a very short time period. It results in temporary increased venous pressures and asystole with transient inversion of intrahepatic flow and sinusoidal blood stasis. Stasis causes enlargement of liver fenestrae followed by generation of membrane pores in hepatocytes resulting in enhancement of membrane permeability and DNA uptake [354, 355, 434]. Side effects are minimal and include transient cardiac irregularity and transient elevation of hepatic transaminases [352, 355]. This technique is commonly used for transfection of the liver. However, transgene expression has also been observed in other organs after hydrodynamic gene transfer [352]. Therefore, it was hypothesized that hydrodynamic gene transfer might also result in transduction of tumor tissue.

Experimental conditions were chosen as previously reported [352, 353]. 50 µg of pCi-luc plasmid DNA was used per mouse. DNA was diluted in sterile PBS in a volume in

milliliters equivalent to 10% of bodyweight in gram. Injection site was the tail vein. Injection time was 5-10 sec. The method was well tolerated by mice with a mortality of 0%. Transgene expression analysis was performed 8, 24 and 48h after injection. Organs of interest were tumor, liver, spleen, kidney, heart, lungs, brain and muscle tissue (Fig. 11).

The highest luciferase activity was observed in the liver with 188808.6 ± 38798.1 RLU/g tissue 8h after injection, followed by a continuous decrease of luciferase activity to 14188.2 ± 12079.2 RLU/g tissue and 1032.9 ± 1026.5 RLU/g tissue 24 and 48h after treatment. Intratumoral luciferase activity was low after treatment. 8h after injection,

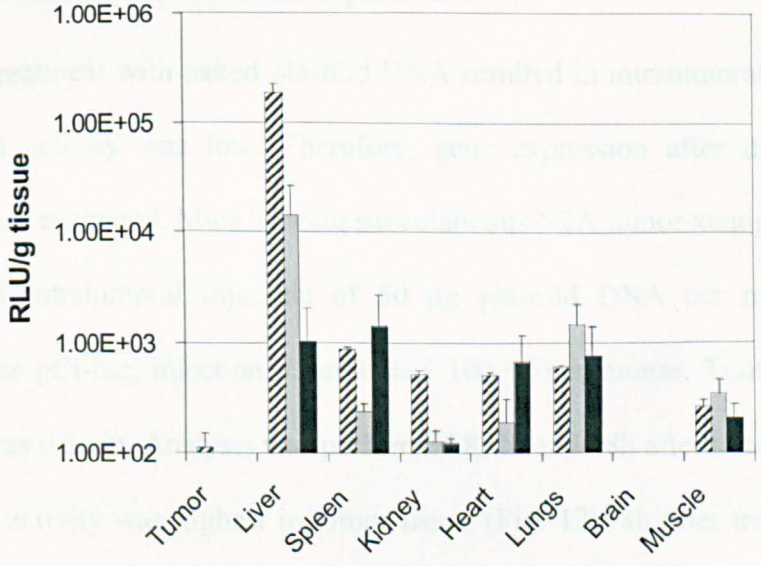

Figure 11: Gene expression after hydrodynamic injection of naked plasmid DNA. Animals bearing subcutaneous N2A-xenografts were treated with 50 µg of pCi-luc plasmid DNA by hydrodynamic gene transfer. DNA was dissolved in a volume equivalent to 10% body weight in milliliters. 8, 24 and 48h after injection, organs were harvested and analyzed for luciferase expression. Shown are means with standard error (n = 3).

(◪ = 8 h p.i., □ = 24 h p.i., ■ = 48 h p.i.)

luciferase activity was 113.0 ± 38.6 RLU/g tissue and decreased to 56.7 ± 30.9 RLU/g tissue and 56.0 ± 35.9 RLU/g tissue 24 and 48h after treatment. Higher levels of transgene expression were measured in other organs. In splenic lysates, luciferase activity fluctuated between 241.6 ± 44.1 RLU/g tissue at 24h and 1418.4 ± 1278.0 RLU/g tissue at 48h after injection. Very high levels of luciferase activity were seen in lung tissue with a peak luciferase activity of 1458.9 ± 761.1 RLU/g tissue 24h after injection. Lower levels of luciferase activity in the range of 129 and 687 RLU/g tissue were observed in renal and cardiac lysates. The lowest luciferase activity levels with a maximum of 347.2 ± 111.9 RLU/g tissue were observed in muscle tissue and in brain lysates.

1.2.4. Intratumoral injection of naked plasmid DNA

Systemic treatment with naked plasmid DNA resulted in intratumoral gene expression, but overall activity was low. Therefore, gene expression after direct intratumoral injection was evaluated. Mice bearing subcutaneous N2A tumor xenografts were treated with direct intratumoral injection of 50 µg plasmid DNA per mouse. Expression plasmid was pCi-luc, injection volume was 100 µl per mouse. Tumor-size at time of injection was 0.5 cm. Analysis was performed 8, 24 and 48h after treatment.

Luciferase activity was highest in tumor tissue (Fig. 12). 8h after treatment, luciferase activity was 179087.5 ± 148338.1 RLU/g tissue. In the following 48h, luciferase activity decreased continuously to 22684.2 ± 18540.4 RLU/g tissue and 10018.5 ± 5786.1 RLU/g tissue 24 and 48h after treatment. Low luciferase activity was observed in all other organs ranging between 10.8 ± 2.4 RLU/g tissue in the liver and 330.5 ± 97.1 RLU/g tissue in muscle tissue.

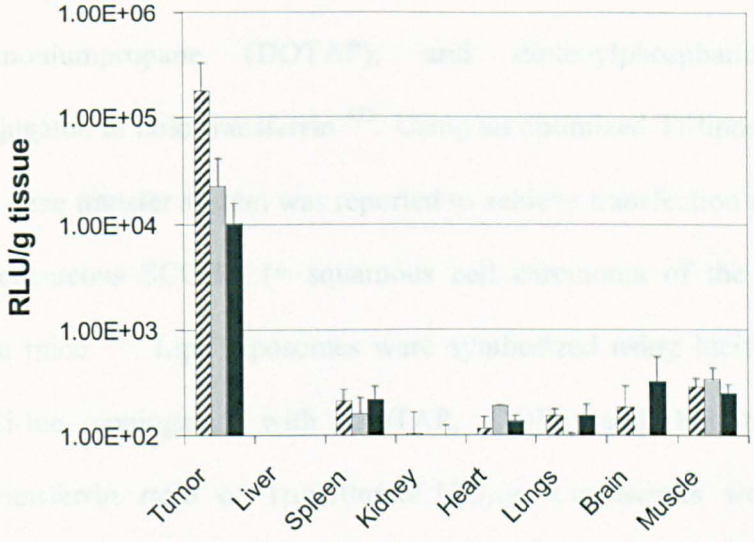

Figure 12: Gene expression after direct intratumoral injection of naked plasmid DNA. Animals bearing subcutaneous N2A-xenografts were treated with 50 µg of pCi-luc plasmid DNA by direct intratumoral DNA injection. DNA was dissolved 100 µl of sterile PBS. 8, 24 and 48h after injection, organs were harvested and analyzed for luciferase expression. Shown are means with standard error (n = 3).

(◪ = 8 h p.i., □ = 24 h p.i., ■ = 48 h p.i.)

1.3. Conjugated DNA transfer systems

The results of the previous studies show the feasibility of unconjugated DNA transfer. However, transgene expression levels are extremely low unless DNA is intratumorally injected. This strategy might be of use for solitary tumors but will not be sufficient for metastatic disease. In the case of proven or suspected metastatic disease, most non-surgical therapeutic approaches to malignancies - including gene therapy - aim at systemically active agents. Conjugation of DNA to different molecules is supposed to protect DNA from extra- and intracellular degradation and clearance, and thereby increase transduction efficiency.

1.3.1. LipT cationic liposomes

LipT cationic liposomes are based on the cationic lipid 1,2-dioleoyl-3-trimethylammoniumpropane (DOTAP), and dioleoylphosphatidyl-ethanolamine (DOPE) conjugated to holo-transferrin [435]. Using an optimized Tf/liposome/DNA ratio, this nonviral gene transfer system was reported to achieve transfection efficiencies up to 30% in subcutaneous SCCHN (= squamous cell carcinoma of the head and neck) xenografts in mice [389]. LipT liposomes were synthesized using luciferase expressing plasmid pCi-luc conjugated with DOTAP, DOPE and holo-transferrin at a DNA:lipid:transferrin ratio of 1µg:10nmol:12.5µg. Lipsosomes were prepared by sonication, dissolved in sterile 5% dextrose and administered systemically via tail vein injection within an hour of preparation. Per mouse a total volume of 300 µl of LipT/pCi-luc was used containing 30 µg of plasmid DNA. 24, 48 and 72h after treatment, organs were analyzed for luciferase expression. As in previous experiments, organs of interest included tumor, liver, spleen, kidneys, lungs, brain, heart and muscle. No luciferase activity above background was detected at any time point in any of the organs using this gene transfer system.

1.3.2. DNA/Tf-PEI25/PEI22-polyplexes

DNA/Tf-PEI25/PEI22-polyplexes are based on the cationic polymer polyethylenimine (PEI) that has been shown to possess high transfection potential *in vitro* and *in vivo* [399]. Further optimization including the use of low molecular weight PEI molecules (22 and 25 kDa) and coupling to cell-binding ligand transferrin, resulted in increased transduction efficiency and specificity, as well as decreased toxicity [393, 436]. Polyplexes were synthesized according to original description by Kircheis et al. using luciferase

expressing plasmid pCi-luc, PEI22 and transferrin conjugated PEI25 [393]. Molar ratio of PEI nitrogen to DNA phosphate was 4.8. Polyplexes were dissolved in sterile 0.5x HBS with 2.5% glucose to a DNA concentration of 200 µg/ml. Animals bearing subcutaneous N2A xenografts were treated systemically with 250 µl of DNA/Tf-PEI25/PEI22 (= 50 µg DNA) via tail vein injection directly after synthesis of polyplexes. 24, 48 and 72h after treatment, organs were analyzed for luciferase expression. As in previous experiments, organs of interest included tumor, liver, spleen, kidneys, lungs, brain, heart and muscle.

The highest transgene expression was observed in tumor tissue (Fig. 13). 24h after injection of the polyplexes, intratumoral luciferase activity was 24138.24 ± 8116.7 RLU/g tissue. In the following 24h, luciferase activity increased to 146244.3 ± 28803.9 RLU/g tissue and decreased to 17351.9 ± 9723.3 RLU/g tissue at 72h after treatment.

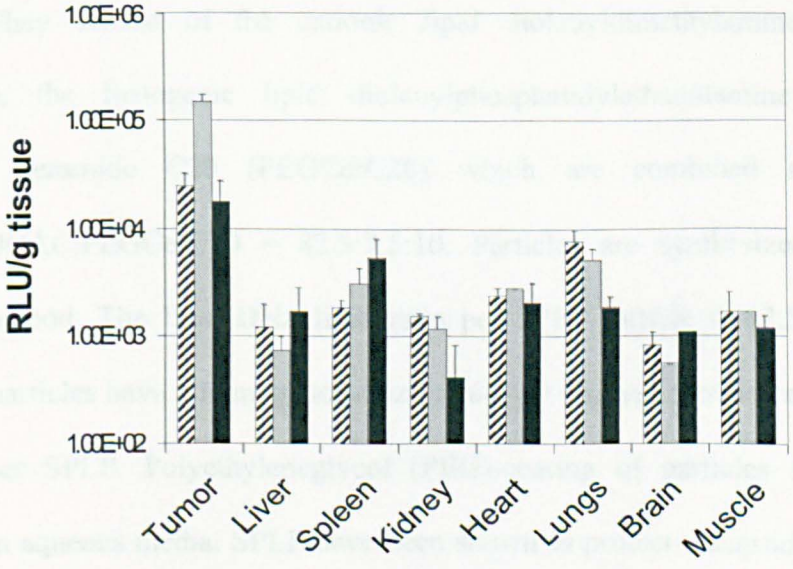

Figure 13: In vivo gene expression after systemic therapy with DNA/Tf-PEI25/PEI22-polyplexes. Animals were treated with 50 µg of pCi-luc conjugated to Tf-PEI25/PEI22-polyplexes per mouse. 24, 48 and 72h after intravenous injection, organs were harvested and analyzed for luciferase expression. Shown are means with standard errors (n=3).

(▨ = 24h p.i., □ = 48h p.i., ■ = 72h p.i.)

Luciferase expression was also detected in lungs, hear, kidney and spleen. However, overall luciferase expression was lower with a maximum of 7526 RLU/g tissue. While, luciferase expression was decreasing over time in most organs, luciferase showed an increasing expression pattern over time in spleen. Low-level luciferase activity was observed in liver, brain and muscle tissue. Luciferase activity in liver lysates fluctuated around 1000 RLU/g tissue with 1200.0 ± 720.0 RLU/g tissue, 720 ± 240 RLU/g tissue and 1680 ± 1200 RLU/g tissue at 24, 48 and 72h after polyplex injection. Also in muscle lysates, luciferase activity was around 1000 RLU/g tissue. The lowest levels of luciferase expression were measured in brain tissue.

1.3.3. Stabilized plasmid lipid particles

Stabilized plasmid lipid particles (SPLP) were first described by Wheeler et al. [437]. SPLP describe liposomal particles in which DNA is encapsulated in a unilamellar lipid bilayer. They consist of the cationic lipid dioleoyldimethylammonium chloride (DODAC), the fusiogenic lipid dioleoylphosphatidylethanolamine (DOPE) and pegylated ceramide C20 (PEGCerC20) which are combined at a ratio of DOPE:DODAC:PEGCerC20 = 82.5:7.5:10. Particles are synthesized by detergent dialysis method. The final DNA:lipid ratio per SPLP-particle is 62.5 µg/µmol. The resulting particles have a homogenous size of 64 ± 9 nm and contain one plasmid copy number per SPLP. Polyethyleneglycol (PEG)-coating of particles stabilizes SPLP particles in aqueous media. SPLP have been shown to protect encapsidated DNA from nuclease digestion, have a systemic half-life of 6.4 ± 1.1 h, preferentially transfect tumor tissue after systemic injection and are non-toxic. In addition, particles can be stored at 4^0 C for up to 2 years [438, 439].

SPLP were synthesized following description by Fenske et al. [432]. Correct particle size was confirmed by QELS-analysis with a mean particle size of 64.7 nm. SPLP encapsulation efficieny was 92% of input DNA. In the following purification steps, 56% was lost, so that of the total input DNA 36% was finally encapsulated in SPLP. The encapsidation efficiencies achieved in this thesis are in accordance with the maximum packing efficiencies achieved by the original laboratory (Dr. MacLachlan, personal communication). Animals were treated systemically with 100 µl of SPLP-solution (= 100 µg DNA) via tail vein injection directly after synthesis of polyplexes. 24, 48 and 72h after treatment, organs were analyzed for luciferase expression. As in previous experiments, organs of interest included tumor, liver, spleen, kidneys, lungs, brain, heart and muscle.

1.3.3.1. Biodistribution

Initial interest was to evaluate the biodistribution of SPLP after intravenous injection in mice bearing subcutaneous N2A-tumors. For this purpose, SPLP were synthesized using DOPE conjugated to fluorescent rhodamine dye. Mice bearing subcutaneous N2A xenografts were treated with SPLP encapsidating GFP-expressing plasmid EGFP-N1. Route of administration was intravenously via tail vein injection, dose per animal was 100 µg. Biodistribution was analyzed over a time course of 72h following treatment. Animals were sacrificed in 24h intervals, organs harvested and analyzed by fluorescence microscopy.

As shown in Fig. 14, SPLP were found to be distributed in all organs. Though, the extent of accumulation per organ differed. 24h after systemic administration, the highest accumulation of SPLP was observed in the liver. At later time points, the highest

accumulation was found to be in the kidneys and spleen. SPLP accumulation in the spleen started 48h after injection and persisted at a steady state. In the kidneys, SPLP accumulation was observed already after 24h and increased over time. The pattern of

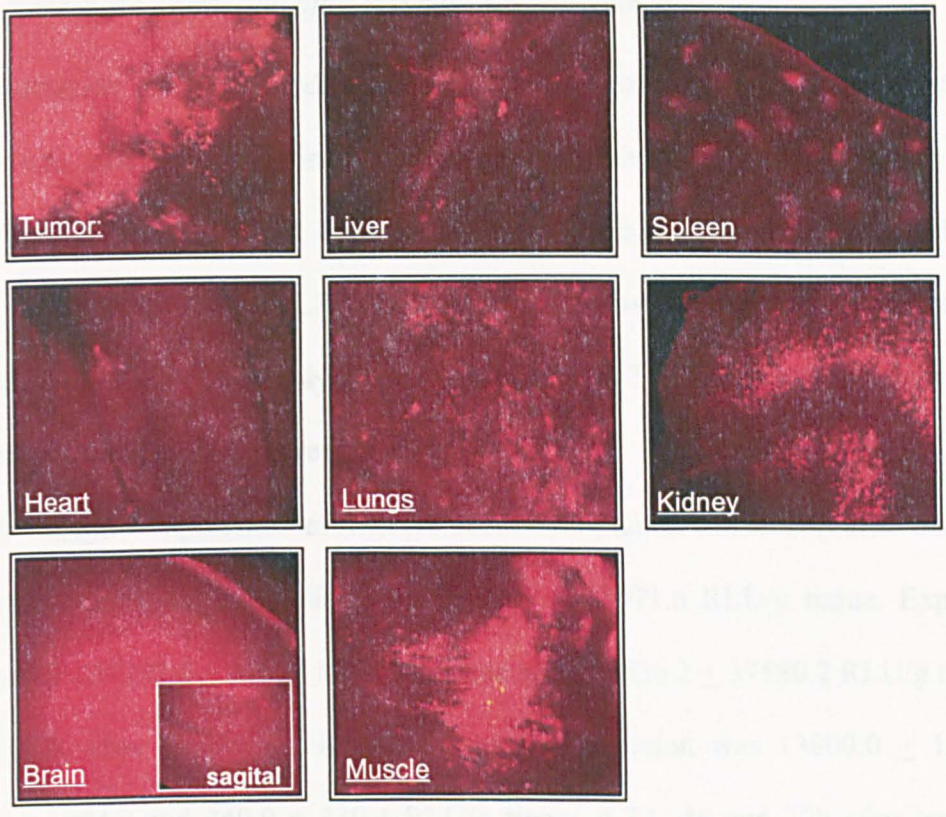

Figure 14: SPLP biodistribution. Mice bearing subcutaneous N2A xenografts were treated intravenously with SPLP conjugated to rodamine. 24, 48 and 72h after treatment animals were sacrificed, organs harvested and analyzed using fluorescence microscopy. Shown is representative SPLP biodistribution at 72h after systemic administration.

renal SPLP-distribution was between cortex and medulla. Relatively high accumulation of SPLP was found within the tumor tissue. Particles were predominantly located perivascular distribution. Lower accumulation was observed in liver (following the initial high accumulation in the initial 24h) and lungs. Very low accumulation of SPLP was seen in heart and brain tissue. In the brain, SPLP were observed in the meningeal

vessels to a high degree at 24h post administration, but none were detected within the brain parenchyma thoughout the 72h time course. Low SPLP accumulation was observed in muscle tissue.

1.3.3.2. Transgene expression after systemic SPLP treatment

After evaluation of SPLP biodistribution, transgene expression after systemic SPLP therapy was analyzed. Experimental settings were identical to the previous SPLP-biodistribution studies. Briefly, mice bearing subcutaneous N2A-tumor xenografts were treated systemically with SPLP. Dose per mouse was 100 pCi-luc DNA, route of administration was intravenously via tail vein injection. Total observation time was 72h, with analysis of transgene expression every 24h.

Highest transgene expression levels were observed in tumor tissue. 24h after treatment, intratumoral transgene expression was 90936.9 $\pm$ 15071.6 RLU/g tissue. Expression increased to 257293.4 $\pm$ 35097.5 RLU/g tissue and 355536.2 $\pm$ 37580.2 RLU/g tissue at 48 and 72h after treatment. Hepatic transgene expression was 13800.0 $\pm$ 16122.0, 2370.0 $\pm$ 1994.0 and 240.0 $\pm$ 339.4 RLU/g tissue at 24, 48 and 72h after treatment. Transgene expression levels measured in spleen were 1415.1 $\pm$ 50.0, 667.6 $\pm$ 97.0 and 632.3 $\pm$ 14.3 RLU/g tissue at the same time points. In the kidneys, transgene expression was highest after 48 h with 2964.8 $\pm$ 3078.0 RLU/g tissue followed by a decrease to 1047.8 $\pm$ 1481.8 RLU/g tissue. In all other organs except muscle, expression was highest after 24h and decreased rapidly over the next 48h to less than 1000 RLU/g tissue. In muscle tissue, transgene expression was stable over time with 1596.7 $\pm$ 116.6 RLU/g tissue after 24h, 1055.1 $\pm$ 260.9 RLU/g tissue after 48h and 2026.1 $\pm$ 1442.6 RLU/g tissue after 72 h.

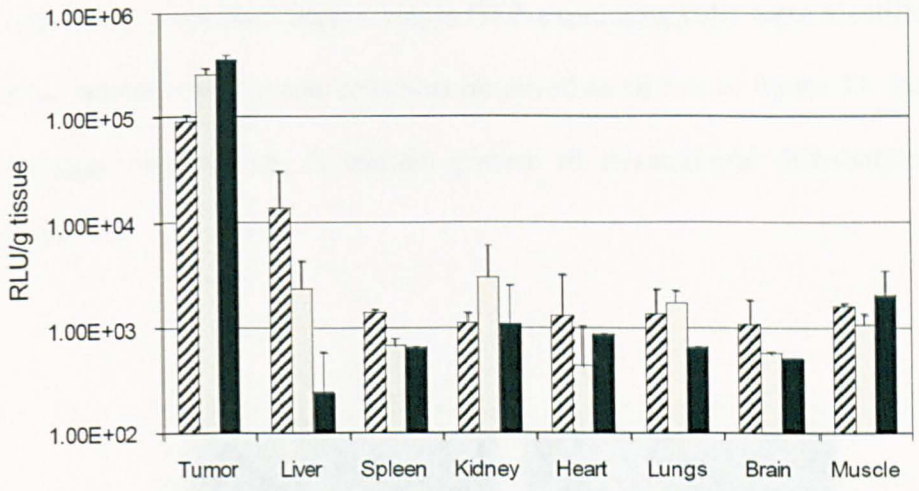

Figure 15: *In vivo* gene expression after systemic therapy with SPLP. Each animal was treated with 100 µg DNA encapsidated in SPLP. 24, 48 and 72h after intravenous injection, organs were harvested and analyzed for luciferase expression. Shown are means with standard errors (n=3).

(▨ = 24h p.i., □ = 48h p.i., ■ = 72h p.i.)

1.3.3.3. Intratumoral distribution of transduced cells

Intratumoral biodistribution of transduced cells is an important factor for the therapeutic efficacy of an agent. The aim of the following experiment was to evaluate the intratumoral distribution of transduced cells after treatment with SPLP. With the exception of the encapsidated plasmid (GFP-expressing pCi-GFP), experimental conditions were identical to the previous SPLP-studies. Briefly, mice bearing subcutaneous N2A-tumor xenografts were treated systemically with pCi-GFP packaged in SPLP. Dose per mouse was 100 µg pCi-GFP DNA, route of administration was intravenously via tail vein injection. Analysis was performed after 72h, based upon previous experiments showing this to be the time point with the highest transgene expression. Analysis was performed by fluorescence microscopy.

Intratumoral biodistribution of transduced cells was very low. The tumor was sectioned in multiple layers. In several layers, single GFP-expressing cells were identified. In one layer, an accumulation of seven cells was observed as shown in figure 33. Intracellular GFP-expression was strong. A distinct pattern of intratumoral distribution was not identifiable.

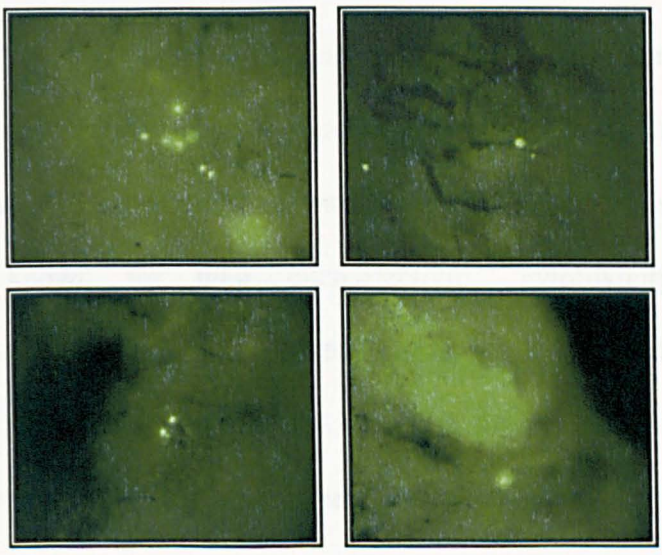

Figure 16: Intratumoral distribution of transduced cells after SPLP treatment. Animals bearing subcutaneous N2A xenografts were treated intravenously with 100 μg of GFP-expressing plamsid EGFP-N1 encapsidated in SPLP. 72h after treatment, animals were sacrificed, tumors harvested and analyzed for GFP-expression using fluorescence microscopy.

2. Expanded parvoviral replicons as novel nonviral gene therapy vectors

2.1. Introduction

The evaluation of non-viral gene delivery systems was able to identify promising non-viral gene delivery systems. However, intratumoral biodistribution and maximum transgene expression were low. Therefore, it was hypothesized in the course of this thesis that the use of replicating expression systems might be able to compensate in part for the low transduction efficiency. In order avoid adverse effects in organ systems other than the tumor, tumor-selectivity was desired. Autonomously replicating parvoviruses are known for their oncoselectivity, cytotoxicity and human apathogenicity. However, their use is impaired by viral immunogenicity. Expansion of parvoviral genome by 6% results in a 10% decrease in encapsidation efficiency of recombinant parvoviruses [133]. This size limitation restricts the choice of transgenes to genes of approximately 0.3 kb as exceeding this size will lead to a significant decrease of viral titers [133, 251]. One of the hypotheses of this study is that the use of the parvoviral genome as a non-viral replication-competent plasmid will allow expansion of the size above these limitations and facilitate the use of large transgenes or transgene combinations. Transfection with parvoviral replicon vectors is hypothesized to result in tumor specific DNA-replication, high-level transgene expression and cytotoxicity. In order to test this hypothesis, recombinant MVMp replicon vectors were generated with expansion of their genome up to 3.5-fold the size of the wildtype.

2.2. Generation of recombinant MVM-replicons

2.2.1. Restoration of the left palindrome

The MVMp genome is available as an infectious plasmid [440]. Parvoviral plasmids used in this study are based on this MVMp plasmid. The original pUC-MVM plasmid was provided by Dr. A. Brandenburger. It contains a pUC18-based plasmid-backbone and the MVMp genome. It has been described that existing infectious parvoviral MVMp clones had an incomplete origin of replication with a defective NS1-nicking site resulting in incomplete parvoviral genome excision (Fig. 17).

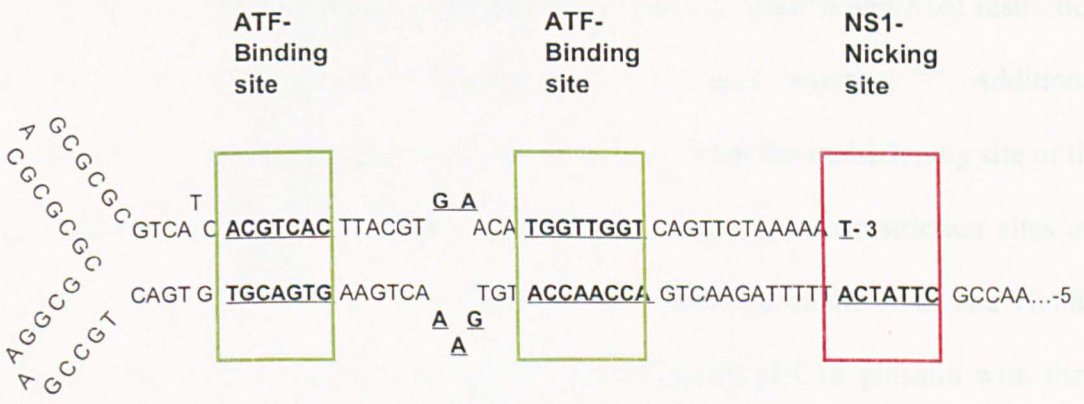

Figure 17: Parvovirus MVM left palindrome. Figure 1 shows an overview over the left palindrome of parvovirus MVM. Indicated are the ATF binding sites as well as the incomplete NS1-nicking site. The "bubble' is also shown

Reconstitution of the NS1 consensus sequence was reported to results in 5-20 times higher parvoviral excision and replication rates [133]. In order to optimize and enhance amplification of MVM-based replicon vectors, the origin of replication site was restored by exchange of the incomplete left palindromic sequence of pUC-MVM with the corresponding sequence of pORI3375, a MVMp-clone containing the correct left palindromic sequence (provided by Dr. A. Brandeburger) [441]. A 407 bp fragment

including the left palindromic sequence was excised from pUC-MVMp using restriction enzymes KpnI and EcoRV, and replaced with the corresponding DNA fragment from KpnI/EcoRV-treated pORI3375. Control digest as well as sequencing analysis confirmed intact sequence of right and left MVMp palindromes. The resulting modified MVM-vector was named pUC-MVMp+.

2.2.2. Genetic modification of pUC-MVMp+

2.2.2.1. Deletion of interfering restriction sites

In order to achieve transgene expression under control of the P38 promoter and maintain the functional elements within the MVM genome, HindIII and XbaI restriction sites of the parvoviral genome were chosen for transgene insertion [218]. Additional HindIII and XbaI restriction sites were also identified within the multicloning site of the pUC18-backbone of pUC-MVMp+ requiring their deletion; both restriction sites are located in 5'-direction of a BamHI restriction site. Deletion of the XbaI and HindIII restriction sites was achieved by restriction hydrolysis of pUC18 plasmid with these enzymes, followed by blunt-ending with exonuclease treatment and religation. The MVMp+ genome was excised from the original pUC-MVMp+ vector by restriction hydrolysis with BamHI and inserted in the corresponding site of the modified pUC18 plasmid vector. Successful deletion of the XbaI and HindIII restriction sites in the modified pUC18 backbone of the newly generated pUC-MVMp+ was confirmed by restriction hydrolysis with HindIII and XbaI followed by agarose gel electrophoresis.

2.2.2.2. Insertion of polylinker sequence

In order to expand the parvoviral genome without interference of transcriptionally essential sequences, a region between the functional element A/B and the right end palindrome was chosen as insertion site for stuffer DNA (Fig. 18). In order to create an insertion site for stuffer DNA of different length, a polylinker containing unique restriction sites was designed (AscI, NheI, AvrII, BsiWI, AflII, SacII, AscI). This

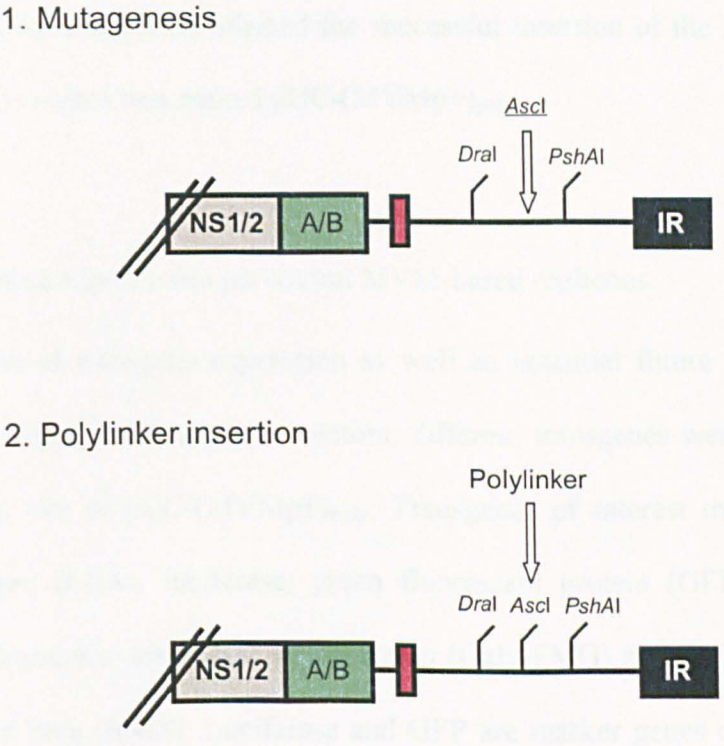

Figure 18: Cloning strategy for insertion of stuffer DNA. MVM PshAI was subcloned into pUC18. A AscI restriction site was inserted between the DraI and PshAI site by mutagenesis. The modified PshAI fragment was cloned back into the original MVM vector. Subsequently, a polylinker was cloned into the AscI site. The polylinker was later used for insertion of stuffer DNA derived from Λ-DNA.

polylinker contained restriction sites neither present in the stuffer DNA nor in the pUC-MVMp+ sequence. For insertion of this polylinker, an AscI restriction site needed to be created in between the DraI and PshAI restriction sites of pUC-MVMp+. This was achieved by restriction hydrolysis of pUC-MVMp+ with PshAI, followed by subcloning

of the resulting 4.25 kb parvoviral PshAI-fragment into the SmaI restriction site of pUC18 by blunt-end ligation. An AscI restriction site was inserted between the DraI and PshAI restriction site by mutagenesis. After confirmation of successful generation of the AscI site by restriction hydrolysis, the modified PshAI fragment was reinserted in the parvoviral genome in its prior position. Next, the above-described polylinker was generated by nucleic acid synthesis followed by annealing of the complementary DNA strands. The resulting polylinker was inserted in the AscI restriction site of pUC-MVMp+. Restriction analysis confirmed the successful insertion of the polylinker into MVMp+. The new vector was named pUC-$(MVMp+)_{poly}$.

2.2.3. Insertion of transgenes into parvoviral MVM-based replicons

For quantification of transgene expression as well as potential future diagnostic and therapeutic use of parvoviral replicon vectors, different transgenes were inserted into the HindIII/XbaI site of pUC-$(MVMp+)_{poly}$. Transgenes of interest included carcino embryonic antigen (CEA), luciferase, green fluorescent protein (GFP), gibbon ape leukemia virus-fusogenic membrane glycoprotein (Galv-FMG) and the human sodium iodide symporter gene (hNIS). Luciferase and GFP are marker genes commonly used for detection of gene expression. Soluble human carcinoembryonic antigen (hCEA) is a 677 amino-acid glycoprotein of molecular weight 180kD with a circulating half-life of 36 hours and no known biological activity in humans. Its normal serum concentrations are less than 5 ng/ml but it is commonly elevated in gastrointestinal and gynecologic human malignancies and therefore used as a tumor-marker in these conditions [106]. Its cloning into a gene therapy vector provides important information about successful tumor tranduction as well as tumor growth and viral amplification kinetics [106]. The

human sodium iodide symporter (hNIS) is an intrinsic membrane glycoprotein mainly expressed in the follicular cells of the thyroid. It facilitates iodine uptake in thyrocytes by a symporter mechanism transporting one iodine ion together with two Na-ions against the Na-gradient maintained by the Na-K-ATPase resulting in an intracellular concentration of iodide 20- to 40-fold above plasma concentration. Its function as an iodine transport protein makes it an intresting candidate as a cancer gene therapy transgene. Expression of this transgene followed by administration of radioiodine results in accumulation of the isotope in hNIS-expressing cells. Tumor-selective hNIS expression can be used diagnostically or for therapeutic purposes. For example, administration ^{123}I followed by imaging analysis allows non-invasive detection of hNIS overexpressing cells. If administered by a systemic gene therapy vector, it can also provide information about systemic and intratumoral biodistribution. If hNIS expression is followed by systemic administration of ^{131}I, it serves as a tumor specific therapeutic gene for radio-sensitive malignancies [431]. The potential of this transgene has been shown in several tumor models including myeloma and prostate cancer [108, 304, 307, 431]. Viral fusogenic membrane glycoproteins (FMG) and (NIS) are therapeutic genes which proved their strong antitumor potential in different tumor-models. Galv-FMG normally restricts fusion of the envelope until it is cleaved during viral infection. By truncating the C-terminus of the wildtype-protein, GALV-FMG becomes highly fusogenic to human cells. Its expression in human tumor cells results in syncytia formation and induction of immune stimulatory heat shock proteins, leading to cell death. Transgenes were synthesized by PCR-techniques, gel-purified and directly cloned in the pUC-$(MVMp+)_{poly}$ plasmid.

Figure 19 (see below): Cloning strategy of recombinant parvoviral replicons vectors. A) Shown is a schematic overview of the MVMp genome (middle). The internal repeats (IR) are indicated as black boxes, the coding regions of the non-structural proteins 1 and 2 (NS1/2) as light-grey box, the coding regions for capsid proteins (VP1/2) as dark-grey box and the poly A location as a white-and-black-hatched box. Also shown are the relative position of the promoter P4 and P38 as well as the restriction sites used for insertion of the transgenes. For insertion of transgenes, a DNA fragment of the coding region for VP1/2 was excised with HindIII and and XbaI restriction hydrolysis, followed by insertion of PCR-generated transgenes into the corresponding restriction sites. Transgenes included marker genes such as carcinoembryonic antigen (CEA), green-fluorescent protein (GFP) and luciferase, and the diagnostic as well as therapeutic human iodide symporter (hNIS) and therapeutic gibbon ape leukaemia virus hyperfusogenic glycomembrane protein (Galv-FMG). Insertion of the genes resulted in alterations of the parvoviral genome size as indicated next to the transgenes. In a second step, a polylinker sequence was inserted between the poly A sequence and the right IR. Using the polylinker restriction sites, 6 kb or 13 kb Lambda DNA-derived stuffer DNA was inserted into predefined polylinker restriction sites. B) Schematic overview of generated, recombinant MVM replicon vectors. For further details, see text.

Fig. 19 A:

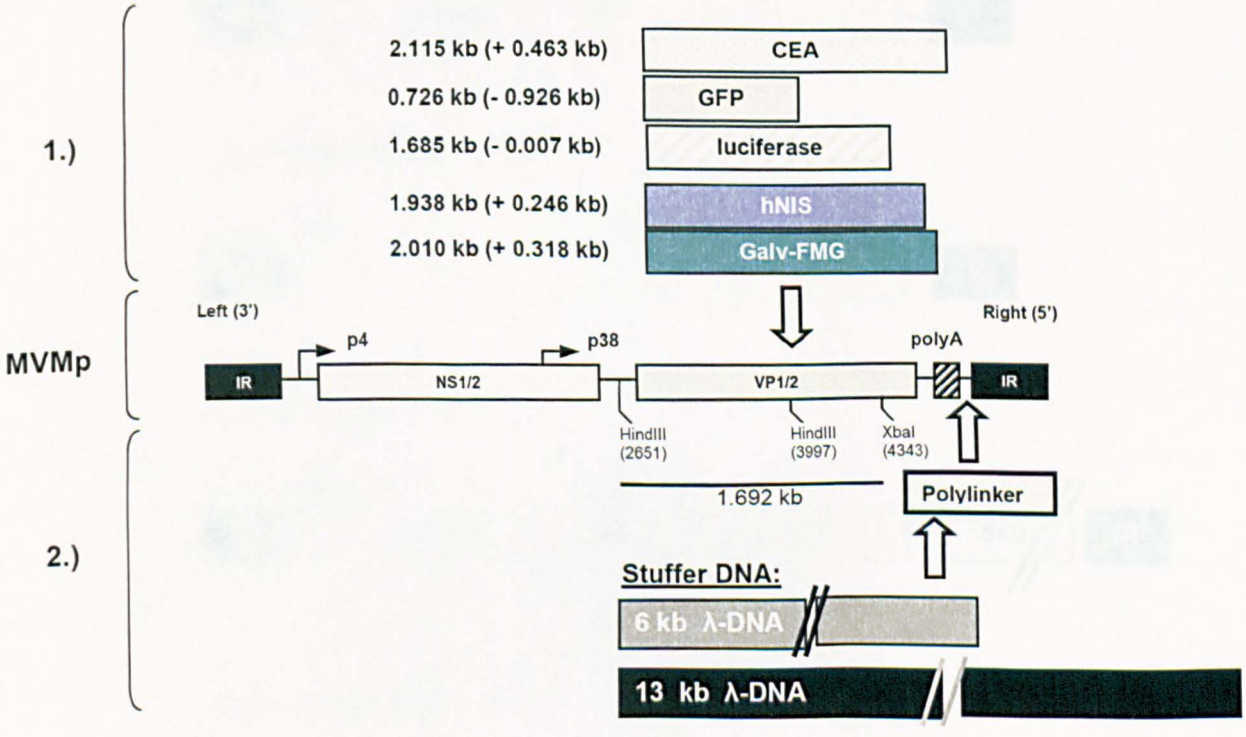

Fig. 19 B:

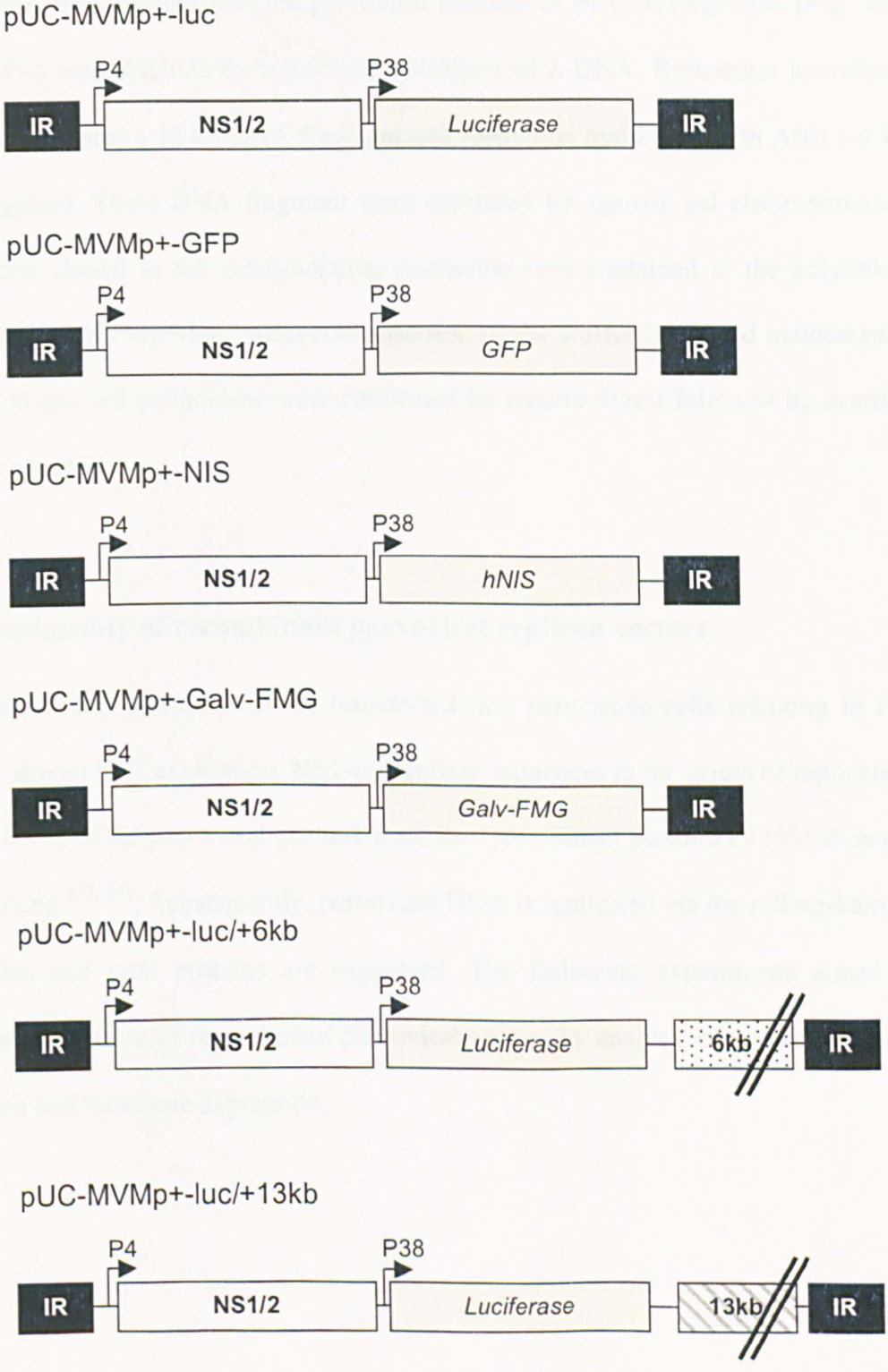
pUC-MVMp+-luc
P4
P38
IR
NS1/2
Luciferase
IR
pUC-MVMp+-GFP
P4
P38
IR
NS1/2
GFP
IR
pUC-MVMp+-NIS
P4
P38
IR
NS1/2
hNIS
IR
pUC-MVMp+-Galv-FMG
P4
P38
IR
NS1/2
Galv-FMG
IR
pUC-MVMp+-luc/+6kb
P4
P38
IR
NS1/2
Luciferase
6kb
IR
pUC-MVMp+-luc/+13kb
P4
P38
IR
NS1/2
Luciferase
13kb
IR

2.2.4. Expansion of parvoviral MVM-based replicon vectors

In order to evaluate the expansion potential of parvoviral replicon vectors, 6 and 13 kb stuffer DNA was inserted into the parvoviral genome of pUC-MVMp+-luc (Fig. 20). Stuffer DNA was obtained by restriction hydrolysis of λ-DNA. Restriction hydrolysis with AscI generated a 13 kb DNA fragment and restriction hydrolysis with AflII a 6 kb DNA fragment. These DNA fragment were separated by agarose gel electrophoresis, isolated and cloned in the corresponding restriction sites contained in the polylinker region of pUC-MVMp+-luc. Successful insertion of the stuffer DNA and maintenance of the right and left palindrome were confirmed by control digest followed by agarose gel-electrophoresis.

2.3. Functionality of recombinant parvoviral replicon vectors

Infectious MVMp plasmids can be transfected into permissive cells resulting in P4-promoter driven NS1-expression. NS1-recognition sequences in the origin of replication allow excision of the parvoviral genome from the recombinant plasmid by NS1-directed DNA nicking [133, 440]. Subsequently, parvoviral DNA is replicated via the rolling-hairpin mechanism and viral proteins are expressed. The following experiments aimed at functional evaluation of recombinant parvoviral vectors by analysis of parvoviral DNA replication and transgene expression.

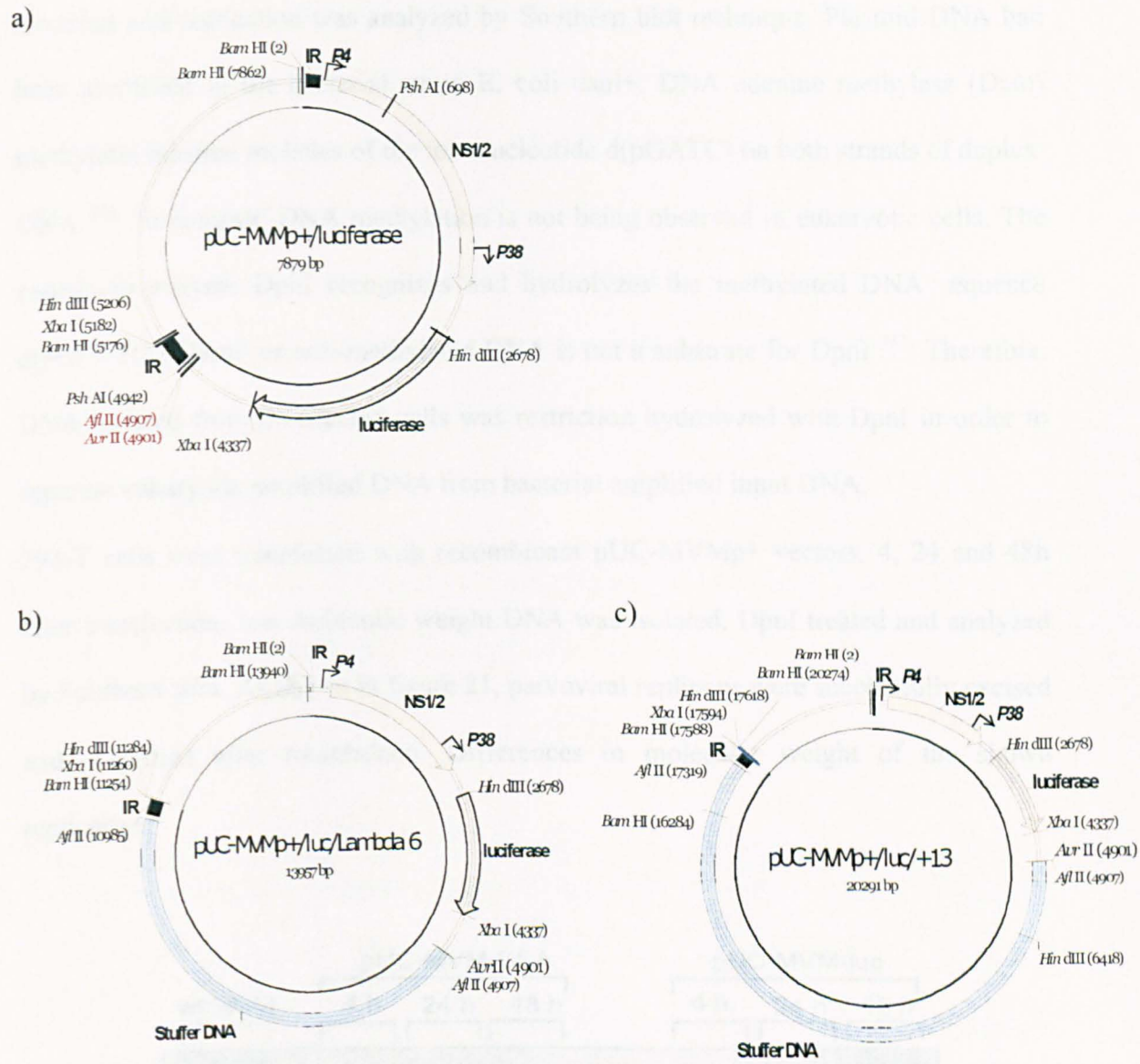

Figure 20: Parvoviral replicons vectors. Plasmid vector maps of luciferase expressing parvoviral replicon vectors pUC-MVMp+/luc as well as the expanded parvoviral replicons pUC-MVMp+/luc/Lambda 6 and MVMp+/luc/+13. Indicated are internal repeats (IR, black box), coding regions of viral non-structural proteins 1 and 2 (NS1/2, grey box), the luciferase transgene (black-and-white-hatched box) and promoters P4 and P38. The plasmid backbone is shown as black double line and stuffer DNA, derived from Lamda vector, is shown as blue-and-white-hatched box. Also, different restriction sites are shown which have been used for cloning of these recombinant parvoviral vectors. The circle in the inside of the vector map indicates the parvoviral genome (solid black line) and the backbone derived from pUC18 (interrupted black line).

2.3.1. Excision and amplification of parvoviral DNA

Excision and replication was analyzed by Southern blot technique. Plasmid DNA had been amplified in the bacterial strain E. coli dam+. DNA adenine methylase (Dam) methylates adenine moieties of the tetranucleotide d(pGATC) on both strands of duplex DNA [442]. In contrast, DNA methylation is not being observed in eukaryotic cells. The restriction enzyme DpnI recognizes and hydrolyzes the methylated DNA sequence d(pG^{m}ATC). Hemi- or non-methylated DNA is not a substrate for DpnI [443]. Therefore, DNA isolated from transfected cells was restriction hydrolyzed with DpnI in order to separate eukaryotic amplified DNA from bacterial amplified input DNA.

293-T cells were transfected with recombinant pUC-MVMp+ vectors. 4, 24 and 48h after transfection, low molecular weight DNA was isolated, DpnI treated and analyzed by Southern Blot. As shown in figure 21, parvoviral replicons were successfully excised and amplified after transfection. Differences in molecular weight of the shown replicative

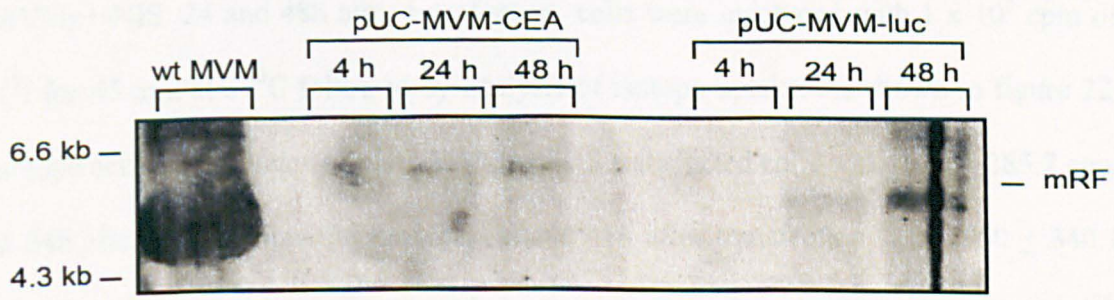

Figure 21: Excision and amplification of recombinant parvoviral replicons. 293-T cells were transfected with pUC-MVMp+-CEA and pUC-MVMp+-luc. 4, 24 and 48 h after transfection, low molecular weight DNA was isolated from cells, DpnI-digested and analyzed by Southern blot technique. As a size marker, pUC-MVMp+ was digested with BamHI resulting in excision of parvoviral genome from its backbone (left lane). It serves as a size marker for identification of parvoviral DNA in the other lanes. Molecular size of MVMp+-CEA is 0.46 kb larger than MVMp+. The first replication intermediate appears after 4h followed by increasing intensity of the band. pUC-MVMp+-luc replication intermediates can first be seen clearly at 24h post transfection. It also increases in its intensity over time.

forms are consistent with length differences of recombinant parvoviral vectors: MVMp+ is 5.1 kb, MVMp+-luc is 5.1 kb and MVMp+-CEA is 5.6 kb in size. Very low intensity signals of monomeric replicative intermediates of parvoviral DNA were observed 4h after transfection. Clear detection of monomeric forms was observed 24h after transfection and signal intensity increased over the following 24h indicative of continuous intracellular parvoviral DNA amplification. As expected, single-stranded parvoviral DNA was not detected, as generation ssRF requires VP2 protein.

2.3.2. Transgene expression

Analysis of transgene expression showed high-level transgene expression of all recombinant MVM-based replicon vectors (Fig. 22-24).

2.3.2.1. pUC-MVMp+-hNIS

In order to evaluate NIS-transgene expression, 293-T cells were transfected with pUC-MVMp+-NIS. 24 and 48h after transfection, cells were incubated with 1 x 10^5 cpm of ^{125}I for 45 min at 37^0C followed by analysis of isotope uptake. As shown in figure 22, isotope activity in lysates of pUC-MVMp+-NIS transfected cells was 1976 $\pm$ 285.2 cpm at 24h after transfection and remained stable 48h after transfection with 1950 $\pm$ 340.1 cpm. In comparison, isotope activity in lysates of untransfected cells incubated with ^{125}I was 287 $\pm$ 58.4 cpm at 24h and 367.7 $\pm$ 34.4 cpm at 48h. In order to test NIS-specificity of ^{125}I-uptake, cells were co-incubated with ^{125}I and potassium perchlorate – a known inhibitor of hNIS-mediated iodine uptake. pUC-MVMp+-NIS transfected cells were co-treated with 1 x 10^5 cpm ^{125}I and 1µM potassium perchlorate followed by gamma

counter analysis of cell lysates. 24 and 48h after transfection, ^{125}I-activity in cell lysates was 129.7 $\pm$ 59.8 cpm and 653 $\pm$ 22.9 cpm.

The results of these studies show that transfection with pUC-MVMp+-NIS results in expression of hNIS-protein facilitating a 5.3 to 6.9-time increase in iodine uptake in transfected cells.

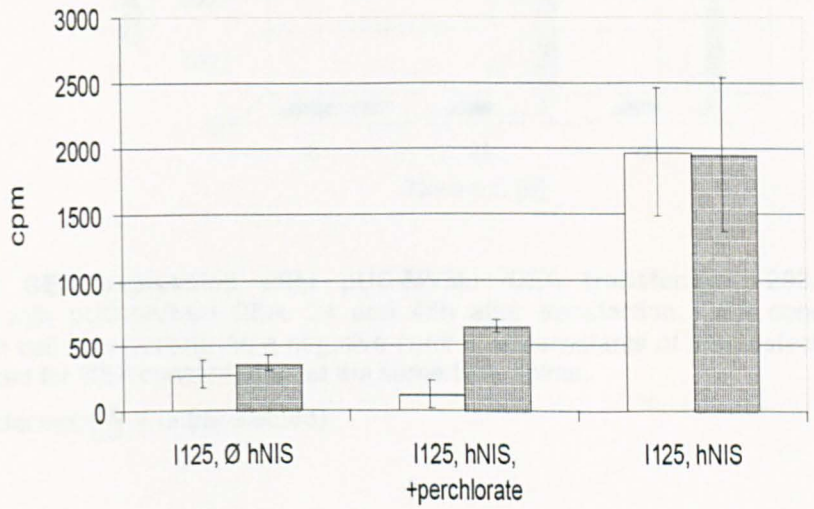

Figure 22: ^{125}I-uptake after pUC-MVMp+-NIS transfection. 293-T cells were transfected with pUC-MVMp+-NIS followed by incubation with ^{125}I or co-treatment with ^{125}I and NIS-inhibitor potassium perchlorate 24h and 48h after transfection. As a negative control, untransfected 293-T cells were also treated with ^{125}I in the presence and absence of potassium perchlorate treatment at the same time points. Isotope incubation of cells was followed by cell lysis and gamma radiation emission analysis using a gamma counter.
(□ = 24h post transfection, ■ = 48h post transfection)

2.3.2.2. pUC-MVMp+-CEA

CEA-expression after pUC-MVMp+-CEA transfection was analyzed in 293-T cells. Analysis was performed by quantification of CEA concentration in the cell supernatant as described in material and methods. 24h after transfection, CEA concentration was 194.3 ng/ml and increased to 532.2 ng/ml 48h post transfection. In contrast, CEA concentration in the supernatant of untransfected 293-T cells was <0.5 ng/ml at all time points (Fig. 23).

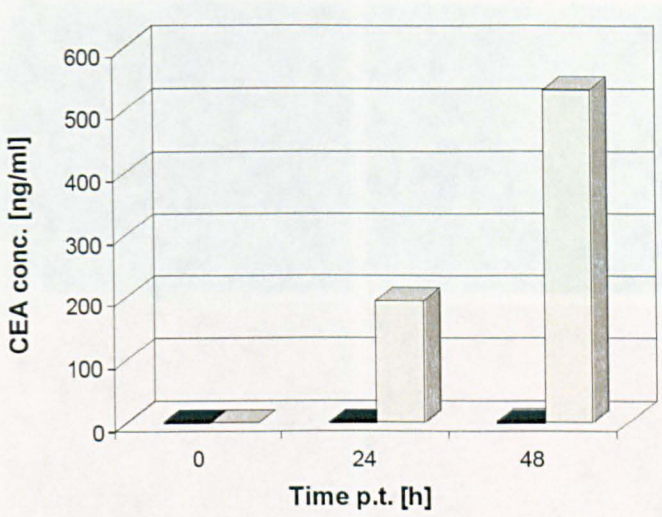

Figure 23: CEA expression after pUC-MVMp+-CEA transfection. 293-T cells were transfected with pUC-MVMp+-CEA. 24 and 48h after transfection, CEA concentration was measured in cell supernatant. As a negative control, supernatants of untransfected 293-T cells were analyzed for CEA concentration at the same time points.

(■ = transfected, □ = untransfected)

2.3.2.3. pUC-MVMp+-GFP

GFP-expression after transfection with pUC-MVMp+-GFP was evaluated in 293-T cells. Cells were transfected using lipotransfection methods followed by fluorescence microscopic evaluation. Transfection with pUC-MVMp+-GFP resulted in strong GFP-expression in transfected cells. GFP-expressing cells were first detectable 24h after transfection and continuously increased over the following 48h in number of cells expressing GFP and intracellular intensity of GFP-expression (Fig. 24).

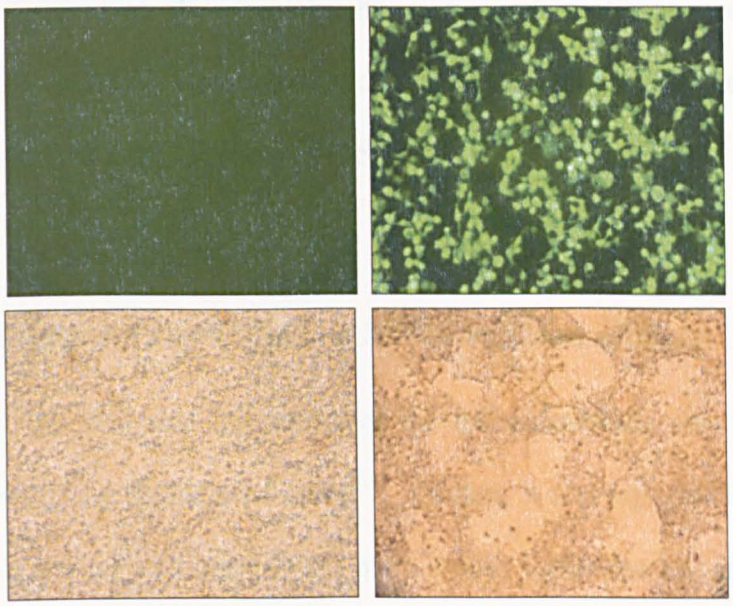

Figure 24: Transgene expression after transfection with recombinant parvoviral replicons. Shown are 293-T cells after transfection with recombinant parvoviral replicons vectors. The bottom panel represents lightmicroscopic analysis of 293-T cells 48h after transfection with pUC-MVM-FMG showing extensive syncytia formation and cell death. The upper panel represents fluorescence microscopic analysis of cells 48h after transfection with pUC-MVM-GFP. Left on the upper and bottom panel, untransfected cells are shown serving as a negative control.

2.3.2.4. pUC-MVM-FMG

Expression of Galv-FMG-expression was analyzed by light microscopy after transfection of 293-T cells with with pUC-MVMp+-FMG. Expression of Galv-FMG causes syncytium formation followed by cell death [305]. Transfection of 293-T cells with pUC-MVMp+-FMG resulted in significant syncytia formation starting 24h after transfection with continuously increasing syncytia size and number (Fig. 24). 72h after transfection the complete cell layer was destroyed.

2.3.3. Summary

The data demonstrate, that the recombinant parvoviral replicons are functional. Parvoviral genome excision, replication and protein expression are not negatively influenced by above described genetic modifications.

2.4. Effect of palindrome restoration on MVM-replicon efficacy

Previously, it was reported that restoration of the left palindrome resulted in higher replication rates as well as higher viral titers [133]. Further, it was reported that transgene expression of parvoviruses with restored left-palindromic sequences was at least 6-timer higher than with defective viruses [444]. Within the 3'-end of existing infectious clones, a NS1-nicking site is deleted, causing decreased excision of parvoviral DNA from the plasmid backbone. Based upon the previous observation of increased replication rates following restoration of the left palindrome, it was hypothesized for this thesis that restoration of the left palindrome will also result in increased MVM genome copy numbers, higher transgene expression levels and thereby increased efficacy of MVM-replicons. Restoration of the left palindrome was achieved as described in section 2.2.1..

2.4.1. Replication

A9-cells were transfected with pUC-MVMp/luc containing the incomplete left palindromic sequence or with pUC-MVMp+/luc containing the restored NS1 nicking site. 24 and 48h after transfection, low-molecular weight DNA was isolated, DpnI treated and analyzed by Southern blot analysis (Fig. 25). 24h post transfection,

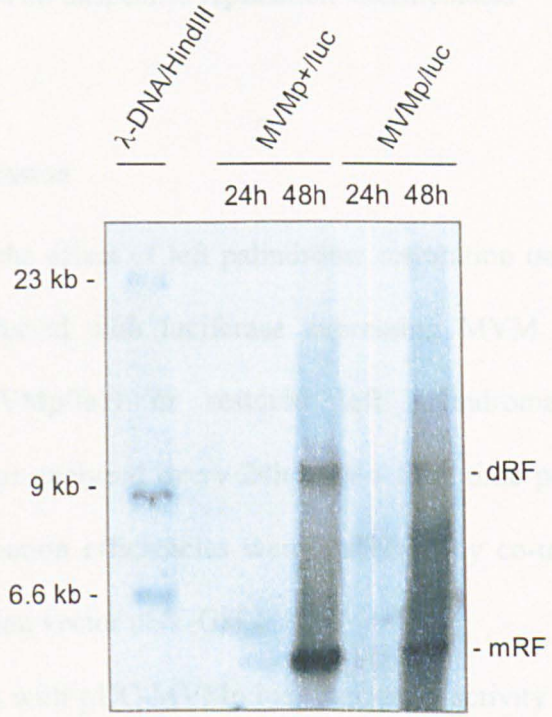

Figure 25: Comparison of parvoviral DNA-replication with incomplete and restored left palindrome. A9-cells were transfected with parvoviral replicons with incomplete (MVMp/luc) or restored left palindrome (MVMp+/luc). 24 and 48h after transfection, low molecular weight DNA was isolated, DpnI treated and analyzed by Southern blot technique. HindIII treated λ-DNA was used as a size marker (6.6, 9 and 23 kb DNA fragments are shown on the left). Parvoviral replicative intermediates are indicated on the right side (mRF = monomeric replicative form, dRF = dimeric replicative form).

monomeric, replicative intermediate forms of parvoviral DNA were detected in cells transfected with pUC-MVMp+-luc and pUC-MVMp/luc. However, signal intensity was higher in cells transfected with pUC-MVMp+-luc. In the following 24h, signal intensity

of monomeric as well as duplex replciative intermediates continued to increase. Also 48h after transfection, signal intensity of intracellular amplified parvoviral DNA was significantly higher after transfection with pUC-MVMp+-luc than after transfection with pUC-MVMp/luc. A single band was detected in cell lysates of pUC-MVMp/luc transfected cells at ~7.0 kb. This band was also seen at increased intensity 48 h after transfection and

correlates most likely with unspecific replication intermediates [251].

2.4.2. Transgene expression

For quantification of the effect of left palindrome restoration on transgene expression, A9 cells were transfected with luciferase expressing MVM replicon vectors with incomplete (pUC-MVMp/luc) or restored left palindrome (pUC-MVMp+/luc). Luciferase activity was analyzed every 24h over a total time period of 96h (Fig. 26). Differences in transfection efficiencies were corrected by co-transfection with the β-galactosidase expression vector pSV-Gal.

24h after transfection with pUC-MVMp/luc, luciferase activity in A9 cell lysates was 6.69×10^6 RLU/mg protein/β-gal. Luciferase activity increased in the following 72h to 1.66×10^7, 2.46×10^7 and 2.96×10^7 RLU/mg protein/β-gal at 48, 72 and 96h after transfection. In comparison, luciferase activity in cells transfected with MVMp+/luc was 3.59×10^7, 8.48×10^7, 2.02×10^8 and 2.50×10^8 RLU/mg protein/β-gal at 24, 48, 72 and 96h after transfection.

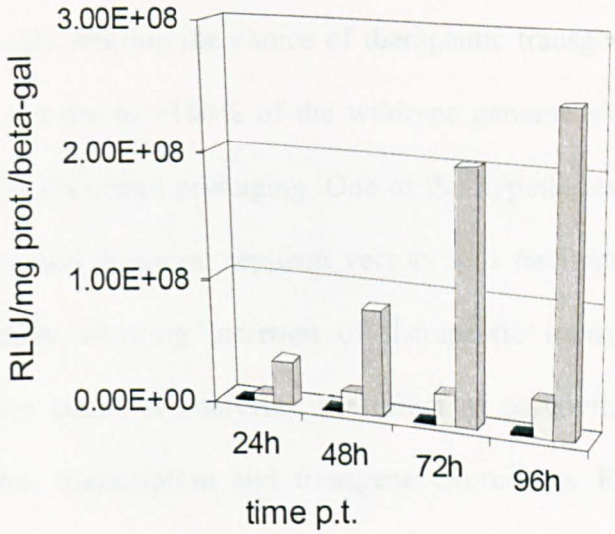

Figure 26: Effect of left palindrome restoration on transgene expression. A9 cells were transfected with MVMp/luc containing the incomplete left palindrome or MVMp+/luc containing the restored left palindrome. Differences in transfection efficiency were corrected by cotransfection with pSV-Gal. Luciferase and β-Gal activity were analyzed 24, 48, 72 and 96h after transfection (p.t.), n=8.

(■ = neg. control, □ = pUC-MVMp/luc, ▨ = pUC-MVMp+/luc)

In summary, restoration of the left palindrome results in an increase in transgene expression of factor 5.4 already 24h after transfection. 96h after transfection, this difference in expression level increased to an 8.4-fold difference. These data demonstrate that restoration of the left palindrome results in significant improvement of parvoviral expression plasmids with almost 10-fold difference in expression levels.

2.4.3. Summary

The results of these studies show that restoration of the left palindrome of MVMp-based non-viral replicons achieves a significant increase in parvoviral replication and transgene expression levels, thereby increasing their efficacy.

2.5. Expanded parvoviral replicons

Parvovirus H1 and MVM are restricted as viral gene therapy vectors by genome size limitations severely limiting the choice of therapeutic transgenes [133, 441]. Expansion of the parvoviral genome to >106% of the wildtype genome size results in decrease of viral titers due to decreased packaging. One of the hypotheses of this thesis is that the use of MVMp-based non-viral replicon vectors will facilitate expansion beyond this size limit, thereby allowing insertion of therapeutic transgenes of any size. The following studies aimed at analyzing the effect of parvoviral genome-expansion on DNA replication, transcription and transgene expression. Expanded MVMp+-based replicon vectors were generated as described above (section 2.2.4.); the genome sizes of these vectors were 255% and 355% of the wildtype MVMp genome.

2.5.1. Transcription

293-T cells were transfected with $4.5x10^4$ plasmid copy numbers per cell of pUC-MVMp+/luc, pUC-MVMp+/luc/+6kb or pUC-MVMp+/luc/+13kb; the non-replicating expression plasmid pCi/luc was used as a negative control. 48 and 72h after transfection, cellular RNA was isolated and analyzed by Reverse Transcriptase-PCR (RT-PCR) using parvoviral NS1-specific primers.

No transcription product was observed in pCi-luc transfected cellular RNA at any timepoint (Fig. 27). In contrast, the first transcription products in parvoviral DNA transfected cells were observed 48h after transfection. Intensities of RT-PCR products

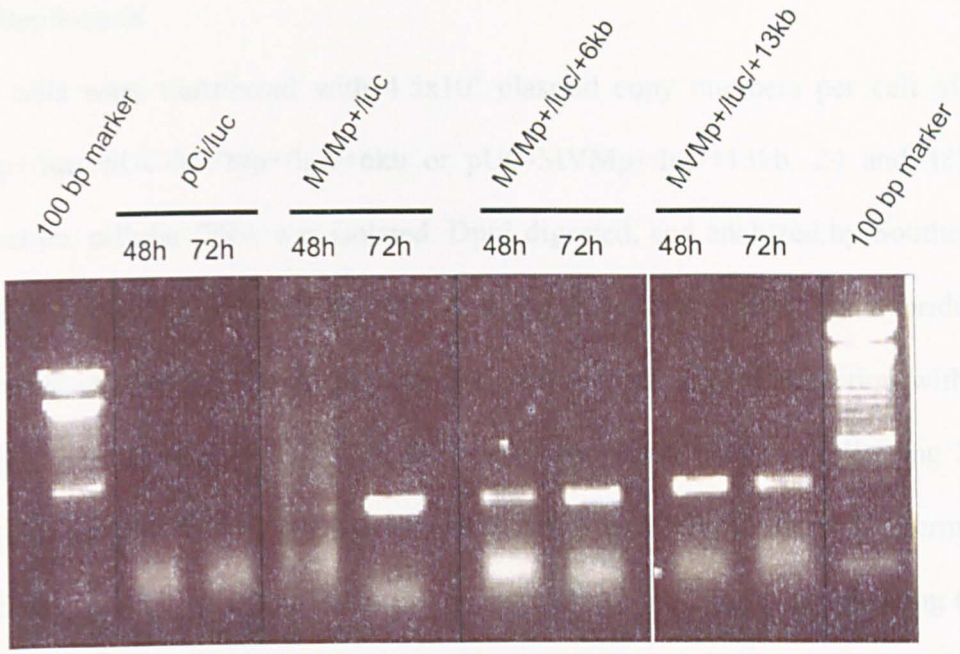

Figure 27: Transcriptional efficiency of expanded parvoviral replicon vectors. 293-T cells were transfected with pCi-luc, pUC-MVMp+/luc or expanded parvoviral replicon vectors pUC-MVMp+/luc/+6 kb or pUC-MVMp+/luc/+6 kb. 48 and 72h after transfection, RNA was isolated and transcription products visualized by RT-PCR followed by gel-electrophoresis. The very left and the very right lane are loaded with a 100 bp DNA-marker. No band was observed in pCi/luc transfected cellular RNA. In contrast, in parvoviral and expanded parvoviral DNA transfected cellular RNA, the NS1-specific band can be identified.

differed between all three plasmids. 48h post transfection, the lowest intensity was observed in pUC-MVMp+-luc transfected cells and the highest in MVMp+-luc/+13 transfected cells. Signal intensity of MVMp+-luc and MVMp+-luc/+6 RNA RT-PCR products increased markedly over the following 24h. Interstingly, RT-PCR products of MVMp+-luc/+13 transfected cells were found to be the highest 48h after transfection followed by a mild decrease. Overall comparison of the three parvoviral constructs showed efficient transcription in all of them. Expansion of the parvoviral genome had resulted in mildly decreased transcription efficiency and had also altered transcription kinetics.

2.5.2. Replication

293-T cells were transfected with $4.5x10^4$ plasmid copy numbers per cell of pUC-MVMp+/luc, pUC-MVMp+/luc/+6kb or pUC-MVMp+/luc/+13kb. 24 and 48h after transfection, cellular DNA was isolated, DpnI digested, and analyzed by Southern blot technique (Fig. 28). A 390 bp NS1 specific probe was used for hybridization. Replicative intermediates were observed as early as 24h after transfection with pUC-MVMp+/luc. Intensity of mRF and dRF bands increased over the following 24h. In DNA-extracts of MVMp+/luc/+6 transfected cells, parvoviral replication intermediates were observed 48 h after transfection. The intensity of the band corresponding to mRF was decreased in comparison to the corresponding bands of MVMp+/luc. In DNA extracts of cells transfected with pUC-MVMp+/luc/+13, the first parvoviral replicative intermediates were observed 48h after transfection. The intensity of this mRF-corresponding band of MVMp+/luc/+13 was very low compared to corresponding bands in MVMp+/luc and MVMp+/luc/+6kb DNA extracts. Unspecific bands were seen. These bands have been described previously by Brandenburger et al. as multimeric replicative forms [251]. Our data demonstrate, that parvoviral replicon vectors tolerate expansion of up to 355%. However, size increase results in reduction of genome replication.

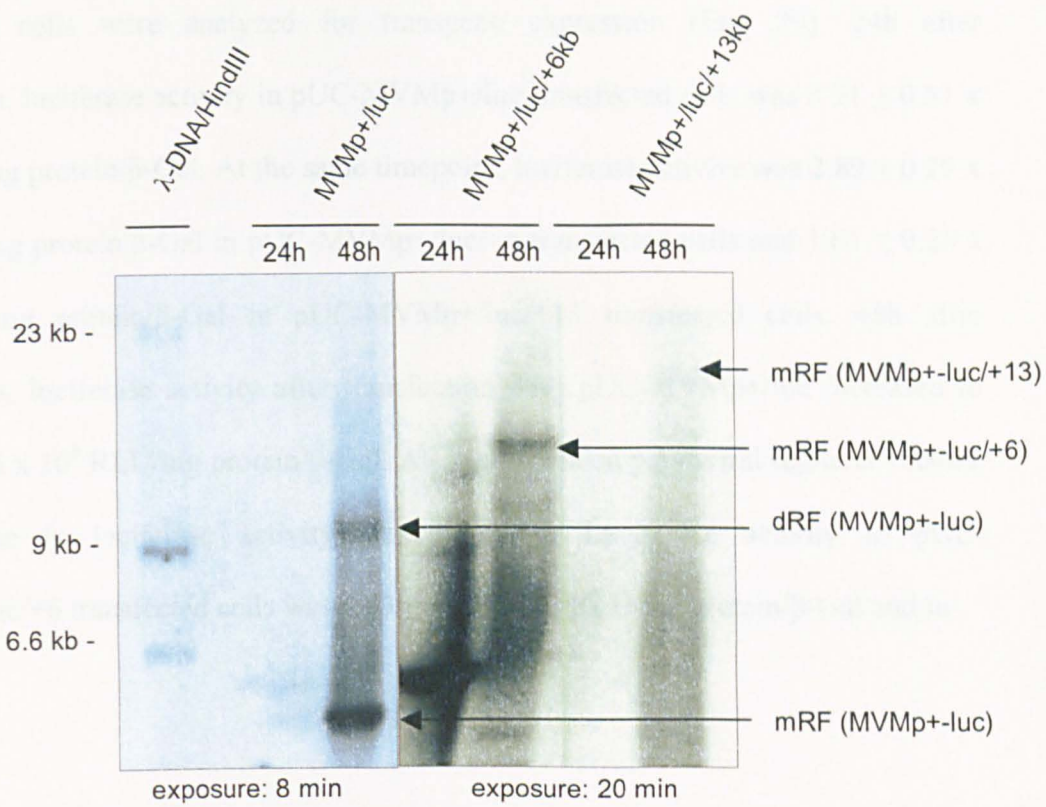

Figure 28: Replication of expanded parvoviral replicon vectors. Figure 28 shows results of the southern blot analysis of total cellular DNA isolated from 293-T cells transfected with pUC-MVMp+/luc or expanded parvoviral replicons pUC-MVMp+/luc/+6kb and pUC-MVMp+/luc/+13kb Time points of analysis are 24 and 48h after transfection. HindIII digested λ-DNA was used as a size marker. On the left, 6.6, 9 and 23 kb fragments are indicated. On the right, parvoviral replication intermediates are indicated (mRF = monomeric replicative form, dRF = duplex replicative form).

2.5.3. Transgene expression

After confirmation of functional replication and transcription of expanded parvoviral replicon vectors, transgene expression of expanded parvoviral replicons was evaluated. 293-T cells were transfected with 1.3 x 10^5 plasmid copy numbers of MVMp+/luc, MVMp+/luc/+6 and MVMp+/luc/+13 per cell. Cells were co-transfected with pSV-Gal for correction of differences in transfection efficiency. 24, 48 and 72h after transfection,

transfected cells were analyzed for transgene expression (Fig. 29). 24h after transfection, luciferase activity in pUC-MVMp+/luc transfected cells was 5.31 ± 0.51 x 10^8 RLU/mg protein/β-Gal. At the same timepoint, luciferase activity was 2.89 ± 0.29 x 10^7 RLU/mg protein/β-Gal in pUC-MVMp+/luc/+6 transfected cells and 1.64 ± 0.26 x 10^7 RLU/mg protein/β-Gal in pUC-MVMp+/luc/+13 transfected cells. 48h after transfection, luciferase activity after transfection with pUC-MVMp+/luc increased to 9.78 ± 0.85 x 10^8 RLU/mg protein/β-Gal. Also in expanded parvoviral replicon vectors, an increase in luciferase activity was observed. Luciferase activity in pUC-MVMp+/luc/+6 transfected cells was 6.53 ± 0.45 x 10^7 RLU/mg protein/β-Gal and in

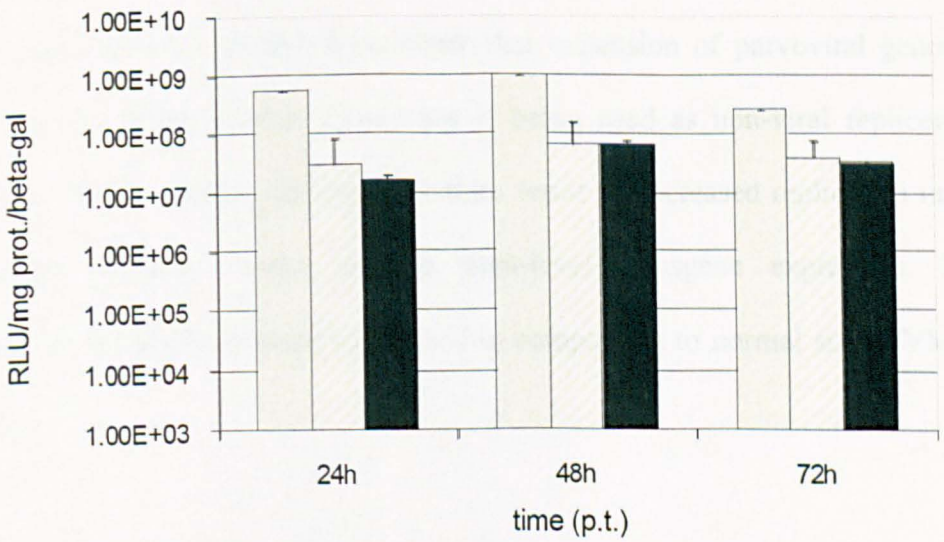

Figure 29: Transgene expression after transfection with expanded parvoviral replicon vectors. 293-T cells were transfected with wildtype-sized and expanded parvoviral replicon vectors. Co-transfection was performed with pSV-Gal for correction of differences in transfection efficiency. 24, 48 and 72 h after transfection, cells were analyzed for luciferase expression

(□ = pUCMVMp+, ▨ = pUC-MVMp+/luc/+6kb, ■ = pUC-MVMp+/luc/+13kb)

pUC-MVMp+/luc/+13 transfected cells 6.69 ± 0.37 x 10^7 RLU/mg protein/β-Gal. 72h after transfection, transgene expression slightly decreased. In pUC-MVMp+/luc transfected cells, luciferase activity was 2.61 ± 0.03 x 10^8 RLU/mg protein/β-Gal. At the same time point, luciferase activity in pUC-MVMp+/luc/+6 transfected cells was 3.93 ± 0.2 x 10^7 RLU/mg protein/β-Gal and in pUC-MVMp+/luc/+13 3.35 ± 0.2 x 10^7 RLU/mg protein/β-Gal. Comparison between wildtype-sized and expanded parvoviral replicon vectors shows that expansion to 255% of the wildtype size results in 18.3, 14.9 and 6.6-fold reduction of transgene expression levels at 24, 48 and 72 h after transfection. Expansion up to 355% results in reduction of transgene expression of factor 32.4, 14.6 and 7.7 at 24, 48 and 72 h after transfection.

2.5.4. Summary

The results of these studies demonstrate that expansion of parvoviral genome up to 355% of the wildtype size is tolerated if being used as non-viral replicon vectors. However, the increase in genome size does result in decreased replication rates. Also, expanded replicon vectors achieve high-level transgene expression. However, expression levels are reduced up 30-fold in comparison to normal size MVM replicon vectors.

2.6. Parvoviral replicons in comparison to other expression systems

In permissive cells, parvoviral replicon vectors provide high-level transgene expression due to their persistent replication and amplification through NS1-mediated transactivation of the P38-promoter, which regulates transgene expression in the MVMp+-based vectors. In order to compare their expression potential and pattern,

parvoviral replicon vectors were compared with other replicating and non-replicating expression plasmids chosen for their ability to provide high-level transgene expression. These included pCi-luc, a non-replicating plasmid expressing luciferase under the control of an enhanced CMV promoter, as well as the replicating expression plasmid pCEP4/luc. pCEP4/luc is based on EBV and contains the EBV sequences OriP and EBNA-1 which facilitate plasmid replication. pCEP4/luc expresses luciferase under the control of the CMV promoter. Cotransfection of the beta-gal expressing plasmid pSV-GAL was performed in order to correct for differences in transfection efficiency.

Transfection of MRC-5 cells with pCi-luc resulted in maximum luciferase activity 24h after transfection with $1.42 \pm 0.52 \times 10^8$ RLU/mg protein/β-gal followed by a continous decrease of luciferase activity to $7.70 \times 10^6 \pm 2.45 \times 10^6$ RLU/mg protein/β-gal at 96h after transfection. Transfection with pCEP4/luc resulted in relatively stable luciferase expression starting 24h after transfection with $6.59 \pm 4.07 \times 10^7$ RLU/mg protein/β-gal followed by $1.22 \pm 0.6 \times 10^8$, $7.51 \pm 1.80 \times 10^7$ and $6.94 \pm 3.82 \times 10^7$ RLU/mg protein/β-gal at 48, 72 and 96h after transfection. Transfection with pMVMp+/luc resulted in luciferase expression levels in the range of the negative control due to the non-malignant origin of the cell line. In the negative control group, luciferase expression fluctuated around 6×10^6 RLU/mg protein/β-gal over the 96h time course. Maximum luciferase activity in pUC-MVMp+/luc transfected cells was $4.45 \pm 0.5 \times 10^5$ RLU/mg protein/β-gal (Fig. 30 a).

As shown in figure 30 b, transfection of A9 cells with pCi-luc results in luciferase expression up to $8.41 \pm 0.12 \times 10^7$ RLU/mg protein/β-gal within the first 24h. Luciferase activity stayed stable during the following 24h, followed by a sharp decrease in luciferase activity to $3.91 \pm 0.34 \times 10^7$ RLU/mg protein/β-gal after 96h. Transfection with pCEP4/luc resulted only in low-level luciferase activity up to 8.72×10^6 RLU/mg

a)

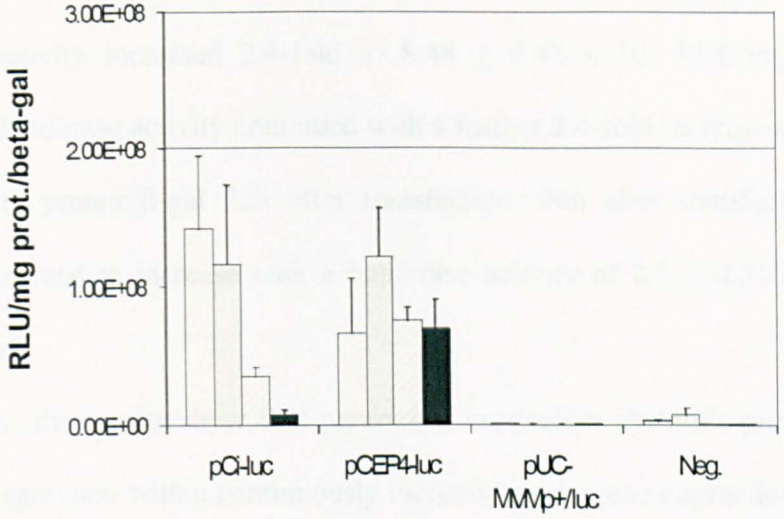

b)

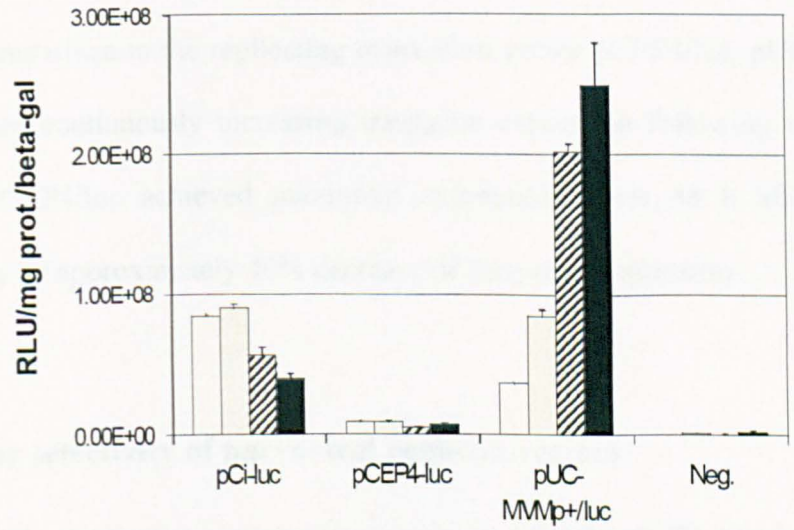

Figure 30: Comparison of parvoviral replicon vectors with replicating and non-replicating high-level expression vectors. MRC-5 (Fig. a) and A9 (Fig. b) cells were transfected with non-replicating expression vector pCi-luc or replicating parvoviral vector pMVMp+-luc or EBV-based vector pCEP4/luc. Differences in transfection efficiency were corrected by co-transfection with β-Gal expressing plasmid pSV-Gal. 24, 48, 72 and 96h after transfection, transfected and untransfected cells (neg. contr.) were analyzed for luciferase expression (n=3).

(⊡ = 24 h p.t., □ = 48h p.t., ◪ = 72h p.t., ■ = 96h p.t.)

protein/β-gal. Transfection with the parvoviral replicon vector pUC-MVMp+/luc resulted in increasing high-level luciferase expression. 24h after transfection, luciferase

activity was 3.59 ± 0.13 x 10^7 RLU/mg protein/β-gal. During the following 24h, luciferase activity increased 2.4-fold to 8.48 ± 0.42 x 10^7 RLU/mg protein/β-gal. Increase in luciferase activity continued with a further 2.4-fold increase to 2.02 ± 0.05 x 10^8 RLU/mg protein/β-gal 72h after transfection. 96h after transfection, luciferase activity continued to increase with a luciferase activity of 2.5 ± 0.31 x 10^8 RLU/mg protein/β-gal.

In summary, the results show that parvoviral expression plasmids provide high-level transgene expression with a continuously increasing transgene expression pattern. pUC-MVMp+-luc replicon vectors achieved 2.81-fold higher expression levels than pCi-luc in permissive cells but protein expression was suppressed in non-malignant human cells. In comparison to the replicating expression vector pCEP4/luc, pUC-MVMp+-luc demonstrated continuously increasing transgene expression following transfection. In contrast, pCEP4/luc achieved maximum expression levels 48 h after transfection followed by an approximately 40% decrease of transgene expression.

2.7. Tumor selectivity of parvoviral replicon vectors

Autonomously replicating parvoviruses such as MVM and H1 are known for their oncoselectivity. It is unknown if their oncoselectivity is preserved if parvoviruses are used as non-viral, infectious DNA plasmids. Therefore, the following studies aimed at evaluating the tumor-selectivity of non-viral MVMp-based replicon vectors. Transformation of cells has been shown to sensitize them toward autonomously parvoviruses allowing parvoviral replication and expression. Therefore, normal cell lines (NIH-3T3, Wi38 and MRC-5) and their transformed derivatives (V12-3T3, Wi38/V13 and MRC-5/V1) were used for analysis. Parvoviral replicon vectors

MVMp+-GFP and MVMp+-luc were used for fluorescence microscopic analysis and quantification of oncoselectivity. Non-tumor selective expression vectors EGFP-N1 and pCi-luc were used as controls for specificity of parvoviral tumor-selectivity

As shown in figure 31, transfection of untransformed NIH-3T3 and Wi38 cells as well as transformed V12-3T3 and Wi38/V13 cells with EGFP-N1 resulted in strong GFP expression. In contrast, no GFP-expression was observed after transfection of untransformed NIH-3T3 and Wi38 cells with MVMp+/GFP. However, transfection of their transformed derivatives V12-3T3 and Wi38/V13 with pUC-MVMp+/GFP resulted in strong GFP-expression.

Transformation of MRC-5 cells and Wi38 with MVMp+/luc resulted in sensitization to parvoviral replicon mediated transgene expression (Fig. 32). 24h after transfection, luciferase activity in MRC-5 cells was 8 RLU/β-Gal compared to 7151 RLU/ β-Gal in MRC-5/V1 cells. 48h after transfection, luciferase activity in MRC-5 cells was relatively unchanged with 16 RLU/β-Gal compared to increasing transgene expression with 8614 RLU/ β-Gal in MRC-5/V1 cells. 24h later, luciferase activity was 47 RLU/ β-Gal in MRC-5 cells and in MRC-5/V1 cells had continued to increase to 12393 RLU/ β-Gal. Similar results were obtained in Wi38 and their transformed counterpart Wi38/V13. 24h after transfection, luciferase activity in Wi38 cells 8 RLU/ β-Gal, and in Wi38/V13 cells 8526 RLU/ β-Gal. Luciferase activity 48h after transfection was stable at 8 RLU/ β-Gal in Wi38 cells and increased to 15622 RLU/ β-Gal in Wi38/V13 cells. 72h after transfection, luciferase activity in Wi38 cells was 119 RLU/ β-Gal and in Wi38/V13 24949 RLU/ β-Gal.

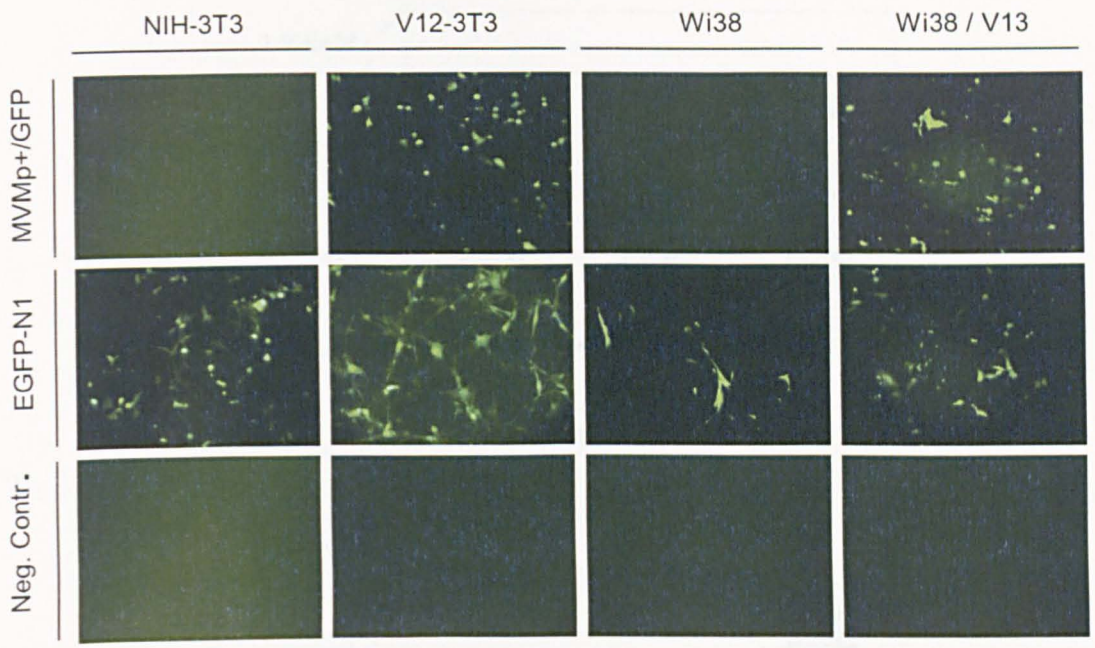

Figure 31: Tumorselectivity of parvoviral replicon vectors. Untransformed NIH-3T3 and Wi38 cells were transfected with parvoviral replicon vector pUC-MVMp+/GFP or expression plasmid EGFP-N1. 48 h after transfection, cells were analyzed by fluorescence microscopy for GFP-expression. For demonstration of background fluorescence, untransfected cells are shown (bottom row). As a positive control, cells were transfected with EGFP-N1 (middle row). Top row shows normal cells and their transformed counterparts transfected with parvoviral replicon vector pUC-MVMp+-GFP.

These results confirm the results of the first experiment using pUC-MVMp+-GFP. Transformation of cell lines MRC-5 and Wi38 resulted in their sensitization toward parvoviral replicon vectors. Comparison between normal cells and their transformed counterparts shows that transfection with parvoviral replicon vectors results in up to 893.9-fold higher transgene expression in MRC-5/V1 cells compared to MRC-5 cells, and up to 1952.8-fold higher transgene expression in Wi38/V13 cells compared to Wi38 cells.

b)

a)

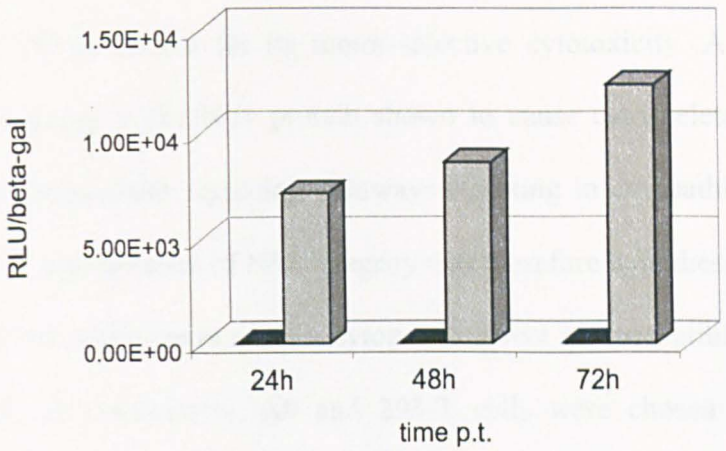

b)

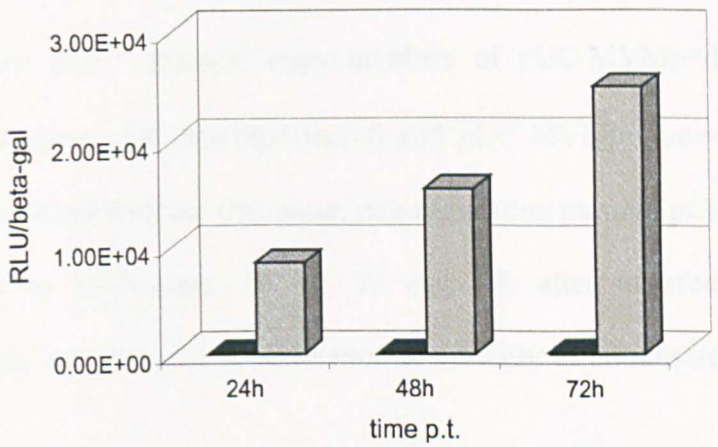

Figure 32: Tumorselectivity of parvoviral replicon vectors. Untransformed MRC-5 and Wi38 cells and their transformed counterparts MRC-5/V1 and Wi38/V13 were transfected with parvoviral replicon vector pUC-MVMp+-luc. For correction of differences in transfection efficiency, cells were co-transfected with β-Gal expressing pSV-Gal. 24, 48 and 72 h after transfection, luciferase activity was analyzed. a) Cell lines MRC-5 and MRC-5/V1. b) Cell lines Wi38 and Wi38/V13.

(■ = normal cell line, □ = transformed cell line).

In summary, no significant transgene expression was observed in normal cells after transfection with parvoviral replicon vectors. Transformation of normal cells resulted in sensitization toward parvoviral replicon vectors with high-level transgene expression. These results demonstrate that tumor selectivity is conserved if parvoviral vectors are used as replicating, double-stranded DNA expression plasmids.

2.8. MVM-replicon cytotoxicity

Parvovirus MVM is known for its tumor-selective cytotoxicity. A key mediator of parvoviral cytoxicity is the NS1 protein shown to cause cytoskeletal changes and to interfere with intracellular signaling pathways resulting in cytopathic effects and cell death [161, 445-447]. Maintenance of NS1 integrity was therefore hypothesized to enable also parvovirus MVM replicons to elicit a cytopathic effect on susceptible target cells. For the evaluation of cytotoxicity, A9 and 293-T cells were chosen based upon their susceptibility toward parvoviral cytotoxicity. Using lipotransfection, $2x10^4$ cells were transfected with $2x10^{10}$ plasmid copy numbers of pUC-MVMp+/luc or one of its expanded derivatives pUC-MVMp+/luc/+6 and pUC-MVMp+/luc/+13. As a control, cells were transfected with the non-toxic, non-replicating plasmid pCi-luc. Cell viability was analyzed by MTS-assay 24, 48, 72 and 96h after transfection. Viability of transfected cells was assessed in correlation to viability of untransfected A9 and 293-T cells.

The data show that none of the parvoviral replicon vectors elicited a cytotoxic effect on transfected cells. Viability of MVM-transfected cells fluctuated between $99.3\pm16.7\%$ and $162.3\pm37.3\%$ of untransfected cells over the time course of 96h (Fig. 33). Statistical analysis showed no significant difference in viability of cells transfected with parvoviral versus non-parvoviral plasmids ($p>0.05$).

In summary, parvoviral replicon vectors do not maintain the cytotoxic potential of the parental virus.

a)

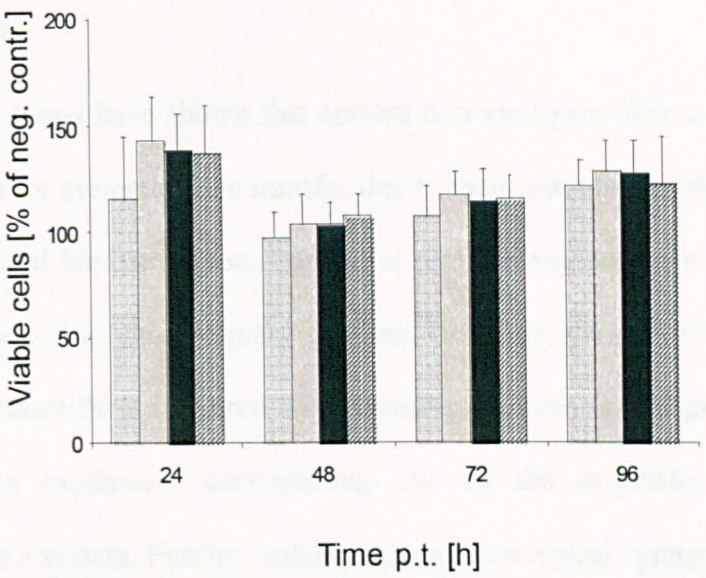

b)

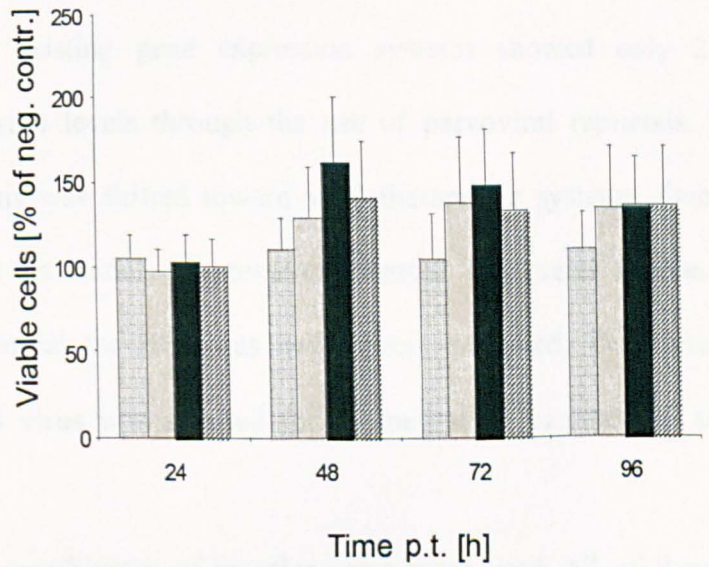

Figure 33: MVM replicon cytotoxicity. Cells were transfected with pCi-luc as a control, or with one of the MVM-replicons pUC-MVM, pUC-MVM/+6 or pUC-MVM/+13. 24, 48, 72 and 96h after transfection (p.t.), cell viability was measured using MTS-assay. Viability is shown as percent of untransfected cells. A) Viability of A9 cells, B) viability of 293-T cells. (n=16, shown are average values with standard deviation).
(▩= pCi-luc, □= pUC-MVMp+-luc, ■= pUC-MVMp-luc/+6, ◪= pUC-MVMp-luc/+13)

3. Viral gene therapy using recombinant measles virus

3.1. Introduction

The results of this thesis have shown that current non-viral gene delivery systems are suboptimal vectors for systemic gene transfer due to their low transduction efficiencies and poor intratumoral biodistribution. Parvoviral replicon vectors were developed for encapsidation in non-viral gene delivery systems. However, the parvoviral data show that their use as plasmids is impaired by decreasing replication and gene expression with genome size expansion, contradicting one of the originally hypothesized advantages of such a system. Further, wildtype parvovirus typical cytotoxicity was lost. Maintained were the ability for replication and the tumorselectivity. However, comparison with existing gene expression systems showed only 2.8-fold higher maximum expression levels through the use of parvoviral replicons. Therefore, the focus of this thesis was shifted toward viral therapeutic systems. Oncolytic measles virus has proven its tumor suppressive potential in several human malignancies. However, its potential for HCC has never been evaluated. Therefore, recombinant, oncolytic measles virus was selected for evaluation of its potential as a therapeutic vector for HCC.

Three different recombinants of measles virus were used, all of them based on the Edmonston strain of measles virus (MV-Edm) and genetically modified to express different transgenes as previously described: CEA-expressing measles virus (MV-CEA), GFP-expressing measles virus (MV-eGFP) and NIS-expressing measles virus (MV-NIS) (Fig. 34).

a) MV-CEA:

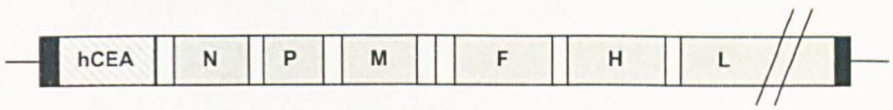

b) MV-eGFP:

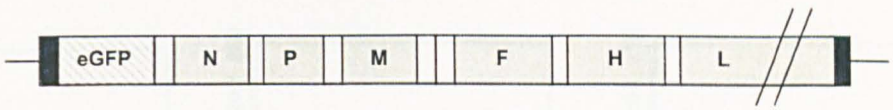

c) MV-NIS:

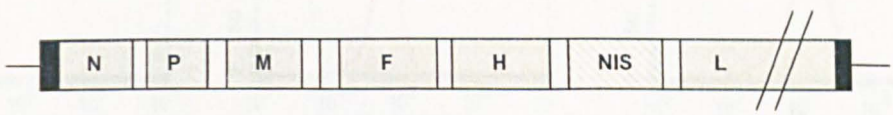

Figure 34: Schematic representation of recombinant MV-Edm. Schematic representation of the genome of recombinant MV-Edm constructs showing the coding regions for viral proteins and the intergenic regions. *N*, nucleoprotein gene; *P*, phosphoprotein gene; *M*, matrix protein gene; *F*, fusion protein gene; *H*, hemagglutinin gene; *L*, polymerase gene. The P cistron encodes two additional proteins: C protein and V protein. Figure a) is an overview of the genome of recombinant MV-Edm coding for the human carcinoembryonic antigen (hCEA) as described previously (Peng et al., 2002). Figure b) shows the genome of recombinant MV-Edm encoding enhanced green fluorescent protein (eGFP) as described previously (Duprex et al., 2000). Below in figure c), the genome of recombinant MV-Edm coding for the human sodium iodide symporter (NIS) is shown, as described previously (Dingli et al., 2002).

3.2. Human HCC express high levels of CD46

MV-Edm induced syncytia formation requires CD46 overexpression. Therefore, the initial studies focused on the evaluation of CD46 expression by human HCC cell lines compared to primary human hepatocytes, and in intraoperatively obtained human HCC tumor samples. CD46 expression levels of human HCC cell lines, HUH-7 and Hep-3B, and primary human hepatocytes were analyzed by flow cytometry. Human HCC cell lines express high levels of CD46 compared to primary human hepatocytes. In

comparison to isotype control, a 2.68-fold increase in median fluorescencnce in primary human hepatocytes incubated with a FITC-labeled monoclonal anti human CD46 antibody was observed. In HUH-7 cells, the increase in median fluorescence was 17.47-

a)

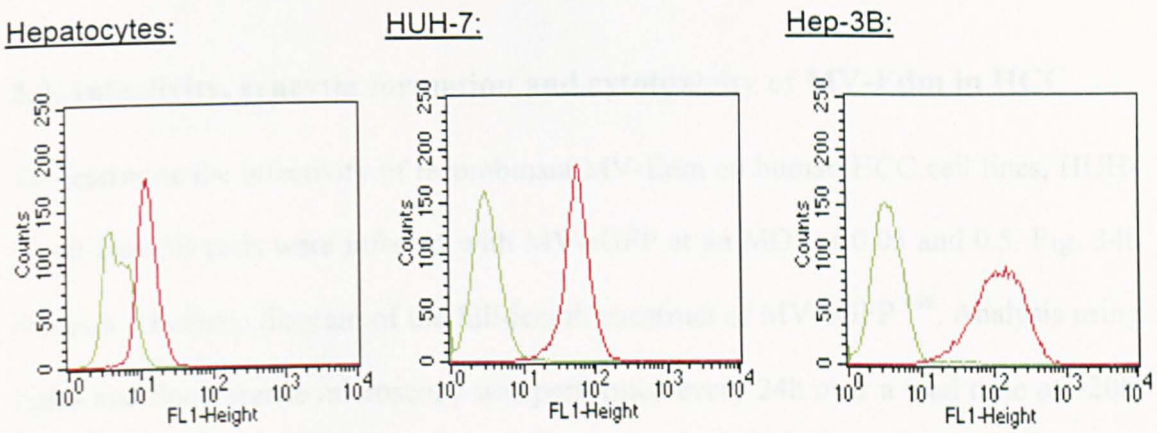

b

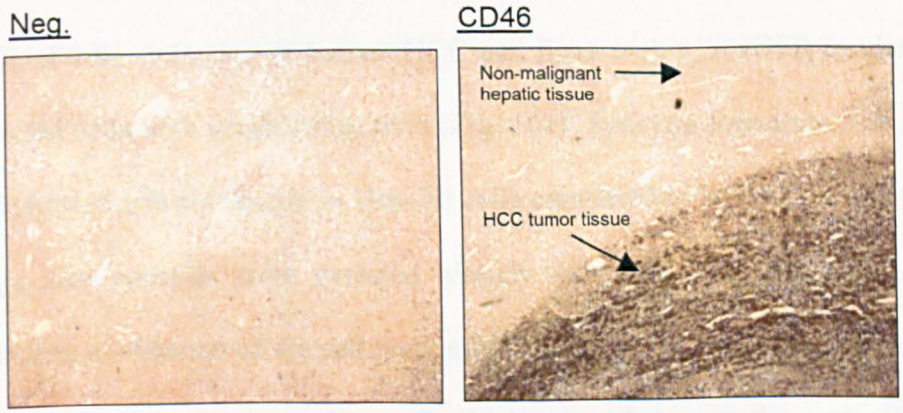

Figure 35: CD46-overexpression in HCC in comparison to normal hepatic tissue. Figure a) shows high expression of the CD46-receptor on human HCC cell lines HUH-7and Hep-3B but low expression on primary human hepatocytes. Analysis was performed by flowcytometry using a monoclonal CD46-antibody (*red histogram*: anti-CD46 FITC antibody; *green histogram*: isotype control). b) Immunofluorescence for CD46-receptor in HCC-tissue samples and non-malignant hepatic tissue using a anti-human CD46 primary antibody and a fluorescein isothiocyanate-conjugated secondary antibody. The arrows highlight the border between normal hepatic tissue and tumor-tissue.

fold and in Hep-3B cells 16.36-fold (Fig. 35a). CD46 expression in HCC in comparison to non-malignant hepatic tissue was analyzed by immunohistochemistry in human hepatic tissue samples of HCC patients (n = 3). As shown in Fig. 35b, CD46 is overexpressed in HCC-tissue compared to surrounding normal hepatic tissue. This result was confirmed in 100% of analyzed human tissue samples.

3.3. Infectivity, syncytia formation and cytotoxicity of MV-Edm in HCC

To determine the infectivity of recombinant MV-Edm on human HCC cell lines, HUH-7 and Hep-3B cells were infected with MV-eGFP at an MOI of 0.05 and 0.5. Fig. 34b shows a schematic diagram of the full-length construct of MV-eGFP [448]. Analysis using light- and fluorescence microscopy was performed every 24h over a total time of 120h. All human HCC cell lines were successfully infected by MV-eGFP (Fig. 36a). As early as 24h after infection, GFP-expression was observed in infected cells even at a low MOI of 0.05. Infection of human HCC cell lines with MV-eGFP resulted in fusion of infected cells with neighboring cells (Fig. 36a). Syncytia formation was more dramatic and showed a faster kinetic in Hep-3B cells compared to HUH-7 cells. In Hep-3B cells, large size syncytia were detected already 48h after infection followed by almost complete eradication of the cell layer after 96h. In HUH-7 cells, infected cells as well as small size syncytia were observed which expanded over the next 48h in size and number.

MV-Edm mediated CPE on HCC cells was quantified. Hep-3B and HUH-7 cells were infected with MV-eGFP at MOI 0.05 and 0.5. Analysis was performed every 24h over a total time course of 120h using crystal violet staining and CellTiter 96 AQueous nonradioactive cell proliferation assay. On both cell lines, recombinant MV-Edm elicited a strong CPE in a MOI dependent manner (Fig. 36b and c). Differences between

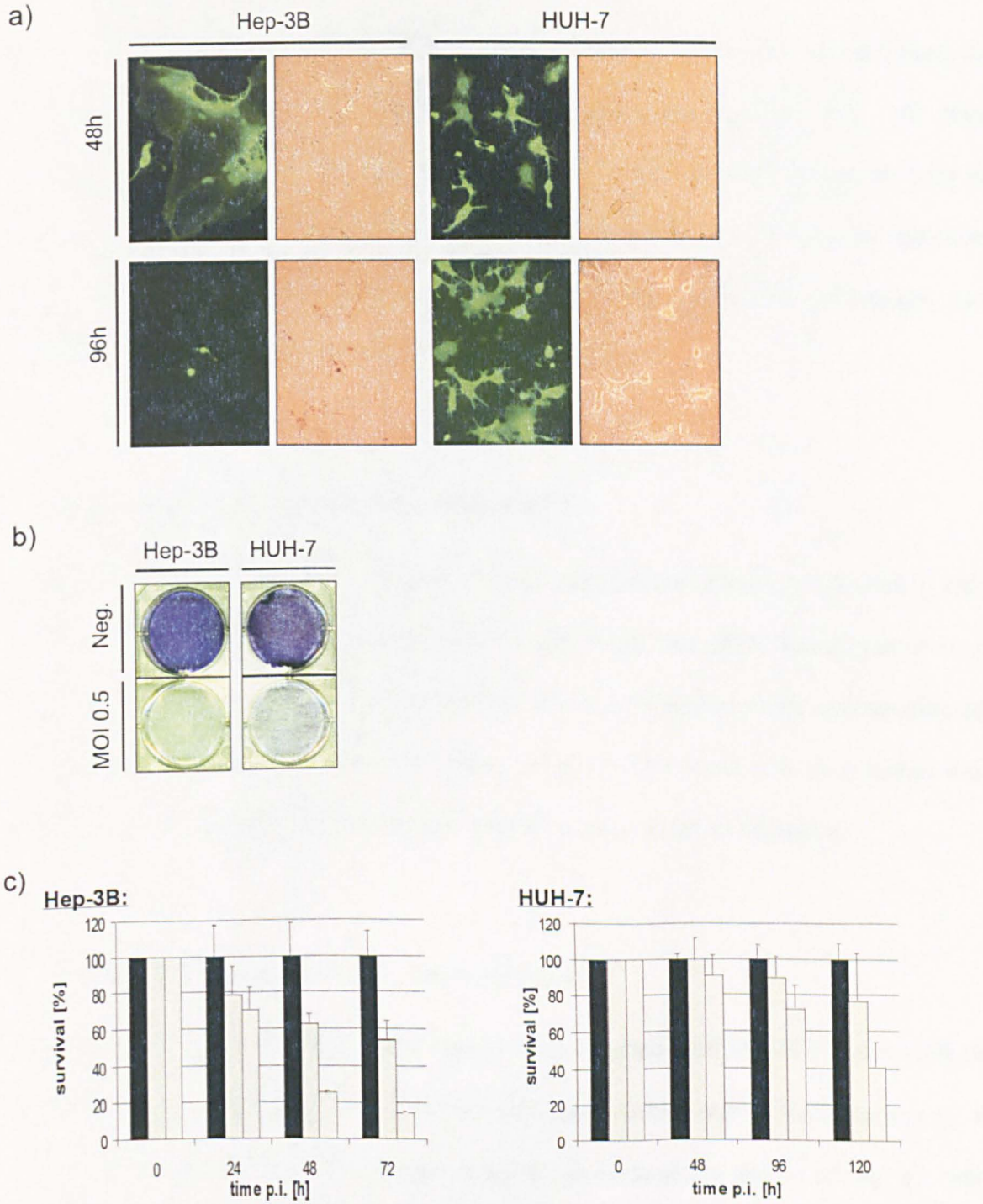

Figure 36: Infectivity, syncytia-induction and CPE of MV-Edm in HCC. a) Human HCC cell lines HUH-7 and Hep-3B were infected with MV-eGFP at an MOI of 0.5. Serial fluorescence microscopic analysis was performed every 24h. The figure shows GFP-expression and syncytia formation in human HCC cells 48 and 96h after MV-GFP infection. Fig. b) and c) show the CPE of recombinant MV-Edm on human HCC cell lines HUH-7 and Hep-3B. HCC cells were infected with MV-Edm at MOI of 0.05 and 0.5. Serial analysis for cytotoxicity was performed every 24h. Fig. b) shows crystal violet staining of infected cells 96h after infection with recombinant MV-Edm. Fig. c) shows the time course of cell viability of HCC cells after infection with recombinant MV-Edm as analyzed by CellTiter 96 AQueous nonradioactive cell proliferation assay kit (n=8).

(■ = Neg. contr., □ = MOI 0.05, □ = MOI 0.5).

the two cell lines were observed in the total susceptibility and kinetics of cell killing. In Hep-3B cells reduction of viability was observed within the first 24h. 72h after infection, viability of Hep-3B cells was reduced to 14.9% at MOI 0.5 and to 54% at MOI 0.05. In HUH-7 cells, the cytotoxic effect of MV-Edm started 48h after infection at MOI 0.5. 120h after infection of HUH-7 cells with MV-eGFP cell vialility had decreased to 41% at MOI 0.5 and 77.2% at MOI 0.05.

3.4. Measles virus induces apoptosis in HCC

Measles virus infection of HCC cell lines results in syncytia formation followed by cell death. The mechanism of syncytia-induced cell death can either be apoptosis or a bioenergetic form of cell death with necrosis. The mechanism of measles virus induced cell death in HCC cell lines has never been evaluated. Aim of the following studies was the evaluation of MV-Edm induced cell death following syncytia formation.

3.4.1. Optical analysis by TUNEL and DAPI-stain

Human HCC cell lines HUH-7 and Hep3B were infected with MV-eGFP at a MOI of 0.05. Cells were evaluated every 24h for apoptosis by DAPI- and TUNEL-staining for a total time period of 96h. The results of these experiments are shown in Fig. 37. 24h after infection first morphologic signs of apoptosis were noted by TUNEL as well as by DAPI-stain. Maximum number of cells undergoing apoptotic morphologic changes was observed 48h after infection. At later time points, the majority of cells were not viable anymore and apoptotic signals had decreased.

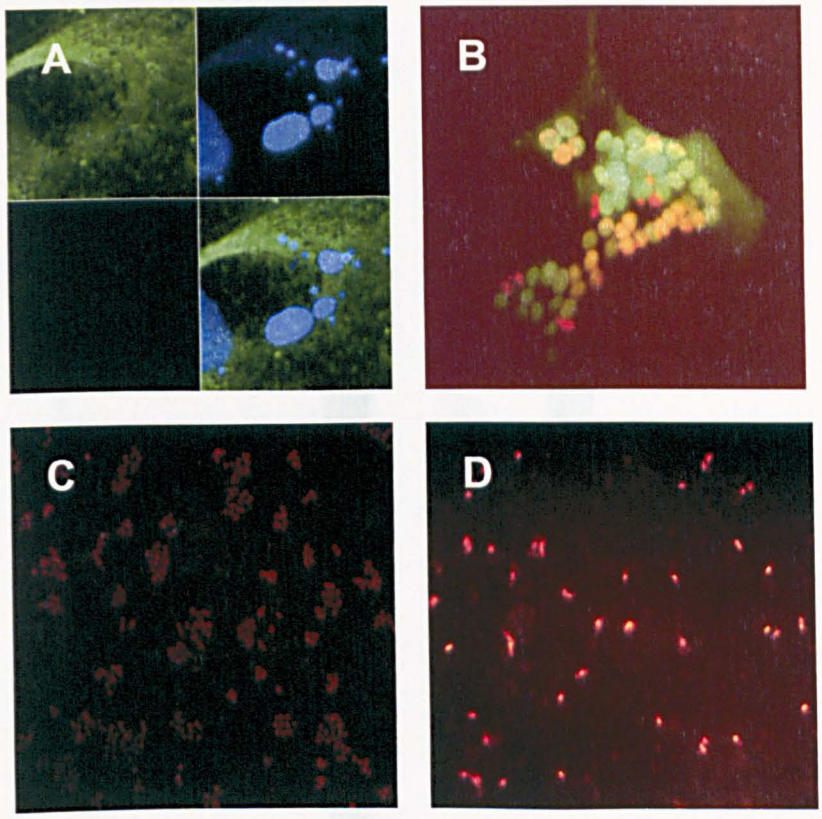

Figure 37: MV-Edm induced apoptosis. Human HCC cell lines Hep-3B and HUH-7 were infected with GFP-expressing MV-eGFP at a MOI of 0.05. 24h after infection, cells were analyzed for apoptosis by TUNEL-staining. Figure 37, shows fluoscence microscopic analysis of treated cells. Green fluorescence indicates GFP-expression. Blue fluorescencent structures are DAPI-stained DNA. Red fluorescence indicates TUNEL-positive cells. A) Negative control showing nuclear DAPI-staining and GFP-expression. B) Overlay image of GFP-expression and TUNEL-stain. C) TUNEL-stain of untreated cells. D) TUNEL-stain of MV-Edm treated cells.

3.4.2. Caspase 3/7-activity after MV-Edm infection

For confirmation of apoptosis induction following MV-Edm induced syncytia formation, activity of caspase 3 and 7 was evaluated. Hep-3B cells and HUH-7 cells were infected with MV-eGFP at a MOI of 0.05. 24h after infection, caspase activity was analyzed (Fig. 38). Uninfected cells served as negative control. For a positive control, cells were treated with TRAIL (100 ng/ml) and actinomycin D (0.5 µg/ml). For confirmation of caspase activitation, MV-Edm and TRAIL-actinomycin D were cotreated with the caspase inhibitor zVAD-FMK (100 µM).

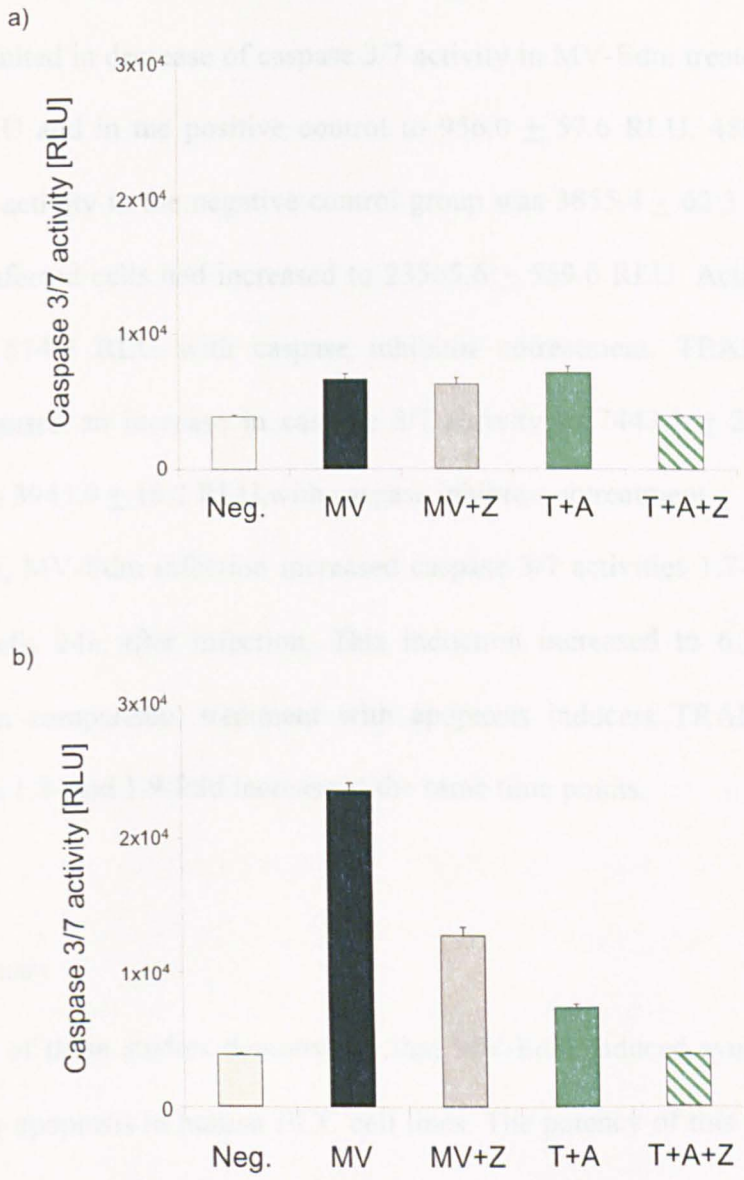

Figure 38: Caspase 3/7 activity after MV-Edm infection. HUH-7 cells were treated with apoptosis inducers TRAIL (100 ng/ml) and actinomycin D (0.5 μg/ml) or infected with MV-Edm (MOI 0.05). Untreated cells were used as a negative control. Cotreatment was used for apoptosis-inhibition. After 24 and 48h cells were analyzed for caspase 3/7 activity. a) 24h post infection, b) 48h post infection.

(□ = neg. contr., ■ = MV-Edm, ▒ = MV-Edm+ZVAD, ▩ = TRAIL+actinomycin D, ▨ = TRAIL+actinomycin D+ZVAD)

24h after treatment, caspase 3/7 activity in the negative control was 3920.3 ± 119.5 RLU. In comparison, activity in MV-Edm infected cells was 6641.1 ± 386.6 RLU.

Activity of the positive control was 7147.6 ± 483.0 RLU. Treatment with caspase inhibitor resulted in decrease of caspase 3/7 activity in MV-Edm treated cells to 6276.8 ± 451.8 RLU and in the positive control to 956.0 ± 57.6 RLU. 48h after treatment, caspase 3/7 activity in the negative control group was 3855.4 ± 62.3 RLU. Activity in MV-Edm infected cells had increased to 23565.6 ± 559.6 RLU. Activity decreased to 12783.6 ± 574.9 RLU with caspase inhibitor cotreatment. TRAIL-actinomycn D treatment caused an increase in caspase 3/7 activity to 7443.1 ± 238.3 RLU which decreased to 3943.9 ± 18.2 RLU with caspase inhibitor cotreatment.

In summary, MV-Edm infection increased caspase 3/7 activities 1.7-fold compared to untreated cells 24h after infection. This induction increased to 6.1-times 48h after infection. In comparison, treatment with apoptosis inducers TRAIL-actinomycin D resulted in a 1.8- and 1.9-fold increase at the same time points.

3.4.3. Summary

The results of these studies demonstrate that MV-Edm induced syncytia formation is followed by apoptosis in human HCC cell lines. The potency of this activation exceeds the stimulus achieved by strong apoptosis inducers such as TRAIL and actinomycin D.

3.5. Transgene expression in MV-Edm infected human HCC cell lines

In order to monitor virus spread and location of infected cells we evaluated recombinant measles viruses expressing CEA and hNIS. Fig. 34 shows schematic diagrams of the full-length constructs of MV-CEA and MV-NIS [107, 304].

2 x 10^5 HUH-7 and Hep-3B cells were infected with MV-CEA at a MOI of 0.05 and 0.5. Supernatant was collected every 24h for a total time period of 72 hours and

analyzed for CEA concentration (Fig. 39a). CEA was detected within the first 24h after infection in both cell lines and continuously increased over the following 48h. In detail, 24h after infection CEA concentration in Hep-3B cell supernatant was 7.05 ng/ml at MOI 0.5 and 0.42 ng/ml at MOI 0.05. At 72 hours after infection, CEA concentrations had increased to 693.3 ng/ml at MOI 0.5 and 44.03 at MOI 0.05. In supernatant of MV-CEA infected HUH-7 cells CEA concentrations were 8.5 ng/ml at MOI 0.5 and 0.8 ng/ml 24h at MOI 0.05 24h after infection, and increased to 6951.7 ng/ml at MOI 0.5 and 691 ng/ml 72h after infection.

HUH-7 and Hep-3B cells were infected with MV-NIS at MOI 0.01, 0.1 and 1.0. 24, 48 and 72h after infection, cells were incubated with $1x10^6$ mCi ^{125}I for 1 h at 37^0C followed by analysis of isotope uptake. In Hep-3B cells, infection with MV-NIS resulted in a MOI-dependent uptake of ^{125}I with a maximum uptake of 1617 cpm at a MOI of 1.0 at 24h post infection (Fig. 39b). At later time points, virus infection had eradicated the cell layer to an extent that overall uptake was reduced. In HUH-7 cells, maximum uptake with 1296.7 cpm was observed 48h after infection at MOI 0.01. In the following 48h activity decreased at MOI 0.1 and 1.0, but increased at MOI 0.01.

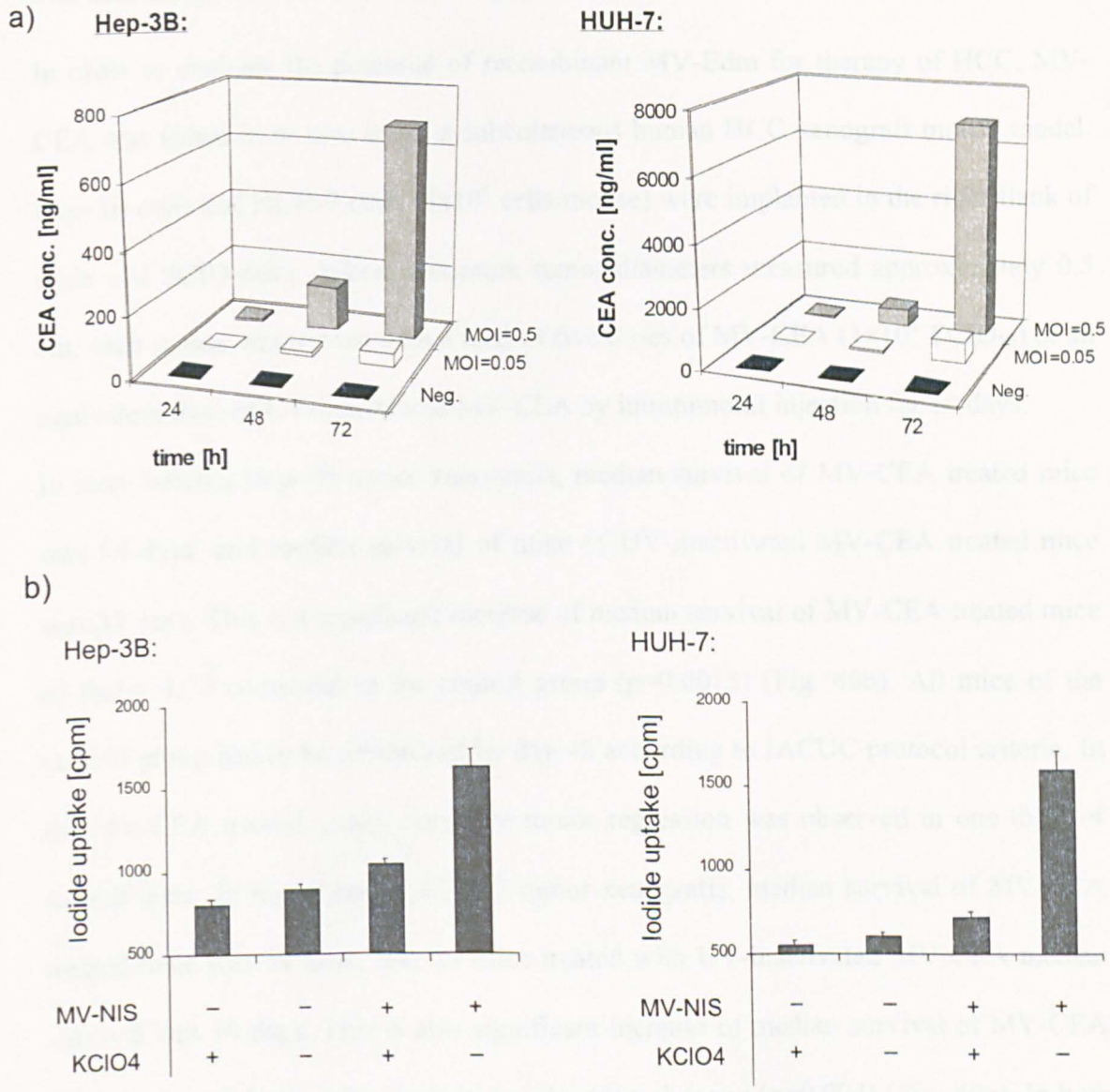

Figure 39: Transgene expression in human HCC cell lines after infection with MV-CEA and MV-NIS. Hep-3B and HUH-7 cells were infected with MV-CEA or MV-NIS at different MOIs and analyzed for transgene expression. Fig. a) shows the time course of CEA-concentration in the supernatant of MV-CEA infected Hep-3B and HUH-7 cells. Data points are mean values with standard deviations (n=6). Data of negative controls are shown as black bars, MOI 0.05 infected cells as white bars and MOI 0.5 infected cells as gray bars. Fig. b) shows isotope activity in MV-NIS infected HCC cells after incubation with ^{125}I. Shown are mean values with standard deviations (n=3). In order to show NIS-mediated ^{125}I-uptake controls co-treated with KClO4 were used.

3.6. Intratumoral MV-Edm therapy in human HCC-xenografts

In order to evaluate the potential of recombinant MV-Edm for therapy of HCC, MV-CEA was tested in *in vivo* using a subcutaneous human HCC xenograft mouse model. Hep-3B cells and HUH-7 cells ($5x10^6$ cells/mouse) were implanted in the right flank of nude and SCID mice. When maximum tumor diameters measured approximately 0.5 cm, each mouse was treated with a total of five doses of MV-CEA ($1x10^7$ $TCID_{50}$) or an equivalent dose of UV-inactivated MV-CEA by intratumoral injection for 10 days.

In mice bearing Hep-3B tumor xenografts, median survival of MV-CEA treated mice was 58 days, and median survival of mice of UV-inactivated MV-CEA treated mice was 33 days. This is a significant increase of median survival of MV-CEA treated mice of factor 1.75 compared to the control group ($p=0.0015$) (Fig. 40b). All mice of the control group had to be euthanized by day 48 according to IACUC protocol criteria. In the MV-CEA treated group, complete tumor regression was observed in one third of treated mice. In mice bearing HUH-7 tumor xenografts, median survival of MV-CEA treated mice was 34 days, and for mice treated with UV-inactivated MV-CEA median survival was 19 days. This is also significant increase of median survival of MV-CEA treated mice of factor 1.79 compared to the control group ($p=0.004$) (Fig. 40b). In both HCC cell line xenografts, the response first became apparent at day 10, the last day of therapy, and increased over time (Fig. 40a).

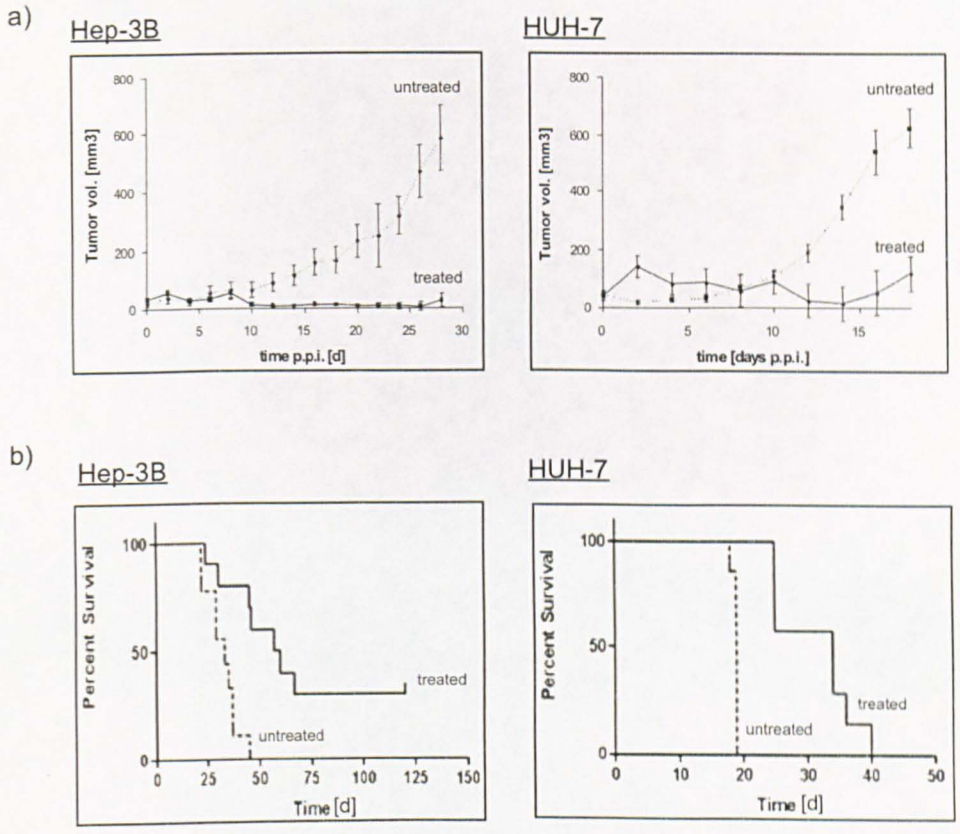

Figure 40: Tumor-suppression and survival after intratumoral MV-CEA therapy of HCC-xenografts. Mice bearing s.c. HCC-xenografts (HUH-7, Hep-3B) were injected intratumorally with $2x10^6$ $TCID_{50}$ of MV-CEA every other day for a total of 5 injections (= $1x10^7$ total $TCID_{50}$/mouse). The groups consisted of 9 mice/group. Treatment groups received active MV-CEA, the negative control mice UV-inactivated MV-CEA. In Fig. a) development of tumor volume after initiation of MV-CEA therapy is shown. The datapoints are medians with standard error. Tumor volume of MV-CEA treated mice is shown as solid line, tumor volume of UV-inactivated MV-CEA treated mice is shown as dashed line. The graph ends at the time point at which the first mouse had to be euthanized. In Fig. b) survival curves are shown for treated mice (solid line) and negative control mice (dashed line).

At the end of the studies, tumors were excised and analyzed histologically. Measles virus therapy resulted in extensive syncytia formation as shown in figure 41.

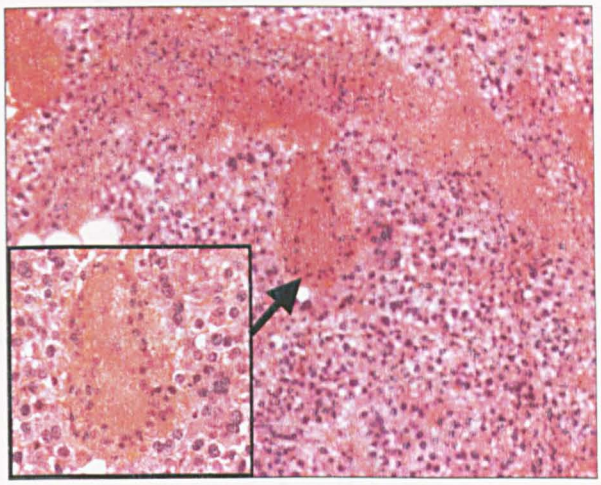

Figure 41: Syncytia formation after intratumoral MV-Edm therapy. Mice bearing subcutaneous Hep-3B tumor xenografts were treated with a single intratumoral dose of MV-CEA at a TCID50 of $2x10^6$ per animal. Three days after therapy tumors were harvested and HE-stained followed by histologic analysis. Figure 41 shows extensive syncytia formation.

3.7. Non-invasive *in vivo* monitoring after MV-CEA therapy of HCC

In order to evaluate the potential of recombinant measles virus for non-invasive *in vivo* monitoring, MV-CEA was tested in a subcutaneous human HCC xenograft mouse model. Hep-3B cells and HUH-7 cells ($5x10^6$ cells/mouse) were implanted in the right flank of nude and SCID mice. When maximum tumor diameters measured approximately 0.5 cm, each mouse was treated with a total of five doses of MV-CEA ($1x10^7$ $TCID_{50}$) or an equivalent dose of UV-inactivated MV-CEA for 10 days by intratumoral injection.

CEA was detected in MV-CEA treated but not in UV-inactivated MV-CEA treated mice. In both, Hep-3B and HUH-7, HCC-xenograft models serum CEA concentrations could be detected as early as 5 days after initiation of therapy and increased over time. In Hep-3B xenografts model, CEA concentrations reached a maximum of 312.3 ng/ml

at day 35. In HUH-7 xenografts a maximum of 10360 ng/ml was reached at day 12. Following these maximum CEA concentrations, the mean CEA-levels started to decrease.

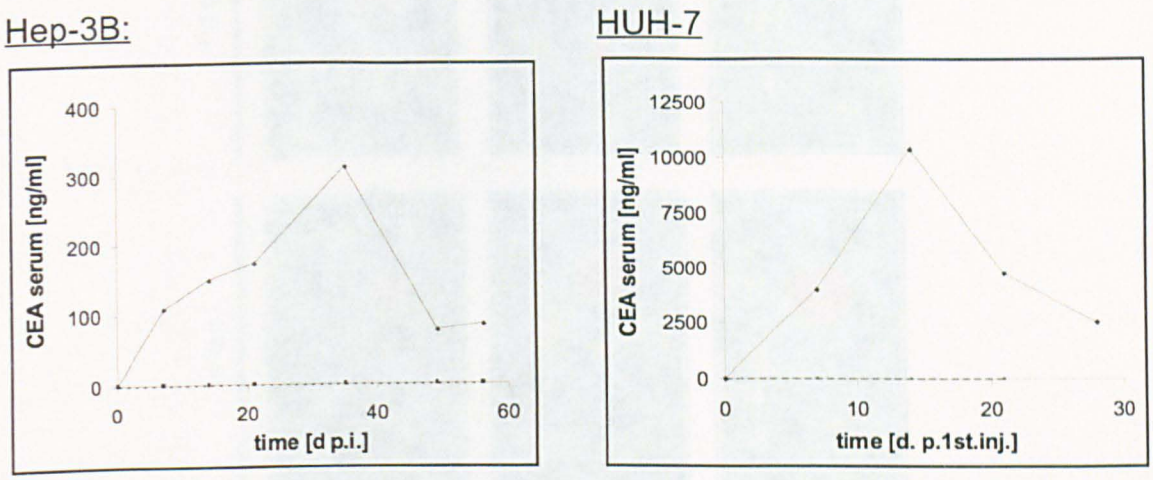

Figure 42: Serum CEA concentrations after intratumoral MV-CEA therapy of HCC-xenografts. Mice bearing s.c. HCC-xenografts (HUH-7, Hep-3B) were injected intratumorally with $2x10^6$ $TCID_{50}$ of MV-CEA every other day for a total of 5 injections (= $1x10^7$ total $TCID_{50}$/mouse). The groups consisted of 9 mice/group. Treatment groups received active MV-CEA, the negative control mice UV-inactivated MV-CEA. The graphs represent the course of serum CEA concentration in HCC xenograft bearing mice after MV-CEA therapy.

3.8. Non-invasive *in vivo* imaging after MV-NIS therapy of HCC

HUH-7 cells were implanted subcutaneously in SCID and nude mice as described above. Once tumors were 0.5 cm in diameter, mice were injected intravenously via the tail vein with a single dose of $2x10^6$ $TCID_{50}$ of MV-NIS or an equivalent dose of UV-inactivated MV-NIS. 7 and 14 days after MV-NIS treatment, mice were injected

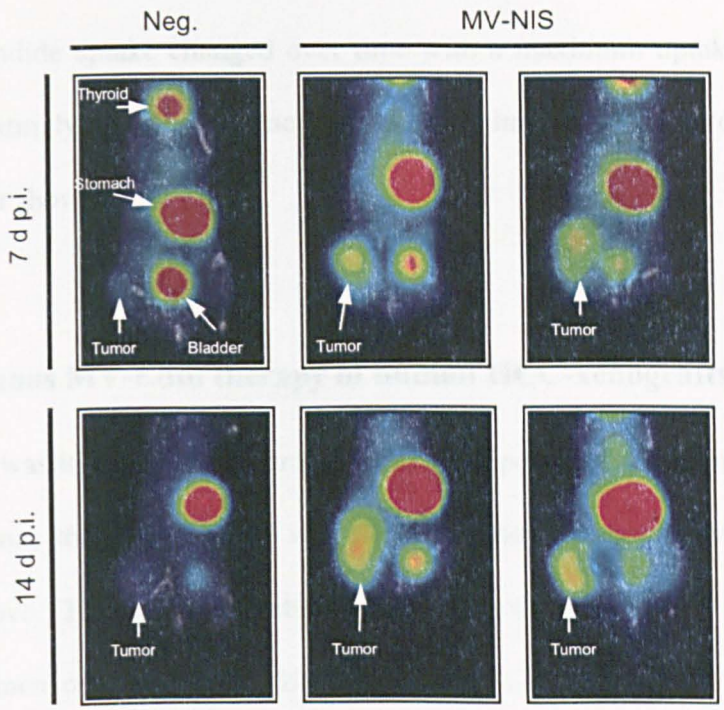

Figure 43: Increased ^{123}I-uptake in HCC-tumors after intravenous MV-NIS therapy. Fig a): Mice bearing subcutaneous HUH-7 tumor xenografts received a single i.v. injection of $2x10^6$ $TCID_{50}$ of MV-NIS. 7d and 14 d after MV-NIS treatment 0.5 mCi ^{123}I was injected intraperitoneally. 1h after application of the isotope, animals were analyzed by whole body gamma-camera imaging. Tumors, located at the right flank of the mice, show increased activity at the tumor site indicating ^{123}I uptake. This uptake is not observed in the negative control mouse. Other organs showing activity are thyroid, stomach and bladder.

intraperitoneally with ^{123}I (500 µCi/mouse) and analyzed one hour later for isotope uptake using whole body gamma-camera imaging. As shown in Fig. 43, in MV-NIS treated animals we observed a strong signal of the HCC tumors indicating high intratumoral uptake of ^{123}I; dosimetric analysis quantified intratumoral isotope accumulation as 7.7% of whole body activity. In contrast, UV-inactivated MV-NIS treated mice did not concentrate ^{123}I intratumorally. Viral gene expression and viral replication are tightly coupled. Serial iodide uptake studies can be expected to reflect NIS expression and serve as a surrogate of MV-NIS replication [304]. Therefore, we

repeated the experiment as described above and performed serial imaging analysis 3, 7, 10 and 14 days after a single dose treatment with MV-NIS. The serial imaging analysis showed that iodide uptake changed over time with a maximum uptake between day 7 and 10. Interestingly, in Hep-3B xenografts only minimal iodide uptake was observed at day 3 (data not shown).

3.9. Intravenous MV-Edm therapy of human HCC-xenografts

The next aim was to evaluate the tumor suppressive potential of recombinant MV-Edm after intravenous therapy. Hep-3B and HUH-7 tumor xenografts were implanted as described above. Therapy was initiated once tumors reached 0.5 cm in diameter. Therapy regimen consisted of 5 doses of $2x10^6$ $TCID_{50}$ MV-NIS every other day; injection was performed intravenously via the tail vein. Mice of the control group were treated with equivalent doses of UV-inactivated MV-NIS. In the Hep-3B xenograft model, median survival of control mice was 15 days compared to 41 days in the treatment group (Fig. 44). This is a significant increase of median survival of factor 2.7 ($p<0.0001$). At day 22 all of the mice of the control group had to be sacrificed. In the MV-NIS treated group, we observed 10% complete regression. In the HUH-7 tumor model, median survival in the control group was 8 days. In the treated group, median survival was 12 days. Intravenous MV-NIS treatment resulted in increase of median survival of factor 1.5 in HUH-7 xenografts ($p=0.0018$).

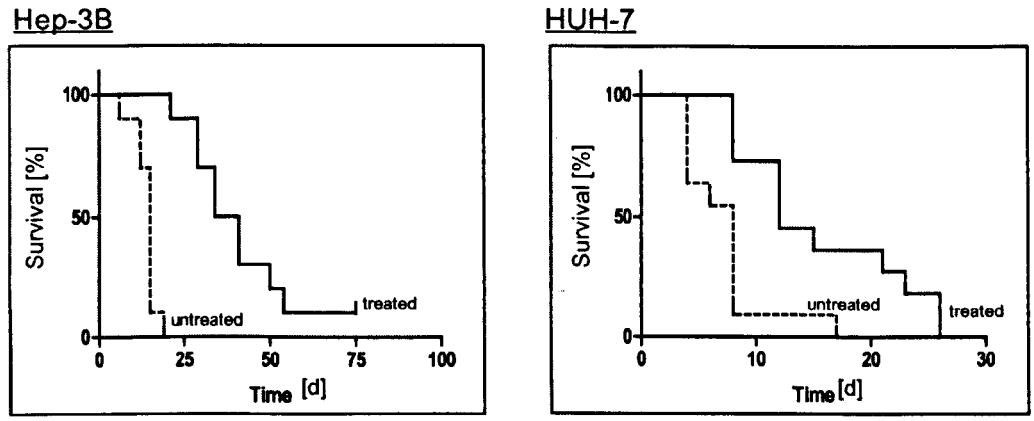

Figure 44: Tumorsuppression in HCC-tumors after intravenous MV-NIS therapy. Mice bearing s.c. HCC-xenografts (HUH-7, Hep-3B) were injected intravenously with $2x10^6$ $TCID_{50}$ of MV-NIS every other day for a total of 5 injections (= $1x10^7$ total $TCID_{50}$/mouse). The groups consisted of 10 mice/group. Treatment groups received active MV-NIS, the negative control mice UV-inactivated MV-NIS. Survival curves are shown for treated mice (solid line) and negative control mice (dashed line).

IV. Discussion

1. Nonviral gene delivery systems

In this thesis, a variety of published non-viral strategies were evaluated. The most efficient of these approaches were chosen for further analysis, and global collaborations with worldwide-leading laboratories specialized in non-viral gene delivery systems established. Independently, synthesis of these carriers was established and their efficacy evaluated *in vivo*. The main findings of these studies are: 1. direct, intratumoral DNA injection is the only physical *in vivo* transfection method achieving significant intratumoral transgene expression levels, but is limited for cancer gene therapy by its low biodistribution, 2. pegylated, PEI-based polyplexes as well as stabilized plasmid lipid particles achieve specific and high levels of intratumoral transgene expression after systemic administration but are limited by their low intratumoral biodistribution.

The first study within this thesis evaluated transgene expression after intravenous injection of unconjugated plasmid DNA. Transgene expression levels were very low with luciferase activity between 0-500 RLU/g tissue. Highest expression levels were observed in lung tissue. These results confirm previous observations. Kawabata et al. had shown that the degradation of plasmid DNA exposed *in vitro* to whole blood results in a DNA half-life of 10 min and even faster degradation rates were observed after intravenous injection of plasmid DNA [319]. These results prompted further biodistribution studies showing that large amounts of DNA were taken up by hepatic endothelial and Kupffer-cells followed by its degradation [449, 450]. The early, relatively high pulmonary transgene expression is also consistent with other reports showing relatively high accumulation of intravenously administered DNA in the lungs, and the

observation that DNA uptake in lungs results in transient gene expression, while hepatic uptake results only in its degradation. [319]. Hence, the results of this thesis are consistent with these observations. However, overall expression levels are extremely low and are hardly above background activity.

Plasmid DNA exposed *in vitro* to whole murine blood has a half-life of 10 min and *in vivo* of less than 5 min [319]. 60% of intravenously administered plasmid DNA accumulates in the liver within the first minute following administration [450]. Hence, it was hypothesized in this thesis that circumvention of liver and lung circulation should decrease hepatic uptake as well as pulmonary filtration of administered DNA resulting in higher systemic plasmid DNA concentration and thereby higher gene delivery to tumor-tissue. The route of administration was shown to influence biodistribution; while intravenous injection of recombinant adenoviral vectors resulted mainly in hepatic transduction, injection into the left cardiac ventricle achieved transduction mostly in cardiac, thymus, intercostal muscles and diaphragm [451]. Results of this thesis show that arterial injection via left cardiac ventricle achieves 2 to 46.5-times higher transgene expression levels than intravenous plasmid DNA injection. The highest transgene expression was observed in cardiac lysates. This observation is most likely explained by an accidental direct myocardial injection on the injection route. Myocardial plasmid injection has been shown to result in transgene expression [452]. However, intratumoral transgene expression was only doubled compared to intravenous administration and overall expression levels were very low. The low tumor transduction efficiency is likely due to persistence of remaining biologic barriers such as serum nuclease–mediated DNA degradation, inefficient extravasation, impaired transport through the extracellular marix, extracellular nuclease-mediated degradation, inefficient cellular uptake, cytosolic transport, cytosolic nuclease degradation and inefficient nuclear transport.

Hydrodynamic gene transfer was first described by Liu et al. and Zhang et al. and is mostly used for gene delivery to the liver [352, 353]. Liu et al. observed in their study transgene expression in all organs; expression levels were dependent on injection rate and volume [352]. This observation was explained by reverse blood flow. Based upon this observation, it was hypothesized in this thesis that the reverse flow could also result in hydrostatic pressure-mediated reverse flow in efferent tumor vessels. The results of this thesis show that the highest transgene expression levels after hydrodynamic gene transfer are in the liver as well as in organs directly linked to the inferior vena cava. However, neither in tumor nor in brain tissue was transgene expression detected. The differences in transgene expression are most likely anatomically explained. Organs such as liver, spleen, kidney and heart as well as their blood supply are directly connected to the inferior vena cava. In contrast, blood supply of a subcutaneous tumor is not directly connected but rather secondary to cutaneous blood supply. It is likely that the hydrostatic pressure is not high enough to result in a reverse blood flow in cutaneous vessels and especially not in tumor capillaries. It could be hypothesized that in an orthotopic HCC model, hydrodnamic gene transfer might be more efficient. However, Tada et al. have previously shown in an orthotopic HCC model in rats, that hydrodynamic gene transfer via the tail vein achieved only 0.16% gene transduction efficiency in tumor tissue but 5% in non-malignant hepatic tissue. Hydrodynamic gene transfer via the portal vein did not result in any transgene expression, neither in tumor nor non-malignant tissue. The only route through which intratumoral transgene expression was achieved, was by hydrodynamic transfer via the hepatic artery and concurrent transient occlusion of portal vein and inferior vena cava; however, gene transfer was not specific to tumor tissue with transduction efficiencies of 7% in malignant and non-malignant hepatic tissue [453].

The feasibility of intratumoral injection of unconjugated plasmid DNA has been shown in several studies [454-456]. The results of this thesis confirm its feasibility in HCC. Intratumoral treatment of subcutaneous HCC tumors with unconjugated plasmid DNA achieved the highest intratumoral transgene expression levels of the physical gene transfer methods evaluated in this thesis. Expression in other organs was minimal and hardly above background. The highest expression was observed 8h after treatment followed by a steady decline in luciferase activity. This decline was expected as a non-replicating expression plasmid was used; however, even after 48h, luciferase activity was still significantly above the levels observed with the other physical gene transfer methods.

In summary, physical gene transfer systems for unconjugated plasmid DNA are suboptimal for gene therapy of HCC. They achieve no to very low transduction efficiencies. The only significant transgene expression was achieved by direct intratumoral injection. This method could be used for cases where patients have single intrahepatic tumors but no signs of extrahepatic or multilocular intrahepatic spread. Failure of other physical methods confirms previous studies and is most likely explained by the above-discussed biologic barriers. An alternative method described in the literature but not evaluated in this thesis, would be selective catheterization of the hepatic artery as it has been used for gene therapy of other cancers [457]. The main blood supply of the liver is provided by the portal vein, while HCC tumors are mainly supplied by the hepatic artery. However, evaluation of this approach were shown to be only effective if DNA was complexed to PEI and co-administered with an embolizing agent or if efferent vessels were occluded and DNA was administered under high hydrostatic pressure in the hepatic artery [453, 458]. As the majority of HCC patients have

multilocular and/or large tumors at the time of diagnosis, none of these physical approaches appears to have therapeutic potential for cytoreductive cancer gene therapy.

Failure of the above discussed physical methods as gene therapy tools for HCC prompted evaluation of different conjugated DNA gene transfer methods. Based upon transfection efficiencies reported in the literature, one targeted and one non-targeted liposomal system as well as one targeted PEI-based systems were tested. The first system established and evaluated for this thesis was the LipT gene transfer system [389, 435]. This system describes a transferrin-receptor targeted, cationic liposomal system using cationic DOTAP and the neutral, fusogenic lipid DOPE. LipT complexes were described to achieve 20-30% transfection efficiencies in a subcutaneous human head and neck cancer xenograft model in mice after treatment with a single dose systemically administered by tail vein injection [389]. For studies in the context of this thesis, LipT complexes were evaluated in the subcutaneous N2A murine neuroblastoma xenograft model. No transgene expression was observed after systemic treatment with LipT complexes. Potential explanations for the discrepancy between the results of this thesis and the published data include the use of a different tumor model or unidentified technical difficulties in LipT synthesis. The N2A murine neuroblastoma model is a frequently used model for evaluation of non-viral gene delivery models. Transferrin-ligand has been used successfully for targeting this tumor model [459]. Differences could also be explained by anatomical differences such as desmoplasticity, extent or structure of tumor vessels. However, the N2A model has successfully been used for a variety of different non-viral gene transfer models including the ones evaluated in this thesis, showing its general amenability to transfection. The components of the LipT complexes, such as DOTAP and DOPE, are commonly used lipids in liposomal

formulations and have successfully been used in lipoplex mediated *in vivo* gene transfer [460]. The use of transferrin-ligand for targeting is highly efficient *in vivo* and has been shown *in vitro* in N2A cells to result in 100-fold increased transfection efficiency [101]. Tf-LipT Lipoplexes were reported to have a diameter of 63.8 ± 6.3 nm and a ζ-potential of +2.3 ± 1.9 mV, physicochemical characteristics qualifying them for efficient transfection [460, 461]. LipT complex preparation was carefully performed according to the originally described protocol, which is essential for achievement of the desired nanostructure; modifications in this protocol have been shown to result in abolishment of LipT nanostructure and transfection potential [101]. Although, the synthesis of defective lipoplex particles secondary to unidentified problems in preparation or due to missing information in the published methodology cannot be excluded with absolute certainty, the data of this thesis do not confirm the published results in regard of the LipT-lipoplex efficiency.

Transferrin-targeted, PEI-based polyplexes were evaluated *in vivo* in a subcutaneous murine neuroblastome xenograft model chosen for comparability with the original published results. Systemic administration of these complexes resulted in intratumoral transgene expression levels in approximately the same range as observed after intratumoral injection. Polyplexes also caused transgene expression in other organs but luciferase activity was still 30-250 times lower in these organs than in tumor tissue. The results of this thesis confirm the previously published results. Kircheis et al. measured under the same experimental conditions intratumoral transgene expression level in the same logarithmic range as observed in this thesis. Similarly, maximum extratumoral transgene expression was observed in lung and spleen with expression levels in the same logarithmic range as in this thesis. Expression kinetic was similar between the thesis results and the original published results with maximum expression 24-48h after

treatment followed by a decline in transgene expression [393]. Interestingly, Kircheis et al. also evaluated expression kinetics after repetitive vector administration showing prolonged though continuously decreasing transgene expression levels after two daily vector administrations.

Hence, this system appears to be highly promising as a systemic non-viral gene delivery system for tumor therapy. However, two disadvantages limit its use. First, its unspecificity despite the use of targeting ligands requires additional targeting strategies in order to avoid significant complications from therapeutic transgene expression in non-tumoral tissue. The second and main limiting factor is the intratumoral biodistribution pattern. Kircheis et al. evaluated intratumoral DNA biodistribution as well as intratumoral transgene expression [393]. Their results showed a heterogenous gene expression pattern with focal areas of strong transgene expression and broad areas without any visible expression. Transfected cells accumulated mostly around lacunar structures thought to be immature vessels indicating that the polyplexes do not migrate efficiently through the tumor tissue. In HCC, the thickness and impermeability of tumor vasculature increases with tumor size [462]. This impermeability could result in significant decrease of extravasation and thereby in a decreased number of transduced cells. The authors also noted that not all of the transduced cells were of tumor origin reducing the number of transduced tumor cells even further.

Stabilized plasmid lipid particles (SPLP) are a liposome-based gene transfer system [437]. They contain the cationic lipid DODAC and the fusogenic lipid DOPE, and are stabilized in aqueous medium by coating with polyethylenglycol (PEG). They are synthezied by the detergent dialysis method. Resulting particles are ~70 nm in diameter, consist of a unilamellar, lipid double layer membrane entrapping one plasmid copy

number per SPLP particle; SPLP protect DNA from serum nuclease degradation [437, 463]. Within this thesis, synthesis of SPLP was successfully achieved with encapsidation efficiencies of 80-90% of input DNA and a total yield of 36% of input DNA after completion of subsequent isolation and purification steps. These yields are consistent with the maximum yields achieved by the original authors describing the method (Dr. I. MacLachlan, personal communication). The initial *in vivo* studies of this thesis focused on SPLP biodistribution. Moderate amounts of SPLP were found intratumorally and appeared to be perivascular located. This is consistent with previous studies reporting intratumoral accumulation of 3% of input SPLP and 1.5% of the total input DNA within 24h [438]. Uptake in other organs was similar to published data, with the exception of high renal SPLP accumulation, which had not been examined in the original reports [432, 438]. The known SPLP half-life of 7.2 + 1.6h combined with the observation of their high renal accumulation after approximately 3 half-lifes indicate a renal excretion mechanism of SPLP. Transgene expression studies were highly interesting and confirmed published data. In comparison to other conjugated non-viral gene transfer systems evaluated in the course of this thesis, systemic SPLP treatment achieved the highest intratumoral transgene expression levels. At the same time, transgene expression in other organs was significantly lower than with the other methods. A striking finding was the increasing pattern of transgene expression over time despite the use of a non-replicating plasmid. These data speak for continuous, new SPLP-mediated transfection of intratumoral cells, as expression patterns of non-replicating vectors would rather be expected to decline over time. The same observation was made by Tam et al. and is possible explained by PEG-ceramide mediated prolonged systemic circulation times with 7.2 $\pm$ 1.6h circulation half-life. The prolonged half-life, increased vasculature and higher cell proliferation rates might explain the preferential

intratumoral transgene expression [432]. Unfortunately, intratumoral biodistribution studies revealed similar problems as observed with the above-discussed PEI-polyplexes. The intratumoral biodistribution analysis demonstrated that the transfected cell population was very heterogeneously and sparcely distributed. Transfected cells appeared to be in groups and intracellular transgene expression was strong. Hence, the same criticism as for PEI-polyplexes applies to SPLP.

In summary, none of the analyzed non-viral gene transfer systems achieved high transfection efficiencies as discussed above. Although, two of the three tested systemic non-viral systems achieved intratumoral transfection, their intratumoral biodistribution was sparce and very heterogenous with very few transfected tumor cells. It is likely, that with increasing size of HCC nodules the low transduction efficiency will further decrease due to decreasing permeability of the tumor vessels [462]. Unfortunately, the initial hypothesis that replicating, high transgene expressing vector systems might compensate for low transfection efficiencies is unlikely to be confirmed as single cell transgene expression was high but total tumor transgene expression was low due to the limited number of transfected cells. In case of a cytoreductive gene therapy –even with the use of a transgene with a strong bystander effect- only few cells would be eliminated at a fast rate. Bystander transfection of initially untransfected cells is highly unlikely as vectors disassemble for successful transgene expression and unspecific DNA-uptake of surrounding tumor cells after tumor lysis is very inefficient due to the above-described biologic barriers. Hence, current non-viral vector systems are severely limited due to their low transduction efficiencies. Future developments should focus on high intratumoral biodistribution. However, it needs to be kept in mind that transduction-focused modifications can also cause increased toxicity and

immunogenicity. For example, it was shown that charge ratio providing optimal transfection efficiencies of PEI-polyplexes and cationic lipoplexes can also be very close to the severly toxic ratio causing complications such as hepatic necrosis and death [464-466]. Immunogenicity of synthetic gene delivery has been described and been attributed to bacterial CpG-motifs [467, 468].

In conclusion, nonviral gene transfer strategies have severe limitations making viral vectors at the current time the more appealing and promising vector systems for genetic approaches of human diseases.

2. Parvoviral replicon vectors

This is the first study to demonstrate the feasibility of parvovirus-based replicon vectors as a novel, efficient and tumor selective expression system. Data of this thesis show: 1) genetically modified and optimized MVM-replicons are efficiently excised, replicated and expressed; 2) MVM-based replicons achieve continuously increasing high-level transgene expression levels compared to other expression systems; 3) MVM-based replicon vectors retain parvoviral tumorselectivity; 4) MVM-replicons tolerate expansion of the parvoviral genome of up to 355% but replication and expression decrease with increasing genome size, and 5.) recombinant MVM-based replicons lost the parvoviral cytotoxicity.

Autonomously replicating parvoviruses are highly qualified as virotherapeutic agents for malignancies due to their oncoselectivity, oncosuppression and human apathogenicity. However, their use is limited by their immunogenicity, genomic size restriction and limitations in achievable vector yields [469]. Their use as non-viral

replicating vector systems has never been evaluated. The problem of most plasmid DNA-based expression systems used for non-viral gene delivery is their lack of sustained transgene expression due to DNA degradation, cell mitosis and gene silencing [470]. There are several strategies to achieve sustained gene expression including the use of constitutive human or tissue-specific promoters or stable chromosomal integration through use of transposons or phage integrase [471-475]. However, these strategies also bear risks such as insertional mutagenesis and are therefore not desirable for transient gene transfer strategies as required for malignancies. Episomally retained, self-replicating vector systems –referred to as replicons- are a reasonable alternative for this indication [470]. There are a variety of different replicon vectors systems currently in use; most of these are based on DNA or negative and positive strand RNA viruses [476-478]. Most of these systems are limited for their use for cancer gene therapy due to non-selectivity, low efficiencies or host range restrictions. Hence, the development of parvoviral replicons for tumor-selective gene therapy is a potentially novel and promising tool.

Several parvovirus MVM-based replicons were generated throughout this study. In order to maximize genomic excision and replication, and as a result transgene expression, the left palindromic end was modified by insertion of a NS1-nicking site. Kestler et al. had found that a NS1-nicking site was deleted in the original MVMp-clone described by Merchlinsky et al. [133]. The missing NS1-nicking site is essential for efficient parvoviral genome excision. Reconstitution of this site achieved a significant increase in parvoviral replication and viral titers. The data of this thesis confirm these findings; restoration of the left parvoviral palindrome resulted in increased replication. The effect of this modification on transgene expression after parvoviral DNA transfection had not been evaluated in previous studies. The data presented as part of this thesis indicate also a significant increase in transgene expression levels through

reconstitution of the NS1 nicking site. The increase in expression levels is possibly related to increased numbers of MVM-DNA copy numbes secondary to increased replication rates. A positive correlation between vector copy number and transgene expression levels has also been observed in other systems [479]. Hence, improved excision results in more efficient replication and thereby higher number of parvoviral DNA copy numbers, which translates into higher transgene expression levels.

Parvoviral replicon vectors achieved high transgene expression levels in susceptible cells. The maximum achieved expression was 2-3-fold higher than with expression systems using an enhanced CMV-promoter. These high expression levels observed after MVM-replicon transfection are the consequence of two factors. First, transgene were cloned in a position in which their expression is controlled by the P38 promotor [218]. Transactivation of P38 through NS1 causes an enhanced transgene expression. The second factor is indicated by the expression profile. Transgene expression increased over time likely due to sustained intracellular parvoviral DNA replication. In contrast, non-replicating systems have their maximum protein expression within the first 24h after transfection followed by a sharp decrease due to input DNA elimination as outlined above. The EBV-based replicating vector system is one of the most commonly used replicating expression systems. However, plasmids containing the oriP and EBNA-1 sequences are maintained at low copy numbers DNA episomes and replicate only once per cell cycle in eukaryotic cells [480]. In conclusion from parvoviral replication data, MVM-based replicons replicate at a higher rate. This conclusion is further supported by the transgene expression data indicating a continuous increase in transgene expression. In contrast, EBV-replicon mediated transgene expression only stabilized after its initial increase 24h after transfection.

Parvoviruses are also known for their tumor suppressive potential [469]. It was hypothesized in this thesis that parvoviral cytotoxicity is an additional advantage of parvoviral replicon vectors. Parvovirus MVM has been shown to elicit cytotoxic effects predominantly mediated by its non-structural protein NS1 [161, 445]. NS1-protein has been shown to induce cytoskeletal changes and to interfere with intracellular signaling pathways resulting in cytopathic effects and cell death [446, 447]. However, NS2 protein also contributed to parvoviral cytotoxicity eliciting an enhancing effect [162]. Earlier studies using stably transfected cell clones expressing parvoviral NS proteins under the control of inducible promoters showed cytopathic effects in colony assays following induction of NS-protein expression [154, 481]. Hence, it was hypothesized in this thesis that parvoviral replicon vectors should maintain their cytotoxic potential as long as NS1 and NS2 coding regions are not interrupted. Unexpectedly, it was found that none of the parvoviral replicon vectors elicited a cytotoxic effect. These results cannot be explained by resistance of the cell lines used for evaluation as they are known to be susceptible to parvoviral cytotoxicity and are commonly used for titration of parvoviral virus stocks. NS1 and NS2 coding regions were kept intact through the choice of the *Xba*I and *Hind*III restriction sites as an insertion site for transgenes excluding a cloning-mediated defect in their expression. Previously, it was shown that mutations in the NS1 coding region causing alterations of protein kinase C (PKC)-phosphorylation sites, significantly reduce parvoviral cytotoxicity [482, 483]. However, MVM-plasmids used for the cytotoxicity studies in this thesis were analyzed carefully by DNA sequencing and found to be negative for these mutations. Most recently, recombinant MVM viral vectors were compared to wildtype MVM [484]. Interestingly, the authors of this study found similar results as the ones described in this thesis. Cytoxicity of recombinant MVM viruses in which capsid coding regions were replaced by interleukin-2 coding

DNA had almost completely lost their cytotoxic potential compared to wildtype MVM even if used at a 10-fold higher multiplicity of infection [484]. It was hypothesized that NS1 is not the only mediator of parvoviral cytoxicity but that factors mediated by the capsid or at least contained in the deleted regions are required for parvoviral cytotoxicity. The results of this study confirm these observations and provide further evidence for additional factors required for parvoviral cytotoxicity warranting further studies. However, the attenuated parvoviral cytotoxicity could also be advantageous for tumor-directed therapy. Wodarz et al. analyzed mathematical models of optimal virotherapeutic strategies and concluded that a fast killing vector will result in a disadvantageous change of infected to uninfected proliferating cell ratio of a tumor cell population with the final outcome of tumor growth [314]. The absent cytotoxicity in parvoviral vectors would allow sustained therapeutic transgene expression and thereby enhancement of its effect even on untransfected cells if therapeutic genes with bystander effects are used.

Genetically unmodified autonomously replicating parvoviruses are not able to achieve complete tumorsuppression [239, 249]. Therefore, genetic modification is required in order to enhance their tumor suppressive potential. However, the choices of therapeutic transgenes for these viruses are very limited due to genomic size restrictions [144]. Kestler et al. as well as Brandenburger et al. have described an optimal genomic size between 90 and 106% for parvovirus MVM. Outside these limitations, viral titers decrease significantly due to inefficient viral packaging [133, 251]. In this thesis, the parvoviral genome was increased to 355% of its wildtype size. Despite the significant increase in genome size, recombinant MVM-replicons were replicated and transgenes expressed. However, the increase in genome size did result in markedly decreased replication rates as well as an up to 30-fold decreae in transgene expression. These data indicate, that the

use of the parvoviral MVM-genome as a replicon does not allow unlimited genome expansion.

Autonomously replicating parvoviruses such as MVM and H1 are known for their tumor-selectivity. Several factors contribute to their oncotropism. The parvoviral P4-promoter is one of the major contributers to their selectivity [144]. Oncogenic transformation has been shown to result in enhanced P4-promoter activity [191, 192]. In addition, cellular transcription factors ATF and E2F-mediated P4-promoter induction is S-phase dependent [176]. However, the P4-promoter dependence alone is not sufficient to guarantee oncoselectivity as the isolated P4-promoter elicits activity even in untransformed cells [144].

The second mechanism contributing to parvoviral oncoselectivity is the strict S-phase dependency of parvoviral genome conversion from single- to duplex DNA which requires cellular factors such as cyclin A and CDK2 kinase activity [174]. Therefore, it was a concern that the use of parvoviral replicons as double-stranded DNA vectors could interfere with these mechanisms and result in loss of oncoselectivity. However, the data presented in this thesis clearly demonstrate that this is not the case. Optical as well as highly sensitive enzymatic analysis confirmed that transfection of untransformed cells with parvoviral replicon vectors does not result in transgene expression. In contrast, high and increasing transgene expression was observed in their transformed counterparts. These results prove the sustained tumor-selectivity of parvoviral replicons.

In summary, this thesis has demonstrated the feasibility of parvoviral replicon as a novel, tumor-selective gene expression system. It provides tumor-selective, high-level

transgene expression. However, the hypothesis that replicons allow unlimited genome size increase could not be confirmed nor did they retain their cytotoxic potential.

3. Viral gene therapy using recombinant measles virus

This thesis is the first study to show the tumor suppressive potential of recombinant MV-Edm as a viral cancer agent for the therapy of HCC. The data show that: 1) CD46 is overexpressed in HCC in comparison to non-malignant hepatic tissue; 2) MV-Edm successfully infects human HCC cells resulting in transgene expression, syncytia formation and tumor cell killing; 3) recombinant MV-Edm has a strong tumorsuppressive effect on human HCC xenografts after intratumoral and intravenous therapy; 4) recombinant MV-Edm expressing either CEA or hNIS allow non-invasive monitoring of viral expression kinetics and localization of infected tumor cells.

MV-Edm is a RNA virus which is characterized by its oncolytic potential and its tumorselectivity [107, 202, 304, 313]. One of the factors contributing to its tumorselectivity is CD46-receptor density [284]. The pathogenic wildtype of measles virus, which is not selectively oncolytic, uses primarily the SLAM receptor [274, 485]. The main receptor used by the vaccine strain MV-Edm is CD46 [275]. Virus entry increases with increasing CD46-receptor density; if CD46 receptor density exceeds a "threshold" density, syncytium formation and cell killing are induced [284]. The data show that CD46 is strongly expressed in human HCC cell lines compared to primary human hepatocytes. Unfortunately, culturing of primary human hepatocytes for more than 48h resulted in upregulation of CD46-receptor expression and cell fusion after MV-Edm infection (data not shown). Since long-term culturing of human HCC cell lines might also have resulted in upregulation of CD46-receptor expression in these cell lines,

immunohistochemical analysis of human hepatic tissue samples of HCC patients was performed. The results of these studies confirmed overexpression of CD46 in HCC tumor tissue compared to non-malignant hepatic tissue. These data are in concordance with earlier studies by Kinugasa et al. [486]. In their studies CD46 expression was compared in normal human hepatic tissue samples, HCC, cirrhosis and chronic hepatitis. Their results showed relative CD46-densities of 0.11 + 0.1 in normal hepatic tissue, 0.63 + 0.23 in HCC, 0.21 + 0.07 in cirrhosis and 0.25 + 0.1 in chronic hepatitis. These data clearly show that CD46-expression is 6-times higher in HCC than in normal hepatic tissue, 3-times higher in HCC than in cirrhotic liver tissue, and 2.52 higher in HCC than in chronic hepatitis without overlap of CD46-density. Therefore, it can be concluded that HCC fulfills the requirements for viral uptake and selective cell fusion and killing.

Additional factors contributing to MV-Edm tumor selectivity are likely. Virally infected cells respond with inhibition of viral protein synthesis through IFN-α/β, double-stranded RNA-dependent protein kinase, 2',5'-oligoadenylate synthetase and Mx-proteins [487-489]. In contrast to non-malignant cells, tumor cells are often defective in IFN-α/β and RNA-dependent protein kinase pathways [284, 300]. This impairment in cellular defense is thought to be one of the mechanisms underlying the tumor selectivity of other RNA viruses used in experimental cancer therapy [490-493]. It might also be one of the mechanisms contributing to MV-Edm tumor selectivity in addition to other yet unknown mechanisms.

Tumor selectivity in the setting of HCC is an important safety concern as 60-80% of HCC patients have reduced liver function due to liver cirrhosis [3]. Based upon the observation that CD46 expression is increased in cirrhosis, though still 3-times lower

than in HCC, clinical Phase I toxicity studies are necessary [3, 486]. Nevertheless, MV-Edm therapy of HCC is not expected to cause damage to surrounding tumor-free hepatic tissue for the following reasons:

a) liver toxicity was not observed in CD46-positive mice and monkeys treated systemically with MV-Edm [494];

b) intraperitoneal treatment of Ifnar^{TM}-CD46Ge transgenic mice with MV-GFP did not result in significant transgene expression, despite the presence of MV-Edm RNA in liver tissue [495];

c) the attenuated Edmonston vaccine strain has successfully been used for vaccination with an excellent safety profile;

d) reports of wildtype measles virus induced hepatic damage are restricted to an extremely rare number of single case reports, are negligible in severity or fail to show intrahepatic presence of measles virus [496, 497];

e) post-transplant measles vaccination in liver transplantation patients did not result in significant complications and was considered safe [498, 499].

In addition, protection of non-malignant cells from the MV-Edm induced cytotoxicity is likely through the following mechanisms:

a) measles virus has the ability to block the intracellular antiviral state by inhibition of IFN-α/β-pathways and inhibition of phosphorylation of STAT1 and STAT2; this suppressive mechanism is mediated by measles virus V and C protein [295-297]. However, recombinant MV-Edm used in this thesis have a mutation in the V protein resulting in loss of IFN-antagonist activity [299]. Therefore, normal cells will be able to efficiently block viral replication;

b) Patients as well as health care personnel will be protected by anti-MV antibodies due to widely used MV vaccination.

MV-Edm resulted in a strong CPE *in vitro* and *in vivo*. Two different human HCC cell lines were used. Both HCC cell lines were susceptible to the cytotoxic effect of MV-Edm but differed in the kinetics of cell death. Hep-3B cells were eliminated very efficiently and quickly while the cytotoxic effect of MV-Edm on HUH-7 cells was observed at a later time point. The *in vivo* data of this thesis show that intratumoral MV-Edm therapy results in significant prolongation of survival, almost doubling median survival times of mice bearing human HCC xenografts and causing complete tumor regression in up to one third of treated animals. Intravenous MV-NIS almost tripled median survival in mice bearing human HCC xenografts and resulted in 10% complete tumor regression in Hep-3B xenografts. Intratumoral MV-Edm therapy has been shown to result in limited intratumoral spread of MV-Edm [255]. Longer median survival after intravenous therapy compared to intratumoral therapy might be explained by better intratumoral MV-Edm distribution after intravenous delivery. Interestingly, the HCC cell lines showed different susceptibilities towards the cytotoxic effect MV-Edm. This difference in susceptibility between different HCC cell lines most likely resembles the situation in primary human tumors which consist of a heterogeneous tumor cell population [500]. Both cell lines express comparable level of CD46 but they differ in other aspects, e.g. their p53 status [501, 502]. Syncytia formation results in cell death either by apoptosis or a bioenergetic form of cell death with necrosis [303, 305]. The data of this thesis indicate apoptosis as the mechanism of cell death in HCC cells after MV-Edm induced syncytia formation. Differences in components of these pathways or other not

yet identified factors in the process of measles induced cytotoxicity could explain the different susceptibility.

The less susceptible HUH-7 tumors showed higher transgene expression levels *in vitro* as well as *in vivo* than the more susceptible Hep-3B tumors. This observation might be explained by the delay of cell death in HUH-7 cells; that is, the increased time interval until cell death results in an overall increase in viral replication and expression. A similar observation was made in an ovarian cancer model and was explained by an intratumoral dynamic equilibrium between formation of new tumor cells and the death of infected tumor cells [313]. The optimal rate of cell killing depends on the growth rate of infected tumor cells relative to uninfected tumor cells [314]. In the case of Hep-3B tumors, the equilibrium is shifted toward the cell killing of infected cells resulting in efficient and rapid destruction of infected tumor tissue. In HUH-7 tumors, the virus would be maintained and viral proteins be expressed until cell death occurs. Infected tumor cells fuse with surrounding uninfected tumor cells resulting in a strong bystander effect [503]. Syncytia formation is CD46 dependent resulting in fusion of tumor cells but not their normal counterparts [284]. Delayed cell death would therefore allow recruitment of more uninfected tumor cells in syncytia. In addition, the increased transgene expression levels in less susceptible cells can be expected to allow further enhancement of the therapeutic effect by the use of therapeutic transgenes, as e.g. hNIS in combination with ^{131}I [304, 431]. ^{131}I is a beta-particle emitting isotope with an average tissue-path length of 0.4 mm, thereby causing a bystander effect. HCC is susceptible toward the therapeutic effect of ^{131}I [504, 505]. It is a future aim to explore the possibility of further enhancement of the therapeutic effect of MV-Edm by combined radiovirotherapy using MV-NIS and ^{131}I.

Another factor influencing the therapeutic outcome of MV-Edm therapy will be the immune response. CTL response and humoral antibodies will influence dynamics of

virus persistance, infection and cell death [314]. It is likely, that virally infected tumor cells will be recognized by the host's immune system and be eliminated, and thereby contributing to the therapeutic effect.

A general concern in systemic viral therapy is the potential decreased efficacy due to the presence of antibodies. HCC offers the possibility of local treatments. The majority of HCC patients do not have extrahepatic metastasis and the liver is easily accessible using ultrasound- or CT-guidance [506]. HCC tumor nodules can easily be localized and injected with a therapeutic agent. In the setting of multilocular HCC, the liver offers the opportunity of intrahepatic delivery by hepatic artery infusion. In either case, the presence of anti-MV antibodies is not expected to result in significant decrease of efficacy. Grote et al. showed in a mouse model, in which mice received passive transfer of anti-MV antibodies, that intratumoral MV-Edm therapy of human lymphoma xenografts resulted in effective tumor regression without compromise through the presence of anti-MV antibodies [255]. This observation was in accordance with results from studies involving intratumoral therapy with reovirus in immune competent C3H mice and a clinical phase II study with a genetically modified adenovirus in patients with advanced head and neck cancer. In both studies, effective tumor-regression was achieved despite the presence of antibodies [492, 507]. Also, in the case of hepatic artery infusion as the route of administration, it has been shown that repeated infusion of replicating results in sufficient viral delivery to elicit therapeutic effects [508].

A major drawback of many cancer agents is the lack of convenient methods of monitoring the agent after application to the patient. This thesis shows that MV-CEA and MV-NIS allow non-invasive tracking of viral gene expression in HCC as well as localization of infected tumor tissue. The *in vivo* studies show transgene expression up

to 58 days after MV-CEA therapy and stable iodine uptake up to 14 days after MV-NIS therapy, which was the endpoint of the study. It has been shown for MV-CEA that the expression profile of the marker gene correlates with viral gene expression and the serum concentration of the marker polypeptide reflects the number of viable cells [106]. Expression of viral proteins lasts for the duration of viability of the infected cell. Once the cell has reached the state of cell death, viral gene expression continues through infection of new cells with progeny virus. Only 15% of HCC patients express CEA. Therefore, MV-CEA would be well suited for the majority of these patients allowing non-invasive monitoring of viral expression kinetics by serum CEA analysis. MV-NIS combined with ^{123}I will allow localization of infected HCC cells by non-invasive imaging techniques. Analysis of these data will help to determine pharmacokinetics and pharmacodynamics of measles therapy in HCC; these informations are essential for optimization of therapy protocols for optimal safety and efficacy.

In conclusion, this thesis has shown that trackable MV-Edm is a very potent novel therapeutic agent for HCC. It has an excellent safety profile and offers the possibility of controlling viral expression kinetics and localization of infected cells by non-invasive methods. The potential of monitoring measles therapy will allow modification of protocols for enhanced safety and efficacy. The accessibility of the liver and the relative low rate of extrahepatic HCC metastasis qualify HCC as an ideal target. Therefore, recombinant MV-Edm should further be explored as a therapeutic agent for HCC.

V. Literature

1. Schafer DF, Sorrell MF. Hepatocellular carcinoma. Lancet 1999;353:1253-7.
2. McGlynn KA, London WT. Epidemiology and natural history of hepatocellular carcinoma. Best Pract Res Clin Gastroenterol 2005;19:3-23.
3. Thomas MB, Zhu AX. Hepatocellular carcinoma: the need for progress. J Clin Oncol 2005;23:2892-9.
4. Bosch FX, Ribes J, Cleries R, Diaz M. Epidemiology of hepatocellular carcinoma. Clin Liver Dis 2005;9:191-211, v.
5. El-Serag HB. Hepatocellular carcinoma: recent trends in the United States. Gastroenterology 2004;127:S27-34.
6. El-Serag HB, Mason AC. Rising incidence of hepatocellular carcinoma in the United States. N Engl J Med 1999;340:745-50.
7. Llovet JM, Burroughs A, Bruix J. Hepatocellular carcinoma. Lancet 2003;362:1907-17.
8. Blum HE. Treatment of hepatocellular carcinoma. Best Pract Res Clin Gastroenterol 2005;19:129-45.
9. Chang MH, Chen CJ, Lai MS, Hsu HM, Wu TC, Kong MS, Liang DC, Shau WY, Chen DS. Universal hepatitis B vaccination in Taiwan and the incidence of hepatocellular carcinoma in children. Taiwan Childhood Hepatoma Study Group. N Engl J Med 1997;336:1855-9.
10. Chang MH, Shau WY, Chen CJ, Wu TC, Kong MS, Liang DC, Hsu HM, Chen HL, Hsu HY, Chen DS. Hepatitis B vaccination and hepatocellular carcinoma rates in boys and girls. Jama 2000;284:3040-2.
11. Bruix J, Sherman M. Management of hepatocellular carcinoma. Hepatology 2005;42:1208-36.
12. Trevisani F, De NS, Rapaccini G, Farinati F, Benvegnu L, Zoli M, Grazi GL, Del PP, Di N, Bernardi M. Semiannual and annual surveillance of cirrhotic patients for hepatocellular carcinoma: effects on cancer stage and patient survival (Italian experience). Am J Gastroenterol 2002;97:734-44.
13. Sheu JC, Sung JL, Chen DS, Yang PM, Lai MY, Lee CS, Hsu HC, Chuang CN, Yang PC, Wang TH, et al. Growth rate of asymptomatic hepatocellular carcinoma and its clinical implications. Gastroenterology 1985;89:259-66.
14. Kubota K, Ina H, Okada Y, Irie T. Growth rate of primary single hepatocellular carcinoma: determining optimal screening interval with contrast enhanced computed tomography. Dig Dis Sci 2003;48:581-6.
15. Nagasue N, Yukaya H, Hamada T, Hirose S, Kanashima R, Inokuchi K. The natural history of hepatocellular carcinoma. A study of 100 untreated cases. Cancer 1984;54:1461-5.
16. Okuda K, Ohtsuki T, Obata H, Tomimatsu M, Okazaki N, Hasegawa H, Nakajima Y, Ohnishi K. Natural history of hepatocellular carcinoma and prognosis in relation to treatment. Study of 850 patients. Cancer 1985;56:918-28.
17. Livraghi T, Bolondi L, Buscarini L, Cottone M, Mazziotti A, Morabito A, Torzilli G. No treatment, resection and ethanol injection in hepatocellular carcinoma: a retrospective analysis of survival in 391 patients with cirrhosis. Italian Cooperative HCC Study Group. J Hepatol 1995;22:522-6.

18. Llovet JM, Bustamante J, Castells A, Vilana R, Ayuso Mdel C, Sala M, Bru C, Rodes J, Bruix J. Natural history of untreated nonsurgical hepatocellular carcinoma: rationale for the design and evaluation of therapeutic trials. Hepatology 1999;29:62-7.
19. Bruix J, Llovet JM. Prognostic assessment and evaluation of the benefits of treatment. J Clin Gastroenterol 2002;35:S138-42.
20. Llovet JM. Updated treatment approach to hepatocellular carcinoma. J Gastroenterol 2005;40:225-35.
21. Pons F, Varela M, Llovet JM. Staging systems in hepatocellular carcinoma. HPB (Oxford) 2005;7:35-41.
22. Wildi S, Pestalozzi BC, McCormack L, Clavien PA. Critical evaluation of the different staging systems for hepatocellular carcinoma. Br J Surg 2004;91:400-8.
23. A new prognostic system for hepatocellular carcinoma: a retrospective study of 435 patients: the Cancer of the Liver Italian Program (CLIP) investigators. Hepatology 1998;28:751-5.
24. Prospective validation of the CLIP score: a new prognostic system for patients with cirrhosis and hepatocellular carcinoma. The Cancer of the Liver Italian Program (CLIP) Investigators. Hepatology 2000;31:840-5.
25. Llovet JM, Bru C, Bruix J. Prognosis of hepatocellular carcinoma: the BCLC staging classification. Semin Liver Dis 1999;19:329-38.
26. Huang YH, Chen CH, Chang TT, Chen SC, Wang SY, Lee HS, Lin PW, Huang GT, Sheu JC, Tsai HM, Lee PC, Chau GY, Lui WY, Lee SD, Wu JC. Evaluation of predictive value of CLIP, Okuda, TNM and JIS staging systems for hepatocellular carcinoma patients undergoing surgery. J Gastroenterol Hepatol 2005;20:765-71.
27. Fong Y, Sun RL, Jarnagin W, Blumgart LH. An analysis of 412 cases of hepatocellular carcinoma at a Western center. Ann Surg 1999;229:790-9; discussion 799-800.
28. Mazzaferro V, Chun YS, Poon RT, Schwartz ME, Yao FY, Marsh JW, Bhoori S, Lee SG. Liver transplantation for hepatocellular carcinoma. Ann Surg Oncol 2008;15:1001-7.
29. Schwartz M. Liver transplantation for hepatocellular carcinoma. Gastroenterology 2004;127:S268-76.
30. Mazzaferro V, Regalia E, Doci R, Andreola S, Pulvirenti A, Bozzetti F, Montalto F, Ammatuna M, Morabito A, Gennari L. Liver transplantation for the treatment of small hepatocellular carcinomas in patients with cirrhosis. N Engl J Med 1996;334:693-9.
31. Roayaie S, Frischer JS, Emre SH, Fishbein TM, Sheiner PA, Sung M, Miller CM, Schwartz ME. Long-term results with multimodal adjuvant therapy and liver transplantation for the treatment of hepatocellular carcinomas larger than 5 centimeters. Ann Surg 2002;235:533-9.
32. Yao FY, Ferrell L, Bass NM, Watson JJ, Bacchetti P, Venook A, Ascher NL, Roberts JP. Liver transplantation for hepatocellular carcinoma: expansion of the tumor size limits does not adversely impact survival. Hepatology 2001;33:1394-403.

33. Yao FY, Bass NM, Nikolai B, Davern TJ, Kerlan R, Wu V, Ascher NL, Roberts JP. Liver transplantation for hepatocellular carcinoma: analysis of survival according to the intention-to-treat principle and dropout from the waiting list. Liver Transpl 2002;8:873-83.
34. Bolondi L, Piscaglia F, Camaggi V, Grazi GL, Cavallari A. Review article: liver transplantation for HCC. Treatment options on the waiting list. Aliment Pharmacol Ther 2003;17 Suppl 2:145-50.
35. Schwartz M, Roayaie S, Uva P. Treatment of HCC in patients awaiting liver transplantation. Am J Transplant 2007;7:1875-81.
36. Ono T, Yamanoi A, Nazmy El Assal O, Kohno H, Nagasue N. Adjuvant chemotherapy after resection of hepatocellular carcinoma causes deterioration of long-term prognosis in cirrhotic patients: metaanalysis of three randomized controlled trials. Cancer 2001;91:2378-85.
37. Schwartz JD, Schwartz M, Mandeli J, Sung M. Neoadjuvant and adjuvant therapy for resectable hepatocellular carcinoma: review of the randomised clinical trials. Lancet Oncol 2002;3:593-603.
38. Ribeiro A, Nagorney DM, Gores GJ. Localized hepatocellular carcinoma: therapeutic options. Curr Gastroenterol Rep 2000;2:72-81.
39. Livraghi T, Giorgio A, Marin G, Salmi A, de Sio I, Bolondi L, Pompili M, Brunello F, Lazzaroni S, Torzilli G, et al. Hepatocellular carcinoma and cirrhosis in 746 patients: long-term results of percutaneous ethanol injection. Radiology 1995;197:101-8.
40. Shiina S, Tagawa K, Niwa Y, Unuma T, Komatsu Y, Yoshiura K, Hamada E, Takahashi M, Shiratori Y, Terano A, et al. Percutaneous ethanol injection therapy for hepatocellular carcinoma: results in 146 patients. AJR Am J Roentgenol 1993;160:1023-8.
41. Pompili M, Rapaccini GL, de Luca F, Caturelli E, Astone A, Siena DA, Villani MR, Grattagliano A, Cedrone A, Gasbarrini G. Risk factors for intrahepatic recurrence of hepatocellular carcinoma in cirrhotic patients treated by percutaneous ethanol injection. Cancer 1997;79:1501-8.
42. Isobe H, Sakai H, Imari Y, Ikeda M, Shiomichi S, Nawata H. Intratumor ethanol injection therapy for solitary minute hepatocellular carcinoma. A study of 37 patients. J Clin Gastroenterol 1994;18:122-6.
43. Castells A, Bruix J, Bru C, Fuster J, Vilana R, Navasa M, Ayuso C, Boix L, Visa J, Rodes J. Treatment of small hepatocellular carcinoma in cirrhotic patients: a cohort study comparing surgical resection and percutaneous ethanol injection. Hepatology 1993;18:1121-6.
44. Gaiani S, Celli N, Cecilioni L, Piscaglia F, Bolondi L. Review article: percutaneous treatment of hepatocellular carcinoma. Aliment Pharmacol Ther 2003;17 Suppl 2:103-10.
45. Jansen MC, van Hillegersberg R, Chamuleau RA, van Delden OM, Gouma DJ, van Gulik TM. Outcome of regional and local ablative therapies for hepatocellular carcinoma: a collective review. Eur J Surg Oncol 2005;31:331-47.
46. Ng KK, Poon RT. Radiofrequency ablation for malignant liver tumor. Surg Oncol 2005;14:41-52.

47. Bruix J, Castells A, Montanya X, Calvet X, Bru C, Ayuso C, Jover L, Garcia L, Vilana R, Boix L, et al. Phase II study of transarterial embolization in European patients with hepatocellular carcinoma: need for controlled trials. Hepatology 1994;20:643-50.
48. Lin DY, Liaw YF, Lee TY, Lai CM. Hepatic arterial embolization in patients with unresectable hepatocellular carcinoma--a randomized controlled trial. Gastroenterology 1988;94:453-6.
49. Simonetti RG, Liberati A, Angiolini C, Pagliaro L. Treatment of hepatocellular carcinoma: a systematic review of randomized controlled trials. Ann Oncol 1997;8:117-36.
50. Llovet JM, Real MI, Montana X, Planas R, Coll S, Aponte J, Ayuso C, Sala M, Muchart J, Sola R, Rodes J, Bruix J. Arterial embolisation or chemoembolisation versus symptomatic treatment in patients with unresectable hepatocellular carcinoma: a randomised controlled trial. Lancet 2002;359:1734-9.
51. Bruix J, Llovet JM, Castells A, Montana X, Bru C, Ayuso MC, Vilana R, Rodes J. Transarterial embolization versus symptomatic treatment in patients with advanced hepatocellular carcinoma: results of a randomized, controlled trial in a single institution. Hepatology 1998;27:1578-83.
52. Llovet JM, Bruix J. Systematic review of randomized trials for unresectable hepatocellular carcinoma: Chemoembolization improves survival. Hepatology 2003;37:429-42.
53. Reidy DL, Schwartz JD. Therapy for unresectable hepatocellular carcinoma: review of the randomized clinical trials-I: hepatic arterial embolization and embolization-based therapies in unresectable hepatocellular carcinoma. Anticancer Drugs 2004;15:427-37.
54. Chang JM, Tzeng WS, Pan HB, Yang CF, Lai KH. Transcatheter arterial embolization with or without cisplatin treatment of hepatocellular carcinoma. A randomized controlled study. Cancer 1994;74:2449-53.
55. Kawai S, Tani M, Okamura J, Ogawa M, Ohashi Y, Monden M, Hayashi S, Inoue J, Kawarada Y, Kusano M, Kubo Y, Kuroda C, Sakata Y, Shimamura Y, Jinno K, Takahashi A, Takayasu K, Tamura K, Nagasue N, Nakanishi Y, Makino M, Masuzawa M, Yumoto Y, Mori T, Oda T. Prospective and randomized trial of lipiodol-transcatheter arterial chemoembolization for treatment of hepatocellular carcinoma: a comparison of epirubicin and doxorubicin (second cooperative study). The Cooperative Study Group for Liver Cancer Treatment of Japan. Semin Oncol 1997;24:S6-38-S6-45.
56. Kawai S, Tani M, Okamura J, Ogawa M, Ohashi Y, Monden M, Hayashi S, Inoue J, Kawarada Y, Kusano M, et al. Prospective and randomized clinical trial for the treatment of hepatocellular carcinoma--a comparison between L-TAE with farmorubicin and L-TAE with adriamycin: preliminary results (second cooperative study). Cooperative Study Group for Liver Cancer Treatment of Japan. Cancer Chemother Pharmacol 1994;33 Suppl:S97-102.
57. Lu W, Li Y, He X, Chen Y. Transcatheter arterial chemoembolization for hepatocellular carcinoma in patients with cirrhosis: evaluation of two kinds of dosages of anticancer drugs and analysis of prognostic factors. Hepatogastroenterology 2003;50:2079-83.

58. Bronowicki JP, Vetter D, Dumas F, Boudjema K, Bader R, Weiss AM, Wenger JJ, Boissel P, Bigard MA, Doffoel M. Transcatheter oily chemoembolization for hepatocellular carcinoma. A 4-year study of 127 French patients. Cancer 1994;74:16-24.
59. Trevisani F, De Notariis S, Rossi C, Bernardi M. Randomized control trials on chemoembolization for hepatocellular carcinoma: is there room for new studies? J Clin Gastroenterol 2001;32:383-9.
60. Geschwind JF, Ramsey DE, Choti MA, Thuluvath PJ, Huncharek MS. Chemoembolization of hepatocellular carcinoma: results of a metaanalysis. Am J Clin Oncol 2003;26:344-9.
61. Hatanaka Y, Yamashita Y, Takahashi M, Koga Y, Saito R, Nakashima K, Urata J, Miyao M. Unresectable hepatocellular carcinoma: analysis of prognostic factors in transcatheter management. Radiology 1995;195:747-52.
62. Ngan H, Lai CL, Fan ST, Lai EC, Yuen WK, Tso WK. Transcatheter arterial chemoembolization in inoperable hepatocellular carcinoma: four-year follow-up. J Vasc Interv Radiol 1996;7:419-25.
63. Yang CF, Ho YJ. Transcatheter arterial chemoembolization for hepatocellular carcinoma. Cancer Chemother Pharmacol 1992;31 Suppl:S86-8.
64. Bismuth H, Morino M, Sherlock D, Castaing D, Miglietta C, Cauquil P, Roche A. Primary treatment of hepatocellular carcinoma by arterial chemoembolization. Am J Surg 1992;163:387-94.
65. Hassoun Z, Gores GJ. Treatment of hepatocellular carcinoma. Clin Gastroenterol Hepatol 2003;1:10-8.
66. Johnson PJ. Systemic chemotherapy of liver tumors. Semin Surg Oncol 2000;19:116-24.
67. Yeo W, Chan PK, Zhong S, Ho WM, Steinberg JL, Tam JS, Hui P, Leung NW, Zee B, Johnson PJ. Frequency of hepatitis B virus reactivation in cancer patients undergoing cytotoxic chemotherapy: a prospective study of 626 patients with identification of risk factors. J Med Virol 2000;62:299-307.
68. Steinberg JL, Yeo W, Zhong S, Chan JY, Tam JS, Chan PK, Leung NW, Johnson PJ. Hepatitis B virus reactivation in patients undergoing cytotoxic chemotherapy for solid tumours: precore/core mutations may play an important role. J Med Virol 2000;60:249-55.
69. Yeo W, Lam KC, Zee B, Chan PS, Mo FK, Ho WM, Wong WL, Leung TW, Chan AT, Ma B, Mok TS, Johnson PJ. Hepatitis B reactivation in patients with hepatocellular carcinoma undergoing systemic chemotherapy. Ann Oncol 2004;15:1661-6.
70. Yang TS, Wang CH, Hsieh RK, Chen JS, Fung MC. Gemcitabine and doxorubicin for the treatment of patients with advanced hepatocellular carcinoma: a phase I-II trial. Ann Oncol 2002;13:1771-8.
71. Taieb J, Bonyhay L, Golli L, Ducreux M, Boleslawski E, Tigaud JM, de Baere T, Mansourbakht T, Delgado MA, Hannoun L, Poynard T, Boige V. Gemcitabine plus oxaliplatin for patients with advanced hepatocellular carcinoma using two different schedules. Cancer 2003;98:2664-70.
72. Poh SB, Bai LY, Chen PM. Pegylated liposomal doxorubicin-based combination chemotherapy as salvage treatment in patients with advanced hepatocellular carcinoma. Am J Clin Oncol 2005;28:540-6.
73. Johnson PJ, Williams R, Thomas H, Sherlock S, Murray-Lyon IM. Induction of remission in hepatocellular carcinoma with doxorubicin. Lancet 1978;1:1006-9.

74. Lai CL, Wu PC, Chan GC, Lok AS, Lin HJ. Doxorubicin versus no antitumor therapy in inoperable hepatocellular carcinoma. A prospective randomized trial. Cancer 1988;62:479-83.
75. Johnson PJ. Hepatocellular carcinoma: is current therapy really altering outcome? Gut 2002;51:459-62.
76. Yang TS, Lin YC, Chen JS, Wang HM, Wang CH. Phase II study of gemcitabine in patients with advanced hepatocellular carcinoma. Cancer 2000;89:750-6.
77. Kubicka S, Rudolph KL, Tietze MK, Lorenz M, Manns M. Phase II study of systemic gemcitabine chemotherapy for advanced unresectable hepatobiliary carcinomas. Hepatogastroenterology 2001;48:783-9.
78. Ulrich-Pur H, Kornek GV, Fiebiger W, Schull B, Raderer M, Scheithauer W. Treatment of advanced hepatocellular carcinoma with biweekly high-dose gemcitabine. Oncology 2001;60:313-5.
79. Fuchs CS, Clark JW, Ryan DP, Kulke MH, Kim H, Earle CC, Vincitore M, Mayer RJ, Stuart KE. A phase II trial of gemcitabine in patients with advanced hepatocellular carcinoma. Cancer 2002;94:3186-91.
80. Guan Z, Wang Y, Maoleekoonpairoj S, Chen Z, Kim WS, Ratanatharathorn V, Reece WH, Kim TW, Lehnert M. Prospective randomised phase II study of gemcitabine at standard or fixed dose rate schedule in unresectable hepatocellular carcinoma. Br J Cancer 2003;89:1865-9.
81. Lersch C, Schmelz R, Erdmann J, Hollweck R, Schulte-Frohlinde E, Eckel F, Nader M, Schusdziarra V. Treatment of HCC with pravastatin, octreotide, or gemcitabine--a critical evaluation. Hepatogastroenterology 2004;51:1099-103.
82. Leung TW, Tang AM, Zee B, Yu SC, Lai PB, Lau WY, Johnson PJ. Factors predicting response and survival in 149 patients with unresectable hepatocellular carcinoma treated by combination cisplatin, interferon-alpha, doxorubicin and 5-fluorouracil chemotherapy. Cancer 2002;94:421-7.
83. Johnson PJ, Alexopoulos A, Johnson RD, Williams R. Significance of serum bilirubin level in response of hepatocellular carcinoma to doxorubicin. J Hepatol 1986;3:149-53.
84. Yeo W, Mok TS, Zee B, Leung TW, Lai PB, Lau WY, Koh J, Mo FK, Yu SC, Chan AT, Hui P, Ma B, Lam KC, Ho WM, Wong HT, Tang A, Johnson PJ. A randomized phase III study of doxorubicin versus cisplatin/interferon alpha-2b/doxorubicin/fluorouracil (PIAF) combination chemotherapy for unresectable hepatocellular carcinoma. J Natl Cancer Inst 2005;97:1532-8.
85. Zhu AX. Systemic therapy of advanced hepatocellular carcinoma: how hopeful should we be? Oncologist 2006;11:790-800.
86. Kouroumalis E, Skordilis P, Thermos K, Vasilaki A, Moschandrea J, Manousos ON. Treatment of hepatocellular carcinoma with octreotide: a randomised controlled study. Gut 1998;42:442-7.
87. Martinez Cerezo FJ, Tomas A, Donoso L, Enriquez J, Guarner C, Balanzo J, Martinez Nogueras A, Vilardell F. Controlled trial of tamoxifen in patients with advanced hepatocellular carcinoma. J Hepatol 1994;20:702-6.
88. Manesis EK, Giannoulis G, Zoumboulis P, Vafiadou I, Hadziyannis SJ. Treatment of hepatocellular carcinoma with combined suppression and inhibition of sex hormones: a randomized, controlled trial. Hepatology 1995;21:1535-42.

89. Elba S, Giannuzzi V, Misciagna G, Manghisi OG. Randomized controlled trial of tamoxifen versus placebo in inoperable hepatocellular carcinoma. Ital J Gastroenterol 1994;26:66-8.
90. Mathurin P, Rixe O, Carbonell N, Bernard B, Cluzel P, Bellin MF, Khayat D, Opolon P, Poynard T. Review article: Overview of medical treatments in unresectable hepatocellular carcinoma--an impossible meta-analysis? Aliment Pharmacol Ther 1998;12:111-26.
91. Chow PK, Tai BC, Tan CK, Machin D, Win KM, Johnson PJ, Soo KC. High-dose tamoxifen in the treatment of inoperable hepatocellular carcinoma: A multicenter randomized controlled trial. Hepatology 2002;36:1221-6.
92. Castells A, Bruix J, Bru C, Ayuso C, Roca M, Boix L, Vilana R, Rodes J. Treatment of hepatocellular carcinoma with tamoxifen: a double-blind placebo-controlled trial in 120 patients. Gastroenterology 1995;109:917-22.
93. Tamoxifen in treatment of hepatocellular carcinoma: a randomised controlled trial. CLIP Group (Cancer of the Liver Italian Programme). Lancet 1998;352:17-20.
94. Liu CL, Fan ST, Ng IO, Lo CM, Poon RT, Wong J. Treatment of advanced hepatocellular carcinoma with tamoxifen and the correlation with expression of hormone receptors: a prospective randomized study. Am J Gastroenterol 2000;95:218-22.
95. Riestra S, Rodriguez M, Delgado M, Suarez A, Gonzalez N, de la Mata M, Diaz G, Mino-Fugarolas G, Rodrigo L. Tamoxifen does not improve survival of patients with advanced hepatocellular carcinoma. J Clin Gastroenterol 1998;26:200-3.
96. Ganne-Carrie N, Trinchet JC. Systemic treatment of hepatocellular carcinoma. Eur J Gastroenterol Hepatol 2004;16:275-81.
97. Yuen MF, Poon RT, Lai CL, Fan ST, Lo CM, Wong KW, Wong WM, Wong BC. A randomized placebo-controlled study of long-acting octreotide for the treatment of advanced hepatocellular carcinoma. Hepatology 2002;36:687-91.
98. Yu AS, Keeffe EB. Management of hepatocellular carcinoma. Rev Gastroenterol Disord 2003;3:8-24.
99. Avila MA, Berasain C, Sangro B, Prieto J. New therapies for hepatocellular carcinoma. Oncogene 2006;25:3866-84.
100. O'Neil BH, Venook AP. Hepatocellular carcinoma: the role of the North American GI Steering Committee Hepatobiliary Task Force and the advent of effective drug therapy. Oncologist 2007;12:1425-32.
101. Ogris M, Wagner E. Tumor-targeted gene transfer with DNA polyplexes. Somat Cell Mol Genet 2002;27:85-95.
102. Miller AD. Nonviral liposomes. Methods Mol Med 2004;90:107-37.
103. Niidome T, Huang L. Gene therapy progress and prospects: nonviral vectors. Gene Ther 2002;9:1647-52.
104. Nishikawa M, Huang L. Nonviral vectors in the new millennium: delivery barriers in gene transfer. Hum Gene Ther 2001;12:861-70.
105. Peng KW, Donovan KA, Schneider U, Cattaneo R, Lust JA, Russell SJ. Oncolytic measles viruses displaying a single-chain antibody against CD38, a myeloma cell marker. Blood 2003;101:2557-62.
106. Peng KW, Facteau S, Wegman T, O'Kane D, Russell SJ. Non-invasive in vivo monitoring of trackable viruses expressing soluble marker peptides. Nat Med 2002;8:527-31.

107. Peng KW, Ahmann GJ, Pham L, Greipp PR, Cattaneo R, Russell SJ. Systemic therapy of myeloma xenografts by an attenuated measles virus. Blood 2001;98:2002-7.
108. Dingli D, Diaz RM, Bergert ER, O'Connor MK, Morris JC, Russell SJ. Genetically targeted radiotherapy for multiple myeloma. Blood 2003.
109. Zhang J. RSJ. Vectors for cancer gene therapy. Cancer and Metastasis Reviews 1996;15:385-401.
110. Waller EK, Ernstoff MS. Modulation of antitumor immune responses by hematopoietic cytokines. Cancer 2003;97:1797-809.
111. Brentjens RJ, Latouche JB, Santos E, Marti F, Gong MC, Lyddane C, King PD, Larson S, Weiss M, Riviere I, Sadelain M. Eradication of systemic B-cell tumors by genetically targeted human T lymphocytes co-stimulated by CD80 and interleukin-15. Nat Med 2003;9:279-86.
112. Becknell B, Caligiuri MA. Cancer T cell therapy expands. Nat Med 2003;9:257-8.
113. Vile RG, Russell SJ, Lemoine NR. Cancer gene therapy: hard lessons and new courses. Gene Ther 2000;7:2-8.
114. Waldmann TA. Immunotherapy: past, present and future. Nat Med 2003;9:269-77.
115. Carrau RL, Barnes EL, Snyderman CH, Petruzzelli G, Kachman K, Rueger R, D'Amico F, Johnson JT. Tumor angiogenesis as a predictor of tumor aggressiveness and metastatic potential in squamous cell carcinoma of the head and neck. Invasion Metastasis 1995;15:197-202.
116. Jaeger TM, Weidner N, Chew K, Moore DH, Kerschmann RL, Waldman FM, Carroll PR. Tumor angiogenesis correlates with lymph node metastases in invasive bladder cancer. J Urol 1995;154:69-71.
117. Weidner N, Folkman J. Tumoral vascularity as a prognostic factor in cancer. Important Adv Oncol 1996:167-90.
118. Dvorak HF, Brown LF, Detmar M, Dvorak AM. Vascular permeability factor/vascular endothelial growth factor, microvascular hyperpermeability, and angiogenesis. Am J Pathol 1995;146:1029-39.
119. Ribatti D, Vacca A, Dammacco F. New non-angiogenesis dependent pathways for tumour growth. Eur J Cancer 2003;39:1835-41.
120. Davis DW, McConkey DJ, Zhang W, Herbst RS. Antiangiogenic tumor therapy. Biotechniques 2003;34:1048-50, 1052, 1054 passim.
121. Maxwell IH, Spitzer AL, Long CJ, Maxwell F. Autonomous parvovirus transduction of a gene under control of tissue-specific or inducible promoters. Gene Ther 1996;3:28-36.
122. Ried MU, Girod A, Leike K, Buning H, Hallek M. Adeno-associated virus capsids displaying immunoglobulin-binding domains permit antibody-mediated vector retargeting to specific cell surface receptors. J Virol 2002;76:4559-66.
123. Flasshove M, Moritz T, Bardenheuer W, Seeber S. Hematoprotection by transfer of drug-resistance genes. Acta Haematol 2003;110:93-106.
124. Laufs S, Buss EC, Zeller WJ, Fruehauf S. Transfer of drug resistance genes in hematopoietic progenitors for chemoprotection: is it still an option? Drug Resist Updat 2003;6:57-69.
125. Halene S, Kohn DB. Gene therapy using hematopoietic stem cells: Sisyphus approaches the crest. Hum Gene Ther 2000;11:1259-67.

126. Strauss LC, Trischmann TM, Rowley SD, Wiley JM, Civin CI. Selection of normal human hematopoietic stem cells for bone marrow transplantation using immunomagnetic microspheres and CD34 antibody. Am J Pediatr Hematol Oncol 1991;13:217-21.
127. Krause DS, Fackler MJ, Civin CI, May WS. CD34: structure, biology, and clinical utility. Blood 1996;87:1-13.
128. Laver J, Traycoff CM, Abdel-Mageed A, Gee A, Lee C, Turner C, Srour EF, Abboud M. Effects of CD34+ selection and T cell immunodepletion on cord blood hematopoietic progenitors: relevance to stem cell transplantation. Exp Hematol 1995;23:1492-6.
129. Berns KI. Parvoviridae: The viruses and their replication. In: Fields BN KD, Howley PM, Channock RM, Melnick JL, Monath TP, Roizman B, Straus SE, ed. Virology. Philadelphia: Lippincott-Raven, 1996:2173-2197.
130. Fields BN KD, Howley PM, Channock RM, Melnick JL, Monath TP, Roizman B, Straus SE. Fields Virology. 2006.
131. Cotmore SF, Tattersall, P. DNA replication in the autonomous parvoviruses. Semin Virol 1995;6:271-281.
132. Cotmore SF, Tattersall P. The autonomously replicating parvoviruses of vertebrates. Adv Virus Res 1987;33:91-174.
133. Kestler J, Neeb B, Struyf S, Van Damme J, Cotmore SF, D'Abramo A, Tattersall P, Rommelaere J, Dinsart C, Cornelis JJ. cis requirements for the efficient production of recombinant DNA vectors based on autonomous parvoviruses. Hum Gene Ther 1999;10:1619-32.
134. Pintel D, Dadachanji D, Astell CR, Ward DC. The genome of minute virus of mice, an autonomous parvovirus, encodes two overlapping transcription units. Nucleic Acids Res 1983;11:1019-38.
135. Astell CR, Thomson M, Merchlinsky M, Ward DC. The complete DNA sequence of minute virus of mice, an autonomous parvovirus. Nucleic Acids Res 1983;11:999-1018.
136. Astell CR, Thomson M, Chow MB, Ward DC. Structure and replication of minute virus of mice DNA. Cold Spring Harb Symp Quant Biol 1983;47 Pt 2:751-62.
137. Cotmore SF, Tattersall P. Organization of nonstructural genes of the autonomous parvovirus minute virus of mice. J Virol 1986;58:724-32.
138. Cotmore SF, McKie VC, Anderson LJ, Astell CR, Tattersall P. Identification of the major structural and nonstructural proteins encoded by human parvovirus B19 and mapping of their genes by procaryotic expression of isolated genomic fragments. J Virol 1986;60:548-57.
139. Spegelaere P, van Hille B, Spruyt N, Faisst S, Cornelis JJ, Rommelaere J. Initiation of transcription from the minute virus of mice P4 promoter is stimulated in rat cells expressing a c-Ha-ras oncogene. J Virol 1991;65:4919-28.
140. Ahn JK, Pitluk ZW, Ward DC. The GC box and TATA transcription control elements in the P38 promoter of the minute virus of mice are necessary and sufficient for transactivation by the nonstructural protein NS1. J Virol 1992;66:3776-83.
141. Christensen J, Cotmore SF, Tattersall P. Minute virus of mice transcriptional activator protein NS1 binds directly to the transactivation region of the viral P38 promoter in a strictly ATP-dependent manner. J Virol 1995;69:5422-30.

142. Lorson C, Pintel DJ. Characterization of the minute virus of mice P38 core promoter elements. J Virol 1997;71:6568-75.
143. Lorson C, Burger LR, Mouw M, Pintel DJ. Efficient transactivation of the minute virus of mice P38 promoter requires upstream binding of NS1. J Virol 1996;70:834-42.
144. Cornelis JJ, Salome N, Dinsart C, Rommelaere J. Vectors based on autonomous parvoviruses: novel tools to treat cancer? J Gene Med 2004;6 Suppl 1:S193-202.
145. Rhode SL, 3rd. trans-Activation of parvovirus P38 promoter by the 76K noncapsid protein. J Virol 1985;55:886-9.
146. Cziepluch C, Kordes E, Poirey R, Grewenig A, Rommelaere J, Jauniaux JC. Identification of a novel cellular TPR-containing protein, SGT, that interacts with the nonstructural protein NS1 of parvovirus H-1. J Virol 1998;72:4149-56.
147. Cziepluch C, Lampel S, Grewenig A, Grund C, Lichter P, Rommelaere J. H-1 parvovirus-associated replication bodies: a distinct virus-induced nuclear structure. J Virol 2000;74:4807-15.
148. Bodendorf U, Cziepluch C, Jauniaux JC, Rommelaere J, Salome N. Nuclear export factor CRM1 interacts with nonstructural proteins NS2 from parvovirus minute virus of mice. J Virol 1999;73:7769-79.
149. Cotmore SF, Christensen J, Nuesch JP, Tattersall P. The NS1 polypeptide of the murine parvovirus minute virus of mice binds to DNA sequences containing the motif [ACCA]2-3. J Virol 1995;69:1652-60.
150. Nuesch JP, Cotmore SF, Tattersall P. Sequence motifs in the replicator protein of parvovirus MVM essential for nicking and covalent attachment to the viral origin: identification of the linking tyrosine. Virology 1995;209:122-35.
151. Cotmore SF, Tattersall P. High-mobility group 1/2 proteins are essential for initiating rolling-circle-type DNA replication at a parvovirus hairpin origin. J Virol 1998;72:8477-84.
152. Christensen J, Cotmore SF, Tattersall P. Minute virus of mice initiator protein NS1 and a host KDWK family transcription factor must form a precise ternary complex with origin DNA for nicking to occur. J Virol 2001;75:7009-17.
153. Skiadopoulos MH, Salvino R, Leong WL, Faust EA. Characterization of linker insertion and point mutations in the NS-1 gene of minute virus of mice: effects on DNA replication and transcriptional activation functions of NS-1. Virology 1992;188:122-34.
154. Caillet-Fauquet P, Perros M, Brandenburger A, Spegelaere P, Rommelaere J. Programmed killing of human cells by means of an inducible clone of parvoviral genes encoding non-structural proteins. Embo J 1990;9:2989-95.
155. Brownstein DG, Smith AL, Johnson EA, Pintel DJ, Naeger LK, Tattersall P. The pathogenesis of infection with minute virus of mice depends on expression of the small nonstructural protein NS2 and on the genotype of the allotropic determinants VP1 and VP2. J Virol 1992;66:3118-24.
156. Cotmore SF, D'Abramo AM, Jr., Carbonell LF, Bratton J, Tattersall P. The NS2 polypeptide of parvovirus MVM is required for capsid assembly in murine cells. Virology 1997;231:267-80.
157. Li X, Rhode SL, 3rd. The parvovirus H-1 NS2 protein affects viral gene expression through sequences in the 3' untranslated region. Virology 1993;194:10-9.

158. Li X, Rhode SL, 3rd. Nonstructural protein NS2 of parvovirus H-1 is required for efficient viral protein synthesis and virus production in rat cells in vivo and in vitro. Virology 1991;184:117-30.
159. Naeger LK, Cater J, Pintel DJ. The small nonstructural protein (NS2) of the parvovirus minute virus of mice is required for efficient DNA replication and infectious virus production in a cell-type-specific manner. J Virol 1990;64:6166-75.
160. Eichwald V, Daeffler L, Klein M, Rommelaere J, Salome N. The NS2 proteins of parvovirus minute virus of mice are required for efficient nuclear egress of progeny virions in mouse cells. J Virol 2002;76:10307-19.
161. Brandenburger A, Legendre D, Avalosse B, Rommelaere J. NS-1 and NS-2 proteins may act synergistically in the cytopathogenicity of parvovirus MVMp. Virology 1990;174:576-84.
162. Legrand C, Rommelaere J, Caillet-Fauquet P. MVM(p) NS-2 protein expression is required with NS-1 for maximal cytotoxicity in human transformed cells. Virology 1993;195:149-55.
163. Brown KE, Anderson SM, Young NS. Erythrocyte P antigen: cellular receptor for B19 parvovirus. Science 1993;262:114-7.
164. Weigel-Kelley KA, Yoder MC, Srivastava A. Recombinant human parvovirus B19 vectors: erythrocyte P antigen is necessary but not sufficient for successful transduction of human hematopoietic cells. J Virol 2001;75:4110-6.
165. Weigel-Kelley KA, Yoder MC, Srivastava A. Alpha5beta1 integrin as a cellular coreceptor for human parvovirus B19: requirement of functional activation of beta1 integrin for viral entry. Blood 2003;102:3927-33.
166. Govindasamy L, Hueffer K, Parrish CR, Agbandje-McKenna M. Structures of host range-controlling regions of the capsids of canine and feline parvoviruses and mutants. J Virol 2003;77:12211-21.
167. Hueffer K, Govindasamy L, Agbandje-McKenna M, Parrish CR. Combinations of two capsid regions controlling canine host range determine canine transferrin receptor binding by canine and feline parvoviruses. J Virol 2003;77:10099-105.
168. Hueffer K, Parker JS, Weichert WS, Geisel RE, Sgro JY, Parrish CR. The natural host range shift and subsequent evolution of canine parvovirus resulted from virus-specific binding to the canine transferrin receptor. J Virol 2003;77:1718-26.
169. Parker JS, Murphy WJ, Wang D, O'Brien SJ, Parrish CR. Canine and feline parvoviruses can use human or feline transferrin receptors to bind, enter, and infect cells. J Virol 2001;75:3896-902.
170. Harbison CE, Chiorini JA, Parrish CR. The parvovirus capsid odyssey: from the cell surface to the nucleus. Trends Microbiol 2008;16:208-14.
171. Mani B, Baltzer C, Valle N, Almendral JM, Kempf C, Ros C. Low pH-dependent endosomal processing of the incoming parvovirus minute virus of mice virion leads to externalization of the VP1 N-terminal sequence (N-VP1), N-VP2 cleavage, and uncoating of the full-length genome. J Virol 2006;80:1015-24.
172. Ros C, Burckhardt CJ, Kempf C. Cytoplasmic trafficking of minute virus of mice: low-pH requirement, routing to late endosomes, and proteasome interaction. J Virol 2002;76:12634-45.

173. Bashir T, Horlein R, Rommelaere J, Willwand K. Cyclin A activates the DNA polymerase delta -dependent elongation machinery in vitro: A parvovirus DNA replication model. Proc Natl Acad Sci U S A 2000;97:5522-7.
174. Bashir T, Rommelaere J, Cziepluch C. In vivo accumulation of cyclin A and cellular replication factors in autonomous parvovirus minute virus of mice-associated replication bodies. J Virol 2001;75:4394-8.
175. Richards RG, Armentrout RW. Early events in parvovirus replication: lack of integration by minute virus of mice into host cell DNA. J Virol 1979;30:397-9.
176. Deleu L, Pujol A, Faisst S, Rommelaere J. Activation of promoter P4 of the autonomous parvovirus minute virus of mice at early S phase is required for productive infection. J Virol 1999;73:3877-85.
177. Bultmann BD, Klingel K, Sotlar K, Bock CT, Kandolf R. Parvovirus B19: a pathogen responsible for more than hematologic disorders. Virchows Arch 2003;442:8-17.
178. Rommelaere J, Cornelis JJ. Antineoplastic activity of parvoviruses. J Virol Methods 1991;33:233-51.
179. Dupressoir T, Vanacker JM, Cornelis JJ, Duponchel N, Rommelaere J. Inhibition by parvovirus H-1 of the formation of tumors in nude mice and colonies in vitro by transformed human mammary epithelial cells. Cancer Res 1989;49:3203-8.
180. Faisst S, Guittard D, Benner A, Cesbron JY, Schlehofer JR, Rommelaere J, Dupressoir T. Dose-dependent regression of HeLa cell-derived tumours in SCID mice after parvovirus H-1 infection. Int J Cancer 1998;75:584-9.
181. Toolan HW, Ledinko N. Inhibition by H-1 virus of the incidence of tumors produced by adenovirus 12 in hamsters. Virology 1968;35:475-8.
182. Guetta E, Mincberg M, Mousset S, Bertinchamps C, Rommelaere J, Tal J. Selective killing of transformed rat cells by minute virus of mice does not require infectious virus production. J Virol 1990;64:458-62.
183. Chen YQ, Tuynder MC, Cornelis JJ, Boukamp P, Fusenig NE, Rommelaere J. Sensitization of human keratinocytes to killing by parvovirus H-1 takes place during their malignant transformation but does not require them to be tumorigenic. Carcinogenesis 1989;10:163-7.
184. Cornelis JJ, Chen YQ, Spruyt N, Duponchel N, Cotmore SF, Tattersall P, Rommelaere J. Susceptibility of human cells to killing by the parvoviruses H-1 and minute virus of mice correlates with viral transcription. J Virol 1990;64:2537-44.
185. Cornelis JJ, Becquart P, Duponchel N, Salome N, Avalosse BL, Namba M, Rommelaere J. Transformation of human fibroblasts by ionizing radiation, a chemical carcinogen, or simian virus 40 correlates with an increase in susceptibility to the autonomous parvoviruses H-1 virus and minute virus of mice. J Virol 1988;62:1679-86.
186. Chen YQ, de Foresta F, Hertoghs J, Avalosse BL, Cornelis JJ, Rommelaere J. Selective killing of simian virus 40-transformed human fibroblasts by parvovirus H-1. Cancer Res 1986;46:3574-9.
187. Van Pachterbeke C, Tuynder M, Cosyn JP, Lespagnard L, Larsimont D, Rommelaere J. Parvovirus H-1 inhibits growth of short-term tumor-derived but not normal mammary tissue cultures. Int J Cancer 1993;55:672-7.
188. Mousset S, Rommelaere J. Minute virus of mice inhibits cell transformation by simian virus 40. Nature 1982;300:537-9.

189. Toolan H, Ledinko N. Growth and cytopathogenicity of H-viruses in human and simian cell cultures. Nature 1965;208:812-3.
190. Salome N, van Hille B, Duponchel N, Meneguzzi G, Cuzin F, Rommelaere J, Cornelis JJ. Sensitization of transformed rat cells to parvovirus MVMp is restricted to specific oncogenes. Oncogene 1990;5:123-30.
191. Fuks F, Deleu L, Dinsart C, Rommelaere J, Faisst S. ras oncogene-dependent activation of the P4 promoter of minute virus of mice through a proximal P4 element interacting with the Ets family of transcription factors. J Virol 1996;70:1331-9.
192. Perros M, Deleu L, Vanacker JM, Kherrouche Z, Spruyt N, Faisst S, Rommelaere J. Upstream CREs participate in the basal activity of minute virus of mice promoter P4 and in its stimulation in ras-transformed cells. J Virol 1995;69:5506-15.
193. Deleu L, Fuks F, Spitkovsky D, Horlein R, Faisst S, Rommelaere J. Opposite transcriptional effects of cyclic AMP-responsive elements in confluent or p27KIP-overexpressing cells versus serum-starved or growing cells. Mol Cell Biol 1998;18:409-19.
194. Legendre D, Rommelaere J. Terminal regions of the NS-1 protein of the parvovirus minute virus of mice are involved in cytotoxicity and promoter trans inhibition. J Virol 1992;66:5705-13.
195. Astell CR, Liu Q, Harris CE, Brunstein J, Jindal HK, Tam P. Minute virus of mice cis-acting sequences required for genome replication and the role of the trans-acting viral protein, NS-1. Prog Nucleic Acid Res Mol Biol 1996;55:245-85.
196. Op De Beeck A, Caillet-Fauquet P. The NS1 protein of the autonomous parvovirus minute virus of mice blocks cellular DNA replication: a consequence of lesions to the chromatin? J Virol 1997;71:5323-9.
197. Op De Beeck A, Caillet-Fauquet P. Viruses and the cell cycle. Prog Cell Cycle Res 1997;3:1-19.
198. Ohshima T, Iwama M, Ueno Y, Sugiyama F, Nakajima T, Fukamizu A, Yagami K. Induction of apoptosis in vitro and in vivo by H-1 parvovirus infection. J Gen Virol 1998;79 (Pt 12):3067-71.
199. Rayet B, Lopez-Guerrero JA, Rommelaere J, Dinsart C. Induction of programmed cell death by parvovirus H-1 in U937 cells: connection with the tumor necrosis factor alpha signalling pathway. J Virol 1998;72:8893-903.
200. Moehler M, Blechacz B, Weiskopf N, Zeidler M, Stremmel W, Rommelaere J, Galle PR, Cornelis JJ. Effective infection, apoptotic cell killing and gene transfer of human hepatoma cells but not primary hepatocytes by parvovirus H1 and derived vectors. Cancer Gene Ther 2001;8:158-67.
201. Haviv YS, Curiel DT. Conditional gene targeting for cancer gene therapy. Adv Drug Deliv Rev 2001;53:135-54.
202. Galanis E, Vile R, Russell SJ. Delivery systems intended for in vivo gene therapy of cancer: targeting and replication competent viral vectors. Crit Rev Oncol Hematol 2001;38:177-92.
203. Maxwell IH, Chapman JT, Scherrer LC, Spitzer AL, Leptihn S, Maxwell F, Corsini JA. Expansion of tropism of a feline parvovirus to target a human tumor cell line by display of an alpha(v) integrin binding peptide on the capsid. Gene Ther 2001;8:324-31.

204. Maxwell IH, Maxwell F. Control of parvovirus DNA replication by a tetracycline-regulated repressor. Gene Ther 1999;6:309-13.
205. Malerba M, Daeffler L, Rommelaere J, Iggo RD. Replicating parvoviruses that target colon cancer cells. J Virol 2003;77:6683-91.
206. Schlehofer JR, Rentrop M, Mannel DN. Parvoviruses are inefficient in inducing interferon-beta, tumor necrosis factor-alpha, or interleukin-6 in mammalian cells. Med Microbiol Immunol (Berl) 1992;181:153-64.
207. Moehler M, Zeidler M, Schede J, Rommelaere J, Galle PR, Cornelis JJ, Heike M. Oncolytic parvovirus H1 induces release of heat-shock protein HSP72 in susceptible human tumor cells but may not affect primary immune cells. Cancer Gene Ther 2003;10:477-80.
208. Anderson KM, Srivastava PK. Heat, heat shock, heat shock proteins and death: a central link in innate and adaptive immune responses. Immunol Lett 2000;74:35-9.
209. Brunda MJ, Luistro L, Warrier RR, Wright RB, Hubbard BR, Murphy M, Wolf SF, Gately MK. Antitumor and antimetastatic activity of interleukin 12 against murine tumors. J Exp Med 1993;178:1223-30.
210. Nastala CL, Edington HD, McKinney TG, Tahara H, Nalesnik MA, Brunda MJ, Gately MK, Wolf SF, Schreiber RD, Storkus WJ, et al. Recombinant IL-12 administration induces tumor regression in association with IFN-gamma production. J Immunol 1994;153:1697-706.
211. Kawai K, Tani K, Asano S, Akaza H. Ex vivo gene therapy using granulocyte-macrophage colony-stimulating factor-transduced tumor vaccines. Mol Urol 2000;4:43-6.
212. Parmiani G, Rivoltini L, Andreola G, Carrabba M. Cytokines in cancer therapy. Immunol Lett 2000;74:41-4.
213. Rosenberg SA. Progress in human tumour immunology and immunotherapy. Nature 2001;411:380-4.
214. Gansbacher B, Zier K, Daniels B, Cronin K, Bannerji R, Gilboa E. Interleukin 2 gene transfer into tumor cells abrogates tumorigenicity and induces protective immunity. J Exp Med 1990;172:1217-24.
215. Siapati KE, Barker S, Kinnon C, Michalski A, Anderson R, Brickell P, Thrasher AJ, Hart SL. Improved antitumour immunity in murine neuroblastoma using a combination of IL-2 and IL-12. Br J Cancer 2003;88:1641-8.
216. Cameron RB, Spiess PJ, Rosenberg SA. Synergistic antitumor activity of tumor-infiltrating lymphocytes, interleukin 2, and local tumor irradiation. Studies on the mechanism of action. J Exp Med 1990;171:249-63.
217. Trinchieri G. Proinflammatory and immunoregulatory functions of interleukin-12. Int Rev Immunol 1998;16:365-96.
218. Russell SJ, Brandenburger A, Flemming CL, Collins MK, Rommelaere J. Transformation-dependent expression of interleukin genes delivered by a recombinant parvovirus. J Virol 1992;66:2821-8.
219. Haag A, Menten P, Van Damme J, Dinsart C, Rommelaere J, Cornelis JJ. Highly efficient transduction and expression of cytokine genes in human tumor cells by means of autonomous parvovirus vectors; generation of antitumor responses in recipient mice. Hum Gene Ther 2000;11:597-609.
220. El Bakkouri K, Servais C, Clement N, Cheong SC, Franssen JD, Velu T, Brandenburger A. In vivo anti-tumour activity of recombinant MVM parvoviral vectors carrying the human interleukin-2 cDNA. J Gene Med 2005;7:189-97.

221. Bonecchi R, Polentarutti N, Luini W, Borsatti A, Bernasconi S, Locati M, Power C, Proudfoot A, Wells TN, Mackay C, Mantovani A, Sozzani S. Up-regulation of CCR1 and CCR3 and induction of chemotaxis to CC chemokines by IFN-gamma in human neutrophils. J Immunol 1999;162:474-9.
222. Dieu-Nosjean MC, Vicari A, Lebecque S, Caux C. Regulation of dendritic cell trafficking: a process that involves the participation of selective chemokines. J Leukoc Biol 1999;66:252-62.
223. Allavena P, Bianchi G, Zhou D, van Damme J, Jilek P, Sozzani S, Mantovani A. Induction of natural killer cell migration by monocyte chemotactic protein-1, -2 and -3. Eur J Immunol 1994;24:3233-6.
224. Noso N, Proost P, Van Damme J, Schroder JM. Human monocyte chemotactic proteins-2 and 3 (MCP-2 and MCP-3) attract human eosinophils and desensitize the chemotactic responses towards RANTES. Biochem Biophys Res Commun 1994;200:1470-6.
225. Sozzani S, Luini W, Borsatti A, Polentarutti N, Zhou D, Piemonti L, D'Amico G, Power CA, Wells TN, Gobbi M, Allavena P, Mantovani A. Receptor expression and responsiveness of human dendritic cells to a defined set of CC and CXC chemokines. J Immunol 1997;159:1993-2000.
226. Taub DD, Proost P, Murphy WJ, Anver M, Longo DL, van Damme J, Oppenheim JJ. Monocyte chemotactic protein-1 (MCP-1), -2, and -3 are chemotactic for human T lymphocytes. J Clin Invest 1995;95:1370-6.
227. Alam R, Forsythe P, Stafford S, Heinrich J, Bravo R, Proost P, Van Damme J. Monocyte chemotactic protein-2, monocyte chemotactic protein-3, and fibroblast-induced cytokine. Three new chemokines induce chemotaxis and activation of basophils. J Immunol 1994;153:3155-9.
228. Proost P, Wuyts A, Van Damme J. Human monocyte chemotactic proteins-2 and -3: structural and functional comparison with MCP-1. J Leukoc Biol 1996;59:67-74.
229. Rosl F, Lengert M, Albrecht J, Kleine K, Zawatzky R, Schraven B, zur Hausen H. Differential regulation of the JE gene encoding the monocyte chemoattractant protein (MCP-1) in cervical carcinoma cells and derived hybrids. J Virol 1994;68:2142-50.
230. Kleine K, Konig G, Kreuzer J, Komitowski D, Zur Hausen H, Rosl F. The effect of the JE (MCP-1) gene, which encodes monocyte chemoattractant protein-1, on the growth of HeLa cells and derived somatic-cell hybrids in nude mice. Mol Carcinog 1995;14:179-89.
231. Wetzel K, Menten P, Opdenakker G, Van Damme J, Grone HJ, Giese N, Vecchi A, Sozzani S, Cornelis JJ, Rommelaere J, Dinsart C. Transduction of human MCP-3 by a parvoviral vector induces leukocyte infiltration and reduces growth of human cervical carcinoma cell xenografts. J Gene Med 2001;3:326-37.
232. Wetzel K, Struyf S, Van Damme J, Kayser T, Vecchi A, Sozzani S, Rommelaere J, Cornelis JJ, Dinsart C. MCP-3 (CCL7) delivered by parvovirus MVMp reduces tumorigenicity of mouse melanoma cells through activation of T lymphocytes and NK cells. Int J Cancer 2007;120:1364-71.
233. Chen L, Ashe S, Brady WA, Hellstrom I, Hellstrom KE, Ledbetter JA, McGowan P, Linsley PS. Costimulation of antitumor immunity by the B7 counterreceptor for the T lymphocyte molecules CD28 and CTLA-4. Cell 1992;71:1093-102.

234. Chen L, McGowan P, Ashe S, Johnston J, Li Y, Hellstrom I, Hellstrom KE. Tumor immunogenicity determines the effect of B7 costimulation on T cell-mediated tumor immunity. J Exp Med 1994;179:523-32.
235. Townsend SE, Allison JP. Tumor rejection after direct costimulation of CD8+ T cells by B7-transfected melanoma cells. Science 1993;259:368-70.
236. Townsend SE, Su FW, Atherton JM, Allison JP. Specificity and longevity of antitumor immune responses induced by B7-transfected tumors. Cancer Res 1994;54:6477-83.
237. Matulonis UA, Dosiou C, Lamont C, Freeman GJ, Mauch P, Nadler LM, Griffin JD. Role of B7-1 in mediating an immune response to myeloid leukemia cells. Blood 1995;85:2507-15.
238. Gancberg D, Zeicher M, Bakkus M, Dupont F, Leo O, Moser M, Spegelaere P, Thielemans K, Urbain J, Horth M. Oncoselective transduction of CD80 and CD86 in tumor cell lines using an autonomous recombinant parvovirus. Anticancer Res 2000;20:1825-32.
239. Giese NA, Raykov Z, DeMartino L, Vecchi A, Sozzani S, Dinsart C, Cornelis JJ, Rommelaere J. Suppression of metastatic hemangiosarcoma by a parvovirus MVMp vector transducing the IP-10 chemokine into immunocompetent mice. Cancer Gene Ther 2002;9:432-42.
240. Angiolillo AL, Sgadari C, Taub DD, Liao F, Farber JM, Maheshwari S, Kleinman HK, Reaman GH, Tosato G. Human interferon-inducible protein 10 is a potent inhibitor of angiogenesis in vivo. J Exp Med 1995;182:155-62.
241. Farber JM. Mig and IP-10: CXC chemokines that target lymphocytes. J Leukoc Biol 1997;61:246-57.
242. Telerman A, Tuynder M, Dupressoir T, Robaye B, Sigaux F, Shaulian E, Oren M, Rommelaere J, Amson R. A model for tumor suppression using H-1 parvovirus. Proc Natl Acad Sci U S A 1993;90:8702-6.
243. Noteborn MH, de Boer GF, van Roozelaar DJ, Karreman C, Kranenburg O, Vos JG, Jeurissen SH, Hoeben RC, Zantema A, Koch G, et al. Characterization of cloned chicken anemia virus DNA that contains all elements for the infectious replication cycle. J Virol 1991;65:3131-9.
244. Danen-Van Oorschot AA, Zhang YH, Leliveld SR, Rohn JL, Seelen MC, Bolk MW, Van Zon A, Erkeland SJ, Abrahams JP, Mumberg D, Noteborn MH. Importance of nuclear localization of Apoptin for tumor-specific induction of apoptosis. J Biol Chem 2003.
245. Leliveld SR, Zhang YH, Rohn JL, Noteborn MH, Abrahams JP. Apoptin induces tumor-specific apoptosis as a globular multimer. J Biol Chem 2003;278:9042-51.
246. Danen-van Oorschot AA, van Der Eb AJ, Noteborn MH. The chicken anemia virus-derived protein apoptin requires activation of caspases for induction of apoptosis in human tumor cells. J Virol 2000;74:7072-8.
247. Zhuang SM, Shvarts A, van Ormondt H, Jochemsen AG, van der Eb AJ, Noteborn MH. Apoptin, a protein derived from chicken anemia virus, induces p53-independent apoptosis in human osteosarcoma cells. Cancer Res 1995;55:486-9.
248. Danen-Van Oorschot AA, Fischer DF, Grimbergen JM, Klein B, Zhuang S, Falkenburg JH, Backendorf C, Quax PH, Van der Eb AJ, Noteborn MH. Apoptin induces apoptosis in human transformed and malignant cells but not in normal cells. Proc Natl Acad Sci U S A 1997;94:5843-7.

249. Olijslagers S, Dege AY, Dinsart C, Voorhoeve M, Rommelaere J, Noteborn MH, Cornelis JJ. Potentiation of a recombinant oncolytic parvovirus by expression of Apoptin. Cancer Gene Ther 2001;8:958-65.
250. Dupont F, Avalosse B, Karim A, Mine N, Bosseler M, Maron A, Van den Broeke AV, Ghanem GE, Burny A, Zeicher M. Tumor-selective gene transduction and cell killing with an oncotropic autonomous parvovirus-based vector. Gene Ther 2000;7:790-6.
251. Brandenburger A, Coessens E, El Bakkouri K, Velu T. Influence of sequence and size of DNA on packaging efficiency of parvovirus MVM-based vectors. Hum Gene Ther 1999;10:1229-38.
252. Bluming AZ, Ziegler JL. Regression of Burkitt's lymphoma in association with measles infection. Lancet 1971;2:105-6.
253. Zygiert Z. Hodgkin's disease: remissions after measles. Lancet 1971;1:593.
254. Mota HC. Infantile Hodgkin's disease: remission after measles. Br Med J 1973;2:421.
255. Grote D, Russell SJ, Cornu TI, Cattaneo R, Vile R, Poland GA, Fielding AK. Live attenuated measles virus induces regression of human lymphoma xenografts in immunodeficient mice. Blood 2001;97:3746-54.
256. Enders JF, Peebles TC. Propagation in tissue cultures of cytopathogenic agents from patients with measles. Proc Soc Exp Biol Med 1954;86:277-86.
257. Rota JS, Wang ZD, Rota PA, Bellini WJ. Comparison of sequences of the H, F, and N coding genes of measles virus vaccine strains. Virus Res 1994;31:317-30.
258. Griffin DE, Pan CH, Moss WJ. Measles vaccines. Front Biosci 2008;13:1352-70.
259. Liu X, Bankamp B, Xu W, Bellini WJ, Rota PA. The genomic termini of wild-type and vaccine strains of measles virus. Virus Res 2006;122:78-84.
260. Zuniga A, Wang Z, Liniger M, Hangartner L, Caballero M, Pavlovic J, Wild P, Viret JF, Glueck R, Billeter MA, Naim HY. Attenuated measles virus as a vaccine vector. Vaccine 2007;25:2974-83.
261. Live attenuated measles vaccine. EPI Newsl 1980;2:6.
262. Duclos P, Ward BJ. Measles vaccines: a review of adverse events. Drug Saf 1998;19:435-54.
263. Radecke F, Spielhofer P, Schneider H, Kaelin K, Huber M, Dotsch C, Christiansen G, Billeter MA. Rescue of measles viruses from cloned DNA. Embo J 1995;14:5773-84.
264. Rager M, Vongpunsawad S, Duprex WP, Cattaneo R. Polyploid measles virus with hexameric genome length. Embo J 2002;21:2364-72.
265. Cattaneo R, Kaelin K, Baczko K, Billeter MA. Measles virus editing provides an additional cysteine-rich protein. Cell 1989;56:759-64.
266. Bellini WJ, Englund G, Rozenblatt S, Arnheiter H, Richardson CD. Measles virus P gene codes for two proteins. J Virol 1985;53:908-19.
267. Cattaneo R, Rebmann G, Schmid A, Baczko K, ter Meulen V, Billeter MA. Altered transcription of a defective measles virus genome derived from a diseased human brain. Embo J 1987;6:681-8.
268. Cathomen T, Naim HY, Cattaneo R. Measles viruses with altered envelope protein cytoplasmic tails gain cell fusion competence. J Virol 1998;72:1224-34.
269. Nussbaum O, Broder CC, Moss B, Stern LB, Rozenblatt S, Berger EA. Functional and structural interactions between measles virus hemagglutinin and CD46. J Virol 1995;69:3341-9.

270. Chu TH, Dornburg R. Toward highly efficient cell-type-specific gene transfer with retroviral vectors displaying single-chain antibodies. J Virol 1997;71:720-5.
271. Wild TF, Malvoisin E, Buckland R. Measles virus: both the haemagglutinin and fusion glycoproteins are required for fusion. J Gen Virol 1991;72 (Pt 2):439-42.
272. Baker KA, Dutch RE, Lamb RA, Jardetzky TS. Structural basis for paramyxovirus-mediated membrane fusion. Mol Cell 1999;3:309-19.
273. von Messling V, Milosevic D, Devaux P, Cattaneo R. Canine distemper virus and measles virus fusion glycoprotein trimers: partial membrane-proximal ectodomain cleavage enhances function. J Virol 2004;78:7894-903.
274. Tatsuo H, Ono N, Tanaka K, Yanagi Y. SLAM (CDw150) is a cellular receptor for measles virus. Nature 2000;406:893-7.
275. Dorig RE, Marcil A, Chopra A, Richardson CD. The human CD46 molecule is a receptor for measles virus (Edmonston strain). Cell 1993;75:295-305.
276. Naniche D, Varior-Krishnan G, Cervoni F, Wild TF, Rossi B, Rabourdin-Combe C, Gerlier D. Human membrane cofactor protein (CD46) acts as a cellular receptor for measles virus. J Virol 1993;67:6025-32.
277. Hashimoto K, Ono N, Tatsuo H, Minagawa H, Takeda M, Takeuchi K, Yanagi Y. SLAM (CD150)-independent measles virus entry as revealed by recombinant virus expressing green fluorescent protein. J Virol 2002;76:6743-9.
278. Andres O, Obojes K, Kim KS, ter Meulen V, Schneider-Schaulies J. CD46- and CD150-independent endothelial cell infection with wild-type measles viruses. J Gen Virol 2003;84:1189-97.
279. Nakamura T, Peng KW, Harvey M, Greiner S, Lorimer IA, James CD, Russell SJ. Rescue and propagation of fully retargeted oncolytic measles viruses. Nat Biotechnol 2005;23:209-14.
280. Dhiman N, Jacobson RM, Poland GA. Measles virus receptors: SLAM and CD46. Rev Med Virol 2004;14:217-29.
281. Veillette A, Latour S. The SLAM family of immune-cell receptors. Curr Opin Immunol 2003;15:277-85.
282. Fishelson Z, Donin N, Zell S, Schultz S, Kirschfink M. Obstacles to cancer immunotherapy: expression of membrane complement regulatory proteins (mCRPs) in tumors. Mol Immunol 2003;40:109-23.
283. Erlenhofer C, Duprex WP, Rima BK, ter Meulen V, Schneider-Schaulies J. Analysis of receptor (CD46, CD150) usage by measles virus. J Gen Virol 2002;83:1431-6.
284. Anderson BD, Nakamura T, Russell SJ, Peng KW. High CD46 receptor density determines preferential killing of tumor cells by oncolytic measles virus. Cancer Res 2004;64:4919-26.
285. Haralambieva I, Iankov I, Hasegawa K, Harvey M, Russell SJ, Peng KW. Engineering oncolytic measles virus to circumvent the intracellular innate immune response. Mol Ther 2007;15:588-97.
286. Ong HT, Timm MM, Greipp PR, Witzig TE, Dispenzieri A, Russell SJ, Peng KW. Oncolytic measles virus targets high CD46 expression on multiple myeloma cells. Exp Hematol 2006;34:713-20.
287. Moss WJ, Griffin DE. Global measles elimination. Nat Rev Microbiol 2006;4:900-8.
288. Schneider-Schaulies S, ter Meulen V. Measles virus and immunomodulation: molecular bases and perspectives. Expert Rev Mol Med 2002;2002:1-18.

289. Dingli D, Peng KW, Harvey ME, Vongpunsawad S, Bergert ER, Kyle RA, Cattaneo R, Morris JC, Russell SJ. Interaction of measles virus vectors with Auger electron emitting radioisotopes. Biochem Biophys Res Commun 2005;337:22-9.
290. Iankov ID, Blechacz B, Liu C, Schmeckpeper JD, Tarara JE, Federspiel MJ, Caplice N, Russell SJ. Infected cell carriers: a new strategy for systemic delivery of oncolytic measles viruses in cancer virotherapy. Mol Ther 2007;15:114-22.
291. Ong HT, Hasegawa K, Dietz AB, Russell SJ, Peng KW. Evaluation of T cells as carriers for systemic measles virotherapy in the presence of antiviral antibodies. Gene Ther 2007;14:324-33.
292. Grandvaux N, tenOever BR, Servant MJ, Hiscott J. The interferon antiviral response: from viral invasion to evasion. Curr Opin Infect Dis 2002;15:259-67.
293. Samuel CE. Antiviral actions of interferons. Clin Microbiol Rev 2001;14:778-809, table of contents.
294. Garcia-Sastre A. Mechanisms of inhibition of the host interferon alpha/beta-mediated antiviral responses by viruses. Microbes Infect 2002;4:647-55.
295. Palosaari H, Parisien JP, Rodriguez JJ, Ulane CM, Horvath CM. STAT protein interference and suppression of cytokine signal transduction by measles virus V protein. J Virol 2003;77:7635-44.
296. Shaffer JA, Bellini WJ, Rota PA. The C protein of measles virus inhibits the type I interferon response. Virology 2003;315:389-97.
297. Takeuchi K, Kadota SI, Takeda M, Miyajima N, Nagata K. Measles virus V protein blocks interferon (IFN)-alpha/beta but not IFN-gamma signaling by inhibiting STAT1 and STAT2 phosphorylation. FEBS Lett 2003;545:177-82.
298. Devaux P, von Messling V, Songsungthong W, Springfeld C, Cattaneo R. Tyrosine 110 in the measles virus phosphoprotein is required to block STAT1 phosphorylation. Virology 2007;360:72-83.
299. Ohno S, Ono N, Takeda M, Takeuchi K, Yanagi Y. Dissection of measles virus V protein in relation to its ability to block alpha/beta interferon signal transduction. J Gen Virol 2004;85:2991-9.
300. Russell SJ. RNA viruses as virotherapy agents. Cancer Gene Ther 2002;9:961-6.
301. Di Carlo E, Forni G, Lollini P, Colombo MP, Modesti A, Musiani P. The intriguing role of polymorphonuclear neutrophils in antitumor reactions. Blood 2001;97:339-45.
302. Grote D, Cattaneo R, Fielding AK. Neutrophils contribute to the measles virus-induced antitumor effect: enhancement by granulocyte macrophage colony-stimulating factor expression. Cancer Res 2003;63:6463-8.
303. Phuong LK, Allen C, Peng KW, Giannini C, Greiner S, TenEyck CJ, Mishra PK, Macura SI, Russell SJ, Galanis EC. Use of a vaccine strain of measles virus genetically engineered to produce carcinoembryonic antigen as a novel therapeutic agent against glioblastoma multiforme. Cancer Res 2003;63:2462-9.
304. Dingli D, Peng KW, Harvey ME, Greipp PR, O'Connor MK, Cattaneo R, Morris JC, Russell SJ. Image-guided radiovirotherapy for multiple myeloma using a recombinant measles virus expressing the thyroidal sodium iodide symporter. Blood 2004;103:1641-6.
305. Higuchi H, Bronk SF, Bateman A, Harrington K, Vile RG, Gores GJ. Viral fusogenic membrane glycoprotein expression causes syncytia formation with bioenergetic cell death: implications for gene therapy. Cancer Res 2000;60:6396-402.

306. Blechacz B, Splinter PL, Greiner S, Myers R, Peng KW, Federspiel MJ, Russell SJ, LaRusso NF. Engineered measles virus as a novel oncolytic viral therapy system for hepatocellular carcinoma. Hepatology 2006;44:1465-77.
307. Spitzweg C, Morris JC. Approaches to gene therapy with sodium/iodide symporter. Exp Clin Endocrinol Diabetes 2001;109:56-9.
308. Heinzerling L, Kunzi V, Oberholzer PA, Kundig T, Naim H, Dummer R. Oncolytic measles virus in cutaneous T-cell lymphomas mounts antitumor immune responses in vivo and targets interferon-resistant tumor cells. Blood 2005;106:2287-94.
309. Kunzi V, Oberholzer PA, Heinzerling L, Dummer R, Naim HY. Recombinant measles virus induces cytolysis of cutaneous T-cell lymphoma in vitro and in vivo. J Invest Dermatol 2006;126:2525-32.
310. McDonald CJ, Erlichman C, Ingle JN, Rosales GA, Allen C, Greiner SM, Harvey ME, Zollman PJ, Russell SJ, Galanis E. A measles virus vaccine strain derivative as a novel oncolytic agent against breast cancer. Breast Cancer Res Treat 2006;99:177-84.
311. Liu C, Sarkaria JN, Petell CA, Paraskevakou G, Zollman PJ, Schroeder M, Carlson B, Decker PA, Wu W, James CD, Russell SJ, Galanis E. Combination of measles virus virotherapy and radiation therapy has synergistic activity in the treatment of glioblastoma multiforme. Clin Cancer Res 2007;13:7155-65.
312. Peng KW, Hadac EM, Anderson BD, Myers R, Harvey M, Greiner SM, Soeffker D, Federspiel MJ, Russell SJ. Pharmacokinetics of oncolytic measles virotherapy: eventual equilibrium between virus and tumor in an ovarian cancer xenograft model. Cancer Gene Ther 2006;13:732-8.
313. Peng KW, TenEyck CJ, Galanis E, Kalli KR, Hartmann LC, Russell SJ. Intraperitoneal therapy of ovarian cancer using an engineered measles virus. Cancer Res 2002;62:4656-62.
314. Wodarz D. Viruses as antitumor weapons: defining conditions for tumor remission. Cancer Res 2001;61:3501-7.
315. Medina-Kauwe LK, Xie J, Hamm-Alvarez S. Intracellular trafficking of nonviral vectors. Gene Ther 2005;12:1734-51.
316. Dean DA, Strong DD, Zimmer WE. Nuclear entry of nonviral vectors. Gene Ther 2005;12:881-90.
317. Miller AD. The problem with cationic liposome/micelle-based non-viral vector systems for gene therapy. Curr Med Chem 2003;10:1195-211.
318. Wiethoff CM, Middaugh CR. Barriers to nonviral gene delivery. J Pharm Sci 2003;92:203-17.
319. Kawabata K, Takakura Y, Hashida M. The fate of plasmid DNA after intravenous injection in mice: involvement of scavenger receptors in its hepatic uptake. Pharm Res 1995;12:825-30.
320. Li S, Tseng WC, Stolz DB, Wu SP, Watkins SC, Huang L. Dynamic changes in the characteristics of cationic lipidic vectors after exposure to mouse serum: implications for intravenous lipofection. Gene Ther 1999;6:585-94.
321. Litzinger DC, Brown JM, Wala I, Kaufman SA, Van GY, Farrell CL, Collins D. Fate of cationic liposomes and their complex with oligonucleotide in vivo. Biochim Biophys Acta 1996;1281:139-49.
322. Wattiaux R, Laurent N, Wattiaux-De Coninck S, Jadot M. Endosomes, lysosomes: their implication in gene transfer. Adv Drug Deliv Rev 2000;41:201-8.

323. Lechardeur D, Sohn KJ, Haardt M, Joshi PB, Monck M, Graham RW, Beatty B, Squire J, O'Brodovich H, Lukacs GL. Metabolic instability of plasmid DNA in the cytosol: a potential barrier to gene transfer. Gene Ther 1999;6:482-97.
324. Pollard H, Toumaniantz G, Amos JL, Avet-Loiseau H, Guihard G, Behr JP, Escande D. Ca2+-sensitive cytosolic nucleases prevent efficient delivery to the nucleus of injected plasmids. J Gene Med 2001;3:153-64.
325. Lukacs GL, Haggie P, Seksek O, Lechardeur D, Freedman N, Verkman AS. Size-dependent DNA mobility in cytoplasm and nucleus. J Biol Chem 2000;275:1625-9.
326. Colin M, Moritz S, Fontanges P, Kornprobst M, Delouis C, Keller M, Miller AD, Capeau J, Coutelle C, Brahimi-Horn MC. The nuclear pore complex is involved in nuclear transfer of plasmid DNA condensed with an oligolysine-RGD peptide containing nuclear localisation properties. Gene Ther 2001;8:1643-53.
327. Dowty ME, Williams P, Zhang G, Hagstrom JE, Wolff JA. Plasmid DNA entry into postmitotic nuclei of primary rat myotubes. Proc Natl Acad Sci U S A 1995;92:4572-6.
328. Labat-Moleur F, Steffan AM, Brisson C, Perron H, Feugeas O, Furstenberger P, Oberling F, Brambilla E, Behr JP. An electron microscopy study into the mechanism of gene transfer with lipopolyamines. Gene Ther 1996;3:1010-7.
329. Tachibana R, Harashima H, Shinohara Y, Kiwada H. Quantitative studies on the nuclear transport of plasmid DNA and gene expression employing nonviral vectors. Adv Drug Deliv Rev 2001;52:219-26.
330. Mehier-Humbert S, Bettinger T, Yan F, Guy RH. Plasma membrane poration induced by ultrasound exposure: implication for drug delivery. J Control Release 2005;104:213-22.
331. Mehier-Humbert S, Bettinger T, Yan F, Guy RH. Ultrasound-mediated gene delivery: kinetics of plasmid internalization and gene expression. J Control Release 2005;104:203-11.
332. Sundaram J, Mellein BR, Mitragotri S. An experimental and theoretical analysis of ultrasound-induced permeabilization of cell membranes. Biophys J 2003;84:3087-101.
333. Mehier-Humbert S, Yan F, Frinking P, Schneider M, Guy RH, Bettinger T. Ultrasound-mediated gene delivery: influence of contrast agent on transfection. Bioconjug Chem 2007;18:652-62.
334. Taniyama Y, Tachibana K, Hiraoka K, Aoki M, Yamamoto S, Matsumoto K, Nakamura T, Ogihara T, Kaneda Y, Morishita R. Development of safe and efficient novel nonviral gene transfer using ultrasound: enhancement of transfection efficiency of naked plasmid DNA in skeletal muscle. Gene Ther 2002;9:372-80.
335. Azuma H, Tomita N, Kaneda Y, Koike H, Ogihara T, Katsuoka Y, Morishita R. Transfection of NFkappaB-decoy oligodeoxynucleotides using efficient ultrasound-mediated gene transfer into donor kidneys prolonged survival of rat renal allografts. Gene Ther 2003;10:415-25.
336. Chen S, Shohet RV, Bekeredjian R, Frenkel P, Grayburn PA. Optimization of ultrasound parameters for cardiac gene delivery of adenoviral or plasmid deoxyribonucleic acid by ultrasound-targeted microbubble destruction. J Am Coll Cardiol 2003;42:301-8.

337. Lu QL, Liang HD, Partridge T, Blomley MJ. Microbubble ultrasound improves the efficiency of gene transduction in skeletal muscle in vivo with reduced tissue damage. Gene Ther 2003;10:396-405.
338. Miao CH, Brayman AA, Loeb KR, Ye P, Zhou L, Mourad P, Crum LA. Ultrasound enhances gene delivery of human factor IX plasmid. Hum Gene Ther 2005;16:893-905.
339. Sakakima Y, Hayashi S, Yagi Y, Hayakawa A, Tachibana K, Nakao A. Gene therapy for hepatocellular carcinoma using sonoporation enhanced by contrast agents. Cancer Gene Ther 2005;12:884-9.
340. Tsunoda S, Mazda O, Oda Y, Iida Y, Akabame S, Kishida T, Shin-Ya M, Asada H, Gojo S, Imanishi J, Matsubara H, Yoshikawa T. Sonoporation using microbubble BR14 promotes pDNA/siRNA transduction to murine heart. Biochem Biophys Res Commun 2005;336:118-27.
341. Neumann E, Schaefer-Ridder M, Wang Y, Hofschneider PH. Gene transfer into mouse lyoma cells by electroporation in high electric fields. Embo J 1982;1:841-5.
342. Titomirov AV, Sukharev S, Kistanova E. In vivo electroporation and stable transformation of skin cells of newborn mice by plasmid DNA. Biochim Biophys Acta 1991;1088:131-4.
343. Mehier-Humbert S, Guy RH. Physical methods for gene transfer: improving the kinetics of gene delivery into cells. Adv Drug Deliv Rev 2005;57:733-53.
344. Teissie J, Golzio M, Rols MP. Mechanisms of cell membrane electropermeabilization: a minireview of our present (lack of ?) knowledge. Biochim Biophys Acta 2005;1724:270-80.
345. Favard C, Dean DS, Rols MP. Electrotransfer as a non viral method of gene delivery. Curr Gene Ther 2007;7:67-77.
346. Dean DA, Machado-Aranda D, Blair-Parks K, Yeldandi AV, Young JL. Electroporation as a method for high-level nonviral gene transfer to the lung. Gene Ther 2003;10:1608-15.
347. Goto T, Nishi T, Kobayashi O, Tamura T, Dev SB, Takeshima H, Kochi M, Kuratsu J, Sakata T, Ushio Y. Combination electro-gene therapy using herpes virus thymidine kinase and interleukin-12 expression plasmids is highly efficient against murine carcinomas in vivo. Mol Ther 2004;10:929-37.
348. Goto T, Nishi T, Tamura T, Dev SB, Takeshima H, Kochi M, Yoshizato K, Kuratsu J, Sakata T, Hofmann GA, Ushio Y. Highly efficient electro-gene therapy of solid tumor by using an expression plasmid for the herpes simplex virus thymidine kinase gene. Proc Natl Acad Sci U S A 2000;97:354-9.
349. Harrison RL, Byrne BJ, Tung L. Electroporation-mediated gene transfer in cardiac tissue. FEBS Lett 1998;435:1-5.
350. Budker V, Zhang G, Danko I, Williams P, Wolff J. The efficient expression of intravascularly delivered DNA in rat muscle. Gene Ther 1998;5:272-6.
351. Budker V, Zhang G, Knechtle S, Wolff JA. Naked DNA delivered intraportally expresses efficiently in hepatocytes. Gene Ther 1996;3:593-8.
352. Liu F, Song Y, Liu D. Hydrodynamics-based transfection in animals by systemic administration of plasmid DNA. Gene Ther 1999;6:1258-66.
353. Zhang G, Budker V, Wolff JA. High levels of foreign gene expression in hepatocytes after tail vein injections of naked plasmid DNA. Hum Gene Ther 1999;10:1735-7.

354. Crespo A, Peydro A, Dasi F, Benet M, Calvete JJ, Revert F, Alino SF. Hydrodynamic liver gene transfer mechanism involves transient sinusoidal blood stasis and massive hepatocyte endocytic vesicles. Gene Ther 2005;12:927-35.
355. Zhang G, Gao X, Song YK, Vollmer R, Stolz DB, Gasiorowski JZ, Dean DA, Liu D. Hydroporation as the mechanism of hydrodynamic delivery. Gene Ther 2004;11:675-82.
356. Suda T, Gao X, Stolz DB, Liu D. Structural impact of hydrodynamic injection on mouse liver. Gene Ther 2007;14:129-37.
357. Kobayashi N, Nishikawa M, Hirata K, Takakura Y. Hydrodynamics-based procedure involves transient hyperpermeability in the hepatic cellular membrane: implication of a nonspecific process in efficient intracellular gene delivery. J Gene Med 2004;6:584-92.
358. Budker V, Budker T, Zhang G, Subbotin V, Loomis A, Wolff JA. Hypothesis: naked plasmid DNA is taken up by cells in vivo by a receptor-mediated process. J Gene Med 2000;2:76-88.
359. Mann MJ, Gibbons GH, Hutchinson H, Poston RS, Hoyt EG, Robbins RC, Dzau VJ. Pressure-mediated oligonucleotide transfection of rat and human cardiovascular tissues. Proc Natl Acad Sci U S A 1999;96:6411-6.
360. Maruyama H, Higuchi N, Nishikawa Y, Hirahara H, Iino N, Kameda S, Kawachi H, Yaoita E, Gejyo F, Miyazaki J. Kidney-targeted naked DNA transfer by retrograde renal vein injection in rats. Hum Gene Ther 2002;13:455-68.
361. Zhang G, Budker V, Williams P, Subbotin V, Wolff JA. Efficient expression of naked dna delivered intraarterially to limb muscles of nonhuman primates. Hum Gene Ther 2001;12:427-38.
362. Alino SF, Herrero MJ, Noguera I, Dasi F, Sanchez M. Pig liver gene therapy by noninvasive interventionist catheterism. Gene Ther 2007;14:334-43.
363. Yoshino H, Hashizume K, Kobayashi E. Naked plasmid DNA transfer to the porcine liver using rapid injection with large volume. Gene Ther 2006;13:1696-702.
364. Klein RM, Wolf ED, Wu R, Sanford JC. High-velocity microprojectiles for delivering nucleic acids into living cells. 1987. Biotechnology 1992;24:384-6.
365. Williams RS, Johnston SA, Riedy M, DeVit MJ, McElligott SG, Sanford JC. Introduction of foreign genes into tissues of living mice by DNA-coated microprojectiles. Proc Natl Acad Sci U S A 1991;88:2726-30.
366. Yang NS, Burkholder J, Roberts B, Martinell B, McCabe D. In vivo and in vitro gene transfer to mammalian somatic cells by particle bombardment. Proc Natl Acad Sci U S A 1990;87:9568-72.
367. Matthews KE, Mills GB, Horsfall W, Hack N, Skorecki K, Keating A. Bead transfection: rapid and efficient gene transfer into marrow stromal and other adherent mammalian cells. Exp Hematol 1993;21:697-702.
368. Uchida M, Natsume H, Kobayashi D, Sugibayashi K, Morimoto Y. Effects of particle size, helium gas pressure and microparticle dose on the plasma concentration of indomethacin after bombardment of indomethacin-loaded poly-L-lactic acid microspheres using a Helios gun system. Biol Pharm Bull 2002;25:690-3.

369. Zelenin AV, Kolesnikov VA, Tarasenko OA, Shafei RA, Zelenina IA, Mikhailov VV, Semenova ML, Kovalenko DV, Artemyeva OV, Ivaschenko TE, Evgrafov OV, Dickson G, Baranovand VS. Bacterial beta-galactosidase and human dystrophin genes are expressed in mouse skeletal muscle fibers after ballistic transfection. FEBS Lett 1997;414:319-22.
370. Chang ML, Chen JC, Yeh CT, Chang MY, Liang CK, Chiu CT, Lin DY, Liaw YF. Gene Gun Bombardment with DNA-Coated Gold Particles Is a Potential Alternative to Hydrodynamics-Based Transfection for Delivering Genes into Superficial Hepatocytes. Hum Gene Ther 2008.
371. Peng S, Trimble C, Alvarez RD, Huh WK, Lin Z, Monie A, Hung CF, Wu TC. Cluster intradermal DNA vaccination rapidly induces E7-specific CD8(+) T-cell immune responses leading to therapeutic antitumor effects. Gene Ther 2008.
372. Dietrich A, Becherer L, Brinckmann U, Hauss J, Liebert UG, Gutz A, Aust G. Particle-mediated cytokine gene therapy leads to antitumor and antimetastatic effects in mouse carcinoma models. Cancer Biother Radiopharm 2006;21:333-41.
373. Kurata S, Tsukakoshi M, Kasuya T, Ikawa Y. The laser method for efficient introduction of foreign DNA into cultured cells. Exp Cell Res 1986;162:372-8.
374. Tao W, Wilkinson J, Stanbridge EJ, Berns MW. Direct gene transfer into human cultured cells facilitated by laser micropuncture of the cell membrane. Proc Natl Acad Sci U S A 1987;84:4180-4.
375. Shirahata Y, Ohkohchi N, Itagak H, Satomi S. New technique for gene transfection using laser irradiation. J Investig Med 2001;49:184-90.
376. Zeira E, Manevitch A, Khatchatouriants A, Pappo O, Hyam E, Darash-Yahana M, Tavor E, Honigman A, Lewis A, Galun E. Femtosecond infrared laser-an efficient and safe in vivo gene delivery system for prolonged expression. Mol Ther 2003;8:342-50.
377. Zeira E, Manevitch A, Manevitch Z, Kedar E, Gropp M, Daudi N, Barsuk R, Harati M, Yotvat H, Troilo PJ, Griffiths TG, 2nd, Pacchione SJ, Roden DF, Niu Z, Nussbaum O, Zamir G, Papo O, Hemo I, Lewis A, Galun E. Femtosecond laser: a new intradermal DNA delivery method for efficient, long-term gene expression and genetic immunization. Faseb J 2007;21:3522-33.
378. Gersting SW, Schillinger U, Lausier J, Nicklaus P, Rudolph C, Plank C, Reinhardt D, Rosenecker J. Gene delivery to respiratory epithelial cells by magnetofection. J Gene Med 2004;6:913-22.
379. Krotz F, Sohn HY, Gloe T, Plank C, Pohl U. Magnetofection potentiates gene delivery to cultured endothelial cells. J Vasc Res 2003;40:425-34.
380. Scherer F, Anton M, Schillinger U, Henke J, Bergemann C, Kruger A, Gansbacher B, Plank C. Magnetofection: enhancing and targeting gene delivery by magnetic force in vitro and in vivo. Gene Ther 2002;9:102-9.
381. Felgner PL, Gadek TR, Holm M, Roman R, Chan HW, Wenz M, Northrop JP, Ringold GM, Danielsen M. Lipofection: a highly efficient, lipid-mediated DNA-transfection procedure. Proc Natl Acad Sci U S A 1987;84:7413-7.
382. Farhood H, Serbina N, Huang L. The role of dioleoyl phosphatidylethanolamine in cationic liposome mediated gene transfer. Biochim Biophys Acta 1995;1235:289-95.
383. Behr JP. Gene transfer with synthetic cationic amphiphiles: prospects for gene therapy. Bioconjug Chem 1994;5:382-9.

384. Mislick KA, Baldeschwieler JD. Evidence for the role of proteoglycans in cation-mediated gene transfer. Proc Natl Acad Sci U S A 1996;93:12349-54.
385. Friend DS, Papahadjopoulos D, Debs RJ. Endocytosis and intracellular processing accompanying transfection mediated by cationic liposomes. Biochim Biophys Acta 1996;1278:41-50.
386. Xu Y, Szoka FC, Jr. Mechanism of DNA release from cationic liposome/DNA complexes used in cell transfection. Biochemistry 1996;35:5616-23.
387. Elouahabi A, Ruysschaert JM. Formation and intracellular trafficking of lipoplexes and polyplexes. Mol Ther 2005;11:336-47.
388. Li S, Ma Z. Nonviral gene therapy. Curr Gene Ther 2001;1:201-26.
389. Xu L, Pirollo KF, Tang WH, Rait A, Chang EH. Transferrin-liposome-mediated systemic p53 gene therapy in combination with radiation results in regression of human head and neck cancer xenografts. Hum Gene Ther 1999;10:2941-52.
390. Baeuerle PA, Huttner WB. Chlorate--a potent inhibitor of protein sulfation in intact cells. Biochem Biophys Res Commun 1986;141:870-7.
391. Lungwitz U, Breunig M, Blunk T, Gopferich A. Polyethylenimine-based non-viral gene delivery systems. Eur J Pharm Biopharm 2005;60:247-66.
392. Laemmli UK. Characterization of DNA condensates induced by poly(ethylene oxide) and polylysine. Proc Natl Acad Sci U S A 1975;72:4288-92.
393. Kircheis R, Wightman L, Schreiber A, Robitza B, Rossler V, Kursa M, Wagner E. Polyethylenimine/DNA complexes shielded by transferrin target gene expression to tumors after systemic application. Gene Ther 2001;8:28-40.
394. Fischer D, Bieber T, Li Y, Elsasser HP, Kissel T. A novel non-viral vector for DNA delivery based on low molecular weight, branched polyethylenimine: effect of molecular weight on transfection efficiency and cytotoxicity. Pharm Res 1999;16:1273-9.
395. Kunath K, von Harpe A, Fischer D, Petersen H, Bickel U, Voigt K, Kissel T. Low-molecular-weight polyethylenimine as a non-viral vector for DNA delivery: comparison of physicochemical properties, transfection efficiency and in vivo distribution with high-molecular-weight polyethylenimine. J Control Release 2003;89:113-25.
396. Demeneix B, Behr JP. Polyethylenimine (PEI). Adv Genet 2005;53:217-30.
397. Roth CM, Sundaram S. Engineering synthetic vectors for improved DNA delivery: insights from intracellular pathways. Annu Rev Biomed Eng 2004;6:397-426.
398. Abdallah B, Hassan A, Benoist C, Goula D, Behr JP, Demeneix BA. A powerful nonviral vector for in vivo gene transfer into the adult mammalian brain: polyethylenimine. Hum Gene Ther 1996;7:1947-54.
399. Boussif O, Lezoualc'h F, Zanta MA, Mergny MD, Scherman D, Demeneix B, Behr JP. A versatile vector for gene and oligonucleotide transfer into cells in culture and in vivo: polyethylenimine. Proc Natl Acad Sci U S A 1995;92:7297-301.
400. Coll JL, Chollet P, Brambilla E, Desplanques D, Behr JP, Favrot M. In vivo delivery to tumors of DNA complexed with linear polyethylenimine. Hum Gene Ther 1999;10:1659-66.
401. Goula D, Becker N, Lemkine GF, Normandie P, Rodrigues J, Mantero S, Levi G, Demeneix BA. Rapid crossing of the pulmonary endothelial barrier by polyethylenimine/DNA complexes. Gene Ther 2000;7:499-504.

402. Goula D, Benoist C, Mantero S, Merlo G, Levi G, Demeneix BA. Polyethylenimine-based intravenous delivery of transgenes to mouse lung. Gene Ther 1998;5:1291-5.
403. Goula D, Remy JS, Erbacher P, Wasowicz M, Levi G, Abdallah B, Demeneix BA. Size, diffusibility and transfection performance of linear PEI/DNA complexes in the mouse central nervous system. Gene Ther 1998;5:712-7.
404. Zou SM, Erbacher P, Remy JS, Behr JP. Systemic linear polyethylenimine (L-PEI)-mediated gene delivery in the mouse. J Gene Med 2000;2:128-34.
405. Lavigne MD, Gorecki DC. Emerging vectors and targeting methods for nonviral gene therapy. Expert Opin Emerg Drugs 2006;11:541-57.
406. Uster PS, Allen TM, Daniel BE, Mendez CJ, Newman MS, Zhu GZ. Insertion of poly(ethylene glycol) derivatized phospholipid into pre-formed liposomes results in prolonged in vivo circulation time. FEBS Lett 1996;386:243-6.
407. Dean DA, Dean BS, Muller S, Smith LC. Sequence requirements for plasmid nuclear import. Exp Cell Res 1999;253:713-22.
408. Wagstaff KM, Jans DA. Nucleocytoplasmic transport of DNA: enhancing non-viral gene transfer. Biochem J 2007;406:185-202.
409. Park TG, Jeong JH, Kim SW. Current status of polymeric gene delivery systems. Adv Drug Deliv Rev 2006;58:467-86.
410. Zhang S, Xu Y, Wang B, Qiao W, Liu D, Li Z. Cationic compounds used in lipoplexes and polyplexes for gene delivery. J Control Release 2004;100:165-80.
411. Daemen T, de Mare A, Bungener L, de Jonge J, Huckriede A, Wilschut J. Virosomes for antigen and DNA delivery. Adv Drug Deliv Rev 2005;57:451-63.
412. Garcia L, Bunuales M, Duzgunes N, Tros de Ilarduya C. Serum-resistant lipopolyplexes for gene delivery to liver tumour cells. Eur J Pharm Biopharm 2007;67:58-66.
413. Luten J, van Nostrum CF, De Smedt SC, Hennink WE. Biodegradable polymers as non-viral carriers for plasmid DNA delivery. J Control Release 2008;126:97-110.
414. Ebert O, Shinozaki K, Huang TG, Savontaus MJ, Garcia-Sastre A, Woo SL. Oncolytic vesicular stomatitis virus for treatment of orthotopic hepatocellular carcinoma in immune-competent rats. Cancer Res 2003;63:3605-11.
415. Huang TG, Ebert O, Shinozaki K, Garcia-Sastre A, Woo SL. Oncolysis of hepatic metastasis of colorectal cancer by recombinant vesicular stomatitis virus in immune-competent mice. Mol Ther 2003;8:434-40.
416. Pawlik TM, Nakamura H, Yoon SS, Mullen JT, Chandrasekhar S, Chiocca EA, Tanabe KK. Oncolysis of diffuse hepatocellular carcinoma by intravascular administration of a replication-competent, genetically engineered herpesvirus. Cancer Res 2000;60:2790-5.
417. Mohr L, Shankara S, Yoon SK, Krohne TU, Geissler M, Roberts B, Blum HE, Wands JR. Gene therapy of hepatocellular carcinoma in vitro and in vivo in nude mice by adenoviral transfer of the Escherichia coli purine nucleoside phosphorylase gene. Hepatology 2000;31:606-14.

418. Palmer DH, Mautner V, Mirza D, Oliff S, Gerritsen W, van der Sijp JR, Hubscher S, Reynolds G, Bonney S, Rajaratnam R, Hull D, Horne M, Ellis J, Mountain A, Hill S, Harris PA, Searle PF, Young LS, James ND, Kerr DJ. Virus-directed enzyme prodrug therapy: intratumoral administration of a replication-deficient adenovirus encoding nitroreductase to patients with resectable liver cancer. J Clin Oncol 2004;22:1546-52.
419. Ohwada A, Hirschowitz EA, Crystal RG. Regional delivery of an adenovirus vector containing the Escherichia coli cytosine deaminase gene to provide local activation of 5-fluorocytosine to suppress the growth of colon carcinoma metastatic to liver. Hum Gene Ther 1996;7:1567-76.
420. Xu GW, Sun ZT, Forrester K, Wang XW, Coursen J, Harris CC. Tissue-specific growth suppression and chemosensitivity promotion in human hepatocellular carcinoma cells by retroviral-mediated transfer of the wild-type p53 gene. Hepatology 1996;24:1264-8.
421. Barajas M, Mazzolini G, Genove G, Bilbao R, Narvaiza I, Schmitz V, Sangro B, Melero I, Qian C, Prieto J. Gene therapy of orthotopic hepatocellular carcinoma in rats using adenovirus coding for interleukin 12. Hepatology 2001;33:52-61.
422. Schmitz V, Barajas M, Wang L, Peng D, Duarte M, Prieto J, Qian C. Adenovirus-mediated CD40 ligand gene therapy in a rat model of orthotopic hepatocellular carcinoma. Hepatology 2001;34:72-81.
423. Habib N, Salama H, Abd El Latif Abu Median A, Isac Anis I, Abd Al Aziz RA, Sarraf C, Mitry R, Havlik R, Seth P, Hartwigsen J, Bhushan R, Nicholls J, Jensen S. Clinical trial of E1B-deleted adenovirus (dl1520) gene therapy for hepatocellular carcinoma. Cancer Gene Ther 2002;9:254-9.
424. Habib NA, Sarraf CE, Mitry RR, Havlik R, Nicholls J, Kelly M, Vernon CC, Gueret-Wardle D, El-Masry R, Salama H, Ahmed R, Michail N, Edward E, Jensen SL. E1B-deleted adenovirus (dl1520) gene therapy for patients with primary and secondary liver tumors. Hum Gene Ther 2001;12:219-26.
425. Makower D, Rozenblit A, Kaufman H, Edelman M, Lane ME, Zwiebel J, Haynes H, Wadler S. Phase II clinical trial of intralesional administration of the oncolytic adenovirus ONYX-015 in patients with hepatobiliary tumors with correlative p53 studies. Clin Cancer Res 2003;9:693-702.
426. Sangro B, Mazzolini G, Ruiz J, Herraiz M, Quiroga J, Herrero I, Benito A, Larrache J, Pueyo J, Subtil JC, Olague C, Sola J, Sadaba B, Lacasa C, Melero I, Qian C, Prieto J. Phase I trial of intratumoral injection of an adenovirus encoding interleukin-12 for advanced digestive tumors. J Clin Oncol 2004;22:1389-97.
427. Penuelas I, Mazzolini G, Boan JF, Sangro B, Marti-Climent J, Ruiz M, Ruiz J, Satyamurthy N, Qian C, Barrio JR, Phelps ME, Richter JA, Gambhir SS, Prieto J. Positron emission tomography imaging of adenoviral-mediated transgene expression in liver cancer patients. Gastroenterology 2005;128:1787-95.
428. Warren RS, Kirn DH. Liver-directed viral therapy for cancer p53-targeted adenoviruses and beyond. Surg Oncol Clin N Am 2002;11:571-88, vi.
429. Weiss SJ, Philp NJ, Grollman EF. Iodide transport in a continuous line of cultured cells from rat thyroid. Endocrinology 1984;114:1090-8.
430. Hirt B. Selective extraction of polyoma DNA from infected mouse cell cultures. J Mol Biol 1967;26:365-9.
431. Dingli D, Russell SJ, Morris JC, 3rd. In vivo imaging and tumor therapy with the sodium iodide symporter. J Cell Biochem 2003;90:1079-86.

432. Fenske DB, MacLachlan I, Cullis PR. Stabilized plasmid-lipid particles: a systemic gene therapy vector. Methods Enzymol 2002;346:36-71.
433. Tomayko MM, Reynolds CP. Determination of subcutaneous tumor size in athymic (nude) mice. Cancer Chemother Pharmacol 1989;24:148-54.
434. Andrianaivo F, Lecocq M, Wattiaux-De Coninck S, Wattiaux R, Jadot M. Hydrodynamics-based transfection of the liver: entrance into hepatocytes of DNA that causes expression takes place very early after injection. J Gene Med 2004;6:877-83.
435. Xu L, Pirollo KF, Chang EH. Transferrin-liposome-mediated p53 sensitization of squamous cell carcinoma of the head and neck to radiation in vitro. Hum Gene Ther 1997;8:467-75.
436. Kircheis R, Kichler A, Wallner G, Kursa M, Ogris M, Felzmann T, Buchberger M, Wagner E. Coupling of cell-binding ligands to polyethylenimine for targeted gene delivery. Gene Ther 1997;4:409-18.
437. Wheeler JJ, Palmer L, Ossanlou M, MacLachlan I, Graham RW, Zhang YP, Hope MJ, Scherrer P, Cullis PR. Stabilized plasmid-lipid particles: construction and characterization. Gene Ther 1999;6:271-81.
438. Tam P, Monck M, Lee D, Ludkovski O, Leng EC, Clow K, Stark H, Scherrer P, Graham RW, Cullis PR. Stabilized plasmid-lipid particles for systemic gene therapy. Gene Ther 2000;7:1867-74.
439. Fenske DB, MacLachlan I, Cullis PR. Long-circulating vectors for the systemic delivery of genes. Curr Opin Mol Ther 2001;3:153-8.
440. Merchlinsky MJ, Tattersall PJ, Leary JJ, Cotmore SF, Gardiner EM, Ward DC. Construction of an infectious molecular clone of the autonomous parvovirus minute virus of mice. J Virol 1983;47:227-32.
441. Clement N, Velu T, Brandenburger A. Construction and production of oncotropic vectors, derived from MVM(p), that share reduced sequence homology with helper plasmids. Cancer Gene Ther 2002;9:762-70.
442. Geier GE, Modrich P. Recognition sequence of the dam methylase of Escherichia coli K12 and mode of cleavage of Dpn I endonuclease. J Biol Chem 1979;254:1408-13.
443. Vovis GF, Lacks S. Complementary action of restriction enzymes endo R-DpnI and Endo R-DpnII on bacteriophage f1 DNA. J Mol Biol 1977;115:525-38.
444. Clement N, Avalosse B, El Bakkouri K, Velu T, Brandenburger A. Cloning and sequencing of defective particles derived from the autonomous parvovirus minute virus of mice for the construction of vectors with minimal cis-acting sequences. J Virol 2001;75:1284-93.
445. Becquart P, Vanacker JM, Duponchel N, Begue A, Rommelaere J. Expression of the non-structural proteins of parvovirus MVMp from recombinant retroviruses: predominant role of the parvoviral NS-1 product in host cell disturbance. Res Virol 1993;144:465-70.
446. Nuesch JP, Lachmann S, Rommelaere J. Selective alterations of the host cell architecture upon infection with parvovirus minute virus of mice. Virology 2005;331:159-74.
447. Nuesch JP, Rommelaere J. NS1 interaction with CKII alpha: novel protein complex mediating parvovirus-induced cytotoxicity. J Virol 2006;80:4729-39.
448. Duprex WP, McQuaid S, Roscic-Mrkic B, Cattaneo R, McCallister C, Rima BK. In vitro and in vivo infection of neural cells by a recombinant measles virus expressing enhanced green fluorescent protein. J Virol 2000;74:7972-9.

449. Hisazumi J, Kobayashi N, Nishikawa M, Takakura Y. Significant role of liver sinusoidal endothelial cells in hepatic uptake and degradation of naked plasmid DNA after intravenous injection. Pharm Res 2004;21:1223-8.
450. Kobayashi N, Kuramoto T, Yamaoka K, Hashida M, Takakura Y. Hepatic uptake and gene expression mechanisms following intravenous administration of plasmid DNA by conventional and hydrodynamics-based procedures. J Pharmacol Exp Ther 2001;297:853-60.
451. Huard J, Lochmuller H, Acsadi G, Jani A, Massie B, Karpati G. The route of administration is a major determinant of the transduction efficiency of rat tissues by adenoviral recombinants. Gene Ther 1995;2:107-15.
452. Lin H, Parmacek MS, Morle G, Bolling S, Leiden JM. Expression of recombinant genes in myocardium in vivo after direct injection of DNA. Circulation 1990;82:2217-21.
453. Tada M, Hatano E, Taura K, Nitta T, Koizumi N, Ikai I, Shimahara Y. High volume hydrodynamic injection of plasmid DNA via the hepatic artery results in a high level of gene expression in rat hepatocellular carcinoma induced by diethylnitrosamine. J Gene Med 2006;8:1018-26.
454. Ma L, Luo L, Qiao H, Dong X, Pan S, Jiang H, Krissansen GW, Sun X. Complete eradication of hepatocellular carcinomas by combined vasostatin gene therapy and B7H3-mediated immunotherapy. J Hepatol 2007;46:98-106.
455. Nomura T, Yasuda K, Yamada T, Okamoto S, Mahato RI, Watanabe Y, Takakura Y, Hashida M. Gene expression and antitumor effects following direct interferon (IFN)-gamma gene transfer with naked plasmid DNA and DC-chol liposome complexes in mice. Gene Ther 1999;6:121-9.
456. Vile RG, Hart IR. In vitro and in vivo targeting of gene expression to melanoma cells. Cancer Res 1993;53:962-7.
457. Barnett FH, Scharer-Schuksz M, Wood M, Yu X, Wagner TE, Friedlander M. Intra-arterial delivery of endostatin gene to brain tumors prolongs survival and alters tumor vessel ultrastructure. Gene Ther 2004;11:1283-9.
458. Kim YI, Chung JW, Park JH, Han JK, Hong JW, Chung H. Intraarterial gene delivery in rabbit hepatic tumors: transfection with nonviral vector by using iodized oil emulsion. Radiology 2006;240:771-7.
459. Hildebrandt IJ, Iyer M, Wagner E, Gambhir SS. Optical imaging of transferrin targeted PEI/DNA complexes in living subjects. Gene Ther 2003;10:758-64.
460. Kneuer C, Ehrhardt C, Bakowsky H, Kumar MN, Oberle V, Lehr CM, Hoekstra D, Bakowsky U. The influence of physicochemical parameters on the efficacy of non-viral DNA transfection complexes: a comparative study. J Nanosci Nanotechnol 2006;6:2776-82.
461. Xu L, Frederik P, Pirollo KF, Tang WH, Rait A, Xiang LM, Huang W, Cruz I, Yin Y, Chang EH. Self-assembly of a virus-mimicking nanostructure system for efficient tumor-targeted gene delivery. Hum Gene Ther 2002;13:469-81.
462. Bilbao R, Bustos M, Alzuguren P, Pajares MJ, Drozdzik M, Qian C, Prieto J. A blood-tumor barrier limits gene transfer to experimental liver cancer: the effect of vasoactive compounds. Gene Ther 2000;7:1824-32.
463. Zhang YP, Sekirov L, Saravolac EG, Wheeler JJ, Tardi P, Clow K, Leng E, Sun R, Cullis PR, Scherrer P. Stabilized plasmid-lipid particles for regional gene therapy: formulation and transfection properties. Gene Ther 1999;6:1438-47.
464. Chollet P, Favrot MC, Hurbin A, Coll JL. Side-effects of a systemic injection of linear polyethylenimine-DNA complexes. J Gene Med 2002;4:84-91.

465. Loisel S, Le Gall C, Doucet L, Ferec C, Floch V. Contribution of plasmid DNA to hepatotoxicity after systemic administration of lipoplexes. Hum Gene Ther 2001;12:685-96.
466. Lv H, Zhang S, Wang B, Cui S, Yan J. Toxicity of cationic lipids and cationic polymers in gene delivery. J Control Release 2006;114:100-9.
467. Audouy SA, de Leij LF, Hoekstra D, Molema G. In vivo characteristics of cationic liposomes as delivery vectors for gene therapy. Pharm Res 2002;19:1599-605.
468. Yew NS, Scheule RK. Toxicity of cationic lipid-DNA complexes. Adv Genet 2005;53:189-214.
469. Blechacz B, Russell SJ. Parvovirus vectors: use and optimisation in cancer gene therapy. Expert Rev Mol Med 2004;6:1-24.
470. Conese M, Auriche C, Ascenzioni F. Gene therapy progress and prospects: episomally maintained self-replicating systems. Gene Ther 2004;11:1735-41.
471. Herweijer H, Wolff JA. Progress and prospects: naked DNA gene transfer and therapy. Gene Ther 2003;10:453-8.
472. Mikkelsen JG, Yant SR, Meuse L, Huang Z, Xu H, Kay MA. Helper-Independent Sleeping Beauty transposon-transposase vectors for efficient nonviral gene delivery and persistent gene expression in vivo. Mol Ther 2003;8:654-65.
473. Olivares EC, Hollis RP, Chalberg TW, Meuse L, Kay MA, Calos MP. Site-specific genomic integration produces therapeutic Factor IX levels in mice. Nat Biotechnol 2002;20:1124-8.
474. Ortiz-Urda S, Thyagarajan B, Keene DR, Lin Q, Calos MP, Khavari PA. PhiC31 integrase-mediated nonviral genetic correction of junctional epidermolysis bullosa. Hum Gene Ther 2003;14:923-8.
475. Ortiz-Urda S, Thyagarajan B, Keene DR, Lin Q, Fang M, Calos MP, Khavari PA. Stable nonviral genetic correction of inherited human skin disease. Nat Med 2002;8:1166-70.
476. Khromykh AA. Replicon-based vectors of positive strand RNA viruses. Curr Opin Mol Ther 2000;2:555-69.
477. Calos MP. The potential of extrachromosomal replicating vectors for gene therapy. Trends Genet 1996;12:463-6.
478. Oehmig A, Fraefel C, Breakefield XO, Ackermann M. Herpes simplex virus type 1 amplicons and their hybrid virus partners, EBV, AAV, and retrovirus. Curr Gene Ther 2004;4:385-408.
479. Jalanko A, Kallio A, Ruohonen-Lehto M, Soderlund H, Ulmanen I. An EBV-based mammalian cell expression vector for efficient expression of cloned coding sequences. Biochim Biophys Acta 1988;949:206-12.
480. Yates JL, Guan N. Epstein-Barr virus-derived plasmids replicate only once per cell cycle and are not amplified after entry into cells. J Virol 1991;65:483-8.
481. Ozawa K, Ayub J, Kajigaya S, Shimada T, Young N. The gene encoding the nonstructural protein of B19 (human) parvovirus may be lethal in transfected cells. J Virol 1988;62:2884-9.
482. Corbau R, Duverger V, Rommelaere J, Nuesch JP. Regulation of MVM NS1 by protein kinase C: impact of mutagenesis at consensus phosphorylation sites on replicative functions and cytopathic effects. Virology 2000;278:151-67.

483. Daeffler L, Horlein R, Rommelaere J, Nuesch JP. Modulation of minute virus of mice cytotoxic activities through site-directed mutagenesis within the NS coding region. J Virol 2003;77:12466-78.
484. Lang SI, Boelz S, Stroh-Dege AY, Rommelaere J, Dinsart C, Cornelis JJ. The infectivity and lytic activity of minute virus of mice wild-type and derived vector particles are strikingly different. J Virol 2005;79:289-98.
485. Hsu EC, Iorio C, Sarangi F, Khine AA, Richardson CD. CDw150(SLAM) is a receptor for a lymphotropic strain of measles virus and may account for the immunosuppressive properties of this virus. Virology 2001;279:9-21.
486. Kinugasa N, Higashi T, Nouso K, Nakatsukasa H, Kobayashi Y, Ishizaki M, Toshikuni N, Yoshida K, Uematsu S, Tsuji T. Expression of membrane cofactor protein (MCP, CD46) in human liver diseases. Br J Cancer 1999;80:1820-5.
487. Katze MG, He Y, Gale M, Jr. Viruses and interferon: a fight for supremacy. Nat Rev Immunol 2002;2:675-87.
488. Jagus R, Joshi B, Barber GN. PKR, apoptosis and cancer. Int J Biochem Cell Biol 1999;31:123-38.
489. Bose S, Banerjee AK. Innate immune response against nonsegmented negative strand RNA viruses. J Interferon Cytokine Res 2003;23:401-12.
490. Bell JC, Garson KA, Lichty BD, Stojdl DF. Oncolytic viruses: programmable tumour hunters. Curr Gene Ther 2002;2:243-54.
491. Balachandran S, Barber GN. Vesicular stomatitis virus (VSV) therapy of tumors. IUBMB Life 2000;50:135-8.
492. Coffey MC, Strong JE, Forsyth PA, Lee PW. Reovirus therapy of tumors with activated Ras pathway. Science 1998;282:1332-4.
493. Strong JE, Coffey MC, Tang D, Sabinin P, Lee PW. The molecular basis of viral oncolysis: usurpation of the Ras signaling pathway by reovirus. Embo J 1998;17:3351-62.
494. Myers RM, Greiner SM, Harvey ME, Griesmann G, Kuffel MJ, Buhrow SA, Reid JM, Federspiel M, Ames MM, Dingli D, Schweikart K, Welch A, Dispenzieri A, Peng KW, Russell SJ. Preclinical pharmacology and toxicology of intravenous MV-NIS, an oncolytic measles virus administered with or without cyclophosphamide. Clin Pharmacol Ther 2007;82:700-10.
495. Peng KW, Frenzke M, Myers R, Soeffker D, Harvey M, Greiner S, Galanis E, Cattaneo R, Federspiel MJ, Russell SJ. Biodistribution of oncolytic measles virus after intraperitoneal administration into Ifnar-CD46Ge transgenic mice. Hum Gene Ther 2003;14:1565-77.
496. Satoh A, Kobayashi H, Yoshida T, Tanaka A, Kawajiri T, Oki Y, Kasugai K, Tonai M, Satoh K, Nitta M. Clinicopathological study on liver dysfunction in measles. Intern Med 1999;38:454-7.
497. Fimmel CJ, Guo L, Compans RW, Brunt EM, Hickman S, Perrillo RR, Mason AL. A case of syncytial giant cell hepatitis with features of a paramyxoviral infection. Am J Gastroenterol 1998;93:1931-7.
498. Rand EB, McCarthy CA, Whitington PF. Measles vaccination after orthotopic liver transplantation. J Pediatr 1993;123:87-9.
499. Kano H, Mizuta K, Sakakihara Y, Kato H, Miki Y, Shibuya N, Saito M, Narita M, Kawarasaki H, Igarashi T, Hashizume K, Iwata T. Efficacy and safety of immunization for pre- and post- liver transplant children. Transplantation 2002;74:543-50.

500. Wolman SR, Camuto PM, Perle MA. Cytogenetic diversity in primary human tumors. J Cell Biochem 1988;36:147-56.
501. Ponchel F, Puisieux A, Tabone E, Michot JP, Froschl G, Morel AP, Frebourg T, Fontaniere B, Oberhammer F, Ozturk M. Hepatocarcinoma-specific mutant p53-249ser induces mitotic activity but has no effect on transforming growth factor beta 1-mediated apoptosis. Cancer Res 1994;54:2064-8.
502. Hsu IC, Tokiwa T, Bennett W, Metcalf RA, Welsh JA, Sun T, Harris CC. p53 gene mutation and integrated hepatitis B viral DNA sequences in human liver cancer cell lines. Carcinogenesis 1993;14:987-92.
503. Galanis E, Bateman A, Johnson K, Diaz RM, James CD, Vile R, Russell SJ. Use of viral fusogenic membrane glycoproteins as novel therapeutic transgenes in gliomas. Hum Gene Ther 2001;12:811-21.
504. Faivre J, Clerc J, Gerolami R, Herve J, Longuet M, Liu B, Roux J, Moal F, Perricaudet M, Brechot C. Long-term radioiodine retention and regression of liver cancer after sodium iodide symporter gene transfer in wistar rats. Cancer Res 2004;64:8045-51.
505. Risse JH, Grunwald F, Kersjes W, Strunk H, Caselmann WH, Palmedo H, Bender H, Biersack HJ. Intraarterial HCC therapy with I-131-Lipiodol. Cancer Biother Radiopharm 2000;15:65-70.
506. Katyal S, Oliver JH, 3rd, Peterson MS, Ferris JV, Carr BS, Baron RL. Extrahepatic metastases of hepatocellular carcinoma. Radiology 2000;216:698-703.
507. Nemunaitis J, Ganly I, Khuri F, Arseneau J, Kuhn J, McCarty T, Landers S, Maples P, Romel L, Randlev B, Reid T, Kaye S, Kirn D. Selective replication and oncolysis in p53 mutant tumors with ONYX-015, an E1B-55kD gene-deleted adenovirus, in patients with advanced head and neck cancer: a phase II trial. Cancer Res 2000;60:6359-66.
508. Shinozaki K, Ebert O, Kournioti C, Tai YS, Woo SL. Oncolysis of multifocal hepatocellular carcinoma in the rat liver by hepatic artery infusion of vesicular stomatitis virus. Mol Ther 2004;9:368-76.

VI. Abbreviations

AAIR	Age-adjusted incidence rate
AAMR	Age-adjusted mortality rate
AASLD	American Association of the Study of Liver Disease
AAV	Adeno-associated virus
ALDH	Aldehyde dehydrogenase
ARP	Autonomously replicating parvovirus
ATP	Adenosine triphosphate
BCLC	Barcelona Clinic Liver Cancer
bFGF	Basic fibroblast growth factor
bp	Base pairs
CAR	Chimaeric antigen receptor
CDD	Cytidine deaminase
CEA	Carcinoembryonic antigen
Cer	Ceramide
CLIP	Cancer of the Liver Italian Program
cpm	Counts per minute
CPE	Cytopathic effect
CPV	Canine parvovirus
CTCL	Cutaneous T-cell lymphoma
CTL	Cytotoxic T lymphocyte
d	Day
DAPI	4,6-Diamidino-2-phenylidone
DHFR	Dihydrofolate reductase
DIG	Digoxigenin
DMEM	Dulbecco's modified Eagle medium
DMSO	Dimethyl sulfoxide
DODAC	Dileoyldimethylammonium chloride
DOPE	Dioleoyl-L-α-phosphatidylethanolamine
DOTAP	1,2 Dioleoyl 3-trimethyl ammonium propane
DPD	Dihydropyrimidine dehydrogenase
dRF	Dimeric replicative form
EBV	Epstein-Barr virus
EDTA	Ethylenediaminetetraacetic acid
EGFR	Epidermal growth factor receptor
ELISA	Enzyme-linked immunosorbent assay
F	Fusion protein
FPV	Feline parvovirus
g	gram
Galv-FMG	Gibbon ape leukemia virus-fusogenic membrane glycoprotein
GBM	Glioblastoma multiforme
GFP	Green fluorescent protein
GM-CSF	Granulocyte macrophage colony-stimulating factor
GST	Glutathione-S-transferase
H	Hemagglutinine protein
h	hour
HEPES	*N*-2-hydroxyethylpiperazine-*N*'-ethanesulfonic acid

HBSS	Hank's balanced salt solution
HBV	Hepatitis B virus
HCC	Hepatocellular carcinoma
HCV	Hepatitis C virus
HLA	Human leukocyte antigen
HSC	Hematopoietic stem cell
IACUC	Institutional animal care and use committee
IL-2	Interleukin-2
INF	Interferon
IR	Inverted repeat
Kb	Kilobase
kD	Kilo Dalton
L	Polymerase
LMV	Large multilamellar vesicle
LUV	Large unilamellar vesicle
M	Matrix protein
MDR	Multidrug resistance gene
MEM	Minimum essential media
MGMT	O^6-methylguanine-DNA methyltransferase
min	Minutes
MOI	Multiplicity of infection
mRF	Monomer relicative form
MV-Edm	Edmonston strain of Measles virus
MVM	Minute virus of mice
MW	Molecular weight
N	Nucleoprotein
NIS	Sodium iodide symporter
NS1/2	Nonstructural proteins 1/2
ORF	Open reading frame
P	Phosphoprotein
PBS	Phosphate buffered saline
PCR	Polymerase chain reaction
PDGF-β	Platelet-derived endothelial growth factor-β
PEG	Polyethylene glycol
PEI	Poly(ethylenimine)
PEI	Percutaneous ethanol injection
p.i.	Post injection
PKC	Protein kinase C
PLL	Poly(L-Lysine)
p.t.	post transfection
QELS	Quasi elastic light light scattering
RLU	Relative light units
RNA	Ribonucleic acid
RPM	Rounds per minute
RT	Room temperature
RT-PCR	Reverse transcriptase-polymerase chain reaction
SCID	Severe combined immunodeficiency
SDS	Sodium dodecyl sulfate
SHARP	Sorafenib HCC Assessment Randomized Protocol

SLAM	Signaling lymphocyte activation molecule
SPLP	Stabilized plasmid lipid particles
SSC	Saline-sodium citrate buffer
SUV	Small unilamellar vesicle
T4 PNK	T4 polynucleotide kinase
TAA	Tumor-associated antigen
TAE	Tris-acetate-EDTA buffer
TACE	Transarterial chemoembolization
TBS	Tris-buffered saline
$TCID_{50}$	50% Tissue Culture Infective Dose
TCR	T cell receptor
Tf	Transferrin
TGF-β	Transforming growth factor-β
TNF-α	Tumor necrosis factor-α
TRAIL	TNF-related apoptosis-inducing ligand
Tris	Tris(hydroxymethyl)aminomethane
TUNEL	Terminal deoxynucleotidyl transferase dUTP nick end labeling
UNOS	United Network for Organ Sharing
VEC	Vascular endothelial cell
VEGFR	Vascular endothelial growth factor receptor
VP1/2	Viral proteins 1/2